

# **THE ROLE OF HAEM TRANSPORT AND IRON CHELATION IN OESOPHAGEAL CANCER**

SAMUEL JOHN FORD

**A thesis submitted to**

The University of Birmingham

For the degree of

**DOCTOR OF PHILOSOPHY**

School of Cancer Sciences

The University of Birmingham

July 2012

UNIVERSITY OF  
BIRMINGHAM

**University of Birmingham Research Archive**

**e-theses repository**

This unpublished thesis/dissertation is copyright of the author and/or third parties. The intellectual property rights of the author or third parties in respect of this work are as defined by The Copyright Designs and Patents Act 1988 or as modified by any successor legislation.

Any use made of information contained in this thesis/dissertation must be in accordance with that legislation and must be properly acknowledged. Further distribution or reproduction in any format is prohibited without the permission of the copyright holder.

## ABSTRACT

The incidence of oesophageal adenocarcinoma (OAC) is increasing at an alarming rate in the Western World. Despite advances in surgical technique and patient selection, overall survival remains abysmal. Understanding the molecular and genetic events in the evolution of OAC is crucial to improving outcome. The role of iron in the carcinogenesis of OAC is supported by epidemiological and experimental evidence. Oesophageal cancers are iron loaded and aggressively capture systemic iron to potentiate a malignant phenotype. This project aimed to establish that OAC cells are also capable of acquiring haem and to explore the potential of iron chelation therapy in the treatment of oesophageal cancer.

Haem import proteins are sequentially over expressed in the evolution of OAC. Culturing OAC cells with supplementary haem significantly enhances viability, proliferation, migration and anchorage independent growth. Abrogation of haem import protein expression reverses the stimulatory effect of supplementary haem and significantly reduces tumour burden *in-vivo*. Different classes of iron chelators exhibit potent *in-vitro* and *in-vivo* anti-neoplastic action in oesophageal malignancy. Iron chelators demonstrate chemo-sensitising properties and are able to overcome chemo-resistance.

Haem import proteins are potential therapeutic targets in the treatment of oesophageal malignancy. Iron chelation therapy represents an effective, predictable and well tolerated adjunct to standard chemotherapy and should be considered for clinical trial.

## **DEDICATION**

This thesis is dedicated to my lovely wife Abby and baby boy Maxi. Abby's support and understanding during the three years spent away from home studying for this PhD cannot be overstated.

## **ACKNOWLEDGEMENTS**

I am greatly indebted to my supervisor and friend Dr Chris Tselepis for his unerring guidance, support and intellect, without which this project would not have been possible.

Thank you to all my friends in the lab who have offered intellectual support and shared the trials and tribulations of scientific research; especially Keith, Elisabeth and more latterly Matt, who has taken up the gauntlet to further advance this body of work.

I offer my sincere thanks to Cancer Research UK and all those that support this fantastic institution, for fully funding my PhD programme by award of the Cancer Research UK Gordon Hamilton Fairley Clinical Research Fellowship.

# CONTENTS

<b>CHAPTER 1: Introduction .....</b>	<b>1</b>
1.1 Oesophageal Cancer .....	1
1.2 Epidemiology of oesophageal cancer .....	3
1.3 Risk factors for oesophageal malignancy .....	5
1.4 Barrett's oesophagus and gastro-oesophageal reflux.....	7
1.5 Barrett's metaplasia – dysplasia – adenocarcinoma sequence.....	8
1.6 The molecular and genetic basis for the progression of Barrett's metaplasia to adenocarcinoma .....	9
1.6.1 Cellular origin of Barrett's metaplasia .....	9
1.6.2 p16 .....	10
1.6.3 Adenomatous polyposis coli (APC) .....	10
1.6.4 p53 .....	11
1.6.5 p27 .....	11
1.6.6 Cyclin D1.....	11
1.6.7 Retinoblastoma gene (Rb) .....	12
1.6.8 K-ras.....	12
1.6.9 Bcl-2.....	12
1.6.10 Cell adhesion and interaction in the malignant progression of oesophageal adenocarcinoma .	12
1.6.11 The role of growth factors in the malignant progression of oesophageal adenocarcinoma .....	13
1.6.12 Immortalisation of cells in the progression of oesophageal adenocarcinoma .....	13
1.6.13 Other genes involved in the malignant progression of oesophageal adenocarcinoma .....	14
1.7 The role of iron in malignant progression of oesophageal adenocarcinoma.....	16
1.8 Iron and potential mechanisms underlying carcinogenesis .....	19
1.9 Dietary iron .....	22
1.10 Absorption, storage and transport of inorganic iron.....	23
1.10.1 Duodenal cytochrome b (Dcytb) .....	23
1.10.2 Divalent metal transporter 1 (DMT1) .....	24
1.10.3 Ferritin.....	24
1.10.4 Ferroportin (FPN) .....	25
1.10.5 Hephaestin .....	26
1.10.6 Transferrin receptor (TfR1) .....	27
1.11 Cellular regulation of iron transport and storage proteins .....	30

1.12 Systemic regulation of iron .....	32
1.13 Absorption, transport and metabolism of haem iron .....	34
1.13.1 Haem-carrier protein 1 (HCP1).....	40
1.13.2 Low-density lipoprotein receptor related protein (LRP1) .....	41
1.13.3 Feline leukaemic virus, subgroup C receptor (FLVCR) .....	43
1.13.4 Breast cancer resistance protein (BCRP) .....	44
1.14 Iron chelation as a potential anti-neoplastic therapeutic modality .....	45
1.15 Naturally occurring chelators .....	47
1.16 Clinically established iron chelators .....	48
1.16.1 Desferrioxamine (DFO).....	48
1.16.2 Deferasirox .....	50
1.17 Promising experimental chelators with anti-neoplastic properties (Dp44mT).....	56
1.18 Hypothesis .....	61
1.19 Aims .....	62

## **CHAPTER 2: MATERIALS AND METHODS..... 63**

<b>2.1 Materials.....</b>	<b>63</b>
2.1.1 General, Cell Culture and Molecular Biology Reagents .....	63
2.1.2 Primary antibodies.....	68
2.1.3 Secondary Antibodies .....	69
2.1.4 Oligonucleotides.....	70
2.1.5 Ex-vivo tissue Samples .....	71
2.1.6 Cell lines .....	72
<b>2.2 Methods.....</b>	<b>74</b>
2.2.1 Immunohistochemistry .....	74
2.2.2 Evaluation of immunoreactivity .....	75
2.2.3 DAB-enhanced Perls' Prussian blue staining .....	75
2.2.4 Electrophoresis and Western Blotting .....	76
2.2.5 RNA extraction from frozen tissue and cells .....	80
2.2.6 Cell Culture.....	85
2.2.7 MTT cell viability assay.....	87
2.2.8 BrdU proliferation assay.....	88
2.2.9 Ferrozine assay.....	89
2.2.10 Anchorage Independent Growth Assay (colony forming assay) .....	90
2.2.11 Wound healing assay .....	91

2.2.12 Fluorescence-activated cell sorting (FACS) with propidium iodide labelling for cell cycle analysis .....	92
2.2.13 Intracellular reactive oxygen species assay - 2,7-dichloro-fluorescein-diacetate (H2DCF-DA) ..	93
2.2.14 <sup>59</sup> Fe extraction (efflux) with <sup>59</sup> Fe-Tf .....	95
2.2.15 Cellular <sup>59</sup> Fe up-take blocking .....	95
2.2.16 Stable silencing (knock-down) of LRP1 and HCP1 protein expression by pGIPZ construct bearing lenti-viral preparations .....	96
2.2.17 Murine studies .....	103
2.2.18 Statistical Analysis .....	105
2.2.19 Ethical approval .....	106

### **Chapter 3: Characterisation of Haem Transport Proteins in the Progression of Barrett’s Metaplasia to Oesophageal Adenocarcinoma .....**

3.1 Introduction .....	107
3.2 Aims.....	109
3.3 Results.....	110
3.3.1 mRNA expression of the haem import proteins LRP1 and HCP1 and haem export proteins BCRP and FLVCR in the malignant progression of BM to OAC.....	110
3.3.2 Protein expression of the haem import proteins LRP1 and HCP1 and export proteins BCRP and FLVCR in the malignant progression of BM to OAC.....	114
3.3.3 Immunolocalisation of the haem import proteins LRP1 and HCP1 and haem export proteins BCRP and FLVCR in the malignant progression of BM to OAC.....	117
3.3.4 Haem transport protein immunoreactivity stratified by tumour stage .....	124
3.4 Conclusions .....	126

### **Chapter 4: The *In-vitro* and *In-vivo* Effects of Haem and Abrogation of Haem Transport Proteins on Oesophageal Cancer Cells.....**

4.1 Introduction .....	130
4.2 Aims.....	132
4.3 Results.....	133
4.3.1 Abrogation of LRP1 and HCP1 protein expression (LRP1 and HCP1 knock-downs) .....	133
4.3.2 Characterisation of the influence of LRP1 and HCP1 protein abrogation on cellular iron loading and iron transport protein expression <i>in-vitro</i> .....	136
4.3.3 Determination of the impact of LRP1 and HCP1 silencing on cell viability, proliferation and phenotype .....	154
4.3.4 The impact of LRP1 and HCP1 silencing on OE33, OE19 and OE21 cell cycle <i>in-vitro</i> .....	168
4.3.5 <i>In-vivo</i> effects of LRP1 and HCP1 protein silencing .....	171

4.4 Conclusions .....	180
-----------------------	-----

## **Chapter 5: The *in-vitro* and *in-vivo* anti-neoplastic activity of iron chelators in oesophageal cancer ..... 186**

5.1 Introduction .....	186
5.2 Aims.....	189
5.3 Results.....	190
5.3.1 Cell lines and iron chelators .....	190
5.3.2 Generation of IC50 values .....	190
5.3.3 Determine the ability of iron chelators to block iron up-take and extract iron from oesophageal cancer cells .....	191
5.3.4 The <i>in-vitro</i> effects of iron chelation on iron and haem transport protein expression in oesophageal cancer cells .....	195
5.3.5 The <i>in-vitro</i> effect of iron chelation on oesophageal cancer cell phenotype .....	206
5.3.6 Characterisation of the <i>in-vitro</i> effect of iron chelation on oesophageal cancer cell cycle .....	226
5.3.7 The <i>in-vivo</i> activity of oral Deferasirox on tumour burden in murine xenograft models of oesophageal cancer and quantification of systemic toxicity.....	231
5.3.8 Exploration of the anti-neoplastic potential of iron chelators in combination with standard chemotherapeutic agents for oesophageal cancer treatment and possible action on chemoresistant lineages.....	247
5.4 Conclusions .....	257

## **Chapter 6: Discussion ..... 264**

6.1 Conclusions .....	264
6.2 Future work.....	268
6.2.1 Laboratory experimental work .....	268
6.2.2 Clinical experimental work .....	269

## **References ..... 271**

## Figures

<b>Figure 1.1</b> Disease free and overall survival from oesophageal adenocarcinoma - long term results of Medical Research Council OE02 oesophageal cancer trial.....	2
<b>Figure 1.2</b> Stage-specific incidence trends in oesophageal adenocarcinoma 1973-2006....	4
<b>Figure 1.3</b> Summary of the genetic basis for progression through the Barrett's Metaplasia-dysplasia-adenocarcinoma sequence .....	15
<b>Figure 1.4</b> The Fenton reactions.....	20
<b>Figure 1.5</b> Haem – ferrous protoporphyrin IX.....	22
<b>Figure 1.6</b> Iron and haem transport proteins in the human enterocyte .....	28
<b>Figure 1.7</b> The IRE-IRP regulatory system .....	31
<b>Figure 1.8</b> Homeostatic regulation of plasma iron.....	32
<b>Figure 1.9</b> Overview of systemic haem and inorganic iron metabolism.....	38
<b>Figure 1.10</b> Molecular structures of iron chelators Deferasirox, DFO and Dp44mT .....	46
<b>Figure 1.11</b> Mean plasma concentrations (+ SD) of Deferasirox are proportional to dose	52
<b>Figure 2.1</b> pGIPZ Construct Design .....	97
<b>Figure 3.1</b> mRNA expression for the haem transport proteins is not significantly altered in the metaplastic transformation of NS to BM .....	112
<b>Figure 3.2</b> mRNA expression for the haem transport proteins is significantly up-regulated in the malignant progression of dysplastic BM to invasive OAC.....	113
<b>Figure 3.3</b> The expression of proteins capable of haem transport is up-regulated in the malignant progression of dysplastic BM to invasive OAC.....	116
<b>Figure 3.4</b> LRP1 immunoreactivity .....	120
<b>Figure 3.5</b> HCP1 immunoreactivity.....	121

<b>Figure 3.6</b> BCRP Immunoreactivity.....	122
<b>Figure 3.7</b> FLVCR immunoreactivity .....	123
<b>Figure 3.8</b> Semi-quantitative immunohistochemistry analysis of haem transport proteins by tumour stage.....	125
<b>Figure 4.1</b> OE33 cell line expressing GFP after successful infection with lenti-virus vector containing pGIPZ constructs and culture with Puromycin .....	134
<b>Figure 4.2</b> Confirmation of successful silencing of LRP1 and HCP1 protein expression in OE33, OE19 and OE21 cell line knock-downs.....	135
<b>Figure 4.3</b> LRP1 and HCP1 knock-down suppresses cellular ability to acquire haem to augment the intracellular iron pool compared to control .....	137
<b>Figure 4.4</b> knock-down of LRP1 or HCP1 proteins alters TfR1, FPN and ferritin mRNA expression.....	140
<b>Figure 4.5</b> Knock-down of LRP1 and HCP1 proteins in the OE33 cell line alters TfR1, FPN and ferritin protein expression.....	143
<b>Figure 4.6</b> Knock-down of LRP1 and HCP1 proteins in the OE19 cell line alters TfR1, FPN and ferritin protein expression.....	144
<b>Figure 4.7</b> Knock-down of LRP1 and HCP1 proteins in the OE21 cell line alters TfR1, FPN and ferritin protein expression.....	145
<b>Figure 4.8</b> knock-down of LRP1 or HCP1 proteins alters mRNA expression of haem transport proteins .....	149
<b>Figure 4.9</b> Confirmation of knock-down of LRP1 and HCP1 proteins in OE33 cell line and altered expression of haem transporting proteins .....	151
<b>Figure 4.10</b> Confirmation of knock-down of LRP1 and HCP1 proteins in OE19 cell line and altered expression of haem transporting proteins .....	152

<b>Figure 4.11</b> Confirmation of knock-down of LRP1 and HCP1 proteins in OE21 cell line and altered expression of haem transporting proteins .....	153
<b>Figure 4.12</b> LRP1 and HCP1 knock-down reduces oesophageal cancer cell viability and proliferation and neutralises the stimulatory effect of supplementary haem .....	156
<b>Figure 4.13</b> LRP1 and HCP1 knock-down prevents the stimulatory effect of supplementary haem on OE33 cell line migration .....	158
<b>Figure 4.14</b> LRP1 and HCP1 knock-down prevents the stimulatory effect of supplementary haem on OE33 cell line migration .....	159
<b>Figure 4.15</b> LRP1 and HCP1 knock-down prevents the stimulatory effect of supplementary haem on OE19 cell line migration .....	160
<b>Figure 4.16</b> LRP1 and HCP1 knock-down prevents the stimulatory effect of supplementary haem on OE19 cell line migration .....	161
<b>Figure 4.17</b> LRP1 and HCP1 knock-down prevents the stimulatory effect of supplementary haem on OE21 cell line migration .....	162
<b>Figure 4.18</b> LRP1 and HCP1 knock-down prevents the stimulatory effect of supplementary haem on OE21 cell line migration .....	163
<b>Figure 4.19</b> LRP1 and HCP1 knock-down suppresses independent colony formation with or without supplementary haem in OE33 cell line.....	165
<b>Figure 4.20</b> LRP1 and HCP1 knock-down suppresses independent colony formation with or without supplementary haem in OE19 cell line.....	166
<b>Figure 4.21</b> LRP1 and HCP1 knock-down suppresses independent colony formation with or without supplementary haem in OE21 cell line.....	167
<b>Figure 4.22</b> LRP1 and HCP1 protein knock-down neutralises the stimulatory effect of supplementary haem on the cycle cell.....	169

<b>Figure 4.23</b> Silencing of LRP1 and HCP1 in OE33 cell line xenografts significantly reduced tumour burden in a murine model.....	172
<b>Figure 4.24</b> Silencing of LRP1 and HCP1 in OE33 cell line xenografts significantly alters mRNA expression of iron transport proteins but has little impact on haem transport mRNA expression.....	174
<b>Figure 4.25</b> Semi-quantitative immunoreactivity scoring - silencing of LRP1 and HCP1 in OE33 cell line xenografts is maintained and significantly increases TfR1 and decreases ferritin immunoreactivity .....	177
<b>Figure 4.26</b> Representative immunolocalisation of LRP1 and HCP1 for OE33 LRP1 and HCP1 knock-down xenografts .....	178
<b>Figure 4.27</b> Representative immunolocalisation of TfR1 and ferritin for OE33 LRP1 and HCP1 knock-down xenografts .....	179
<b>Figure 5.1</b> Iron chelators DFO, Deferasirox and Dp44mT can block the up-take of <sup>59</sup> Fe-Tf by oesophageal cancer cells <i>in-vitro</i> .....	193
<b>Figure 5.2</b> Iron chelators DFO, Deferasirox and Dp44mT can efflux iron from oesophageal cancer cells <i>in-vitro</i> .....	194
<b>Figure 5.3</b> Culture with iron chelators Deferasirox and DFO alters mRNA expression of iron transport proteins <i>in-vitro</i> .....	197
<b>Figure 5.4</b> Culture with iron chelators Deferasirox and DFO alters iron transport protein expression <i>in-vitro</i> .....	199
<b>Figure 5.5</b> Culture with iron chelators Deferasirox and DFO influences mRNA expression of haem transport proteins <i>in-vitro</i> .....	202
<b>Figure 5.6</b> Culture with iron chelators Deferasirox and DFO influences haem transport protein expression <i>in-vitro</i> .....	205

<b>Figure 5.7</b> Iron chelators Deferasirox and DFO inhibit oesophageal cancer cell viability	207
<b>Figure 5.8</b> Iron chelators Deferasirox and DFO inhibit oesophageal cancer cell proliferation.....	208
<b>Figure 5.9</b> Dp44mT inhibits oesophageal cancer cell viability and proliferation <i>in-vitro</i>	210
<b>Figure 5.10</b> Iron chelators inhibit OE33 cell line anchorage independent growth .....	212
<b>Figure 5.11</b> Iron chelators inhibit OE19 cell line anchorage independent growth .....	213
<b>Figure 5.12</b> Iron chelators inhibit OE21 cell line anchorage independent growth .....	214
<b>Figure 5.13</b> Iron chelator Dp44mT inhibits OE33 cell line anchorage independent growth .....	215
<b>Figure 5.14</b> Iron chelator Dp44mT inhibits OE19 cell line anchorage independent growth .....	216
<b>Figure 5.15</b> Iron chelator Dp44mT inhibits OE21 cell line anchorage independent growth .....	217
<b>Figure 5.16</b> Deferasirox inhibits oesophageal cancer cell migration <i>in-vitro</i> .....	219
<b>Figure 5.17</b> Deferasirox inhibits oesophageal cancer cell migration <i>in-vitro</i> .....	221
<b>Figure 5.18</b> DFO inhibits oesophageal cancer cell migration <i>in-vitro</i> .....	222
<b>Figure 5.19</b> Dp44mT inhibits oesophageal cancer cell migration <i>in-vitro</i> .....	223
<b>Figure 5.20</b> Dp44mT inhibits oesophageal cancer cell migration <i>in-vitro</i> .....	225
<b>Figure 5.21</b> Iron chelation significantly inhibits the oesophageal cancer cell cycle .....	228
<b>Figure 5.22</b> Deferasirox increases expression of the cell cycle related nuclear protein CDC45L in oesophageal cancer cells.....	230
<b>Figure 5.23</b> Oral Deferasirox significantly reduces xenograft tumour burden in a murine model of oesophageal cancer .....	232

<b>Figure 5.24</b> Oral administration of Deferasirox (20mg/Kg) does not adversely affect mouse weight .....	233
<b>Figure 5.25</b> Oral administration of Deferasirox (20mg/Kg) does not alter major organ iron content in murine models .....	237
<b>Figure 5.26</b> Representative images of major organ immunoreactivity following oral administration of Deferasirox or control vehicle alone .....	238
<b>Figure 5.27</b> Oral administration of Deferasirox (20mg/Kg) for 21 days significantly reduces iron content in oesophageal cancer xenografts.....	240
<b>Figure 5.28</b> Oral administration of Deferasirox significantly alters mRNA expression of the iron transport proteins in oesophageal cancer xenografts.....	242
<b>Figure 5.29</b> Oral administration of Deferasirox alters iron transport protein expression (immunohistochemistry) in oesophageal cancer xenografts.....	245
<b>Figure 5.30</b> Representative images of xenograft immunoreactivity following oral administration of Deferasirox or control vehicle alone .....	246
<b>Figure 5.31</b> Effect of iron chelators and standard chemotherapeutic agents on oesophageal cancer cellular viability.....	250
<b>Figure 5.32</b> Effect of iron chelators and standard chemotherapeutic agents on oesophageal cancer cellular proliferation.....	252
<b>Figure 5.33</b> The effect of iron chelators on TE-4 cellular viability .....	256

## Tables

<b>Table 1.1</b> The numerous and diverse ligands associated with LRP1.....	42
<b>Table 2.1</b> Primary antibodies, origin, class, positive controls and optimum working concentrations.....	68
<b>Table 2.2</b> Oligonucleotides.....	70
<b>Table 2.3</b> SDS-PAGE gels.....	79
<b>Table 2.4</b> Volumes of optimised fluorogenic probe used for TaqMan q-RT-PCR reactions.....	84
<b>Table 2.5</b> Sense, anti-sense and loop sequences for shRNA control, LRP1 and HCP1 knockdown .....	102
<b>Table 3.1</b> Immunoreactivity score for organic iron transport proteins in the progression of NS to invasive OAC .....	119
<b>Table 5.1</b> Oral administration of Deferasirox (20mg/Kg) does not impact on systemic haematological and biochemical indices in murine models .....	235
<b>Table 5.2</b> Oral administration of Deferasirox (20mg/Kg) does not alter major organ weights in murine models .....	236
<b>Table 5.3</b> Assessment of the statistical significance of treating oesophageal cancer cell lines with chelator alone compared to a combination of chelator and standard chemotherapeutic agent .....	253
<b>Table 5.4</b> Concentration/range of iron chelators indicating a chemo-sensitising potential in the presence of standard chemotherapeutic agents.....	254

## ABBREVIATIONS

ABC	ATP-binding cassette
ABC-me	ABC-mitochondrial erythroid transporter
ALB	Albumin
ALT	Alanine transferase
APC	Adenomatous polyposis coli
ApoE	Apolipoprotein E
AST	Aspartate transaminase
BCA	Bicinchoninic acid
Bcl2	B-cell lymphoma 2
BCRP	Breast cancer resistance protein (ABCG2, MXR and ABCP)
BCS	Bathocuproine disulfonate
BHT	Hydroxyamino triazine
BM	Barrett's metaplasia
BMP	Bone morphogenetic protein
Brdu	5-bromo-2'-deoxyuridine
CD163	Haptoglobin receptor
CDC	Cell division cycle
CDK	Cyclin dependent kinase
CDKI	Cyclin dependent kinase inhibitor
cDNA	Complementary deoxyribonucleic acid
CDX2	Homeobox transcription factor
COX2	Cyclo-oxygenase 2
Ct	Cycle number
DCF	Dichloro-fluorescein-diacetate
Dcytb	Duodenal cytochrome b
DFO	Desferrioxamine
DMEM	Dulbecco's modified eagles medium
DMSO	Dimethyl sulfoxide
DMT1	Divalent metal transporter 1
DNA	Deoxyribonucleic acid
Dp44mT	Di-2-pyridylketone-4,4-dimethyl-3-thiosemicarbazone
DpT	Di-2-pyridylketone thiosemicarbazone
dsRNA	Double-strand ribonucleic acid
ECL	Enhanced chemiluminescence
EDTA	Ethylenediaminetetraacetic acid
EGRF	Epidermal growth factor receptor
FACS	Fluorescence-activated cell sorting
FBC	Full blood count
FCS	Foetal calf serum
FLVCR	Feline leukaemic virus, subgroup C receptor
FLVCR2	Feline leukaemic virus, subgroup C receptor 2

FPN	Ferroportin
GFP	Green fluorescent protein
GORD	Gastro-oesophageal reflux disease
GSK	Glycogen synthase kinase
Hb	Haemoglobin
HCP1	Haem-carrier protein 1 (SLC46A1)(PCFT/HCP1)
HCT	Haematocrit
HEPES	4-(2-hydroxyethyl)-1-piperazineethanesulfonic acid
HFE	Haemochromatosis gene
H-ferritin	Heart or heavy chain ferritin
HGD	High grade dysplasia
HIF	Hypoxia-inducible factor
HIF1	Hypoxia-inducible factor 1
HJV	Hemojuvelin
HL	Haem loaded
HO1	Haem oxygenase 1
Hp	Haptoglobin
HU	Hydroxyurea
HUH	Human hepatoma
Hx	Haemopexin
IC	Inhibitory concentration
IHC-P	Paraffin embedded immunohistochemistry
IL6	Interleukin 6
iNOS	Inducible nitric oxide synthase
IRE	Iron responsive element
IRP1	Iron regulatory protein 1
IRP2	Iron regulatory protein 2
KD	Knock-down
kDa	Kilo Dalton
k-ras	Kirsten rat sarcoma
L-ferritin	Liver or light chain ferritin
LGD	Low grade dysplasia
LOH	Loss of heterozygosity
LREC	Local Research Ethics Committee
LRP1	Low-density lipoprotein receptor-related protein (CD91) (Haemopexin receptor)
MALT	Mucosa-associated lymphoid tissue
MCH	Mean cell haemoglobin
MCHC	Mean cell haemoglobin concentration
MCV	Mean cell volume
Mdm	Murine double minute
mRNA	Messenger ribonucleic acid
m-Tor	Mammalian target of rapamycin
MTT	3-(4,5-dimethylthiazol-2-yl)-2,5-diphenyltetrazolium bromide

NdrG1	N-myc downstream regulated gene 1
NEUT	Neutrophil count
NF-κB	Nuclear factor κB
NOD-SCID	Non-obese diabetic-severe combined immunodeficiency
NS	Normal squamous mucosa
OAC	Oesophageal adenocarcinoma
PBS	Phosphate buffered saline
PCFT/HCP1	Proton coupled folate transporter/haem carrier protein 1 (HCP1)
PI	Propidium iodide
PLT	Platelets
pRb	Retinoblastoma gene product
PVDF	Polyvinylidene difluoride
q-RT-PCR	Quantitative real-time polymerase chain reaction
Rb	Retinoblastoma
REDD1	Regulated in development and DNA damage response
RET	Reticulocyte count
RIPA	Radio-immuno-precipitation buffer
RISC	RNA induced silencing complex
RNAi	Ribonucleic acid interference
RNR	Ribonucleotide reductase
ROS	Reactive oxygen species
RPMI	Roswell Park Memorial Institute medium
rRNA	Ribosomal ribonucleic acid
SCC	Squamous cell carcinoma
SDS	Sodium dodecyl sulphate
SDS-PAGE	Sodium dodecyl sulphate -Polyacrylamide Gel Electrophoresis
SEM	Standard error of the mean
siRNA	Short interfering ribonucleic acid
sla	sex-linked anaemic
SP1	Specificity protein 1
SPSS	Statistical package for the social sciences
STAT3	Signal transducer and activator of transcription 3
Steap 3	6-transmembrane epithelial antigen of the prostate 3
TBS	Tris-buffered saline
TBST	Tris-buffered saline tween
T-CA	Tri-carboxylic acid
TCA	Trichloroacetic acid
Tf	Transferrin
TfR1	Transferrin receptor 1 (CD71)
TfR2	Transferrin receptor 2
TIBC	Total iron binding capacity
TM	Tetrathiomolybdate
TMB	tetramethyl-benzidien
TMED	Tetramethylethylenediamine

TP	Total protein
UIBC	Unstaturated iron binding capacity
UICC	Union for International Cancer Control
UTR	Untranslated region
VEGF	vascular endothelial growth factor
VEGFR	vascular endothelial growth factor receptor
WB	Western blotting
WBC	Total white blood cell count

# CHAPTER 1: INTRODUCTION

## 1.1 Oesophageal Cancer

Oesophageal cancer is responsible for 5% of all cancer deaths in the UK and is the sixth most common cancer in Western populations<sup>1</sup>. There are two major histological subtypes of oesophageal cancer, squamous cell carcinoma (SCC) and adenocarcinoma (OAC). SCC and OAC differ substantially with respect to patterns of incidence and aetiological factors; however, both are associated with an extremely poor overall five year survival rate of just 10%<sup>2,3</sup>. The incidence of OAC has risen alarmingly over the past 25 years and is finally starting to become the focus of clinical and laboratory based research<sup>4,5</sup>. Surgical resection is the only curative treatment for OAC, however, the majority of patients present with advanced disease or are unsuitable for radical intervention<sup>3</sup>. Of the minority that undergo surgery, the outlook remains bleak with only 20-30% surviving two years<sup>3</sup>. Oesophagectomy carries a 30 day mortality rate of 5-10% and the associated morbidity impacts on quality of life scores for three years before returning to pre-operative levels<sup>6</sup>. Locally advanced disease and undiagnosed metastatic spread greatly contribute to failure of treatment with curative intent<sup>3</sup>. High rates of loco-regional and distant recurrence has led to much interest in pre-operative (neoadjuvant) combination chemotherapy with response rates of up to 30-40%<sup>3,7</sup>. Cisplatin and 5-fluorouracil (5-FU) based chemotherapy, combined with surgery, increases overall survival by 6% at five years, compared to surgery alone<sup>7</sup>.

**Figure 1.1 Disease free and overall survival from oesophageal adenocarcinoma - long term results of Medical Research Council OE02 oesophageal cancer trial**

Figure A: Disease free survival and figure B: Overall survival determined by surgery alone (S) or neoadjuvant chemotherapy followed by surgery (CS). All patients considered potentially curable at allocation. CS: two cycles of combination Cisplatin and 5-fluorouracil before surgery.

Adapted from Allum et al<sup>7</sup>

Despite the addition of neoadjuvant chemotherapy and refinement of surgical technique, the vast majority of patients still die from overwhelming malignant disease progression. It would appear that further advances in treatment will be governed by understanding the molecular events involved in oesophageal cancer evolution and the development of novel therapeutic strategies where side effects, complications and mortality associated with existing forms of treatment can be minimised.

The focus of this body of work is principally OAC, however, oesophageal SCC is largely included throughout to reflect the importance of this histological entity and the considerable overlap in clinical oncological and surgical treatment of OAC and SCC.

## 1.2 Epidemiology of oesophageal cancer

The incidence of OAC has dramatically increased over the last 25 years and is now rising faster than any other malignant disease in Western nations<sup>8-12</sup>. The magnitude of such an increase is truly alarming considering the extremely poor survival rate, advanced stage at presentation, lack of therapeutic options, deficient knowledge of the disease process and an underfunded research programme.

In the USA the absolute incidence of OAC increased approximately seven-fold, from 3.6 million in 1973 to 25.6 per million in 2005<sup>13,14</sup>. From the early 2000s the annual increase in cases has just started to show signs of slowing from an average of 8.2% to 1.3%<sup>14</sup>. Upon sub-classification of OAC stage at presentation, there is a drop off in the numbers of early stage disease that accounts for this seeming improvement, whereas the incidence of late regional or metastatic cases continues unabated<sup>14</sup>. This may be explained by improved staging techniques, leading to greater detection of regional lymph nodes or metastatic lesions, termed stage migration<sup>14</sup>.

## Figure 1.2 Stage-specific incidence trends in oesophageal adenocarcinoma 1973-2006

Adapted from Pohl et al<sup>14</sup>.

For the majority of the early twentieth century, OAC was a rare entity representing only 0.8-3.7% of all oesophageal cancers<sup>15-19</sup>. In contrast, recent publications from the United States<sup>4,20</sup>, United Kingdom<sup>21</sup>, Switzerland<sup>22</sup> and Australia<sup>23</sup> demonstrate that 30-70% of all oesophageal cancers are adenocarcinomas. Within Western populations, there is a fair degree of heterogeneity in annual incidence, for example, the United Kingdom has nearly twice the incidence of OAC (5-8.7/100,000) as the United States (3.7/100 000) and other European countries with annual reported cases varying in incidence by up to 30%<sup>24-26</sup>.

In contrast to the West, the Middle East and Asia-Pacific has seen very little in the way of an OAC epidemic<sup>27</sup>. SCC retains its predominance as the major histological subtype, principally in the lower third of the oesophagus<sup>27,28</sup>. Regions with a high incidence of SCC tend to be less prosperous with some geographical locations yielding an extremely dense disease prevalence, up to 1:1000 adults<sup>28</sup>. One such area, the so-called "Asian

oesophageal cancer belt” stretches from Eastern Turkey, through Iran and southern areas of the former Soviet Union<sup>28-30</sup>.

### **1.3 Risk factors for oesophageal malignancy**

The contrasting spectrum of risk factors for OAC and oesophageal SCC suggest markedly different pathological origins. A large study from the United States, examining the racial preponderances of the two histological subtypes, confirmed previous observations that oesophageal SCC was much more common in those of Afro-Caribbean origin (SCC >90%, OAC 5%) compared to Caucasians (SCC 32%, OAC 66%), typically males<sup>31</sup>. Consumption of alcohol and smoking is much more prevalent in American Afro-Caribbeans<sup>31</sup> and conversely, prevalence of Barrett’s metaplasia (BM) is low (BM is the major risk factor for OAC; discussed in more detail below)<sup>31,32</sup>. Tobacco and alcohol are extremely strong synergistic risk factors for SCC whereas tobacco alone is only weakly associated with OAC (2.5 times risk of non-smokers)<sup>33-35</sup>. Smoking cessation decreases the relative risk of SCC within a decade, however the modest increase in relative risk of OAC persists<sup>36</sup>.

Diet appears to play a moderate role in oesophageal cancer risk. Akin to many cancers, the incidence of oesophageal malignancy is inversely proportional to fruit and vegetable intake<sup>37</sup>. Evidence supporting micronutrient intake is less robust with a modest benefit seen in high incidence areas of China, following micronutrient supplementation<sup>37,38</sup>. Chronic thermal injury, from consuming hot drinks, may increase risk but this is largely tempered by tea drinking; especially green tea in China<sup>37,39,40</sup>. Areas of intensely high SCC incidence, such as Linxian, China, are associated with dietary nitrosamines<sup>41</sup>.

Nitrosamines are highly carcinogenic and widely used in Asia and the Far East for food preservation<sup>41</sup>.

Obesity increases the risk of OAC 2-3-fold but is not associated with an increased risk of SCC<sup>42-44</sup>. Obesity has been proposed as an indirect risk factor for OAC by increasing the risk of gastro-oesophageal reflux disease (GORD) and BM. However, some studies have shown the impact of obesity on OAC incidence to be independent for GORD<sup>42,43,45</sup>. Chronic inflammation seems to have a central role in the development of OAC<sup>46</sup>. Abdominal obesity (visceral fat) is increasingly being recognised as causing low level systemic inflammation, characterised by increased plasma levels of pro-inflammatory cytokines and receptors, such as interleukin-6, tumour necrosis factor- $\alpha$  and its receptor, C-reactive protein and leptin<sup>42,46-48</sup>.

*Helicobacter pylori* has been associated with several benign and malignant gastrointestinal diseases<sup>48,49</sup>. *H. pylori* causes non-cardia gastric adenocarcinoma and gastric MALT lymphoma<sup>48,49</sup>. Specific eradication therapy and casual exposure to antibiotics has led to a marked decrease in *H. pylori* colonisation in Western countries<sup>48</sup>. The pattern of increasing OAC incidence and reducing incidence of non-cardia gastric adenocarcinoma fits geographically with *H. Pylori* eradication, drawing a tentative conclusion that the organism may have a protective role against OAC<sup>48,50-52</sup>. One proposed mechanism is acidification of refluxing gastric content in patients with GORD secondary to loss of the inhibitory effect of *H. pylori* on gastric acid production<sup>52</sup>.

#### 1.4 Barrett's oesophagus and gastro-oesophageal reflux

Barrett's oesophagus describes an acquired condition in which squamous epithelium of the distal oesophagus is replaced by metaplastic columnar epithelium<sup>53-55</sup>. BM is the most significant risk factor for the development of OAC with a relative risk of 30-120 compared to BM free subjects<sup>55-58</sup>. Dysplasia in BM, particularly high grade, is considered a precursor for invasive OAC<sup>59,60</sup>.

BM is likely to represent a tissue response to the chronic reflux of acidified bile into the oesophagus<sup>55</sup>. GORD affects 40% of adults in the United States and BM is thought to develop in 5-20% of patients with chronic GORD<sup>61,62</sup>. Despite the high prevalence of BM, the absolute risk of developing invasive OAC on an individual basis is minimal. Estimates of cancer risk in BM are variable, ranging from 0.5-1% of patients with BM per year<sup>63-65</sup>. Recent meta-analysis of larger longitudinal studies placed the risk for progression to OAC at 0.5% per year<sup>66</sup>. Publication bias may play a role in over estimating the incidence of BM, favouring small studies with a tendency to over estimate cancer risk<sup>66</sup>. The relationship between severity and longevity of GORD symptoms, compared to OAC risk, has been characterised by a series of case-control studies<sup>55,67,68</sup>. Severe and prolonged GORD symptoms (>20 years) produced an odds ratio of 43.5 for developing OAC, compared to a cohort with short-term minor symptoms<sup>55</sup>. No association between GORD and SCC risk has been noted<sup>55</sup>. Despite the association between GORD and developing OAC, a lack of symptoms does not eliminate the risk of developing OAC with as many as 40% of cases presenting with no appreciable history of GORD<sup>55</sup>. Endoscopic surveillance of patients with BM is recommended with the intention to identify early and potentially curable cancers<sup>60,69</sup>. However, the very low absolute risk of developing OAC brings into

question the value, cost effectiveness and timing interval of sequential endoscopies<sup>60,70</sup>. Furthermore, observer variation in histological diagnosis and sampling bias compound the difficulty in assessing the risk of progression to invasive OAC<sup>71</sup>.

### **1.5 Barrett's metaplasia – dysplasia – adenocarcinoma sequence**

The molecular evolution of BM to OAC is similar to the well established paradigm of the colorectal adenoma-carcinoma sequence<sup>72,73</sup>. A progressive alteration from benign BM, through stages of dysplasia and ultimately Barrett's associated OAC can be observed<sup>74</sup>. The degree of dysplasia is proportional to the risk of malignant transformation<sup>74</sup>. Subjects with benign BM (non-dysplastic) and low grade dysplasia (LGD) have minimal risk of malignant progression, whereas those with high grade dysplasia (HGD) experience disease progression of up to 10% per annum<sup>58,60,74</sup>. Data on disease progression is compromised by random sampling biopsy techniques that leave the majority of mucosa unsampled and therefore the potential for small foci or mosaic areas of more advanced dysplasia to remain undetected<sup>74</sup>. Indeed, a series of surgical resection specimens demonstrated concurrent undetected OAC in 50% of patients with HGD, adding significantly to the argument that patients with HGD should undergo prophylactic oesophagectomy<sup>75,76</sup>. Furthermore, progression of disease is not necessarily orderly or inexorable<sup>74</sup>. Patients with benign BM may progress to HGD or OAC without LGD and patients with LGD or HGD can regress to a non-dysplastic status<sup>77</sup>. A high degree of inter-observer variation exists in the histological diagnosis of LGD, at least in part accounting

for the apparent ability of benign BM to transform directly to HGD<sup>78</sup>. The histological diagnosis of HGD is consistently far more reliable and reproducible<sup>79</sup>.

Given the relatively high mortality and morbidity associated with oesophagectomy, attempts to identify cases of HGD that will rapidly progress to OAC have been the subject of investigation<sup>76,80</sup>. Features of HGD that herald malignant transformation include increased expression of Ki-67, abnormalities of DNA content or loss of tumour suppressor genes such as p53<sup>60,81</sup>. New treatment modalities including endoscopic mucosal resection and radiofrequency ablation have long term curative potential and may negate the need for radical oesophageal surgery<sup>82-84</sup>.

## **1.6 The molecular and genetic basis for the progression of Barrett's metaplasia to adenocarcinoma**

The replacement of distal oesophageal squamous mucosa with BM and the potential for evolution through dysplasia to invasive OAC is associated with accumulative molecular and genetic aberrations. A generic feature of malignancy is the abrogation or loss of regulatory proteins governing the cell cycle and avoidance of apoptosis<sup>85</sup>. Molecular alterations are described at various stages of OAC tumourigenesis including point mutations, loss of heterozygosity and hypermethylation at multiple tumour suppressor gene loci such as p16, APC, Rb, p27, and k-ras<sup>86</sup>. The origin and pertinent aberrations involved in the BM-dysplasia-OAC sequence are discussed in more detail below.

**1.6.1 Cellular origin of Barrett's metaplasia** The exact origin of the progenitor cells leading to BM is a matter for conjecture. However, BM may arise from the stem cells of

squamous mucosa or associated glandular ducts, which in the presence of an acid milieu, differentiate into unique glandular phenotypes distinct from adjacent gastric mucosa<sup>73,87</sup>. An alternative explanation, using a rodent model of BM, suggests that progenitor cells arise from the bone marrow<sup>74,87,88</sup>. The mechanisms by which these cells differentiate and the factors leading to the propagation of columnar, instead of squamous mucosa, are still largely unknown<sup>74</sup>.

**1.6.2 p16** Loss of cell cycle control at the G<sub>1</sub>/S checkpoint appears to be a critical and early step in the progression of BM<sup>86,89</sup>. G<sub>1</sub>/S transition is modulated by cyclin dependent kinases (CDKs) and cyclin dependent kinase inhibitors (CDKIs)<sup>90</sup>. The p16 gene encodes the CDKI, p16, which acts ultimately to inhibit phosphorylation of the retinoblastoma gene product (pRb) and subsequent G<sub>1</sub>/S progression, by limitation of the CDK 4/6-cyclin D complex<sup>91</sup>. p16 hypermethylation has been demonstrated in 75% of BM and 90% of dysplasia arising within BM and is considered to be integral to pathological progression<sup>92,93</sup>.

**1.6.3 Adenomatous polyposis coli (APC)** APC protein is essential to the control of the canonical oncogenic Wnt signalling pathway where the APC-axin-GSK complex phosphorylates  $\beta$ -catenin, mediating its destruction<sup>94</sup>. Loss of APC function results in an accumulation of nuclear  $\beta$ -catenin, leading to activation of downstream effects including increased expression of the oncogenes c-Myc and cyclin D1<sup>95</sup>. The APC protein also binds to the ends of microtubules that form the spindle apparatus during chromosome segregation<sup>96</sup>. Thus, APC abrogation could mediate chromosomal instability during metaphase<sup>89,96</sup>. In contrast to point mutations that are classically seen in colorectal malignancies, hypermethylation of the promoter region of the APC gene is strongly

associated with silencing of its expression in OAC. APC hypermethylation occurs early in the metaplasia-dysplasia-OAC sequence and has been described in 39% of BM and 92% of OAC resection specimens<sup>97,98</sup>.

**1.6.4 p53** The p53 suppressor protein is involved in multiple central cellular processes, including transcription, DNA repair, genomic stability, cell cycle control and apoptosis<sup>99,100</sup>. The major function of p53 is arresting the cell cycle at the G<sub>1</sub> and G<sub>2</sub> check points, in the presence of DNA damage<sup>101</sup>. If DNA irregularities are not successfully repaired then the cell is destined for apoptosis<sup>101</sup>. p53 is the most commonly mutated gene in human cancers and appears to occur relatively early in the metaplasia-dysplasia-OAC progression with p53 inactivation noted in 60% of BM, 66% of BM associated dysplasia and 88% of OAC<sup>99,102-104</sup>. p53 loss appears to follow abrogation of p16 in almost all resection specimens of OAC and is a major mutation in oesophageal SCC<sup>103,105,106</sup>.

**1.6.5 p27** The CDKI, p27, is a negative regulator of the cell cycle and is highly expressed during the quiescent G<sub>0</sub> and pre-replicative G<sub>1</sub> phases<sup>107</sup>. p27 degradation is required for the cell to enter S phase<sup>107</sup>. Loss of p27 is associated with aggressive behaviour in a variety of tumour types and p27 protein suppression has been observed in 83% of OAC and 50% of BM associated HGD<sup>107,108</sup>. High levels of p27 mRNA expression suggests post-transcriptional modification of the protein in OAC cells<sup>107</sup>.

**1.6.6 Cyclin D1** Cyclin D1 positively regulates transmission of the cell cycle through the G<sub>1</sub>/S interface by promoting CDK4 and CDK6 and inactivating pRb<sup>109-111</sup>. Over expression of this proto-oncogene has been observed in a variety of cancers, including oesophageal SCC<sup>112</sup>. Cyclin D1 is over expressed in 46% of BM biopsies and is associated with a 6-7 fold increase in progression to OAC<sup>113,114</sup>.

**1.6.7 Retinoblastoma gene (Rb)** The Rb gene product (pRb) halts the cell cycle at G<sub>1</sub>/S with a requirement to be phosphorylated to allow progression to S, G<sub>2</sub> and M<sup>115,116</sup>. pRb is also linked to apoptotic pathways mediated by p53<sup>117</sup>. Loss of heterozygosity and expression of the Rb gene are seen in the development of retinoblastoma and several other cancers<sup>115</sup>. The Rb gene locus appears to be aberrant in 36-48% of OAC and has been observed in BM<sup>118-121</sup>.

**1.6.8 K-ras** The K-ras proto-oncogene encodes a highly conserved protein involved with growth and differentiation signal transduction<sup>122</sup>. K-ras mutations have been identified in 40% of BM associated HGD and 30% of OAC<sup>123</sup>. Although thought to be an early event in the development gastrointestinal cancers, K-ras mutations have not been detected in non-dysplastic BM<sup>122-124</sup>.

**1.6.9 Bcl-2** In addition to cellular proliferation, malignant cells can exhibit avoidance of apoptosis. The Bcl-2 oncogene is able to repress a number of apoptotic programs by inhibiting activation of caspases that dismantle the cell through protease activity<sup>125,126</sup>. Weak bcl-2 expression is seen in oesophagitis uncomplicated by BM. However, BM and BM associated LGD exhibit marked bcl-2 over expression (72% and 100% of biopsies) suggesting an early role for bcl-2 deregulation in the BM-dysplasia-carcinoma sequence<sup>127</sup>. Bcl-2 expression in HGD and OAC is much less frequent, indicating that established OAC avoids apoptosis via alternative mechanisms<sup>127</sup>.

**1.6.10 Cell adhesion and interaction in the malignant progression of oesophageal adenocarcinoma** Tumour infiltration and metastatic spread is strongly influenced by the ability to modify adhesions between cells and the supporting extracellular matrix<sup>128</sup>. E-cadherins are calcium dependent transmembrane glycoproteins responsible for cell

adhesion in epithelial tissues<sup>128,129</sup>. Cadherins are anchored to the axin cytoskeleton maintaining cell-cell contact, signal transduction and cell polarity<sup>130</sup>. Loss of E-cadherin aids cell invasion and has been proposed as an important suppressor of malignant activity in numerous cancers<sup>131,132</sup>. Progressive loss of E-cadherin expression has been observed through the BM-dysplasia-OAC sequence and further loss of E-cadherin, in established OAC, is associated with poor differentiation and lymph node metastasis<sup>128,133,134</sup>.

#### **1.6.11 The role of growth factors in the malignant progression of oesophageal**

**adenocarcinoma** Signalling pathways that mediate the normal functions of growth factors are commonly subverted in cancer. OAC is no exception and is associated with a number of growth factor aberrations<sup>135</sup>. Epidermal growth factor receptor (EGFR) activation results in a cascade of cellular responses associated with cell division, proliferation and angiogenesis<sup>135</sup>. EGFR is over expressed in 55% of OAC cases and has been correlated with poor survival<sup>135</sup>. The c-erbB-2 oncogene codes for a transmembrane growth factor receptor with ligands including, Neu-differentiating factor and heregulin<sup>136-138</sup>. Over expression in human cancers is associated with increased risk of metastasis and amplification of the gene has been suggested as an important prognostic marker in OAC<sup>135,139,140</sup>. Over expression of c-erbB-2 occurs in between 16-25% of OAC cases and first appears in the late stages of dysplasia<sup>135,141</sup>.

#### **1.6.12 Immortalisation of cells in the progression of oesophageal adenocarcinoma**

Telomeres are highly conserved specialised structures at the ends of eukaryotic chromosomes that slowly shorten with each round of replication<sup>142</sup>. Telomeric shortening ultimately leads to cell death, limiting proliferation and aiding cell senescence<sup>143</sup>. Telomerase activity confers immortalisation to cells by maintaining telomeric length and

facilitating accumulation of genetic defects<sup>143</sup>. Increasing telomerase activity is widely evident in the progression from BM to invasive OAC<sup>144</sup>.

**1.6.13 Other genes involved in the malignant progression of oesophageal adenocarcinoma** Repeated reflux of acidified bile into the lower oesophagus can promote mucosal oxidative stress and induce transcription of genes associated with malignant progression<sup>55</sup>. Inducible nitric oxide synthase (iNOS) is over expressed in 76% of BM and 80% of OAC biopsies<sup>145</sup>. Nitric oxide is a potent ROS, capable of inducing DNA mutations<sup>146</sup>. BM, when exposed to acidified bile, is known to express the endoperoxidase cyclo-oxygenase-2 (COX2); downstream effects include expression of the apoptosis avoidance oncogene Bcl-2, inhibition of immune surveillance and promotion of angiogenesis<sup>147</sup>.

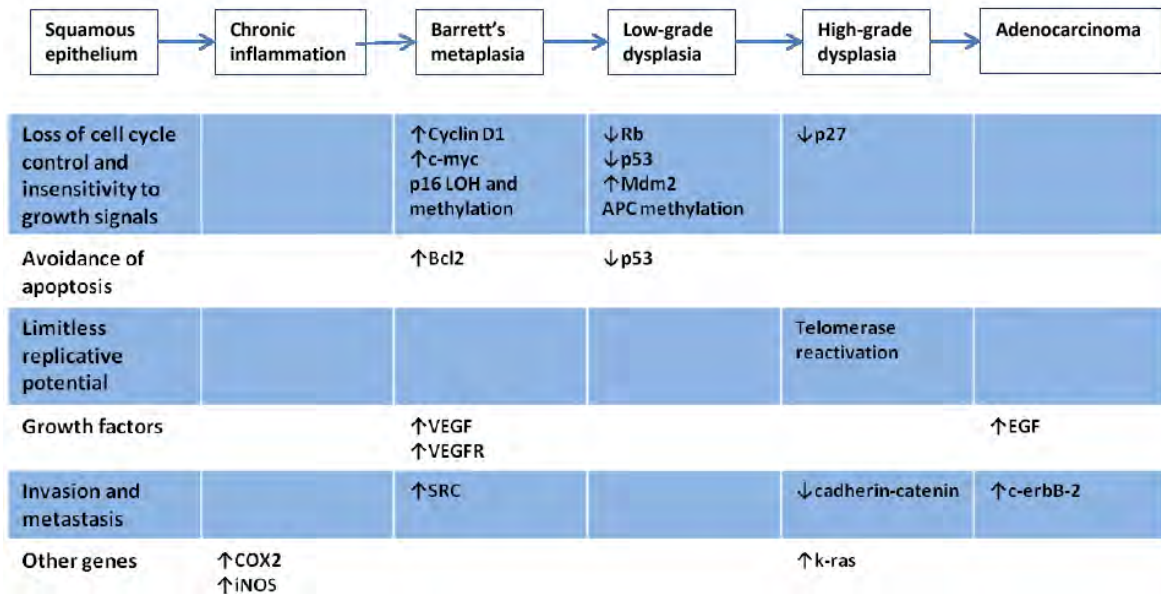


**Figure 1.3 Summary of the genetic basis for progression through the Barrett's Metaplasia-dysplasia-adenocarcinoma sequence**

LOH - loss of heterozygosity; Rb - retinoblastoma gene; Mdm - murine double minute; APC - adenomatous polyposis coli gene; Bcl - B cell lymphoma; VEGF - vascular endothelial growth factor; VEGFR - vascular endothelial growth factor receptor; EGF - epidermal growth factor; COX - cyclooxygenase; iNOS - inducible nitric oxide synthase; k-ras - Kirsten rat sarcoma

Reproduced with the kind permission of Dr JK Roberts, University of Birmingham, UK.

## 1.7 The role of iron in malignant progression of oesophageal adenocarcinoma

The weight of epidemiological and experimental evidence associating iron with cancer incidence and progression is mounting<sup>148-155</sup>. Global variation in the incidence of cancer has been attributed to environmental influences, including dietary preferences<sup>148</sup>. Diets high in red and processed meats have been associated with carcinogenesis at numerous anatomical sites, most thoroughly explored in the case of colorectal adenocarcinoma<sup>148,153,156-162</sup>. The presence of heterocyclic amines, polycyclic aromatic hydrocarbons and *N*-nitroso compounds in consumed meat, created during high temperature cooking methods or preservation techniques, have been extensively evaluated as risk factors for the development of gastric adenocarcinoma and OAC<sup>148,163</sup>. More recently, in a large prospective trial, high red meat consumption, independent of cooking or preservation technique, was associated with OAC and oesophageal SCC<sup>149</sup>. Furthermore, haem and iron derived from dietary meat has been significantly correlated with oesophageal and gastric adenocarcinoma occurrence<sup>164</sup>.

Whole body iron stores slowly accumulate with ageing, as intake gradually exceeds loss<sup>165</sup>. Cohort studies have correlated a replete iron state with increased risk of cancer mortality<sup>151,154,166</sup>. The genetic disorder hereditary haemochromatosis, characterised by excessive gastrointestinal absorption and storage of iron, is strongly associated with hepatocellular carcinoma and other non-hepatic malignancies, including oesophageal and colorectal cancer<sup>152,155</sup>. A randomised trial, allocating patients to regular venesection or control, found a significant correlation between reduced ferritin levels in venesected patients and reduced overall risk of developing visceral malignancy over a 4 year

period<sup>167</sup>. More specifically, increased frequency of blood donation is associated with a decreased incidence of OAC among men with a latency period of 3-7 years<sup>168</sup>.

In addition to epidemiological evidence, animal studies have started to yield experimental evidence implicating iron in OAC carcinogenesis<sup>150,169,170</sup>. Investigators produced a rat model of GORD to explore the association between BM and OAC in humans<sup>150</sup>. GORD was reproduced with a surgical oesophagogastro-duodenal anastomosis, however development of OAC was an infrequent event and the rats developed anaemia<sup>150</sup>. In an attempt to prevent anaemia, intra-peritoneal injections of iron dextran were administered whereupon, it was observed that animals receiving supplementary iron had a very high incidence of BM and OAC (91% and 73%, respectively, at 31 weeks)<sup>170</sup>. Iron supplemented rats demonstrated progressive epithelial cell proliferation, hyperplasia, inflammation and iron deposition in the distal oesophagus, compared to control counterparts<sup>170</sup>. The investigators' resolve further advanced the cause by assigning rats to four experimental arms: non-operated controls +/- iron dextran supplementation; oesophagogastro-duodenal anastomosis +/- supplementary iron dextran<sup>169</sup>. After 40 weeks, the rats were culled. All non-operated controls showed no evidence of BM, dysplasia or OAC. In the surgical GORD models, 53% of non-supplemented rats developed BM compared to 78% of the iron supplemented cohort. OAC was present in 26% and 54% of non-supplemented and iron supplemented GORD models, respectively. Histologically, all tumours were adenocarcinoma and of larger volume in the iron supplemented cohort<sup>169</sup>. Iron deposition and evidence of over expression of oxidative response genes was noted in the distal oesophagus of all rats with oesophagogastro-duodenal reflux but much more marked in the presence of supplementary iron. The investigators concluded

that iron, in the presence of GORD, was driving oxidative stress and initiating metaplasia, dysplasia and invasive adenocarcinoma<sup>169</sup>.

Studies of *ex-vivo* human OAC and associated dysplastic BM, have shown that progression to invasive OAC is associated with increased expression of the iron import proteins, transferrin receptor 1 (TfR1), divalent metal transporter 1 (DMT1) and duodenal cytochrome b (Dcytb)<sup>171</sup>. Protein expression of the iron efflux protein ferroportin (FPN) was paradoxically increased in OAC however; FPN localisation was cytoplasmic, representing functional loss of iron export. These changes were not just confined to late stage disease but evident in the early change of low to high grade Barrett's dysplasia. The authors postulated that over expression of iron transport proteins was unlikely to represent increased luminal iron uptake, rather the acquisition of systemic iron, through TfR1 mediated endocytosis<sup>171</sup>. Gross OAC iron content was significantly raised, compared to associated dysplastic BM, suggesting paradoxical over expression of TfR1 and DMT1 potentially mediated by an aberration of the iron regulatory protein/iron responsive element (IRP-IRE) system, which is responsible for regulating cell iron content and discussed in more detail below<sup>171</sup>. Alternatively, these proteins may have been modulated by other factors that, despite normal IRP-IRE iron sensing, skew the balance towards induced expression<sup>171</sup>. One suggested factor was c-MYC, an oncogene reported to induce TfR1 and iron regulatory protein 2 (IRP2), whilst repressing H-ferritin expression<sup>172,173</sup>. c-MYC expression has previously been demonstrated in BM<sup>174</sup>. Indeed, the authors compared mRNA expression of c-MYC and TfR1 in OAC and found a positive correlation, suggesting c-MYC mediated TfR1 induction rather than an IRE-IRP mediated TfR1 suppression<sup>171</sup>. These observations, mirrored those of earlier work on colorectal

adenocarcinoma where iron transport proteins were up-regulated, promoting paradoxical cancer cell iron loading<sup>175,176</sup>. Furthermore, *in-vitro* culture of OAC cell lines with supplementary iron prompted avid proliferation and significant gross intracellular iron loading compared to control. TfR1 mRNA expression was significantly suppressed and H-ferritin protein levels increased on iron loading in keeping with an IRE-IRP mediated response<sup>171</sup>.

### **1.8 Iron and potential mechanisms underlying carcinogenesis**

Molecular mechanisms underlying the initiation or promotion of carcinogenesis, secondary to systemic and cellular iron loading, are likely to be driven by multiple downstream effects.

Iron is essential for all organisms and is the most abundant metal in humans with the average adult containing approximately 4g<sup>177</sup>. The highly reactive and toxic nature of free iron makes its abundance something of an enigma. However, it is this reactivity that lends iron a vital and diverse biochemical role in: catalysing enzymatic reactions, energy metabolism, oxygen transport and DNA synthesis<sup>178</sup>. Electron transfer is easily accomplished between ferric and ferrous iron and in the presence of oxidative stress, ferrous iron can reduce oxygen to produce superoxide and subsequently, hydroxyl radical formation (Fenton reaction)<sup>178</sup>. Hydroxyl radicals are very potent reactive oxygen species (ROS) with the ability to indiscriminately oxidise nucleic acids, proteins and initiate lipid peroxidation<sup>178,179</sup>. In order to safely access the redox potential of iron, biological

processes require iron to be continuously complexed with protein<sup>180</sup>. *In-vitro* studies, have clearly shown that iron can induce oxidative damage to DNA and furthermore, rat models of GORD suggest that iron mediated oxidative stress is central to oesophageal carcinogenesis; exemplified by marked over expression of oxidative stress responsive genes<sup>169-171,181,182</sup>.

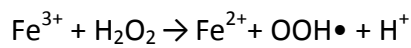


#### **Figure 1.4 The Fenton reactions**

In states of oxidative stress  $\text{Fe}^{2+}$  ferrous and  $\text{Fe}^{3+}$  ferric iron undergo electron transfer generating  $\text{OH}\cdot$  hydroxyl and  $\text{OOH}\cdot$  peroxide free radicals

The antioxidant  $\beta$ -carotene can prevent or even reverse BM and has been epidemiologically associated with decreased risk of OAC<sup>183</sup>. The severity of oesophagitis is positively correlated with evidence of mucosal oxidative stress and most intensely displayed in BM<sup>184</sup>. It has been postulated that supplementary systemic iron, in rats with iatrogenic GORD, leaks via capillary permeability into inflamed tissue and explains the presence of free iron deposition in oesophagitis<sup>181</sup>. Systemic iron, bound to the soluble protein transferrin (Tf) in the serum, may also be endocytosed by macrophages and translocated to areas of inflammation and deposited<sup>185</sup>.

Iron is essential for cellular metabolism and is intrinsic to cell growth and replication<sup>186</sup>. It has long been known that iron plays a crucial role in the conversion of ribonucleotides to deoxyribonucleotides, a rate limiting step in DNA synthesis, catalysed by ribonucleotide reductase (RNR)<sup>187,188</sup>. Recent analysis of cell cycle regulation has implicated iron in the control of numerous checkpoints including, p53, p27<sup>kip1</sup>, cyclin D1 and CDK2<sup>186,189-192</sup>. Iron depletion classically arrests the cell cycle at G<sub>1</sub>/S<sup>193,194</sup>. It follows that a selective advantage is conferred upon cancer cells that are able acquire iron in greater quantities, to drive the cell cycle and enhance proliferation. This is reflected by the overexpression of TfR1, greater up-take of iron from Tf and high expression of RNR in malignant transformation<sup>171,195-197</sup>.

Inorganic iron and haem have both been shown to induce Wnt signalling, a major oncogenic signalling pathway in carcinogenesis<sup>176,198</sup>. Investigators propose a role for iron in the regulation of  $\beta$ -catenin, allowing nuclear accumulation and activation of Wnt target genes, including the oncogene, c-MYC<sup>176</sup>. This phenomenon appeared to be dependent on the background loss of functioning APC, a common finding in gastrointestinal cancers, suggesting that excess iron could exacerbate tumorigenesis<sup>176</sup>. Protein encoded by the c-MYC proto-oncogene is a transcription factor that can activate or repress the expression of target genes. c-MYC has been shown to repress the expression of H-ferritin and stimulate expression of IRP2 and thus increase the intracellular iron pool; whether this is the driver for iron loading in OAC is yet to confirmed<sup>173</sup>. In addition, E-cadherin, a cell adhesion molecule commonly repressed in epithelial carcinogenesis and associated with Wnt signalling, has also been shown to be down-regulated in cellular iron loading, aiding cellular invasion and metastasis<sup>175,199,200</sup>.

## 1.9 Dietary iron

Dietary iron exists in two main forms: inorganic iron, derived from fruit, cereals and vegetables and organic iron, principally derived from meat in the form of haem (ferrous protoporphyrin IX), which is released following digestion of haemoglobin and myoglobin<sup>180</sup>. The amount of iron absorbed from the diet is dependent on the content of inorganic and organic iron, bioavailability and iron status of the consumer<sup>201</sup>. Differences in the bioavailability of iron can lead to a 10-fold variation in iron absorption. Certain dietary constituents such as ascorbic acid can increase absorption, whereas phytate, calcium and polyphenols inhibit bioavailability<sup>201</sup>.

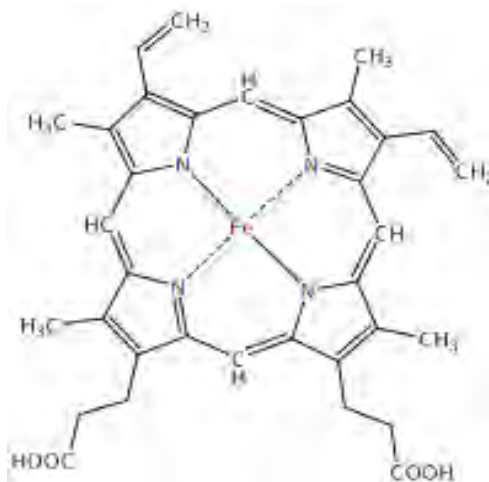


**Figure 1.5 Haem – ferrous protoporphyrin IX**

## 1.10 Absorption, storage and transport of inorganic iron

The absorption of iron occurs almost entirely in the duodenum<sup>202</sup>. Dietary inorganic iron is in the form of ferric iron ( $\text{Fe}^{3+}$ ) complexes and must be reduced to ferrous iron ( $\text{Fe}^{2+}$ ) before active transport across the brush border of the enterocyte<sup>202</sup>. Iron reduction is performed by a brush border surface ferric reductase protein, known as duodenal cytochrome b (Dcytb)<sup>202</sup>. Ferrous iron is then imported, via the divalent metal transporter (DMT1), to be stored bound to ferritin, utilised within the enterocyte or systemically exported via ferroportin (FPN), a basolateral iron transporter<sup>203,204</sup>. FPN mediated export is facilitated by ferroxidase activity of the ceruloplasmin homologue hephaestin; producing ferric iron, in preparation for systemic transport bound to serum transferrin (Tf)<sup>177,205-207</sup>. Serum Tf is secreted by hepatocytes and has two iron binding sites, each capable of binding a single atom of ferric iron<sup>178</sup>. Nearly all inorganic iron is bound to Tf in the circulation, exhibiting a large degree of redundant capacity as only 30% of binding sites are normally occupied (Tf is termed holo or diferric Tf when iron loaded and apo-Tf when unoccupied)<sup>178</sup>. All non-enterocyte cells, requiring iron, express TfR1 which selectively binds diferric Tf<sup>178,208</sup>. The TfR-Tf complex is endocytosed and by a process of endosomal acidification ferric iron is released and the receptor complex re-cycled<sup>209</sup>. Released ferric iron is reduced to ferrous by the ferrireductase, steap3 and transported out of the endosome, via DMT1, to be utilised or stored in the cell bound to ferritin<sup>210,211</sup>.

**1.10.1 Duodenal cytochrome b (Dcytb)** Dcytb is a plasma membrane b-type cytochrome with ferric reductase activity and is highly expressed on the apical border of human duodenal enterocytes adjacent to DMT1<sup>202,212</sup>. Dcytb mRNA and protein levels are up-regulated by several independent stimulators of iron absorption, including chronic

anaemia, iron deficiency and hypoxia<sup>202</sup>. Dcytb mRNA lacks a definable IRE suggesting that iron dependent regulation is via an unconventional mechanism<sup>202</sup>. The physiological role or contribution made by Dcytb to iron absorption is debatable. In murine studies, involving Dcytb silencing, animals did not become iron deficient when fed a balanced diet<sup>213</sup>. It is possible that dietary constituents, such as ascorbate are responsible for ferric iron reduction, marginalising the role of Dcytb<sup>213</sup>.

**1.10.2 Divalent metal transporter 1 (DMT1)** The biological function of DMT1 was determined through phenotypic analysis of the microcytic anaemia (mk) mouse and Belgrade rat; both have spontaneous mutations in DMT1 genes and develop severe impairment of iron transport function<sup>210,214,215</sup>. DMT1 appears to mediate the absorption of numerous divalent metals ( $\text{Fe}^{2+}$ ,  $\text{Zn}^{2+}$ ,  $\text{Mn}^{2+}$ ,  $\text{Co}^{2+}$ ,  $\text{Cd}^{2+}$ ,  $\text{Cu}^{2+}$ ,  $\text{Ni}^{2+}$  and  $\text{Pb}^{2+}$ ), although its prime role is ferrous iron transport<sup>203</sup>. Transcription of the DMT1 gene involves two splice variants at the 5'-end and a further two variants at the 3'-end<sup>216,217</sup>. The 5'-end variants produce DMT1A, found on the apical border of the enterocyte and DMT1B, which is more ubiquitously expressed in the TfR1 endosome where it is responsible for liberating endocytosed iron from Tf<sup>218</sup>. One of the 3'-end untranslated region (UTR) splice variants contains an IRE (DMT1 IRE+ve) that is able to bind IRP and appears to respond to cellular iron levels *in-vitro*<sup>214,219</sup>.

**1.10.3 Ferritin** Ferritins are highly conserved in species from bacteria and plants to man<sup>178</sup>. Human ferritin is a heteropolymer composed of 24 subunits. These subunits, designated H for heavy and L for light (alternatively for heart and liver), have a molecular weight of 21K and 19.5KDa, respectively. Heavy polymers predominate in the heart and striated muscle whereas light ferritin polymers are more abundant in the liver<sup>178</sup>. Despite

the differing contributions, both heavy and light chains are required for normal function; heavy chain knock-out mice die *in-utero*<sup>220</sup>.

The vast majority of ferritin is found in the cytoplasm of cells. If intracellular iron exceeds requirements, ferritin is able to capture and compartmentalise free iron to prevent ROS generation and subsequent cellular damage<sup>178,221</sup>. The internalisation and storage of iron within ferritin is a complex process. Firstly two Fe<sup>2+</sup> ions are bound by H-chain ferroxidase centres and rapidly oxidised forming transient diferric intermediates. The resulting Fe<sup>3+</sup> ions are freed from the ferroxidase and transferred to a nucleation centre on the inner surface of the ferritin shell<sup>222</sup>. Iron mineralisation then occurs to produce polynuclear cores of ferrihydrite (5Fe<sub>2</sub>O<sub>3</sub>)<sup>223</sup>. The exact mechanism of iron liberation from ferritin is poorly understood but may involve lysosomal degradation<sup>224</sup>.

Ferritin mRNA contains a 5'–UTR IRE allowing translational control of ferritin protein by the IRE-IRP system, dependent on intracellular labile iron concentration<sup>225-227</sup>.

**1.10.4 Ferroportin (FPN)** Ferroportin is the sole cellular efflux protein for iron and is principally localised on the basolateral membrane of duodenal enterocytes<sup>204</sup>. FPN is also expressed at other sites of major iron efflux, namely the liver, spleen, placental trophoblast and macrophages<sup>228</sup>. FPN is a highly conserved protein and is essential for maintaining extracellular iron homeostasis; total FPN deficiency is universally lethal *in-utero*, blocking placental iron transport<sup>229</sup>. FPN function is governed by the systemic iron regulatory hormone hepcidin. In high iron states, elevated serum hepcidin levels bind to FPN resulting in phosphorylation, internalisation and degradation<sup>230,231</sup>. In this manner, iron efflux from enterocytes is prohibited, curtailing contribution to the systemic iron pool. Iron efflux is also prevented from the liver and macrophages leading to

sequestration<sup>180,229</sup>. In addition to systemic control by hepcidin, labile iron within the enterocyte can regulate FPN expression at a local level. FPN mRNA contains a 5'-UTR IRE, bringing FPN mRNA translation under control of the IRE-IRP regulatory system. However, the exact interaction of the IRE-IRP system with FPN mRNA is not clear<sup>204,232</sup>.

Iron exporting cells have no significant alternative to the FPN iron efflux pathway, underlining the fundamental role of the hepcidin-FPN interaction in systemic iron homeostasis. The excessively high intestinal iron absorption, characteristic of the haemochromatosis group of diseases, results from inappropriately high FPN activity because of either hepcidin deficiency or FPN mutation, rendering it insensitive to degradation<sup>233,234</sup>. At the other end of the spectrum, haemoglobin production can be impaired as a result of inflammatory cytokine induced hepcidin excess, trapping recycled iron within the liver and macrophages<sup>229,235</sup>.

**1.10.5 Hephaestin** Hephaestin is co-localised on the basolateral border of the enterocyte with FPN<sup>205,236</sup>. Hephaestin was cloned as the defective gene in sex-linked anaemic (sla) mice<sup>237</sup>. The sla mouse develops microcytic anaemia as a result of diminished transfer of iron across the basolateral membrane of the mature enterocyte<sup>237</sup>. Hephaestin has extensive homology with the copper containing serum ferroxidase ceruloplasmin and is thought to assist in the efflux of iron across the basolateral border of enterocytes by oxidising ferrous to ferric iron, ready for systemic transport bound to Tf<sup>206,207</sup>. The regulation of hephaestin appears to be in response to systemic and intracellular iron status by expression of the homeobox transcription factor CDX2<sup>206,238</sup>.

**1.10.6 Transferrin receptor (TfR1) (CD71)** The transferrin receptor is an essential protein involved in cellular iron up-take and regulation of cell growth<sup>209,239</sup>. TfR1 is a transmembrane glycoprotein, existing principally as a homodimer of 90,000 kDa subunits joined by two disulphide bonds<sup>240</sup>. Each monomer consists of a large extracellular C-terminal domain that contains the Tf binding site, a single pass transmembrane domain and an intracellular N-terminal domain that requires glycosylation for receptor functionality<sup>240</sup>.

Diferric Tf binds TfR1, prompting receptor mediated endocytosis and subsequent internalisation of the complex bound by clathrin-coated pits<sup>209</sup>. A reduction in endosomal pH induces a conformational change in Tf, leading to iron release and an increased affinity of apo-Tf for its receptor<sup>241</sup>. The apo-Tf-TfR1 complex is then returned to the cell surface whereupon apo-Tf is released<sup>209</sup>. Ferric iron is reduced to ferrous iron by the actions of steap3<sup>211</sup> and subsequently exported from the endosome via DMT1B<sup>210</sup>. TfR1 expression is principally regulated at the post transcriptional level, in response to intracellular iron status<sup>209,242</sup>. The large 3' UTR of the TfR1 transcript contains 5 IREs which are recognised by both IRP1 and IRP2; without recognition and binding, TfR1 mRNA is degraded, decreasing TfR1 protein expression<sup>242</sup>.

TfR1 is ubiquitously expressed at low levels on many cell types but is especially well represented on cells with a high rate of proliferation such as the basal epidermis<sup>243</sup>. A second transferrin receptor (TfR2) has been identified and displays some homology to TfR1 except in the N-terminal domain<sup>244</sup>. In contrast to TfR1, TfR2 is not regulated in response to intracellular iron levels<sup>209</sup>, being entirely without IREs and its expression is

limited to hepatocytes and small bowel enterocytes<sup>244,245</sup>. TfR2 appears to have a significant role in sensing systemic iron status and control of hepcidin production<sup>246</sup>.

### **Figure 1.6 Iron and haem transport proteins in the human enterocyte**

Dietary inorganic iron (mostly ferric) is reduced by the actions of the ferric reductase Dcytb and reducing agents in the diet to yield  $\text{Fe}^{2+}$  which enters the enterocyte via the divalent metal transporter 1 (DMT1). Haem is transported from the lumen by haem-carrier protein 1 (HCP1) and broken down by haem-oxygenase 1 (HO-1) to liberate  $\text{Fe}^{2+}$  to join the common labile iron pool. Intracellular haem or the by-product of haem metabolism, bilirubin (bil), may be effluxed from the enterocyte back to the lumen by the feline leukaemic virus receptor (FLVCR) or the breast cancer resistance protein (BCRP) to prevent toxicity. If body iron stores are high, iron may be diverted into ferritin to be

stored and lost when the enterocyte is shed at the villous tip. Alternatively, iron passes into the labile iron pool and is subsequently processed for efflux via ferroportin (FPN) as  $\text{Fe}^{2+}$ . Exiting iron is re-oxidised to  $\text{Fe}^{3+}$  through hephaestin (heph) to enable loading on to transferrin (Tf) for systemic distribution. Potential exists for intact haem to be effluxed through the basolateral membrane by FLVCR or BCRP to the systemic circulation. Modified from Sharp and Srai<sup>247</sup>.

### 1.11 Cellular regulation of iron transport and storage proteins

The role of iron in a variety of metabolic processes necessitates that cellular levels are tightly controlled<sup>186</sup>. Cellular iron concentration is elegantly regulated by the interaction between two iron regulatory proteins (IRP1 and IRP2) and iron responsive elements (IREs)<sup>248,249</sup>. IRPs are ubiquitously expressed members of the aconitase gene family and register iron availability mainly through direct interactions with iron in the cytosol<sup>242,249,250</sup>. IREs are highly conserved stem-loop IRP binding structures, found on either the 5' or 3'-UTRs of mRNA encoding proteins involved with iron metabolism<sup>248,250</sup>. The IRP-IRE interaction provides a mechanism for post-transcriptional regulation and subsequent expression of iron transport or storage proteins<sup>250</sup>. In iron depleted cells, IRPs bind to IREs, either repressing mRNA translation or stabilising mRNA to prolong its half-life<sup>242,250</sup>. IRP binding to a 3'-UTR promotes mRNA translation by stabilisation whereas, 5'-UTR binding marks mRNA for degradation, preventing translation<sup>248,250</sup>. DMT1 and TfR1 exhibit 3'-UTR IREs, increasing protein expression and iron influx, during low iron states. In contrast, ferritin and FPN have 5'-UTR IREs reducing storage capacity and preventing iron efflux<sup>248,250</sup>. Although IRP1 and IRP2 are similar in structure, IRP2 regulation appears to be post translational, mediated by proteasomal degradation<sup>251</sup>. In addition, the relative contribution of IRP1 and IRP2 to cellular iron homeostasis varies. Under normal levels of oxygen tension, IRP2 is the principal protein to bind mRNA; IRP1 is dominant during conditions of oxidative stress<sup>252</sup>.

### **Figure 1.7 The IRE-IRP regulatory system**

Proteins involved in iron storage, iron transport, erythroid haem synthesis and TCA cycle are regulated by the interaction of IRPs with IREs. The binding of IRPs to a single IRE in the 5' –UTR region of mRNA blocks translation, whereas, IRP binding to multiple IREs in the 3' –UTR region stabilises TfR1 mRNA and increases protein expression.

IRP: iron regulatory protein; IRE: iron-responsive element; TCA: tri-carboxylic acid.

Adapted from Hentze et al<sup>253</sup>.

## 1.12 Systemic regulation of iron

A stable systemic iron state is required for normal biochemical function and avoidance of toxicity. Systemic iron homeostasis can be achieved by control of three major iron fluxes: absorption of dietary iron; regulation of iron storage (principally in the liver); and recycling of senescent erythrocytes by macrophages<sup>233</sup>. There is no excretory pathway for iron apart from the small, theoretical loss of iron sequestered in enterocytes which are lost to the bowel lumen during mucosal regeneration<sup>233,254</sup>.

### Figure 1.8 Homeostatic regulation of plasma iron

Ferroportin functions as a hepcidin-regulated valve that controls the efflux of recycled, dietary and stored iron into plasma transferrin.

Adapted from Ganz<sup>233</sup>.

The identification of a master iron regulatory hormone, hepcidin, has been the catalyst to unravelling mammalian iron homeostasis<sup>255</sup>. Hepcidin was discovered by chance during an attempt to knock-out an adjacent gene in murine studies. The mice inexplicably developed systemic iron overload, mimicking the phenotype of hereditary hemochromatosis<sup>256</sup>. Hepcidin is a small polypeptide secreted by hepatocytes, circulated in the serum and excreted in urine<sup>255,257</sup>. An increase in serum hepcidin reduces Tf saturation and conversely, decreased circulating hepcidin, increases Tf saturation<sup>258</sup>. Hepcidin acts by binding to FPN, triggering tyrosine phosphorylation, internalisation and lysosomal degradation<sup>259,260</sup>. Loss of functioning FPN from the basolateral surface of enterocytes blocks the systemic export of dietary iron from the duodenum<sup>258</sup>. Similarly, reticuloendothelial iron, derived mainly from senescent erythrocytes, remains sequestered and unavailable for haemopoiesis<sup>235,258</sup>. Hepcidin is homeostatically regulated by iron, erythropoietic activity and inflammation<sup>261</sup>. Hepcidin production is increased in states of iron excess and suppressed in iron deficiency anaemia<sup>261</sup>. Hepcidin is likely to be regulated by both circulating holo-Tf and intracellular iron stores<sup>261</sup>. The bone morphogenetic protein (BMP) pathway has gained eminence as the critical regulator of hepcidin expression, acting via a common mediator, Smad4, that in turn, up-regulates transcription of HAMP, the gene encoding hepcidin<sup>262</sup>. BMP signalling can be modulated by co-receptors, in particular, hemojuvelin (HJV); a common cause of juvenile hemochromatosis in HJV gene mutations<sup>263</sup>. In addition to the BMP/HJV pathway, other factors are necessary for hepcidin regulation, these include Tfr1, Tfr2 and HFE<sup>261</sup>. Tf bound iron stabilises Tfr2 and causes HFE to displace from Tfr1 and shift to Tfr2<sup>246</sup>. The HFE-Tfr2 complex then interacts with the HJV-BMP receptor (BMPRII) potentiating HAMP transcription and hepcidin secretion<sup>264</sup>. Mutations in Tfr2 and HFE genes can cause adult

onset hemochromatosis<sup>261</sup>. The regulation of hepcidin expression, by erythropoietic activity, is not clearly delineated, however soluble proteins (growth differentiation factor 15) produced by developing erythroblasts in the bone marrow reduce hepcidin production<sup>265</sup>. Hepcidin is decreased by hypoxia, possibly through alterations in the hypoxia-inducible factor (HIF) pathway<sup>266</sup>. Hepcidin synthesis is rapidly increased in infection and inflammation by the production of IL-6. IL-6 is a prominent inducer of hepcidin by a STAT3 dependent process<sup>267</sup>. The sequestration of iron, in the reticuloendothelial system, during infection or inflammation is part of the innate immune system, depriving infecting pathogens of iron required for replication<sup>268</sup>. Indeed, hepcidin was originally described for its antimicrobial properties (*hepatic bactericidal protein*)<sup>231</sup>. In chronic inflammatory processes, hepcidin production is responsible for the associated anaemia of chronic disease<sup>267</sup>.

### **1.13 Absorption, transport and metabolism of haem iron**

Haem and porphyrins have fundamental roles in many cellular processes. Haem is a complex of iron and protoporphyrin IX and is an important co-factor in oxygen transport, iron storage (haemoglobin and myoglobin), mitochondrial electron transport, steroid metabolism and signal transduction<sup>269,270</sup>. Haem iron is the most bio-available form of iron from the gastrointestinal tract and is absorbed with far greater affinity than inorganic iron, contributing significantly to body iron stores<sup>271</sup>. The duodenum is the principle site of dietary haem absorption, aided by the relatively low pH of gastric acid, which prevents haem forming insoluble aggregates<sup>272</sup>. Conventionally, haem was thought

to diffuse across biological membranes due to its lipophilic nature, however it is now appreciated that haem and porphyrins carry anionic side chains that produce a negative charge, inhibiting entry to biological compartments by diffusion alone<sup>273</sup>. Haem is therefore transported into the enterocyte in an active energy dependent manner by the apically located haem carrier protein 1 (HCP1)<sup>274</sup>. HCP1 is also expressed in the liver and proximal tubule of the kidney, potentially to scavenge free haem<sup>275</sup>.

In a similar manner to free iron, haem is capable of inducing ROS formation by the Fenton reaction and is therefore toxic to cells in excessive amounts<sup>270</sup>. Within the enterocyte, haem is degraded to release ferrous iron, biliverdin and carbon monoxide by the action of haem oxygenase 1 (HO1)<sup>276</sup>. Free ferrous iron is then readily incorporated into the inorganic iron regulatory pathway bound to ferritin or exported via FPN<sup>270</sup>. Very little dietary haem is exported from enterocytes intact, although haem efflux pathways have recently been recognised<sup>270</sup>. Haem excretory pathways are currently thought to be protective mechanisms, exporting excess haem to prevent acute toxicity, rather than a process for systemic haem distribution, in a manner analogous to inorganic iron efflux by FPN<sup>270</sup>. Two haem efflux proteins have been reported, namely, Feline leukaemic virus, subgroup C receptor (FLVCR) and breast cancer resistance protein (BCRP)<sup>270</sup>. FLVCR appears to have a major role in protecting developing erythroid cells from haem toxicity during maturation and has since been recognised to be highly expressed in tissues involved in haem trafficking namely, hepatocytes, macrophages and duodenum<sup>270,277</sup>. The regulation of FLVCR expression remains unknown, although could potentially be regulated by a transcription factor that senses intracellular haem concentration<sup>270</sup>. BCRP is abundantly expressed by enterocytes at an apical location; positioned perfectly for

effluxing dietary carcinogens back into the intestinal lumen<sup>278,279</sup>. The exact role and contribution of FLVCR and BRCP to intestinal haem trafficking and regulation is still to be determined.

Mitochondrial iron metabolism is a complex and incompletely understood process. Mitochondria are the principal site of cellular haem synthesis<sup>253,279</sup>. In murine erythroblasts, iron appears to be transported into mitochondria by the transporter mitoferrin<sup>280</sup>. Iron is utilised for haem production which is required to be transported across the mitochondrial membrane for insertion into proteins such as cytochromes<sup>281</sup>. FLVCR, BRCP and the ABC-mitochondrial erythroid transporter (ABC-me) are candidates for exporting this newly synthesised mitochondrial haem into the cytoplasm<sup>273,282,283</sup>.

Erythroid precursors require efficient iron acquisition for adequate haemoglobin (Hb) production. This is achieved primarily through recycling of iron through erythrophagocytosis of senescent erythrocytes and to a lesser degree, dietary iron acquisition<sup>281</sup>. Circulating erythrocytes represent a huge potential source of haem iron and undergo degradation within the liver, spleen and marrow. Iron from phagocytosed erythrocytes is liberated from haem by the action of HO1 and enters the systemic iron pool in an orderly fashion via FPN, to be acquired by erythroid precursors through TfR1 mediated endocytosis<sup>274</sup>. However, approximately 10-20% of erythrocytes are lost to intravascular haemolysis, releasing free Hb into the systemic circulation<sup>284</sup>. Free Hb is ultimately scavenged by the liver, as the principal organ of detoxification, storage and buffering of systemic iron<sup>285</sup>. Free Hb can bind to haptoglobin (Hp), a  $\alpha_2$  acid acute phase glycoprotein produced in the liver and endocytosed, as an Hb-Hp complex, by the Hb scavenger receptor CD163<sup>286</sup>. The endocytosed Hb-Hp complex is broken down to

produce haem, globin and unconjugated bilirubin by hepatocytes or macrophages<sup>287-289</sup>. Free Hb is also oxidised to methaemoglobin, which dissociates to form free haem<sup>285</sup>. The toxic potential of free haem requires it to be protein bound within the circulation. This function is performed by haemopexin, a 60kDa  $\beta$ -globulin also excreted by the liver<sup>290</sup>. Haemopexin is another acute phase reactant and has the highest affinity for haem of all proteins<sup>285,291</sup>. Once bound to haemopexin, the haem-haemopexin complex is endocytosed by a receptor-mediated mechanism, in the liver, akin to the diferric TfR1 mediated up-take of inorganic iron<sup>285,292</sup>. A recent report has identified the human haemopexin receptor as the low-density lipoprotein receptor-related protein LRP1 (CD91) that is highly expressed in the liver<sup>292</sup>. The functional overlap between Hp and haemopexin highlights the importance of haem scavenging to iron homeostasis and the prevention of systemic toxicity<sup>293</sup>.

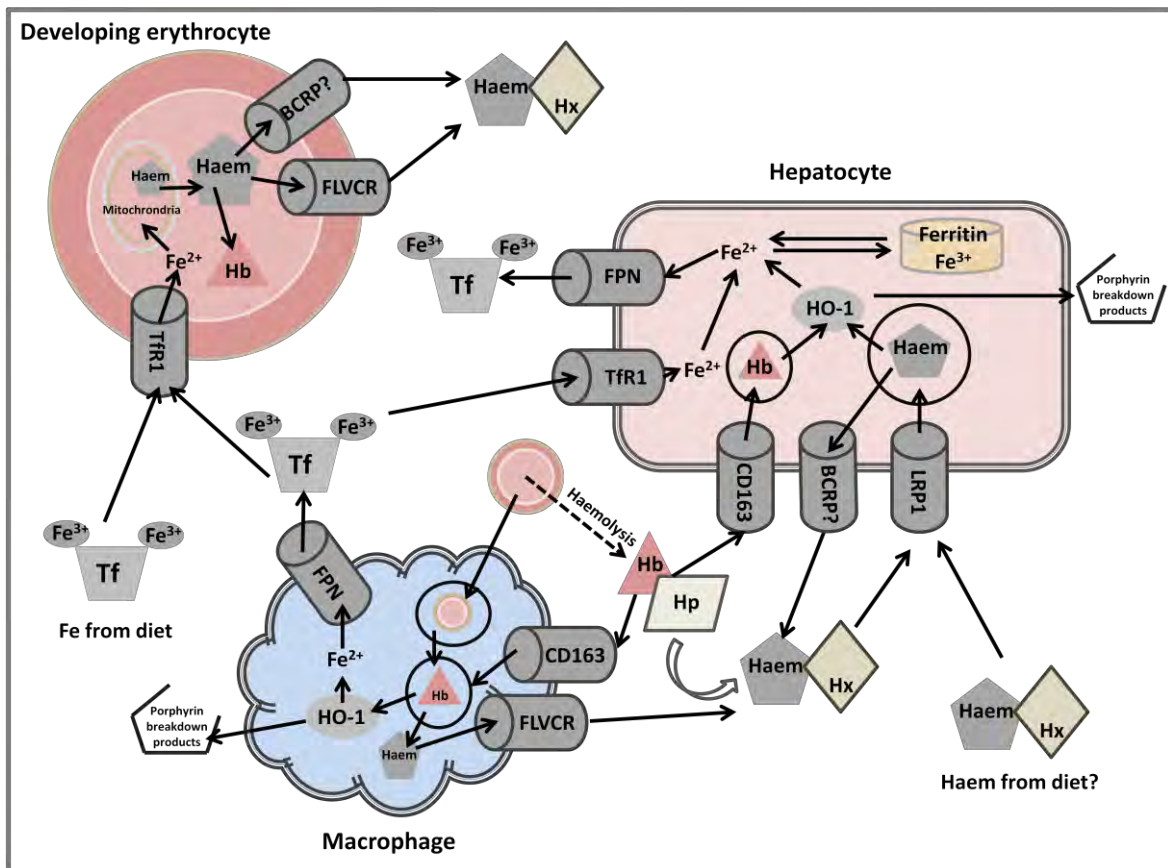


**Figure 1.9 Overview of systemic haem and inorganic iron metabolism**

Haem is trafficked between developing erythrocytes, senescent erythrocytes, hepatocytes and scavenging macrophages. Haem is produced in the mitochondria of developing erythrocytes and incorporated into haemoglobin (Hb) or effluxed to prevent haem toxicity by the feline leukaemic virus receptor (FLVCR) or breast cancer resistance protein (BCRP). Free extracellular haem is rapidly complexed to haemopexin (Hx) to prevent formation of reactive oxygen species. Senescent erythrocytes are either endocytosed directly by macrophages to metabolise Hb or undergo intravascular haemolysis. Free Hb released during haemolysis, is rapidly complexed to haptoglobin (Hp) and scavenged by liver and macrophage expressed haptoglobin receptors (CD163) or oxidised to release free haem which complexes with haemopexin. Haemopexin bound haem is scavenged by low-density lipoprotein receptor related protein (LRP1) expressed

by the liver and metabolised via haem-oxygenase 1 (HO1) to release  $\text{Fe}^{2+}$  that is either exported through ferroportin (FPN) or stored in ferritin.  $\text{Fe}^{2+}$  exported from the liver and macrophages is bound to transferrin (Tf) and joins the circulating pool of transferrin bound iron from the diet that is available to all systemic (non-enterocyte lineages) via transferrin receptor 1 (TfR1) mediated endocytosis. Haem may also be exported from the liver by BCRP and potentially exported intact from enterocytes via the actions of BCRP and FLVCR.

**1.13.1 Haem-carrier protein 1 (HCP1) (SLC46A1)(PCFT/HCP1)** HCP1 was first isolated from a mouse duodenum, utilising suppression subtractive hybridisation<sup>274</sup>. The search for an enterocytes-based protein, capable of transporting haem, was sparked by an earlier observation that haem is imported intact across the enterocyte brush border<sup>294</sup>. HCP1 is highly hydrophobic, contains nine transmembrane domains and has considerable homology to the bacterial metal tetracycline transporters, as members of the major facilitator superfamily<sup>274</sup>. HCP1, when functionally expressed in *Xenopus* oocytes, demonstrates an ability to carry haem in a temperature-dependent and saturable manner<sup>274</sup>. Furthermore, HCP1 dependent import of haem is blocked in the presence of HCP1 antibody and appears specific for the porphyrin ring<sup>274</sup>. HCP1 mRNA expression is strongly regulated by hypoxia and relatively insensitive to changes in iron stores<sup>274,285,295</sup>. However, the protein is post-translationally regulated by redistribution between the apical and cytosolic compartments, depending in iron status; iron deficient mice exhibit apical localisation, and in iron replete states, HCP1 is confined to the cytosolic compartment<sup>274</sup>. The mechanism behind HCP1 distribution is yet to be elucidated<sup>285</sup>.

HCP1 has very recently been described to bind and transport folate, with high affinity, across the duodenal brush border and placenta<sup>296,297</sup>. Patients suffering from hereditary familial folate malabsorption are homozygous for a mutation in the HCP1 gene and the protein has recently been re-named the proton coupled folate transporter/haem carrier protein 1 (PCFT/HCP1)<sup>296</sup>.

### **1.13.2 Low-density lipoprotein receptor related protein (LRP1) (CD91) (Haemopexin**

**receptor)** LRP1 is an extremely diverse protein that consists of five domains: the ligand binding cystein rich repeats; the epidermal growth factor receptor like cystein repeats; YWTD domains; membrane spanning segment and a cytoplasmic tail<sup>298</sup>. It has long been known as a multifunctional scavenger and signalling receptor that recognises a host of different ligands via multiple binding clusters<sup>298</sup>. At least 30 different ligands, drawn from several families of proteins, are represented including lipoproteins, proteinases, bacterial toxins, extracellular matrix proteins and inhibitor complexes<sup>298</sup>. In addition, an increasing number of cytoplasmic proteins have been found to interact with the tail of LRP1 to mediate rapid endocytosis of the receptor<sup>298,299</sup>. LRP1 is highly expressed in the liver and brain, originally suggesting its main role to be related to lipoprotein metabolism, reasoned not solely by location but also by virtue of its ability to bind chylomicron remnants<sup>300</sup> and apoE, which is closely associated with Alzheimer's disease<sup>301</sup>. However, LRP1 appears to have another specific role involving scavenging systemic haem. The haem-haemopexin complex is endocytosed by isolated hepatocytes in a manner similar to TfR1 mediated up-take of inorganic iron<sup>285,291,302</sup>. Extensive ligand affinity studies<sup>292</sup> have identified LRP1 as the responsible protein. LRP1 also exerts effects on certain serine proteinases and metalloproteinases, promoting it as an important regulator of extracellular proteolytic activity with implications for wound repair, tumour invasion and cellular migration<sup>298,303,304</sup>.

Ligand	Ligand function
ApoE	Lipoprotein metabolism and transport
Lipoprotein lipase	
Hepatic lipase	
tPA	Fibrinolysis, signalling function in brain
uPA	Cell migration, wound healing
Factors IXa, VIIIa, VIIa/TFP1	Coagulation
MMP-13 and MMP-9	Angiogenesis and metastasis
Spingolipid activator protein (SAP)	
Pregnancy zone protein	Pan-proteinase inhibitors, infection
$\alpha$ 2M	
Complement C3	Infection
PAI-1	Regulates tPA/uPA activity
C1 inhibitor	Regulates C1r/C1s activity
Antithrombin III	Regulates clotting
TFPI	
Heparin cofactor II	
$\alpha$ 1-antitrypsin	Regulates neutrophil elastase
APP	Role unclear
Thrombospondin 1	TGF- $\beta$ activation, matrix cell interactions
Thrombospondin 2	Collagen assembly, matrix cell interactions
<i>Pseudomonas</i> exotoxin A	
Lactoferrin	Antibacterial
Rhinovirus	
RAP	Chaperone
HSP-96	Chaperone
HIV-Tat protein	Transcriptional activation

**Table 1.1 The numerous and diverse ligands associated with LRP1**

List adapted from Hvidberg<sup>292</sup>

**1.13.3 Feline leukaemic virus, subgroup C receptor (FLVCR)** FLVCR was originally identified as the cell surface receptor for feline leukaemic virus which causes fatal erythrocyte aplasia in cats<sup>285,305</sup>. FLVCR was subsequently described in humans to export cytoplasmic haem from developing erythroid cells, protecting them from haem toxicity, acting as a safety valve<sup>273</sup>. FLVCR-null mice lack definitive erythropoiesis and die in mid gestation<sup>277</sup>. FLVCR mediated haem export is time and temperature dependent<sup>273</sup>. Antibody mediated inhibition of FLVCR decreases haem export, impeding maturation and ultimately leading to apoptosis<sup>273</sup>. FLVCR appears to mediate unidirectional haem transport and does not reverse its export function even when intracellular haem levels are depleted<sup>273</sup>. The expression of FLVCR on cell lines derived from hepatocyte and intestinal lineages, where haem biosynthesis or trafficking occurs, adds credence to the hypothesis that FLVCR is instrumental in maintaining haem homeostasis at these sites<sup>273,306</sup>. More recently, FLVCR has been described on the surface of macrophages, facilitating the export of haem derived from ingested senescent erythrocytes<sup>277</sup>. FLVCR is a member of the Major Facilitator Superfamily and shares a degree of structural homology with HCP1<sup>273,307,308</sup>. The regulation of FLVCR expression is yet to be ascertained, however, expression is down-regulated when globin synthesis increases<sup>273</sup>. FLVCR, in a similar manner to BCRP, may act as a supplement for haem regulation by HO1 in the relatively hypoxic conditions found within the bone marrow, especially as the action of HO1 is largely oxygen dependent<sup>285</sup>. Very recently, a further receptor with marked homology to FLVCR1 has been reported. Named FLVCR2, this protein appears to have the potential to import haem *in-vitro*, however, the exact role of FLVCR2 is still to be elucidated<sup>309</sup>.

**1.13.4 Breast cancer resistance protein (BCRP) (ABCG2, MXR and ABCP)** BCRP is a member of the ATP-binding cassette transporter superfamily<sup>310,311</sup>. BCRP is expressed abundantly on the apical membrane of normal intestinal and colonic epithelium<sup>278</sup> where its function is thought to be integral to the efflux of diet derived carcinogens<sup>279,312</sup>. Similarly, BCRP has a role in detoxifying drugs, toxins and metabolites which flux across the hepatic canalicular membranes, proximal renal tubules and placenta<sup>313</sup>. This protective role can be turned to the advantage of malignant cells where membrane-embedded BCRP is able to limit the intracellular concentrations of chemotherapy agents, conferring a degree of chemoresistance<sup>310,314</sup>. A BCRP  $-/-$  murine model provided evidence for the ability of BCRP to efflux protoporphyrins, conferring cellular protection from photosensitivity<sup>282</sup>. Down-regulation of BCRP in colorectal cancer may explain its particular propensity to accumulate phototoxins with subsequent susceptibility to red light induced apoptosis (photodynamic therapy)<sup>312</sup>.

BCRP has only one ABC cassette, in a single peptide of 70 KDa, that consists of six putative transmembrane domains<sup>315</sup>. BCRP has several regulatory elements in its promoter region including a hypoxia response element<sup>316</sup>. BCRP transcription is partly regulated by HIF1 and AKt1, an upstream regulator of HIF1, that can signal BCRP to locate on the plasma membrane<sup>316</sup>. The regulation of BCRP expression by HIF and its ability to transport haem under hypoxic conditions, confers cellular survival benefit during hypoxic stress<sup>285,317</sup>. The action of BCRP probably reduces the generation of ROS by haem and also prevents mitochondrial damage leading to apoptosis<sup>285,318</sup>.

### 1.14 Iron chelation as a potential anti-neoplastic therapeutic modality

Iron is essential for cellular metabolism, participating in a wide variety of cellular functions such as electron transport, energy metabolism, DNA synthesis and modulation of the molecules involved in cell cycle regulation<sup>191,319-322</sup>. Rapidly proliferating cancer cells are particularly susceptible to iron deprivation; in part due to the expression of the iron dependent enzyme RNR, promoting iron chelation as an attractive potential anti-neoplastic treatment strategy<sup>319,322-324</sup>. RNR is essential for the conversion of ribonucleotides into deoxyribonucleotides and represents a rate limiting step in DNA synthesis<sup>322</sup>. RNR consists of two subunits: an R1 subunit tasked with binding ribonucleotides and allosteric effectors and an R2 subunit, containing a tyrosyl radical that is stabilised by iron<sup>187,188,322,325</sup>. Without a constant supply of oxygen and labile iron, RNR rapidly becomes inactivated<sup>322,325</sup>. The overall result is a change in the expression of cyclins and CDK proteins, essential for cell cycle progression, causing cell arrest in G<sub>1</sub>/S phase and apoptosis<sup>319</sup>. The RNR inhibitor hydroxyurea (HU) has long been used in clinical practice as an agent for treating chronic myelocytic leukemia, although limited by a short biological half life and poor affinity to RNR, HU demonstrates the clinical effectiveness of RNR inhibition in malignant disorders<sup>325-327</sup>. Akin to all chemotherapeutic agents, clinical use of iron chelators as anti-neoplastic agents depends on at least some selectivity for inhibiting neoplastic cells, compared to benign parental lineages<sup>323,325,328</sup>. Indeed, the differences in iron metabolism between normal and neoplastic cells are quantitative rather than qualitative; comparison of a number of key enzymes shows RNR to have the greatest increase in activity between neoplastic and benign tissue<sup>325,329,330</sup>. Although, malignancy specific iron dependent pathways must exist; iron chelators have

been shown to inhibit the canonical Wnt/ $\beta$ -catenin oncogenic pathway in colorectal adenocarcinoma lineages, in an iron dependent manner<sup>331</sup>. A number of therapeutic strategies, based on iron deprivation, have been attempted including dietary iron restriction, anti-TfR1 antibodies and various iron chelating compounds<sup>319,323,325,332</sup>. Iron chelators alter cellular iron homeostasis either by preventing iron acquisition or if lipid soluble, binding the intracellular labile iron pool<sup>322,333</sup>. Broadly, iron chelators can be divided into three categories: naturally occurring iron chelators; clinically established chelators and experimental agents.

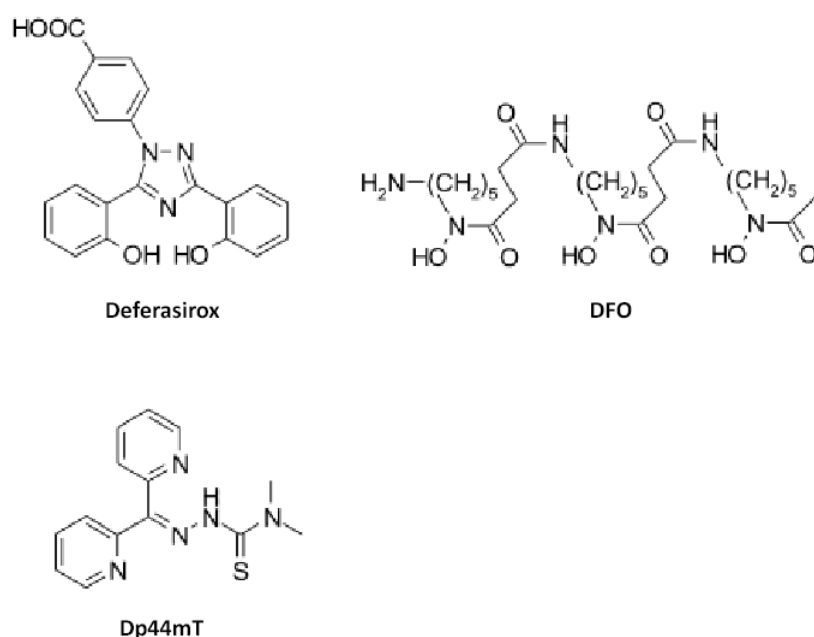


**Figure 1.10 Molecular structures of iron chelators Deferasirox, DFO and Dp44mT**

### 1.15 Naturally occurring chelators

Epidemiological evidence has long been established for the inverse relationship between dietary fibre intake and colorectal carcinoma<sup>334-336</sup> and more recently, distal gastric adenocarcinomas<sup>337</sup>. Intuitively, increased dietary fibre increases colonic transit time and limits mucosal exposure to potential dietary carcinogens<sup>338</sup>. Fibre exhibits the ability to bind numerous toxic agents within the gastrointestinal tract<sup>339,340</sup>.

Alginates, derived from seaweeds and brown algae, are another group of organic compounds that bind iron and various heavy metals<sup>341</sup>. Alginates are salts of alginic acid and are composed of linear polysaccharides containing various quantities of 1,4-linked  $\beta$ -D-mannuronic and  $\alpha$ -L-gluronic acid residues, arranged in irregular blocks along the chain<sup>342</sup>. Alginate, derived from *Sargassum Fluitans*, binds 0.99 mmolFe<sup>2+</sup>/g and sequesters 66 atoms of Fe<sup>3+</sup> per chain<sup>343,344</sup>. In the gastrointestinal tract, alginate binds iron rendering it unavailable for absorption<sup>345</sup>. In a study of ileostomy patients receiving supplemental oral alginate, iron excreted via the ileostomy, was greater than the oral intake at +12  $\mu$ M Fe compared to control (no alginate) at -8  $\mu$ M Fe<sup>345</sup>. Epidemiological evidence, mainly from Japan, associates a high intake of dietary seaweed with decreased incidence of various tumours including colorectal adenocarcinoma, oesophageal SCC and breast cancer<sup>346-348</sup>. Seaweed extracts have also been demonstrated *in-vitro* to induce apoptosis in gastric carcinoma derived cell lines and induce chemo-sensitivity in human malignant lymphoid cells to etoposide<sup>349,350</sup>.

Phytic acid is a major component of cereals and pulses<sup>351</sup> with the ability to bind and maintain iron in the Fe<sup>3+</sup> state, preventing the creation of destructive ROS for seed preservation<sup>352</sup>. In a rat model, additional dietary phytic acid decreased colonic cell

proliferation and in those exposed to the carcinogen, azoxymethane, supplementary phytic acid significantly reduced tumour burden<sup>353,354</sup>. Most pertinently, induced colorectal carcinogenesis in a rat model, using 1,2 dimethylhydrazine, was significantly augmented by supplementary iron and then subsequently suppressed with the addition of phytic acid<sup>355</sup>.

### **1.16 Clinically established iron chelators**

Iron chelators have been used for many years in the treatment of iron overload disorders. The clinically established iron chelators Desferrioxamine and Deferasirox are hereby discussed with reference to potential anti-neoplastic activity.

**1.16.1 Desferrioxamine (DFO)** Desferrioxamine is the archetypal iron chelator used in clinical practice for the treatment of iron overload diseases, such as  $\beta$ -thalassemia, for over thirty years. DFO is a hexadentate siderophore, produced by *Streptomyces Pilosus*, that has a very high affinity for  $\text{Fe}^{3+}$ , resulting in a stable 1:1 complex. Once bound, iron is metabolically inactive and does not produce ROS<sup>325,356</sup>. Although clinically effective at promoting iron excretion, DFO is orally inactive and requires administration by a long subcutaneous/parenteral infusion (12-24 hours/day, 5-6 days/week) due to a short plasma half life so long term compliance with treatment is challenging<sup>357</sup>. DFO exhibits relatively low lipophilicity and therefore has limited access to intracellular iron pools<sup>358</sup>. Despite the disadvantages of DFO, it has been shown to have marked anti-proliferative activity in a number of cellular *in-vitro* studies, animal models and some therapeutic effect in clinical trials<sup>325,328,359-362</sup>. DFO has a potent cytotoxic effect on neuroblastoma

cells whilst exerting very little effect on normal benign cell lines, suggesting a heightened sensitivity to iron deprivation in malignant cells, compared to benign parent tissue<sup>325,360,361</sup>. Furthermore, bone marrow cells, as a classical model of rapidly dividing benign tissue, were quantified as being ten-fold less sensitive to DFO than neuroblastoma cells<sup>360</sup>. Breast cancer cells incubated with DFO exhibit reduced proliferation and increased apoptosis<sup>362</sup> and in a Fisher rat model of breast cancer, DFO significantly inhibited xenograft growth<sup>363</sup>. In further examples of the therapeutic action of DFO in animal models, DFO treatment induced significant regression in hepatocellular carcinoma xenografts and prolonged the life of mice with L1210 leukemia<sup>325,364</sup>. More pertinently, within the clinical setting, administration of a five day course of DFO, delivered as an 8 hour IV infusion at 150 mg/Kg/day, resulted in a very prompt 50% reduction in malignant bone marrow infiltration in seven of nine participants with advanced neuroblastoma<sup>365</sup>. In the same trial, a single patient demonstrated a 48% reduction in tumour burden and encouragingly, in marked contrast to conventional chemotherapy, no toxic side effects were recorded<sup>365</sup>. Following on from this success, when DFO therapy was combined with standard cytotoxic drugs in the treatment of patients with stage III or IV neuroblastoma, objective responses were observed in 12 of 13 patients<sup>366</sup>. Expanded further, combination therapy with DFO in a large cohort of some 57 patients with neuroblastoma resulted in 24 complete responses, 5 very good responses, 21 partial, 3 minor and 4 had progressive disease<sup>367</sup>. It must be stressed, however, that these clinical trials had a single arm with no controls. Limited *in-vitro* evidence exists to suggest that DFO has a synergistic effect on neuroblastoma cell viability in combination with doxorubicin<sup>368</sup>. Haematological malignancies also appear to be sensitive to DFO exposure with numerous reports of marked improvements in the haematological profiles of patients with a broad

spectrum of highly proliferative malignancies: a neonate with refractory lymphoid leukaemia responded to DFO with blast cell reduction and several fold increase in haematological progenitor cells<sup>369</sup>. Combined with low dose cytosine arabinoside, DFO caused significant leukaemic cyto-reduction<sup>369</sup> and DFO administration to a patient in a chronic blast crisis induced a major reduction in circulating blast count<sup>370</sup>.

DFO arrests cells in the G<sub>1</sub>/S phase of the cell cycle<sup>189,194,371</sup>. The action of DFO on the cell cycle is complex but appears to be mediated by a decrease in the hyperphosphorylated form of pRb via suppression of cyclins D1, D2 and D3 which bind with CDK 4 to phosphorylate pRb<sup>189</sup>. In addition, cyclins A and B1 are also decreased in contrast to the action of the RNR inhibitor hydroxyurea, which increased the expression of all cyclins, suggesting that DFO does not directly inhibit RNR<sup>189</sup>.

#### **1.16.2 Deferasirox (Exjade® / ICL670, Novartis Pharma AG, Basel, Switzerland)**

Deferasirox is a recently licensed once-daily, oral iron chelator approved for the treatment of transfusional iron overload<sup>372,373</sup>. Deferasirox is a hydroxyphenyl-triazole class of tridentate chelator; two molecules are required to form a stable complex with each iron (Fe<sup>3+</sup>) atom. The active molecule (ICL670) is highly lipophilic and 99% albumin bound. Deferasirox has a high and specific affinity for Fe<sup>3+</sup> (approximately 14 and 21 times greater than its affinity for copper [Cu<sup>2+</sup>] and zinc [Zn<sup>2+</sup>], respectively)<sup>372,374</sup>. The long half-life means that Deferasirox can be taken once daily (standard dose of 20–30 mg/kg/day) and the oral formulation confers ease-of-use ideal for self-administration at home (Novartis Pharmaceuticals Corporation; Deferasirox Prescribing information).

*In-vivo* animal pharmacokinetic studies demonstrate that Deferasirox is rapidly absorbed and can efficiently and selectively mobilise iron from various organ systems including hepatocytes and cardiomyocytes<sup>374,375</sup>. The main metabolic pathway for Deferasirox is glucuronidation with subsequent biliary excretion. Consequently, Deferasirox and metabolites are primarily excreted in the faeces with a remainder eliminated by renal filtration (Novartis Pharmaceuticals Corporation 2009).

The impact of oral Deferasirox on normal iron absorption was evaluated in a rat model and no appreciable impairment of homeostatic mechanisms of dietary iron uptake was demonstrated<sup>374,375</sup>. Deferasirox was generally well tolerated across a wide range of doses in toxicology studies with no data prohibiting administration to humans.

Phase 1 clinical trials for use in iron overloaded individuals showed that the serum concentration of Deferasirox is proportional to the dose administered<sup>376</sup>. Unbound Deferasirox had a mean half-life of 11–19 hours, supporting the once-daily dosing regimen used throughout the clinical trial programme<sup>376</sup>. Deferasirox plasma levels were also shown to be maintained within a therapeutic range over a 24-hour period (20 mg/kg/day: peak levels ~60–100µmol/L, trough levels ~15–20µmol/L), providing constant chelation activity<sup>377</sup>.

**Figure 1.11 Mean plasma concentrations (+ SD) of Deferasirox are proportional to dose**

Adapted from Raffin et al<sup>376</sup>.

The proof of concept for Deferasirox in humans was achieved by a dose escalation study in patients with  $\beta$ -thalassemia and transfusional iron overload that demonstrated a chelation efficiency of up to 20.5%,<sup>377</sup> establishing an effective dose between 20–30 mg/kg/day. Data from subsequent phase II and III comparative studies in transfusion dependent  $\beta$ -thalassemia patients, provided evidence that Deferasirox efficacy is comparable with DFO<sup>378,379</sup>.

Deferasirox has been shown to be generally well tolerated in adults and children with a variety of chronic anemias<sup>379</sup>. A total of 652 patients received Deferasirox during core clinical trials; none experienced drug related neutropenia or agranulocytosis, which has been observed during treatment with other chelators<sup>379-381</sup>. The most frequent adverse events reported during chronic treatment with Deferasirox include transient mild to moderate gastrointestinal disturbances and skin rashes. These events rarely required drug discontinuation and many resolved spontaneously<sup>379</sup>. Mild, non-progressive increases in serum creatinine (generally within upper limit of normal) were observed in 34% of patients, although these are not thought to be clinically significant as they were temporary and reversible.

Post marketing experience of Deferasirox has involved very rare cases of renal and liver failure in patients with multiple co-morbidities. In addition, a small number of patients have developed a cytopenia which could be associated with Deferasirox treatment but all had advanced haematological disease (Novartis Pharmaceuticals Corporation; Deferasirox prescribing information).

Over the past few years, encouraged by the antiproliferative effects of other chelators, ease of dosing and apparent lack of serious side effects, the potential cytotoxic effects of Deferasirox have come under scrutiny. Investigations are currently confined to *in-vitro* studies with the exception of a limited number of clinical observational reports involving haematological malignancies<sup>322,382-387</sup>. Deferasirox was found to exhibit a greater *in-vitro* cytotoxic effect on the human hepatoma cell line HUH7 than the hexadentate hydroxyquinoline chelator, O-trensox<sup>387</sup>. Specifically Deferasirox decreased cellular viability, inhibited DNA replication and induced DNA fragmentation. Interestingly, in

contrast to O-trensox and other chelators, Deferasirox induced cell cycle blockade during S phase rather than  $G_1$ <sup>387</sup>. Furthermore, much higher concentrations of Deferasirox were required to induce cytotoxicity in primary hepatocyte cultures compared to hepatoma cells (25 $\mu$ M versus >200 $\mu$ M) suggesting that malignant lines are more sensitive to Deferasirox exposure than benign tissues, an observation previously seen with DFO, Deferiprone and O-trensox<sup>360,384,387</sup>. Deferasirox has also been shown as a potent iron dependent inhibitor of the canonical Wnt/ $\beta$ -catenin oncogenic signalling pathway in colorectal lineages, although the exact mechanism and iron dependent enzymes involved are yet to be elucidated<sup>331</sup>.

Experimental tridentate  $Fe^{3+}$  chelators, structurally similar to Deferasirox (2,6-Bis-hydroxyamino-1,3,5-triazine [BHT family]), were synthesised as potential anti-neoplastic agents<sup>322</sup>. Characteristics of the BHT derived chelators that conferred cytotoxic activity were: strong binding of  $Fe^{3+}$  along with high  $Fe^{3+}/Fe^{2+}$  selectivity resulting in a low redox potential of the formed complex, limiting uncontrolled formation of ROS in normal cells; rigidity of the ligand resulting in size selectivity towards iron binding; and balanced hydrophobicity of the ligand, allowing it to be soluble in aqueous media and retain membrane permeability<sup>322,388,389</sup>. Substantially higher anti-proliferative activity has been achieved with tridentate chelators based on semicarbazone and semithiocarbazone such as Triapine<sup>390-392</sup>, however these agents have a relatively high  $Fe^{2+}/Fe^{3+}$  potential and are capable of redox cycling to produce ROS. The resulting hydroxyl radicals are capable of directly attacking cellular components resulting in DNA damage, lipid peroxidation and protein oxidation<sup>322,333,393</sup>.

The usefulness of iron chelation therapy in transfusion dependent myelodysplastic syndromes is debated but some authors suggest that it may induce a marginal survival benefit<sup>385</sup>. Intriguingly, haematologists noticed that patients treated with Deferasirox developed rapid improvement in haemoglobin levels and in some cases the need for recurrent blood transfusions relented<sup>383,386,394</sup>. Nuclear factor –  $\kappa$ B (NF–  $\kappa$ B) plays a pivotal role in the pathogenesis of myelodysplastic syndromes and haematological malignancies by regulating several fundamental cellular processes such as apoptosis, proliferation, differentiation and tumour migration<sup>382,386</sup>. The possible action of Deferasirox on the NF–  $\kappa$ B pathway was assessed by taking samples of peripheral blood from patients with myelodysplastic disorders and incubating them with 50  $\mu$ M Deferasirox for 18 hours<sup>386</sup>. NF–  $\kappa$ B activity was found to be dramatically reduced in samples showing high basal activity. The addition of ferric hydroxyquinoline during incubation did not reinstate NF–  $\kappa$ B activity suggesting that the effect produced by Deferasirox is independent of chelation induced iron deprivation<sup>386</sup>. In addition, inhibition of the NF–  $\kappa$ B pathway was seen solely with Deferasirox and not alternative chelators, despite the anticipated reduction in ROS. The authors concluded that Deferasirox inhibition of NF–  $\kappa$ B should be further explored given that normal haematological cell lines lack activation of NF–  $\kappa$ B with potential for selective therapy<sup>386</sup>.

Deferasirox appears to induce other changes in cell physiology not seen with other chelators. Human hepatoma cells exhibit a marked reduction in polyamine synthesis, normally highly expressed in rapidly dividing tumour cells, when exposed to Deferasirox, possibly by inhibition of ornithine decarboxylase<sup>387,395</sup>. Deferasirox also appears to have anti-proliferative effects on myeloid leukaemia cells, perhaps due to suppression of

signalling through the mTOR (mammalian target of rapamycin) pathway by enhancing expression of REDD1 (regulated in development and DNA damage response)<sup>396</sup>. The mTOR pathway is known to demonstrate aberrant activity in malignant tissue, culminating in de-regulation of the cell cycle and cellular proliferation<sup>397</sup>.

It would appear that the cytotoxic action of Deferasirox is mediated through a series of oncological pathways and not restricted simply to the action of iron deprivation through chelation. Considering a potential multi-modal therapeutic action, clinical experience and ease of dosing, Deferasirox makes for an attractive chemotherapeutic agent in the treatment of cancer. Yet, *in-vivo* replication of the *in-vitro* anti-neoplastic action of Deferasirox is still to be established. In addition, it is not known if Deferasirox has a chemo-sensitising or synergistic effect when combined with standard chemotherapy regimens; a pertinent consideration, as the clinical role for Deferasirox would be as an adjunct to established combination chemotherapy.

### **1.17 Promising experimental chelators with anti-neoplastic properties (Dp44mT)**

Although the development of Deferasirox has been a huge leap in improving the treatment of patients with iron overload disorders, experimental chelating compounds remain a focus for improvement, especially if the anti-neoplastic effects of these agents can be enhanced. A series of very promising chelating agents has been identified based on a di-2-pyridylketone thiosemicarbazone (DpT) backbone<sup>323,398,399</sup>. The most potent of this series, di-2-pyridylketone-4,4-dimethyl-3-thiosemicarbazone (Dp44mT), showed highly significant cytotoxic *in-vitro* and *in-vivo* activity<sup>323,399</sup>. Extremely low IC50

concentrations (0.005-0.4  $\mu$ M) of Dp44mT were used to inhibit the growth of a panel of malignant human cell lines (DMS-53,SK-N-MC and SK-Mel-28) and subsequent murine xenografts were massively inhibited by intravenous administration of Dp44mT over a seven week period (SK-Mel-28, an aggressive melanoma xenograft, demonstrated just 8% growth in the Dp44mT treated mice compared to control)<sup>323</sup>. Captivatingly, the cytotoxic action of Dp44mT was retained when deployed against cell lines known to be highly resistant to standard chemotherapeutic agents (Etoposide resistant MCF-7/VP - breast cancer; Vinblastine resistant KB-V1; epidermal carcinoma) and in all cases was vastly more cytotoxic than equivalent doses of Doxorubicin and DFO<sup>323</sup>. Furthermore, the action of Dp44mT appears to be independent of p53 status<sup>323</sup>. Dp44mT treatment over four weeks induced minimal murine morbidity with retained organ-to-total-body-weight ratios<sup>323</sup>. Over seven weeks a marginal increase in myocardial weight was noted along with patchy necrosis of the myocardium and early fibrosis<sup>323</sup>. Haematological parameters were unchanged, apart from a slight increase liver weight secondary to hemosiderin deposition, however, intriguingly, myocardial iron concentration was increased and in some cases, tumour iron was up or unchanged compared to control<sup>323</sup>. TfR1 mRNA expression was significantly decreased in the livers of Dp44mT treated mice and conversely, significantly increased in xenograft tissue. This observation led the authors to conjecture that Dp44mT may redistribute iron away from compartments controlling gene or TfR1 expression, and may be driven by up-regulating HIF-1 in response to ROS generation<sup>323</sup>.

The ability of Dp44mT to induce such marked cytotoxicity, without significant systemic or specific xenograft iron stripping, may be explained by a dual mechanism of

action<sup>323,390,398-400</sup>. The DpT series mode of action is not solely dependent on iron chelation as their iron complexes redox cycle generating ROS<sup>323,390,398-400</sup>. In the reduced ferrous form, these complexes can react with molecular oxygen and the resulting ferric complexes may subsequently interact with cellular reductants<sup>401-404</sup>. This circumstance culminates in the catalytic generation of ROS leading to indiscriminate damage to essential biomolecules within the cancer cell<sup>398</sup>. The DpT series analogue, Dp2mT has a hypermethylated and inactive iron binding site which precludes iron chelation and therefore eliminates all cytotoxic activity<sup>399,405</sup>. The DpT series ligands are also strongly lipophilic affording permeability across cellular compartments and access to intracellular iron pools<sup>323,404</sup>.

A further potential anti-neoplastic action of Dp44mT may stem from its ability to up-regulate the iron-responsive, tumour growth and metastasis suppressor NdrG1 (N-myc downstream regulated gene 1); up regulation suppresses tumour growth and inhibits metastatic activity<sup>399,405-408</sup>. *In-vitro* exposure of human pancreatic cancer cells to Dp44mT demonstrated marked increase in expression and phosphorylation of NdrG1, essential for its anti-cancer activities. In addition, Dp44mT increased the expression of the CDK inhibitor p21 and decreased cyclin D1<sup>406,408</sup>.

The DpT series has been further developed to include copper complexes. Copper is able to form complexes with a number of chelating ligands (thiosemicarbazones, imidazoles and phosphines) and has intrinsic anti-neoplastic properties, affected through redox activity<sup>409-411</sup>. Indeed, copper complexes can interact with molecular oxygen, cellular oxidants and reductants, allowing copper to redox cycle between its mono and divalent oxidative states<sup>398,412</sup>. As predicted, Cu-Dp44mT exhibited a marked reduction in cellular

viability in the SK-N-MC cell line (neuroepithelioma cells) and evoked powerful ROS generation in SK-N-MC cells labelled with the fluorescent probe DCF, a method well established for assessing intracellular ROS activity in combination with flow cytometry<sup>398,399,413</sup>. There was a pronounced increase in the redox activity of the Dp44mT 1:1 ligand/Cu complex compared to its 2:1 complex, markedly more than CuCl<sub>2</sub> or ligand alone<sup>400</sup>. Co-incubation with copper chelators, tetrathiomolybdate (TM) and bathocuproine disulfonate (BCS), caused near complete cessation of all ROS generation<sup>400</sup>. Curiously, Dp44mT and its analogues, exhibit selective cytotoxicity against malignant cell lines and spare benign parental lines<sup>323,391,399,400,414</sup>. The reason for this, considering the apparently indiscriminate mode of action, may partly be due to differences in how malignant cells metabolise iron and copper ions and the potential for divalent complexes of the DpT series to act as lipophilic vehicles, facilitating intracellular delivery of the free ligand upon metal dissociation<sup>390,410,415</sup>. Direct comparison of the cytotoxic effect of Dp44mT iron complexes to Dp44mT copper complexes demonstrated marked temporal differences in action. Copper complexes exhibit dramatic cytotoxicity after just 3 hours, whereas, iron complexes have a slightly more tardy effect with maximal activity at 24 hours<sup>415</sup>. Furthermore, DpT chelators prevent <sup>64</sup>Cu mobilisation but markedly induce <sup>59</sup>Fe efflux<sup>415</sup>. <sup>64</sup>Cu[Dp44mT] accumulates within the lysosomal/mitochondrial fraction by the following proposed mechanism: i) the neutral ligand enters the lysosome; ii) the ligand becomes protonated and charged at lysosomal pH (pH5), preventing passage out of the organelle; iii) the charged ligand binds copper in the lysosome; and iv) since the formed copper complex is positively charged it cannot escape the lysosome, accounting for <sup>64</sup>Cu accumulation in this compartment<sup>415</sup>. Ensuing

ROS generation causes lysosomal disruption, redistributing cathepsin D to the cytosol with subsequent cleavage of the pro-apoptotic BH3 protein Bid<sup>415</sup>.

Thus, it is likely that the Dp44mT series delivers selective cytotoxic action via a combined cytotoxic approach: iron chelation, early lysosomal disruption secondary to Dp44mT copper complex induced ROS and late ROS generation via Dp44mT Fe complexes with induction of pro-apoptotic pathways.

### **1.18 Hypothesis**

OAC cells are able to capture haem in a manner analogous to inorganic iron acquisition and abrogation of LRP1 and HCP1 will reverse haem mediated effects on OAC cell phenotype.

Oesophageal cancer cells are sensitive to iron deprivation and iron chelating agents may represent valuable adjuncts in the treatment of oesophageal malignancy.

### 1.19 Aims

1. Characterise the expression of haem import and export proteins in oesophageal adenocarcinoma compared to Barrett's metaplasia and normal oesophageal epithelia
2. Determine the *in-vitro* and *in-vivo* effects of abrogating the expression of haem transport proteins on OAC phenotype and iron transport protein expression
3. Evaluate the potential anti-neoplastic properties of iron chelating agents using *in-vitro* and *in-vivo* models of oesophageal cancer

## CHAPTER 2: MATERIALS AND METHODS

### 2.1 Materials

#### 2.1.1 General, Cell Culture and Molecular Biology Reagents

General, cell culture and molecular biology reagents were obtained from the following sources:

##### **Abbott, Global**

Isoflurane

##### **Abcam, Cambridge UK**

Anti CDC-14A (mouse IgG, clone DCS-291)

##### **Amersham Pharmacia, Amersham, Buckinghamshire**

ECL reagent; Hybond PVDF, Hyperfilm X-ray film, Peroxidase linked secondary antibodies; RPN800 rainbow ladder,

##### **Antec International, Sudbury, UK**

Virkon

##### **Applied biosystems, Cheshire**

96-well optical plate; optical adhesive covers; RNAlater; TaqMan ribosomal RNA control reagent

##### **Appleton Woods, Selly Oak, Birmingham**

All disposable plastic ware

##### **Becton Dickinson (BD), Plymouth UK**

Falcon 5ml round bottom counting tubes; FACS tubes (5ml 12/75mm); BD Matrigel

**Bioline, Humber Road, London, UK**

Competent cells; SensiMix<sup>tm</sup> II qRT-PCR probe kit

**Biological Industries, Kibbutz Beit, Haemek, Israel**

DMEM concentrate x2 without L-Glutamine

**Bio-optica, Milano, Italy**

Tris Buffered Saline, W-CAP TEC Buffer<sup>©</sup>

**Boehringer Mannheim, Lewes, East Sussex**

Ampicillin; Mycoplasma detection Kit

**Cambrex Bio Science Wokingham, Ltd**

ViaLight HS kit (ATP assay)

**Chance Propper, Smethwick, West Midlands**

Glass coverslips

**DAKO UK Ltd, Cambridge, UK**

DAKO Antibody Diluent; DAKO ChemMate substrate buffer; DAKO REAL DAB and Chromogen Kit; DAKO Pen

**Difco, West Moseley, Surrey**

Bactoagar; Bacto Tryptone; Yeast Extract

**Dp44mT and 59Fe-Tf: Kind gift of Professor Des Richardson, University of Sydney,**

**Australia**

**Ecole Polytechnique, Federale De Lausanne**

Lenti Viral packaging plasmids (via Dr Chris Dawson)

**Eurogentec, Seraing, Belgium**

Reverse transcriptase core kit

**Fisher Scientific, Loughborough, Leicestershire**

BCA protein assay

**Frontier Scientific, Logan, UT, USA**

Zinc protoporphyrin

**Geneflow, Southampton**

Acrylamide

**Genus Pharmaceuticals, Newbury, Berkshire**

Ciprofloxacin

**Invitrogen, Paisley, Renfrewshire (incorporating Gibco BRL)**

Dulbecco's Modified Eagles Medium (DMEM) with Glutamax-1, pyridoxine and 4500mg/L glucose; Foetal Calf Serum; Geneticin G418; LTX Reagent; Normal goat serum; Optimem medium; Penicillin and Streptomycin solution; PLUS Reagent; PureLink HiPure Plasmid Filter Purification Kits – Maxi Prep; Puromycin; RPMI medium with 25mM HEPES buffer and L-glutamine; S.O.C media; Trizol reagent; Trypsin EDTA

**Iwaki, Stone, Staffordshire (Subsidiary of Barloworld scientific)**

25, 75 and 150cm<sup>2</sup> tissue culture flasks; 96 well culture plates; 12 well culture plates

**Mayne Pharma**

Desferrioxamine mesilate (DFO) 500mg

**Millipore, Watford, UK**

Hexadimethrene Bromide (Polybrene)

**Novartis, UK**

Deferasirox

**Open Biosystems (Thermo Fisher Scientific) Huntsville, Alabama, US**

pGIPZ lenti-viral constructs

**Pall Corporation, Newquay, Cornwall**

0.2µm filters

**Peptides International, Louisville, Kentucky, USA**

Hepcidin peptide

**Promega, Chilworth Research Centre, Southampton**

Dual-Luciferase Reporter Assay System; Nuclease free water

**Roche Applied Science, Lewes, East Sussex**

BrdU proliferation assay; Proteinase inhibitor cocktail

**Sigma Chemical Company Limited, Poole, Dorset**

Agarose; Ammonium acetate; Ammonium persulphate; Aprotinin; β-mercaptoethanol; Bromophenol Blue; Calcium chloride; Citric acid (tri-sodium citrate); DAB (3,3'-diaminobenzidine tetrahydrochloride) tablets; DAPI (4',6-diaminido-2-phenylindole); Deoxynucleotide (dNTP) mix; Dimethyl Formamide; Dimethyl Sulfoxide (DMSO); Dithiothreitol (DTT); DNase I; Ferric chloride; Ferrous cyanate; Ferrous sulphate; Ferrozine (3-(2-Pyridyl)-5,6-diphenyl-1,2,4-triazine-4,4-disulfonic acid); Formalin; GenElute Mammalian Genomic DNA kit; Glycerol; Glycine; N-[2-Hydroxyethyl]piperazine-n'-[2-ethanesulfonic acid] (HEPES); H2DCF-DA (2,7-dichloro-fluorescein-diacetate); HCl; Hydrogen Peroxide 30% w/v; Hydroquinone (1,4-Benzenediol); Immunofluorescence Mounting Media; LB Broth EZMix powder; Isopropanol; Lauryl sulphate; Lithium Chloride; MgCl<sub>2</sub>; Mayer's Haematoxylin 0.1% Solution; Methanol; MTT (3-(4,5-dimethylthiazol-2-yl)-2,5-diphenyltetrazolium bromide); NP40; Paraformaldehyde; Polyoxyethylenesorbitan monolaurate (Tween 20); Phosphate buffered saline; Potassium Acetate; Potassium Chloride; Pronase from *Streptomyces Griseus*; 1,2-propanediol; Propidium Iodide; RNase A; Sodium Acetate; Sodium Ascorbate; Sodium Bicarbonate; Sodium Bisulfite; Sodium

Carbonate; Sodium Chloride; Sodium Citrate; Sodium Deoxycholate; Sodium dodecyl sulphate (SDS); Sodium Fluoride; Sodium Pyrophosphate; Sucrose; TEMED; Trichloroacetic Acid, Trichostatin A; Tris HCl; Trizma base; Urea; Xylene Cyanol

**Sarstedt Limited, Leicester, UK**

Small and Large Culture Dishes

**TPP, Switzerland**

6-well plates for tissue culture

**Turumo, Europe**

Capijet blood tubes

## 2.1.2 Primary antibodies

Target Antigen	Molecular weight	Source and clone	Antibody class	Positive control	Optimum Dilution
Beta- actin	42kDa	Abcam Ab8226	Mouse IgG anti-human		WB: 1/1000
BCRP	72kDa	Abcam Ab3380	Mouse IgG anti-human	Duodenum	WB: 1/250 IHC- P: 1/100
CDC-45L	83kDa	Abcam ab56476	Mouse IgG anti-human	Hydroxy-urea treatment	WB: 1/300
c-Myc	41kDa	Abcam ab32	Mouse IgG anti-human		WB: 1/500
FLVCR	35kDa	Abcam ab57317	Mouse IgG anti-human	Duodenum	WB: 1/350 IHC-P: 1/250
Ferritin	40kDa dimer, 20kDa subunit	Kind gift of Prof A Mckie	Rabbit IgG anti-human	Liver	WB: 1/500 IHC-P: 1/200
Ferroportin	63kDa	Abcam Ab85370	Rabbit IgG anti-human	Duodenum	WB: 1/300 IHC-P: 1/200
HCP1	55kDa	Abcam ab25134	Rabbit IgG anti-human	Duodenum	WB: 1/500 IHC-P: 1/200
IRP2	105kDa	Abcam ab80339	Rabbit IgG anti-human	Duodenum	WB: 1/500
LRP1	85kDa	Abcam ab28320	Mouse IgG anti-human	Liver	WB: 1/250 IHC-P: 1/150
TfR1	190kDa dimer, 95kDa subunit	Invitrogen 13-6800	Mouse IgG anti-human	Liver	WB : 1/500 IHC-P: 1/250

**Table 2.1 Primary antibodies, origin, class, positive controls and optimum working concentrations**

(WB= Western Blotting; IHC-P= paraffin embedded immunohistochemistry)

### **2.1.3 Secondary Antibodies**

Amersham Pharmacia, Amersham, Buckinghamshire

Peroxidase conjugated anti-mouse IgG (WB: 1:10,000); Peroxidase conjugated anti-rabbit IgG (WB: 1:10,000)

## 2.1.4 Oligonucleotides

The following oligonucleotides were used in qRT-PCR reactions (F=Forward, R=Reverse).

	<b>Probe (5'FAM 3'TAMRA)</b>	<b>Forward Primer, 5'-3'</b>	<b>Reverse Primer, 5'-3'</b>
c-MYC	CAGCACAACACTACGCAGCG CCTCC	TCAAGAGGTGCCACGTC TCC	TCTTGGCAGCAGGATAGTC CTT
Ferritin H	CCAACGAGGTGGCCGAAT CTTCCTT	GGAACATGCTGAGAAA CTGATGAA	CATCACAGTCTGGTTTCTTG ATATCC
Ferroportin	AGGATTGACCAGTTAACC AACATCTTAGCCCC	AGCAAATATGAATGCCA CAATACG-	CAAATGTCATAATCTGGCC AACAG
HCP1	ATG GGT TGC TTT TCC TGT CAT TAG TCA TCA CA	CTA TCA CGC CTC TCA TGT TCA CA	GGA GAG TTT AGC CCG GAT GAC
IRP-2	TTTGACAAACAGAGGCCT TACCCC	AGGAATAGTGCTGCCGC TAAGT	TCGAGCTCCGTAAGAGTTG AATT
LRP1	TGC CAT TTA CTC AGC CCG TTA CGA CG	TGG ATT GAC GCC GGT CAG	CCC GAA GCA CCT CCA TGT
TfR1	AAA GAC AGC GCT CAA AAC TCG GTG ATC ATA G	CGT GAT CAA CAT TTT GTT AAG ATT CA	CCA CAT AAC CCC CAG GAT TCT

Pre-optimised TaqMan® gene expression assays (Applied Biosystems) were utilised for BCRP (Hs00184979\_ml) and FLVCR (Hs0017953\_ml) qrt-PCR reactions.

**Table 2.2 Oligonucleotides**

### **2.1.5 Ex-vivo tissue Samples**

The most suitable control tissue for OAC was considered to be adjacent matched BM from the same patient. For benign BM samples, matched normal squamous (NS) mucosa was used as control tissue.

#### **2.1.5.1 Fresh Material**

Oesophageal cancer resection specimens: Samples (n=9) of OAC matched with normal NS and associated BM (immediately adjacent to the tumour) were collected during surgery, snap frozen and stored in liquid nitrogen.

Biopsy samples: Benign BM samples were obtained as biopsies, taken during endoscopy from patients undergoing endoscopic surveillance of benign BM. Written consent was given prior to the procedure. Samples of BM (n=9) were confirmed as non-dysplastic on histological assessment (PT, Consultant Histopathologist, Queen Elizabeth Hospital Birmingham).

Xenografted human oesophageal cell lines and mouse organs were harvested from immunodeficient mice models divided and snap frozen in liquid nitrogen or placed in formalin.

Duodenal and liver biopsies were obtained to act as positive controls as appropriate.

#### **2.1.5.2 Paraffin Embedded Material**

Paraffin sections of OAC with associated BM and NS present in the same section (n=16) and biopsy specimens of benign BM with normal mucosa in the same section (n=26) were selected for immunohistochemistry. Material was screened by a consultant pathologist to confirm the samples contained the relevant tissue types. Normal liver, small bowel and

kidney sections were utilised as appropriate for positive and negative controls during immunohistochemistry.

#### **2.1.5.3 Tissue microarray (paraffin embedded samples)**

78 samples of OAC were used to evaluate the association between haem import and export protein expression and tumour stage. Data was available on: degree of tumour differentiation (well, moderate or poor, as assessed by the original reporting consultant histopathologist); T stage of the tumour (T1: tumour invades lamina propria or submucosa; T2: tumour invades muscularis propria; T3: tumour invades adventia); and presence or absence of lymph node metastases (positive or negative).

To facilitate the screening of multiple tissue blocks from each patient, tissue microarrays were prepared containing 3 representative samples of tumour per patient (kind gift of Dr J Bury, Sheffield Medical School, Sheffield UK).

#### **2.1.6 Cell lines**

##### **OE33 (JROECL33), OE19 (JROECL19) and OE21 (JROECL21)**

OE33, OE19 and OE21 were derived from primary oesophageal tumours in the late 1990's to establish long-term lines for the investigation of oesophageal malignancy<sup>416</sup>. Genetic analysis indicated aberrant karyotypes; all were grossly aneuploid. HLA-A, B and C were expressed constitutively. All three cell lines were shown to have the ability to form xenografts in athymic nude mice.

### **OE33**

Human oesophageal adenocarcinoma cell line established from an adenocarcinoma of the lower oesophagus (Barrett's metaplasia) of a 73-year-old female patient. The tumour was identified as a pathological stage IIA (UICC) and showed poor differentiation<sup>416</sup>.

### **OE19**

Human adenocarcinoma derived from the gastro-oesophageal junction of a 72-year-old male patient. The tumour was identified as a stage III (UICC) and showed moderate differentiation<sup>416</sup>.

### **OE21**

Human oesophageal squamous carcinoma derived from the mid oesophagus of a 74-year-old male patient. The tumour was identified as pathological stage IIa (UICC) and showed moderate differentiation<sup>416</sup>.

### **293FT cell line** (kind gift of NPC Group – University of Birmingham, UK)

The 293FT cell line is a fast-growing, highly transfectable, clonal isolate derived from human embryonic kidney cells<sup>417</sup>. The cell line has been commercially transformed with the SV40 large T antigen making the 293FT line a particularly suitable host for generating lentiviral constructs containing the SV40 origin such as the pGIPZ vectors<sup>418</sup>. 293FT cells stably express the neomycin resistance gene under control of the SV40 enhancer/promoter and can be maintained in media containing Geneticin® 500µg/ml<sup>419</sup>.

## 2.2 Methods

### 2.2.1 Immunohistochemistry

Archived tissues (originally fixed in 10% (v/v) neutral buffered formalin prior to embedding in paraffin) were sectioned at 5µm intervals and applied to SuperFrost glass slides. Sections were softened at 55°C for 30 minutes prior to being submerged in boiling W-CAP TEC buffer<sup>®</sup> (pH 8) (combined solution for wax capture and antigen retrieval) for 45 minutes. Slides were then rinsed in Tris-buffered saline (TBS) pH 7.6, blotted dry and the section outlined by a hydrophobic delineating pen. Sections were blocked with 50-100µl of 20% (v/v) normal goat serum in antibody diluent (Tris buffer pH 7.2 with 15mM sodium azide) for 30 minutes. Sections were incubated for 1 hour with primary antibody in antibody diluent. Antibody concentrations were pre-optimised (table 2.1). Following three washes, sections were then incubated with EnVision reagent (peroxidase-conjugated dextran coupled with goat antibodies against rabbit and mouse immunoglobulins) for 1 hour. Sections were again washed three times and immunoreactivity visualised using DAB+ chromogen (3,3'-diaminobenzidine tetrahydrochloride) in DAB substrate buffer (1:50) for 10 minutes. The slides were rinsed in TBS, counterstained with 0.1% Mayer's haematoxylin (v/v) for 30 seconds and washed in running tap water for approximately 2 minutes for haematoxylin bluing. Sections were then dehydrated in sequential baths of ethanol and xylene before mounting in Depex. Positive controls comprising sections of tissue known to express the protein of interest were included for each series. In addition, a negative control (omission of primary antibody) was used for each tissue type.

Images were visualised from paraffin sections using a Nikon Eclipse E600 microscope and digital image captured using a Nikon DXM1200F camera (Surrey, UK). Nikon ACT-1 version 2.62 software was used for image acquisition (Surrey, UK).

### **2.2.2 Evaluation of immunoreactivity**

Immunoreactivity was scored on a semi-quantitative basis (observers blinded to tissue and antibody identity) by three independent observers, (SF, KR and CT). Staining intensity was scored as a function of two factors: a scale of 0-3 (0= absent, 3=strong); and percentage of positively stained cells within microscopic view (0= no cells, 1= 1-25%, 2= 26-50%, 3= 51-75% and 4=>76%). The two scores were multiplied to give a total score 0-12 (after Di Martino et al)<sup>420</sup>. Slides were further evaluated by a Consultant Histopathologist (PT) to confirm specific cellular location of immunoreactivity (nuclear, cytoplasmic or membranous).

### **2.2.3 DAB-enhanced Perls' Prussian blue staining**

Dilute mineral acid hydrolysis releases ferric ions from protein bound tissue deposits that, in the presence of ferrocyanide ions, are precipitated as a deep purple blue water insoluble complex (potassium ferric ferrocyanide or Prussian blue).

Paraffin sections were de-waxed using a succession of xylene and ethanol baths (x3 for 5 minutes), washed with dH<sub>2</sub>O and incubated in a 1:1 solution of 4% (v/v) HCl and 4% (w/v) ferrous cyanate for 30 minutes. Sections were then washed in PBS for 5 minutes x 3 and incubated in DAB Solution 50X (diluent - Dako ChemMate substrate buffer) 1:200 for 15 minutes. Sections were further incubated for 15 minutes in DAB 1:50 before washing in

PBS and counter staining with haematoxylin for 30 seconds. Slides were then dehydrated in ethanol before mounting. Images were visualised using a Nikon Eclipse E600 microscope and digital images taken using a Nikon DXM1200F camera (Surrey, UK). Nikon ACT-1 version 2.62 software was used for image acquisition (Surrey, UK).

## **2.2.4 Electrophoresis and Western Blotting**

### **2.2.4.1 Sample Preparation**

Samples were derived from *in-vitro* and *in-vivo* sources: Human frozen tissue, mouse frozen tissue, xenografted human cell lines and *in-vitro* cultured cells.

All samples were kept on ice and lysed into RIPA buffer (1% (v/v) NP40, 0.5% (w/v) sodium deoxycholate, 0.1% (w/v) SDS) containing a cocktail of proprietary protease inhibitors (dissolve 1 tablet of Roche “complete” per 50mls RIPA buffer). Tissue samples were homogenised in RIPA buffer with an UltraTurrax homogeniser and cell cultures washed with ice-cold PBS prior to lysis. All samples were then subject to probe sonication x2 for 10 seconds and mixed using a tube rotator for 20 minutes at 4°C. Each sample was then centrifuged for 20 minutes at 13000g. 20µl of the supernatant was used for protein determination and the remainder added to 3x sample loading buffer (Laemmli loading buffer) (0.0625M Tris HCL pH 6.7, 10% (v/v) glycerol, 2% (w/v) sodium dodecyl sulphate (SDS), 1% (v/v) β-mercaptoethanol and 0.001% (w/v) bromophenol blue) and heated to 100°C for 5 minutes.

#### **2.2.4.2 Cellular fractionation (nuclear protein extraction)**

Cells were cultured in 6-well plates. Cells were trypsinised, washed with PBS and centrifuged to form a pellet at 1000 rpm for 4 minutes. The pellet was re-suspended in 5ml ice-cold buffer A (hypotonic buffer – 10mls: 100µl 1M HEPES, pH 7.9; 15µl 1M MgCl<sub>2</sub>; 40µl 2.5M KCl; 5µl 1M DTT, made up to 10ml with dH<sub>2</sub>O; protease inhibitor cocktail) and kept on ice for 5 minutes. Cells were lysed to release nuclei using a pre-chilled Dounce homogeniser.

Dounced cells were centrifuged at 228g for 5 minutes at 4°C to pellet nuclei and other fragments. The supernatant was retained as the cytoplasmic fraction if required.

The nuclear pellet was then re-suspended in 3ml of S1 (S1 – 0.25M sucrose, 10mM MgCl<sub>2</sub>; 20mls: 1.96ml 2.5M sucrose; 200µl 1M MgCl<sub>2</sub>; made up to 20ml with dH<sub>2</sub>O; protease inhibitor cocktail) layered over a 3ml cushion of S3 (S3 – 0.88M sucrose, 0.5mM MgCl<sub>2</sub>; 20mls: 6.9ml 2.5M sucrose; 10µl 1M MgCl<sub>2</sub>; made up to 20mls with dH<sub>2</sub>O; protease inhibitor cocktail) and centrifuge at 2800g for 10 minutes at 4°C. RIPA buffer was then added to the purified nuclear fraction as per protein extraction protocol.

#### **2.2.4.3 Protein assay technique**

Protein concentration of samples was determined using a bicinchoninic acid (BCA™) protein assay and compared with bovine serum albumin at standard concentrations between 0 and 20mg/ml. 25µl of each standard, along with 1:10 diluted tissue or cell lysates, were aliquoted in triplicate onto a clear flat bottomed 96-well plate. 200µl of BCA™ working reagent (reagent B 1:50 in reagent A) was added to each well and incubated for 30 minutes at 37°C. Absorbance was then measured at 562nm using a Bio-Tek ELx800 absorbance microplate reader. The sample protein concentrations were then derived from a graph of standard concentrations plotted against optical density at 562nm.

#### **2.2.4.5 Protein normalisation**

Results of the BCA protein assay were used to calculate the volume of protein lysate required to load 20 $\mu$ g of protein into each sample well. Uniformity of protein loading was further normalised by expressing the optical band densities of the protein of interest as a ratio of the corresponding  $\beta$ -actin band.  $\beta$ -actin blotting was performed on the same PVDF membrane as the probe of interest after antibody stripping (stripping buffer: 200mM glycine, 3.5mM SDS, 1% Tween 20 (v/v), pH to 2.2). (Membrane stripping protocol: cover membrane in stripping buffer for 5 minutes; repeat; wash twice with PBS and twice with TBS-T for 5 minutes each time; block with 10% (w/v) skimmed milk powder). Band optical densities were derived using a Biorad G800 densitometry reader.

#### **2.2.4.6 SDS-Polyacrylamide Gel Electrophoresis (SDS-PAGE)**

A BioRad Protean-II mini-gel apparatus was used and the appropriate percentage resolving gel poured. The stacking gel was added, combs inserted and wells equilibrated with electrophoresis running buffer (0.192 M glycine, 0.01% (w/v) SDS, 25 mM Tris HCl pH 8.3) prior to use. An aliquot of sample equal to 20 $\mu$ g of protein was loaded into each well. One well contained wide range kaleidoscopic pre-stained standards added (5 $\mu$ l) to calibrate protein molecular weights. Electrophoresis was carried out at 200V until the dye front had descended to the lower border of the gel.

Constituent	Stacking Gel	Separating Gel		
	4%	8%	10%	12.5%
Ammonium Persulphate	30mg	30mg	30mg	30mg
Water	3.7ml	4.8ml	3.5ml	1.9ml
Buffer	5ml 0.2% (w/v) SDS; 0.25M Tris HCl, pH 6.8	10ml 0.2% (w/v) SDS; 0.75M Tris HCl, pH 8.8	10ml 0.2% (w/v) SDS; 0.75M Tris HCl, pH 8.8	10ml 0.2% (w/v) SDS; 0.75M Tris HCl, pH 8.8
30% Acrylamide/ 8% bisacrylamide	1.3ml	5.2ml	6.5ml	8.1ml
TEMED	70µl	70µl	70µl	70µl

**Table 2.3 SDS-PAGE gels**

SDS-Polyacrylamide Resolving Gel Composition

#### **2.2.4.7 Western Blotting: Transfer of SDS-PAGE gels and protein detection**

Proteins separated by SDS-PAGE were wet-transferred directly onto Hybond PVDF membranes pre-soaked in methanol for 1 minute. Transfer was performed at 100V for 1 hour in electrophoresis transfer buffer (48mM Tris HCl; 39mM glycine, 20% (v/v) methanol, 0.0375% (w/v) SDS) with constant cooling from an ice pack within the transfer apparatus.

Following transfer, the PVDF membrane was blocked overnight in 10% (w/v) skimmed milk powder in tris-buffered saline tween (TBST) (10mM Tris-Cl pH 8.0, 150mM NaCl, 0.05% tween-20). The PVDF membrane was incubated with the primary antibody for 1 hour at room temperature. Membranes were then washed in TBST (6 x 5 minutes), incubated with secondary peroxidase conjugated antibody for 30 minutes at room temperature and then washed again in TBST (6 x 5min). The membrane was exposed to ECL reagent, placed on Kodak X-OMAT AR film in a darkroom and developed using an X-OGRAPH X2 automatic developer. Band optical densities were derived using a Biorad G800 densitometry reader.

#### **2.2.5 RNA extraction from frozen tissue and cells**

##### **2.2.5.1 RNA extraction from frozen tissue**

Tissue was thawed on ice and homogenised in 750µl Trizol reagent using a PolyTurrax homogeniser. Samples were incubated for 5 minutes at room temperature to allow complete dissociation of nucleoprotein complexes. 100µl of chloroform was added and vortexed for 15 seconds and then incubated at room temperature for 15 minutes. Samples were then centrifuged at 12,000g for 15 minutes at 4°C and the upper aqueous

phase harvested. RNA was precipitated by addition of 250µl isopropanol and incubated for a further 10 minutes at room temperature. RNA was pelleted by centrifugation at 12,000g at 4°C for 10 minutes and washed with 75% ethanol. The 75% ethanol was then aspirated and the residual volume allowed to evaporate followed by RNA re-suspension in 10µl of nuclease free water. Optical density of the re-suspended RNA was measured at 260nm on a spectrophotometer and the concentration of RNA calculated using the equation 1 OD unit= 40µg/ml RNA. RNA was stored at -80 °C.

#### **2.2.5.2 RNA extraction from cells**

Cells were cultured in 6-well plates as per the experimental protocol. At the end of the experiment the cells were washed twice with filter sterilised PBS. 500µl Trizol reagent was added to cells and left at room temperature for 10 minutes. The subsequent Trizol cell mix was aspirated and processed for RNA extraction.

#### **2.2.5.3 cDNA Generation**

cDNA was synthesized from RNA using a reverse transcription system (Eurogentec). 0.4µg of total RNA was added to nuclease free water to attain a total volume of 8.1µl. 11.9µl of reverse transcription mastermix (4µl 25mM MgCl<sub>2</sub>, 2µl of reverse transcription buffer (10x), 4µl 2.5mM dNTP mix, 1µl random nonamer, 0.4µl RNase inhibitor, 0.5µl EuroScript reverse transcriptase) was then added to each RNA sample to achieve a reaction mix volume of 20µl. Each sample was then subjected to the reverse transcription thermal cycle (BioRad My Cycler<sup>tm</sup> thermal cycler) consisting of: initial step - 10 minutes at 25°C; reverse transcriptase step - 30 minutes at 48°C; inactivation of reverse transcriptase enzyme - 5 minutes at 95°C; finally held at 4°C. The synthesized cDNAs were subsequently diluted with the addition of 16µl nuclease free water and stored at -20°C until required for qRT-PCR.

#### **2.2.5.4 TaqMan quantitative real-time polymerase chain reaction (qRT-PCR)**

The technique of qRT-PCR allows quantification of the amplified product; the amount detected at a certain point of the run is directly related to the initial amount of target in the sample. qRT-PCR is initially an exponential process but eventually reaches a plateau phase when one of the reagents becomes limited. Analysis takes the Ct (cycle number) value at the point when the signal is detected above the background and the amplification is in exponential phase. The more abundant the original template, the quicker this point is reached. In conventional PCR the amplified product is quantified at the conclusion of the reactions. Primers were designed to allow the amplicon to span an mRNA exon/exon boundary for the gene of interest in order to eliminate contamination from genomic DNA. Fluorogenic probes incorporating a 5' reporter dye and a 3' quencher dye were designed to a sequence which lay between the two primer annealing sites, the sequences of these and the primers are given in table 2.2. Cleavage of the probe, through a Taq DNA polymerase, separates the two dyes and permits reporter dye fluorescence. Further probing leads to cleavage with every cycle resulting in an increase in the intensity of the fluorescence which is proportional to amount of amplicon produced.

#### **2.2.5.6 qRT- PCR technique**

1µl of newly synthesised cDNA was loaded in triplicate into an optical 96-well reaction plate. 14µl qRT-PCR mastermix (7.5µl 2x PCR reaction buffer 'SensiMix™' (containing dNTPS, DNA polymerase, MgCl<sub>2</sub>, uracil-N-glycosylase, stabilisers and ROX passive reference), 1.5µl to 3µl of 1.25pM gene specific fluorogenic probe (optimised for volume - listed in table 2.4) 1.5µl of 9pM forward and reverse primers specific for the gene of interest, 0.15µl of 18s forward and reverse primers and 0.075µl 18s probe(18s rRNA control kit), nuclease free water to adjust final volume to 14µl for each reaction well). The

reaction mix for each replicate totalled 15 $\mu$ l. In the case of pre-optimised TaqMan<sup>®</sup> gene expression assays (Applied Biosystems) 1 $\mu$ l of pre-optimised probe was added to the reaction mix in place of separate gene specific probe and primers and subsequent reaction volume difference made up with nuclease free water. Once complete, the optical plate was sealed with an optical adhesive cover and loaded into the Applied Biosystems 7500 Fast Real-Time PCR detection system. The standard reaction protocol consisted of 10 minutes at 95°C, 40 cycles of 10 seconds at 95°C and finally 1 minute at 60°C.

#### **2.2.5.7 Probe optimisation**

Each newly designed and synthesised gene-specific fluorogenic probe required optimisation in order to maximize the acquired fluorescent signal. Using 1 $\mu$ l of positive control cDNA reactions were set up as described above but with varying volumes of 1.25 $\mu$ M probe from 0.5 $\mu$ l up to 4 $\mu$ l, the final volume adjusted to 15 $\mu$ l by varying the nuclease free water volume. Following the same thermal cycle real-time protocol the results were graphically analysed as cycle threshold against volume and the point at which the resultant curve levelled off was taken as the optimal volume for subsequent reactions. All optimised specific probes are listed by volume for each reaction in table 2.4.

#### **2.2.5.7 Real-time PCR analysis**

Samples were analysed using SDS software. Each reaction was associated with a fluorescence threshold during exponential replication. The fluorescence baseline tool was optimally adjusted to reflect a best fit for exponential replication across the sample replicates. The cycle number at which fluorescence reached the adjusted baseline threshold was termed the cycle threshold ( $C_T$ ). This value was used for analysis:  $\delta C_T$  value calculated by subtracting the 18s (internal standard)  $C_T$  number from that of the target gene for each replicate; each  $\delta C_T$  value subtracted from the average control  $\delta C_T$  to give

the  $\delta\delta C_T$ ; fold change calculated by using the equation  $2^{-\delta\delta C_T}$ ; average each sample triplicate and divide by control to obtain the normalised fold change value.

Gene	Optimised Volume ( $\mu$ l)	Reaction
<i>c-myc</i>	3	
<i>H-ferritin</i>	2.5	
<i>Ferroportin</i>	2.5	
<i>HCP1</i>	2.5	
<i>IRP2</i>	1.5	
<i>LRP1</i>	2	
<i>TfR1</i>	2	

Pre-optimised TaqMan<sup>®</sup> gene expression assays (Applied Biosystems) were pre-optimised to 1 $\mu$ l per reaction (BCRP and FLVCR).

**Table 2.4 Volumes of optimised fluorogenic probe used for TaqMan q-RT-PCR reactions**

## **2.2.6 Cell Culture**

### **2.2.6.1 Routine cell culture**

All cell culture procedures were performed in a laminar flow tissue culture cabinet using aseptic technique. Cells were cultured in an incubator at 37°C and 5% CO<sub>2</sub> atmosphere. Cell lines were grown in Dulbecco's Modified Eagles Medium (DMEM) with Glutamax-1, pyridoxine and 4500mg/L glucose supplemented with 10% (v/v) Foetal Calf Serum (FCS), 50U/ml penicillin and 50µg/ml streptomycin. All cell lines utilised for study grew as an adherent monolayer and were passaged at ~90% confluence by aspirating the culture medium, washing in media without FCS and incubating with 6 ml of 0.05% (w/v) trypsin EDTA until cells had detached. 5 ml of culture media was added and cells were disaggregated by trituration and then centrifuged at 250g for 3 minutes. The cell pellet was either re-suspended in culture media and reseeded or was re-suspended in 1 ml of 10% (v/v) dimethyl sulphoxide (DMSO) in FCS and placed in a cryovial for cryopreservation. Vials were kept at -70°C for 3 days before transfer to liquid nitrogen storage. Frozen cells were resurrected by rapid warming of the cryovial in a 37°C water bath and the cells were then washed and suspended in pre-warmed culture media. Cells were then seeded into tissue culture flasks and cultured in the standard manner.

### **2.2.6.2 Iron loading of cells and co-culturing with chelators or chemotherapy agents**

Cells were plated out at  $1 \times 10^5$  cells per ml to achieve an initial 50-60% confluence into 6-well (3ml of media per well) or 96-well plates (100 $\mu$ l per well) depending upon the experiment protocol. Cells became adherent to the plastic over a 12 hour period whereupon the media was replaced with experimental media as follows:

#### **2.2.6.2.1 Iron and haem**

**Inorganic Iron:**  $\text{FeSO}_4$  was dissolved in sterilised  $\text{dH}_2\text{O}$  to achieve a stock solution of 100mM. Stock solution was then added to fresh culture media to achieve a final concentration of 100 $\mu$ M.

**Haem:** Haem stock solution (1.5mM) was prepared by dissolving haem in just enough 0.1M NaOH (typically 0.5ml) to create a solution and then made up to 1.5mM with sterilised  $\text{dH}_2\text{O}$ . Stock solution was then added to fresh media to achieve a final concentration of 50 $\mu$ M.

#### **2.2.6.2.2 Iron chelators and chemotherapeutic agents**

The IC50 concentrations of iron chelators and chemotherapeutic agents were determined by dose titration and cell culture for 48 hours followed by and MTT and BrdU assays for viability and proliferation. The IC50 value of each agent was the concentration that reduced viability and proliferation by 50% compared to control. IC50 values were used in all experiments apart from where a dose response was required.

**Deferrioxamine:** A stock solution of 10mM was established by dissolving DFO powder in  $\text{dH}_2\text{O}$ . Stock solution was added to fresh media to achieve the IC50 concentration of 10 $\mu$ M.

**Deferasirox:** A stock solution of 10mM was achieved by dissolving Deferasirox powder in just enough 0.1M NaOH to create a solution and slowly titrating in media (serum free) to avoid precipitation. A final working concentration at an IC50 value of 20  $\mu$ M was made by adding the appropriate volume for stock solution to fresh media.

**Dp44mT:** A 10mM stock solution was made up in DMSO and kept frozen at -20 C until required. A final IC50 concentration of 1 $\mu$ M was achieved by adding the appropriate amount of stock solution to fresh media. Dp2mT (made up as per Dp44mT) was used as the negative control for Dp44mT.

**Chemotherapy agents:** Concentrated vials of chemotherapy agents for clinical intravenous use were used as stock solutions and added to fresh media to attain the following IC50 concentrations: Cisplatin 8 $\mu$ M, 5-FU 8 $\mu$ M and Epirubicin 1 $\mu$ M.

### **2.2.7 MTT cell viability assay**

The MTT [3-(4,5-dimethylthiazol-2-yl)-2,5-diphenyltetrazolium bromide] assay is used to quantify cellular viability following a period of tissue culture<sup>421</sup>. Metabolically active cells cleave the tetrazolium rings of pale yellow MTT, by the action of mitochondrial dehydrogenase, to form dark blue formazan crystals. Upon subsequent cellular lysis the accumulated formazan crystals are solubilised and the colour proportional to the number of viable cells.

1x10<sup>6</sup> cells/ml were plated and cultured in clear, flat-bottomed 96-well plates under the desired experimental conditions, such that a cellular confluence of approximately 70% was achieved at MTT assay.

MTT was freshly dissolved into sterile x1 PBS at 5mg/ml and further filter sterilised to remove any insoluble particles. 10µl of MTT solution was added to each 100µl of culture media per well of the 96-well plate. The plates were then returned to the incubator for a further 3 hours, after which the media was aspirated and replaced with 100µl of DMSO to dissolve the accumulated formazan crystals. After 30 minutes at room temperature, the plates were placed into a Bio-Tek ELx800 absorbance microplate reader and absorbance read at 490nm. The resulting optical densities were used to calculate percentage viability with respect to control.

#### **2.2.8 BrdU proliferation assay**

The pyrimidine analogue 5-bromo-2'-deoxyuridine (BrdU) is incorporated into cellular DNA in place of thymidine during replication and can therefore be used to quantify cellular proliferation<sup>422</sup>. Incorporated BrdU can be detected by the use of a peroxidase conjugated anti-BrdU antibody followed by a colorimetric reaction involving tetramethylbenzidine (TMB).

Cells were plated and cultured in clear, flat-bottomed 96-well plates under the desired experimental conditions, such that a cellular confluence of approximately 70% was achieved to coincide with the BrdU assay. 10µl of BrdU labelling reagent was added to each well (1:100 dilution of the original 10mM stock with culture medium) including a standard-well containing culture medium alone. Plates were then returned to the incubator for a further 4 hours to allow BrdU incorporation. The media/BrdU solution was gently aspirated and 200µl per well of DNA denaturing solution (FixDenat) added to each well and the plate incubated at room temperature for 30 minutes. The FixDenat solution

denatures DNA and increases access to incorporated BrdU. Aspiration of this solution was then followed by the addition of 100µl per well of anti-BrdU-peroxidase antibody and incubated at room temperature for 90 minutes. This solution was then removed and cells gently washed x3 with 200µl of washing solution provided with the assay kit. The washing solution was finally aspirated and replaced with 100µl per well of substrate solution (TMB) and the plate incubated at room temperature for a further 5-30 minutes. The absorbance of each well was determined at 370nm in a Bio-Tek ELx800 absorbance microplate reader and corrected using blank wells (no cells). The resulting optical densities were used to calculate percentage proliferation with respect to control.

### **2.2.9 Ferrozine assay**

The ferrozine assay has been established for decades to quantify intracellular iron levels. Ferrozine forms a stable, water soluble, magenta complex with divalent iron that is suitable for colorimetric quantification<sup>423</sup>.

Cells were cultured in 6-well plates with appropriate media. After a pre-determined incubation period the monolayer was washed three times with 1 ml x1 PBS. The cells were then trypsinised and the cell slurry transferred to Eppendorfs and centrifuged for 5 minutes at 1200 RPM. The supernatant was aspirated and the cell pellet re-suspended in 100µl HEPES saline (10mM HEPES in 0.9% (w/v) sodium chloride at pH 7.4). 90µl of this suspension was removed and added to 200µl 20% (w/v) trichloroacetic acid in 4% (w/v) sodium pyrophosphate (TCA) (5µl of the remainder was added to 95µl RIPA solution and used for protein quantification. This was boiled for 5 minutes then re-centrifuged for a further 5 minutes at 12000 RPM. 200µl of the supernatant was aspirated and added to

100µl of 0.23M sodium ascorbate, 80µl of 10mM ferrozine and 420µl of 2M sodium acetate. This solution was thoroughly mixed and 200µl aliquots placed in triplicate in a flat-bottomed clear 96-well plate. A blank (HEPES + TCA + reaction mix) and a standard (the same mix with 1µl 10mM FeCl<sub>3</sub> added to make a 12.5µM FeCl<sub>3</sub> solution) were included. The colorimetric change in each sample was measured using a Bio-Tek ELx800 plate reader at 550nm. The absorbance in the blank was used to correct each sample. The concentration of iron in each sample was calculated by multiplying the corrected absorbance of the sample by 12.5 and dividing the product by the corrected absorbance of the standard. The protein concentration (analogous to overall cell number) in each sample was determined, as described in section 2.2.4.3, allowing the iron content of each sample to be expressed as a function of protein content.

#### **2.2.10 Anchorage Independent Growth Assay (colony forming assay)**

A malignant cell phenotype is typically capable of growth which is independent of external signals that may restrain or stimulate division. The anchorage independent growth assay measures independent proliferation of an isolated cell in semi-solid culture media; an *in vitro* assay analogous to the ability to form a metastasis *in vivo*<sup>424</sup>.

To make the base gel, 1% (w/v) agar was autoclaved and then kept in a water bath at 40°C. In a tissue culture hood, an equal volume of solution containing 2xDMEM with 20% FCS was warmed to 37°C. The solutions were mixed to give final concentrations of 0.5% agar, 1xDMEM and 10% FCS. 2ml of base agar was pipetted into 6-well plates, using 3 wells per experimental line. Care was taken to avoid air bubble inclusions. Plates were allowed to cool and kept refrigerated at 4°C until adding the superficial agar.

The superficial gel solution was prepared as described above (substituting 0.7% for 1% agar, giving a final concentration of 0.35%) and kept warm in a water bath at 37°C. Appropriate supplementary reagents were added.

Trypsinised cells were passed through a 50µm cell sieve to prevent clumping and then added to the superficial gel solution at a density of  $0.5 \times 10^4$ /ml. 0.5ml of superficial gel solution was then gently pipetted onto the base gel, ensuring even distribution.

Each well was then imaged at random locations using a Zeiss Axiovert 40 CFL microscope and camera with Axiovision Rel. 4.6 imaging software (N=6 for each well). The 6-well plates were then kept in a humidified incubator at 37°C for 14 days after which imaging was repeated to count the total surface area of the colonies within the captured field of view.

### **2.2.11 Wound healing assay**

The scratch or wound healing assay was designed to study cell migration in vitro<sup>425</sup>. The assay involves observing the cellular migration into a wound that is created in a cell monolayer. Migration of cells under these circumstances is regulated by intercellular interactions and is assessed by capturing images of the wound at the beginning and at regular intervals during cell migration, until closure of the wound<sup>425</sup>.

Cells are cultured in 6-well plates until 100% confluent. Once confluent, the growing medium was aspirated and a wound created in the cell monolayer with a fine pipette tip at 45° to the base. An indelible ink line was drawn on the underside of the plate at 90° to the direction of the wound, for orientation and precise positioning during serial

measurements. The cells were then washed with sterile PBS and control or experimental media added. The wound was then imaged using Zeiss Axiovert 40 CFL microscope at 20x magnification and digital images recorded (N=12, two images per wound over 6 wells) with Axiovision Rel. 4.6 imaging software. The total wound surface was measured as a baseline. Plates were replaced in the incubator and at 12 hourly intervals the wounds were photographed, guided by the ink markers to ensure regional consistency of the wound to be imaged. Measurement continued until the wound had healed.

#### **2.2.12 Fluorescence-activated cell sorting (FACS) with propidium iodide labelling for cell cycle analysis**

Propidium iodide (PI) is an intercalating agent that can be used to stain cellular DNA. The quantifiable fluorescent properties of PI can be correlated with the relative amount of cellular DNA and thus, assessment of cell cycle in a given population of cells (fluorescence-activated cell sorting).

$1 \times 10^6$  cells per ml were seeded into T25 flasks such that a confluence of 70% would be achieved at time of FACS. Cells were cultured with media appropriate to the planned experimental conditions (N=3 for each condition including a control cultured in plain media). At a predetermined time point, the cells were trypsinised and centrifuged at 1500g for 5 minutes. The cell pellet, following media aspiration, was washed by re-suspension in PBS containing 1% FCS (v/v) and then centrifuged at 8000g for 5 minutes. Upon re-suspension, cells were adjusted to  $1 \times 10^6$  cells per 1ml PBS. 1ml of PBS containing cells was then vortexed whilst 1ml of ice cold 95% ethanol (v/v) was added drop wise to

fix the cells. Cell suspensions were then stored at -20°C for at least 30 minutes and up to 2 weeks.

Before preparing the cells for analysis, the following solutions were made up:

*10x PI stock solution (0.5mg/ml)* – 0.5mg PI dissolved in 0.038M sodium citrate (pH 7.0), covered and stored at 4 °C. *10 ml PI working solution (50µg/ml)* - 1ml PI stock solution, 100µl 1M TRIS (pH 7.5), 50µl 1M MgCl<sub>2</sub>, 20µl RNase A (20mg/ml), 8.9ml DEPC H<sub>2</sub>O, covered and stored at 4 °C.

For analysis, cells were centrifuged at 2000g for 5 minutes and the supernatant aspirated. The pellet was washed in PBS and centrifuged at 2000g and the supernatant aspirated for the final time. The pellet was then re-suspended in 500µl PI working solution, transferred to FACS tubes and incubated at 37 °C for 30 minutes in the dark. Cells were then gently vortexed immediately prior to being analysed on a Coulter™ EPICS XL™ analyser and Multicycler for Windows.

### **2.2.13 Intracellular reactive oxygen species assay - 2,7-dichloro-fluorescein-diacetate (H2DCF-DA)**

Intracellular reactive oxygen species (ROS) generation can be assessed using 2, 7-dichloro-fluorescein-diacetate (H2DCF-DA)<sup>398,413</sup>. H2DCF-DA diffuses into cells and is hydrolysed to the non-fluorescent derivative H2DCF, which becomes trapped within the cell. H2DCF becomes highly fluorescent when oxidised by O<sub>2</sub><sup>-</sup>, H<sub>2</sub>O<sub>2</sub> or HO<sup>•</sup>. Cellular fluorescence intensity is directly proportional to intracellular ROS.

Cells were seeded at  $7.5 \times 10^4$  per ml to achieve 30% confluence (2mls in small culture dishes 35x10mm) in triplicate for each experimental condition and incubated for 12 hours.

Standard media were removed and replaced with 2mls of media containing 30nM H2DCF-DA (stock solution 10 $\mu$ M in DMSO). Care was taken to minimise light contamination. The cells were incubated for a further 30 minutes. A background control (no H2DCF-DA) was incubated with standard media alone.

The H2DCF-DA media was aspirated and the cells washed three times with warm PBS. 2mls of standard media containing differing concentrations of iron chelators was added and the cells incubated for a pre-optimised period of time (30 minutes–24 hours). A negative control (H2DCF-DA exposed cells and no chelator) and a positive control (pre-optimised concentrations of H<sub>2</sub>O<sub>2</sub> – usually 25-100 $\mu$ M) were utilised.

The media was removed and transferred to 15ml Falcon tubes and kept on ice. Cells were detached with 2mls 0.05% (w/v) trypsin and added to the corresponding Falcon tube. The tubes were centrifuged at 8000g for 4 minutes and the supernatant aspirated and discarded. The cell pellet was re-suspended in 350 $\mu$ l plain culture media (FCS free) and moved to FACS tubes (5ml 12/75mm) kept on ice. Light contamination was kept to a minimum throughout the experiment. FACS analysis for oxidised H2DCF was performed with a BD FACSCanto™ Flow Cytometer and the data analysed using FLOJO software. Background fluorescence was subtracted from all data and results expressed as a percentage of control.

### **2.2.14 <sup>59</sup>Fe extraction (efflux) with <sup>59</sup>Fe-Tf**

Cells were plated at 70% confluence in small culture dishes (35x10mm) n=3. After 12 hours, culture media was removed and replaced with 1ml of media spiked with <sup>59</sup>Fe-Tf (kind gift of Professor Richardson, University of Sydney, Australia) (stock solution 36.7 mg/ml) at 60µg/ml. Dishes were then incubated at 37°C for 3 hours. The media was removed and disposed of as per safety protocol and the cellular monolayer washed on ice with ice cold PBS three times.

1ml of chelator spiked media was added and incubated at 37°C for a further 3 hours. The culture dishes were placed on ice and media removed and transferred to 5ml counting tubes. 1ml ice cold PBS was added and the monolayer scraped off and transferred with the PBS to empty counting tubes.

Gamma counts were then measured using a Perkin Elmer 2480 automated gamma counter for 5 minutes per tube. Three blank tubes were inserted for background counts.

The averaged background counts were subtracted from the media and cellular fraction counts and the results expressed by the culture media fraction as a percentage of the combined culture media and cellular fractions (i.e. total <sup>59</sup>Fe taken up).

### **2.2.15 Cellular <sup>59</sup>Fe up-take blocking**

Cells were seeded to achieve 70% confluence in small culture dishes and cultured for 12 hours (n=3). Growing media was aspirated and replaced with 0.06 µg/ml <sup>59</sup>Fe-Tf media spiked with differing concentrations of iron chelators. Media with <sup>59</sup>Fe-Tf alone was included as a control. Cells were incubated for a further 3 hours. Radiolabelled media was then aspirated and the cells washed with ice cold PBS three times. Ice-cold Pronase (1mg/ml in plain culture media) was added and cells incubated on ice for a further 30

minutes to ensure removal of membrane bound  $^{59}\text{Fe-Tf}$ . The remaining cell monolayer was then scraped from the dish in 1ml PBS and transferred to 5ml counting tubes.

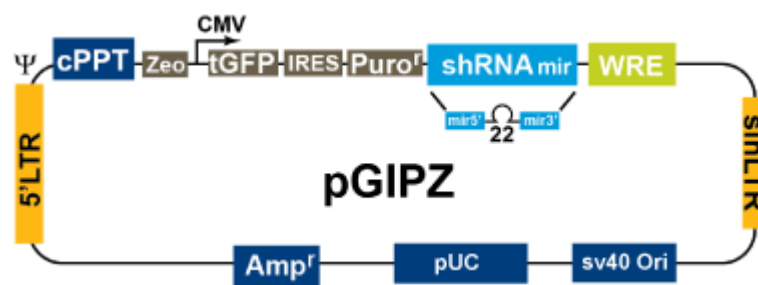
Gamma counts were then measured using a Perkin Elmer 2480 automated gamma counter for 5 minutes per tube. Three blank tubes were inserted for background count estimation and subtracted from the average experimental counts. Results were expressed as a percentage of the control up-take.

## **2.2.16 Stable silencing (knock-down) of LRP1 and HCP1 protein expression by pGIPZ construct bearing lenti-viral preparations**

### **2.2.16.1 RNA interference**

RNA interference (RNAi) inhibits the translation of target mRNA<sup>426,427</sup>. Short hairpin RNA (shRNA) is a method of RNAi that utilises cellular defence mechanisms against viral double stranded (dsRNA) to ultimately cause silencing of a protein of interest by cleavage of its corresponding mRNA to prevent translation<sup>426,427</sup>. shRNAs are transcribed products of plasmid DNA delivered to the cell via the lenti-virus system as part of a pGIPZ construct. The transcribed shRNA nucleotide sequence is specifically created as the antisense sequence to a segment of target mRNA and due to construct design creates a hair-pin looped dsRNA<sup>428</sup>. The RNA endonuclease, Dicer, recognises the dsRNA of shRNA as viral and cleaves it into short interfering RNA (siRNA)<sup>426,427,429</sup>. These siRNA fragments are bound by the RNA induced silencing complex (RISC) where the antisense siRNA strand is used to recognise and bind the corresponding mRNA sequence<sup>430</sup>. Once bound, the mRNA is cleaved by RNase activation preventing translation and protein formation<sup>430</sup>. The pGIPZ construct contains promoters to ensure that shRNA is constitutively expressed to create a

stable knock-down which is passed on to daughter cells. The gene for green fluorescent protein (GFP) is included at the beginning of the pGIPZ construct to allow visual confirmation of gene silencing and antibiotic resistance genes are incorporated to provide a facility to actively select cell lines that have been infected by the lenti-viral vector. As a safety feature, the incorporated viral DNA has been modified to prevent replication of viable lenti-viruses.



	CMV Promoter	RNA Polymerase II promoter
cPPT	Central	Polypurine tract
WRE	Enhances the stability and translation of transcripts	
turbo GFP	Marker to track shRNAmir expression	
Puro <sup>r</sup>	Mammalian selectable marker	
AMP <sup>r</sup>	Ampicillin bacterial selectable marker	
5'LTR	5' long terminal repeat	
pUC ori	High copy replication and maintenance in <i>e.coli</i>	
SIN-LTR	3' Self inactivating long terminal repeat	
RRE	Rev response element	
ZEO <sup>r</sup>	Bacterial selectable marker	

**Figure 2.1 pGIPZ Construct Design**

Reproduced from Open Biosystems product website

The pGIPZ constructs were delivered to the oesophageal cancer cell lines via a competent lenti-virus. Lenti-viruses were manufactured by 293FT cells following transfection of the specifically designed pGIPZ constructs and viral packaging plasmids.

### **2.2.16.2 Lenti-virus production**

All work was carried out in a level II tissue culture hood with full safety clothing. All equipment and waste media were sterilised in 1% Virkon in the tissue culture hood for at least 12 hours and then autoclaved as standard.

### **2.2.16.3 Transfecting 293FT cells for lenti-virus production**

Transfection was performed using lipofectamine LTX and PLUS reagents, a liposomal delivery system (Invitrogen, UK). The optimum number of cells seeded and ratios of plasmid DNA, lipofectamine LTX and PLUS reagents for the highest transfection efficiencies had been previously ascertained by a member of a collaborating group in the laboratory (J O'Neil, personal communication).

293FT cells were cultured in standard media with the addition of Geneticin G418 antibiotic (10µg/ml media). The cells were briefly trypsinised, centrifuged for 5 minutes at 5000g and then washed in PBS. After further centrifugation cells were re-suspended in standard media and  $1 \times 10^6$  cells seeded into each 10cm culture dish (4 dishes per viral preparation). Cellular confluence of approximately 80% was required to proceed to transfection.

All dishes were re-fed with 5mls standard media at least 1 hour before starting transfection. For each viral preparation (4 x 10cm culture dishes) the following were combined and incubated for 15 minutes at room temperature: 16µl (µg) lenti-viral plasmids encoding gene/shRNA of interest (pGIPZ), 16µl (µg) psPAX2, 16µl (µg) pMD2.G, 12ml Optimem, 48µl PLUS reagent.

After 15 minutes, 152µl of LTX reagent was added, gently mixed and further incubated for 30 minutes at room temperature.

The standard culture media was aspirated from the culture dishes and 3062µl of the above reaction mix added in a drop wise fashion to the surface of each culture dish. The reaction mix was gently equilibrated over the cellular monolayer by slowly tilting the culture dish from side to side. Each dish was incubated at 37°C overnight.

The reaction mix was aspirated and replaced with 5mls of standard media, except the added FCS had been heat inactivated (heated to 55°C for 25 minutes) to destroy the complement system that may neutralise any virus produced. Dishes were further incubated for 48 hours for virus production.

#### **2.2.16.4 Concentration of lenti-viral preparations**

The lenti-virus containing media was removed from all 4 dishes and combined. Cellular debris was removed by centrifugation at 12000g for 5 minutes and the supernatant filtered through a 0.45µm acrodisk filter.

The media was then loaded into 12ml Beckman tubes and topped up to the lip of the tube with heat-inactivated media if required. The tubes were then ultra-centrifuged in a Beckman SW40T rotor at 30,000 RPM for 2 hours at 4°C (the centrifuge carousel must be balanced accurately).

The supernatant was then aspirated and 50µl heat inactivated media added to the viral pellet and re-suspended on an orbital shaker at 4°C for 24 hours. The concentrated viral media was stored at 4°C in a Nunc tube for a maximum of 4 weeks.

#### **2.2.16.5 Infecting OE33, OE19 and OE21 cells with concentrated lenti-virus**

Cells to be infected were cultured in 24 well plates until approximately 30% confluent on the day of infection.

The optimal concentration of virus to infect the cells was determined by serial dilutions of the concentrated virus in heat-inactivated media (0.1 - 5  $\mu$ l of virus in 250 $\mu$ l). The percentage of cells infected with lenti-virus was increased by approximately 10% with the addition of hexadimethrene bromide (Polybrene™) 10 $\mu$ g/ml.

Standard media was aspirated from each well and replaced with viral spiked media. The plates were incubated at 37°C for 12 hours with gentle mixing of the virus by tilting the plates every hour for the first 4 hours.

Viral media was then aspirated and replaced with standard media and the cells monitored for expression of GFP for 24, 48 and 72 hours post-infection (infected cells fluoresce green during microscopy under a blue light) . A puromycin resistance gene was incorporated into the lenti-virus to allow for selection of virus infected cells. Selection of infected cells was undertaken at 72 hours with 10 $\mu$ g/ml of puromycin added to the culture media for 12 hours.

Successful silencing of the protein of interest was further confirmed by Western blotting.

#### **2.2.16.6 Preparation of shRNA encoding plasmids**

Plasmids were supplied in transformed *E.coli* bacteria which were amplified by initial culture on agar with 100 $\mu$ g/ml ampicillin (plasmids encoded ampicillin resistance). After overnight culture at 37°C one colony of each plasmid was transferred to 3ml of Luria-Bertani (LB) broth (1% (w/v) Tryptone Peptone, 0.5% (w/v) Yeast Extract, 1% (w/v) NaCl) supplemented with ampicillin (50 $\mu$ g/ml)) for 5 hours of pre-culture at 37°C before transfer to 500ml LB broth for a further 12 hours of incubation in a rotating incubator. 1ml of each culture was aspirated and added to 400 $\mu$ l of glycerol and frozen at -80°C for storage. Having amplified the *E.coli*, plasmids were extracted and purified using PureLink HiPure

Plasmid Filter Purification Kit – Maxi Prep (Invitrogen, UK) as per manufacturer's instructions and using supplied solutions. Briefly, cultures in LB broth were spun at 4000g for 10 minutes, the supernatant discarded, the pellet re-suspended in 20ml of re-suspension buffer and transferred to a 50ml centrifuge tube. 20ml of lysis buffer was added and cells mixed and incubated at room temperature for 5 minutes. 20ml precipitation buffer was then added and mixed by inversion. The solution was passed through a maxi column with filtration cartridge and allowed to flow through by gravity. Columns were then rinsed with 10ml wash buffer and the filtration cartridge was removed and discarded. The column was then washed with 60ml wash buffer and all flow through solution was discarded. 15ml elution buffer was added to the columns and effluent, containing purified plasmids, collected. 10.5ml isopropanol was added and mixed by inversion. Tubes were centrifuged at 15000g for 30 minutes and the supernatant discarded. The pellet was re-suspended in 70% ethanol before being re-spun at 15000g for 5 minutes, supernatant discarded and the pellet air dried at room temperature for 20 minutes. The plasmid DNA pellet was then re-suspended in 500µl TE Buffer (0.1mM EDTA in 10mM Tris-HCl, pH 8) and stored at -20°C.

#### **2.2.16.7 LRP1 and HCP1 shRNA encoding pGIPZ plasmids**

Stable LRP1 and HCP1 knockdowns were created in OE33, OE19 and OE21 cell lines by pGIPZ constructs containing specifically designed shRNA sequences for LRP1 and HCP1. In each case two clones were sourced targeting different mRNA regions. The clone that produced the greatest degree of post-transcriptional mRNA destruction and therefore protein suppression on Western blotting, was chosen for experimentation. A non-silencing shRNA was used as a control and a double LRP1 and HCP1 knock down was created by combining the viral vectors.

pGIPZ plasmids were obtained from (Open Biosystems, UK) and packaging plasmids were received as a kind gift of Dr Chris Dawson, University of Birmingham.

Catalogue number and clone	Function	Sequence		
		Sense	Anti-sense	Loop
RHS4346	Non-silencing	Not disclosed but verified to produce siRNA with no match in mammalian genome		
RHS4531	LRP1	ACCCGCGAGGACTACA	ATCAATGTAGTC	TAGTGAAGCCACA
V2LHS-7406	silencing	TTGAAT	CTCGCGGGC	GATGTA
RHS4531	LRP1	AGGCCTGACTGTGTTT	ATTCTCAAACACA	TAGTGAAGCCACA
V2LHS-134038	silencing	GAGAAT	GTCAGGCCG	GATGTA
RHS4531	HCP1	ACGATCCATTGTCCAG	ATAGAGCTGGAC	TAGTGAAGCCACA
V2LHS-70748	silencing	CTCTAT	AATGGATCGG	GATGTA
RHS4531	HCP1	ACCTCTGTCTAGGATC	ATTCTAGATCCTA	TAGTGAAGCCACA
V2LHS_249843	silencing	TAGAAT	GACAGAGGC	GATGTA

**Table 2.5 Sense, anti-sense and loop sequences for shRNA control, LRP1 and HCP1 knockdown**

### **2.2.17 Murine studies**

All murine work was undertaken at the University of Sydney, Australia, under the guidance of the Animal Ethics Committee, University of Sydney – AEC K20/4-10/3/5299 and the Biomedical Services Unit, University of Birmingham, UK.

Balb/C nu/nu (nude/athymic – T-cell deficient) 6-weeks-old female mice were utilised initially, however xenografts were slow to establish and spontaneously involuted. Mice were then substituted for NOD-SCID (non-obese diabetic-severe combined immunodeficiency – T and B cell deficient, no functioning natural killer cells and lack of complement) murine models which yielded near 100% rate of well established xenografts with OE33, OE19 and OE21 cell lines. The mice were housed under quarantine conditions: air filtered with Techniplast Italy, HEPA-ULPA internal filter; gloves, gown and foot coverings were mandatory. All procedures were performed in a Gelaine biology safety hood. Mice were fed with Riverina rat and mice cubes (an irradiated and balanced composite).

#### **2.2.17.1 Xenograft formation**

The mice were examined to confirm a healthy status before commencing the procedure. Cells were harvested at 70% confluence with 0.05% (w/v) trypsin, washed and re-suspended in plain media for counting. The number of cells required for each xenograft was pre-optimised to  $1 \times 10^6$ . After counting, the cells were centrifuged at 8,000g and re-suspended in 50 $\mu$ l plain media per xenograft and kept on ice. Just before injection, the cell slurry was mixed 50/50 (v/v) with freshly thawed Matrigel (extracellular matrix substitute secreted by Engelbreth-Holm-Swarm mouse sarcoma cells<sup>431</sup>), using ice cold syringes, to form a total volume of 100 $\mu$ l per xenograft and kept on ice.

The mice were anaesthetised in turn (with isoflurane) in an auto-regulated anaesthetising chamber. The thoroughly mixed cell/Matrigel composite was injected in the subcutaneous tissue plane on the left flank of each mouse and allowed to form a solid bleb before the mouse was recovered and returned to the cage.

After receiving xenografts, mice were ear tagged for identification. The health of the mice and size of the xenograft were closely monitored through observation of behaviour, mouse weight and calliper measurements. Established xenografts were seen 2 weeks post injection.

#### **2.2.17.2 Gavarging, culling and tissue collection**

Mice were sorted into treatment groups such that the mean mouse weight and xenograft dimensions were equal in each group.

Mice were gavarged on alternate days using a gavarging needle and luer lock 1ml syringe. A chelator suspension was formed for gavarge in 30% 1,2-propanediol and 70% sterile 0.9% (v/v) sodium chloride solution. Cisplatin was freshly diluted in sterilised dH<sub>2</sub>O for intraperitoneal (IP) injection with a fine bore needle. Control treatment (vehicle alone) consisted of 30% (v/v) 1,2-propanediol and 70% (v/v) sterile 0.9% (w/v) sodium chloride solution for gavarge and sterile dH<sub>2</sub>O for IP injection.

Weight and xenograft dimensions were recorded on non-gavarging days to minimise distress.

After the allotted treatment period the mice were culled under humane conditions. Blood samples were obtained by direct cardiac puncture for full blood count (FBC) and biochemical analysis (blood aliquoted into Capiject<sup>®</sup> blood tubes - lavender, dipotassium EDTA for FBC and cherry red serum gel/clot activator tubes for biochemistry). The biochemistry tube was allowed to clot and spun at 12000g for 10mins; serum aspirated,

transferred to analysis tubes and dispatched to the Veterinary School for analysis of (full blood count, urea, creatinine, ALT, AST, albumin, total bilirubin, serum iron, and total iron binding capacity).

The xenograft, liver, heart and spleen were removed and weighed before being divided and snap frozen in liquid nitrogen or placed in formalin.

### **2.2.18 Statistical Analysis**

Analyses of data were performed using SPSS version 10.0 (SPSS Inc, USA) and Microsoft Excel Professional 2009. Normally distributed data was analysed using paired and independent T-tests and non-parametric data, or where a normal distribution could not be assumed, were analysed using the Mann-Whitney U test. Comparison between categorical variables was made using  $\chi^2$  and formal correlation assessed with Pearson's correlation co-efficient. Significance was accepted at  $\alpha$ -level of 5% ( $p \leq 0.05$ ) and all data means presented with  $\pm 2$  standard error of the mean (SEM).

To assess the performance of two drugs, an iron chelator (Dp44mT, Deferasirox and DFO) and a chemotherapeutic agent (Cisplatin, 5-FU and Epirubicin) in combination, two series of cell counts were observed, one at various concentrations of the iron chelator alone and another in combination with the chemotherapy agent given at IC50 concentration. The additional effect of the iron chelator was estimated from the difference between the two series of counts and significance was assessed using a Wilcoxon signed rank test. Any enhancement of effect from using the two drugs (iron chelator and chemotherapy agent) in combination above that to be expected from observing their performance separately was then estimated by first subtracting the zero concentration cell counts from each

series, and then computing the difference between these two adjusted series (analysis kindly performed by Dr Roger Holder, University of Birmingham, UK).

### **2.2.19 Ethical approval**

This work has been carried out in accordance with the declaration of Helsinki (2008) of the World Medical Association. Ethical approval for this study was approved by the Solihull Local Research Ethics Committee (LREC 06/Q2706/65). All patients providing tissue samples gave informed written consent. Murine studies were performed under the departmental licences of the Department of Pathology, University of Sydney, Australia and the Biomedical Services Unit, University of Birmingham, UK.

# CHAPTER 3: CHARACTERISATION OF HAEM TRANSPORT PROTEINS IN THE PROGRESSION OF BARRETT'S METAPLASIA TO OESOPHAGEAL ADENOCARCINOMA

## 3.1 Introduction

The weight of epidemiological and experimental evidence associating iron with the incidence and progression of cancer is mounting. Iron is essential for cellular metabolism and is intrinsic to cell growth and replication<sup>186</sup>. It has long been known that iron plays a crucial role in the conversion of ribonucleotides to deoxyribonucleotides, a rate limiting step in DNA synthesis, catalysed by RNR<sup>187,188</sup>. Iron depletion classically arrests the cell cycle at G<sub>1</sub>/S<sup>193,194</sup>. It follows that a selective advantage is conferred upon cancer cells that are able to acquire iron in greater quantities, to drive the cell cycle and enhance proliferation.

Recent studies of ex-vivo BM associated OAC resection specimens, have shown that progression to invasive OAC is associated with increased expression of the inorganic iron import proteins, TfR1, DMT1 and DcytB along with the iron storage protein H-ferritin<sup>171</sup>. mRNA and protein expression of the iron efflux protein FPN was paradoxically increased in OAC, however FPN localisation was cytoplasmic, representing functional loss of iron export<sup>171</sup>. Such findings are entirely compatible with previous observations of deranged iron regulation in colorectal carcinogenesis<sup>175</sup>. Alterations in the expression of inorganic iron transport proteins were not just evident in the latter stages of OAC but apparent in

early stages of the dysplastic transformation of BM<sup>171</sup>. DMT1 expression was found to be significantly associated with a more aggressive phenotype and correlated with metastatic potential<sup>171</sup>. The authors postulated that over expression of iron transport proteins was unlikely to culminate in increased luminal iron uptake, rather the acquisition of systemic inorganic iron, through TfR1 mediated endocytosis<sup>171</sup>. Gross OAC iron content was significantly raised (200% increase in mean iron content) compared to adjacent dysplastic BM, supporting a paradoxical over expression of TfR1 and DMT1<sup>171</sup>. Furthermore, *in-vitro* culture of OAC cell lines with supplementary iron prompted avid proliferation and significant gross intracellular iron loading compared to control<sup>171</sup>. TfR1 mRNA expression was significantly suppressed and H-ferritin protein levels increased on iron loading, in keeping with an IRE-IRP mediated response<sup>171</sup>.

The omnivorous human diet contains large quantities of organic iron, principally in the form of haem that is far more readily bio-available than inorganic iron<sup>201</sup>. In addition, there exists a large systemic circulating pool of haem iron bound to haemopexin<sup>290</sup>. Recent identification of haem importing proteins LRP1<sup>298</sup> and HCP1<sup>274</sup> raises the hypothesis that OAC cells express these proteins and acquire systemic haem in a manner analogous to TfR1 mediated endocytosis of transferrin bound inorganic iron. In addition, haem export proteins FLVCR and BCRP are thought to have a role in preventing cellular toxicity from haem and other dietary derived carcinogens<sup>273,279</sup>. Whether haem export protein expression is abrogated in OAC, to mirror the functional loss of inorganic iron efflux, is unknown.

### **3.2 Aims**

1. Characterise the expression of haem import proteins LRP1 and HCP1 in the progression of BM to OAC
2. Characterise the expression of haem export proteins BCRP and FLVCR in the progression of BM to OAC
3. Examine the relationship between haem transport protein expression and OAC pathological stage

### **3.3 Results**

#### **3.3.1 mRNA expression of the haem import proteins LRP1 and HCP1 and haem export proteins BCRP and FLVCR in the malignant progression of BM to OAC**

Fresh OAC resection specimens (n=9) matched with adjacent dysplastic BM and benign non-dysplastic BM (n=9) matched with normal squamous oesophageal mucosa (NS), were obtained from surgical resection specimens and surveillance endoscopy. Histological identities of the samples were confirmed and specifically, benign BM tissue was certified to be columnar epithelium with no evidence of dysplasia or OAC. Samples were snap frozen in liquid nitrogen and subsequently processed for mRNA expression utilising qRT-PCR. Mean fold change in LRP1, HCP1, BCRP and FLVCR mRNA expression were compared between matched samples: benign BM versus NS; and dysplastic BM versus OAC.

##### **3.3.1.1 mRNA expression for the haem import proteins LRP1 and HCP1 in the malignant progression of OAC**

The expression of LRP1 and HCP1 mRNA in benign BM compared to NS was variable with no statistical difference in fold change observed ( $p=0.3$  and  $p=0.1$  for LRP1 and HCP1) (figure 3.1). However, a degree of concordance was noted, at the level of each matched sample as LRP1 and HCP1 mRNA expression appeared to be either raised or decreased in tandem.

In contrast, a marked increase in LRP1 and HCP1 mRNA expression was evident between dysplastic BM and OAC (figure 3.2) ( $p=0.049$  and  $p=0.018$  for LRP1 and HCP1). LRP1 and HCP1 mRNA expression was raised in 8 out of 9 matched samples.

### **3.3.1.2 mRNA expression for the haem export proteins BCRP and FLVCR in the malignant progression of OAC**

No significant differences in haem export protein mRNA expression was seen in the pathological change of NS to benign BM ( $p=0.27$  and  $p=0.7$  for BCRP and FLVCR) (figure 3.1). BCRP and FLVCR mRNA expression was raised in the same samples that exhibited an increase in LRP1 and HCP1.

Overall, a significant increase in BCRP and FLVCR mRNA expression was observed in the progression of dysplastic BM to invasive OAC ( $p=0.05$  and  $p=0.042$  for BCRP and FLVCR) (figure 3.2). A degree of variation between matched dysplastic BM and OAC was noted with BCRP mRNA raised in 6 of 9 and FLVCR mRNA raised in 7 of 9 samples. In the majority of cases, BCRP and FLVCR mRNA expression were raised in the same samples. One matched set of samples (T7) did not exhibit a change in either haem import or export protein mRNA expression.

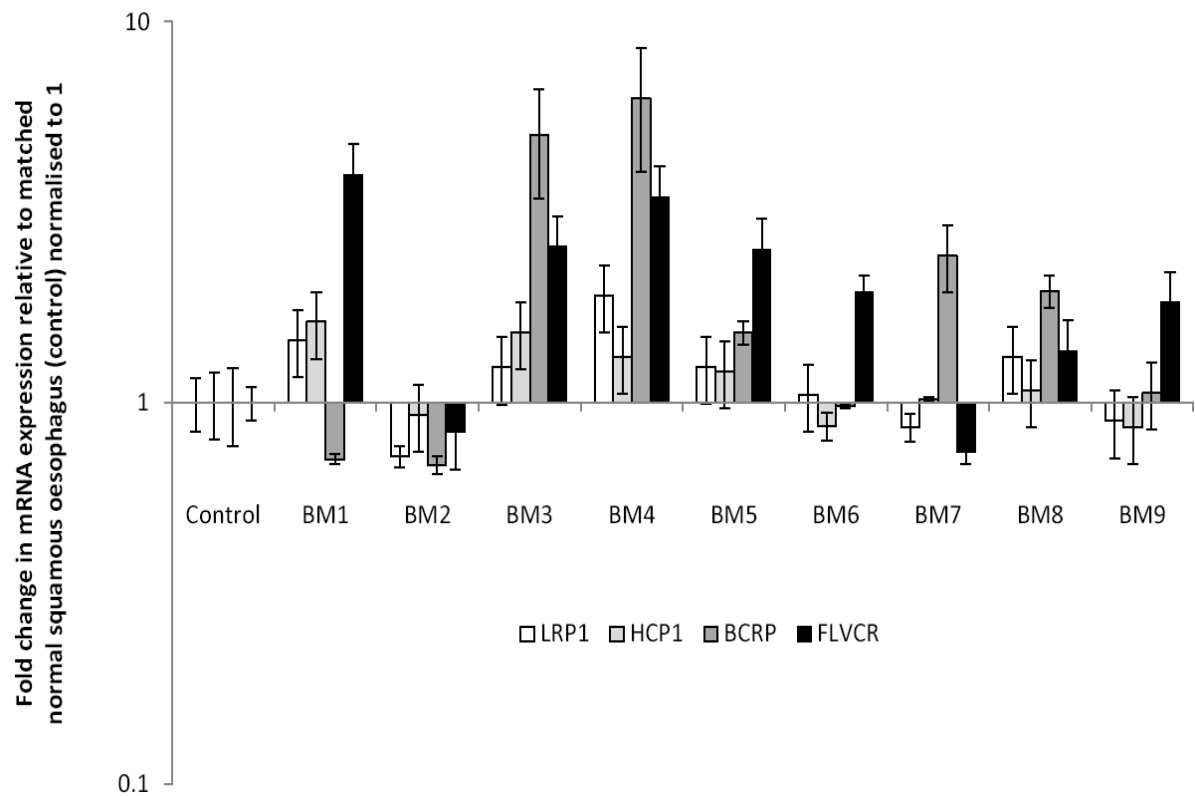


**Figure 3.1 mRNA expression for the haem transport proteins is not significantly altered in the metaplastic transformation of NS to BM**

Matched endoscopic biopsy samples of NS and benign BM (n=9) were processed for LRP1, HCP1, BCRP and FLVCR mRNA expression by qRT-PCR. Results are displayed as a fold change in mRNA expression by benign BM sample compared to average NS control. No change in mRNA expression by benign BM sample compared to average NS control. No significant change in average mRNA fold change was observed in the metaplastic transformation of NS to benign BM for LRP1, HCP1, BCRP or FLVCR. Error bars denote  $\pm$  SEM.

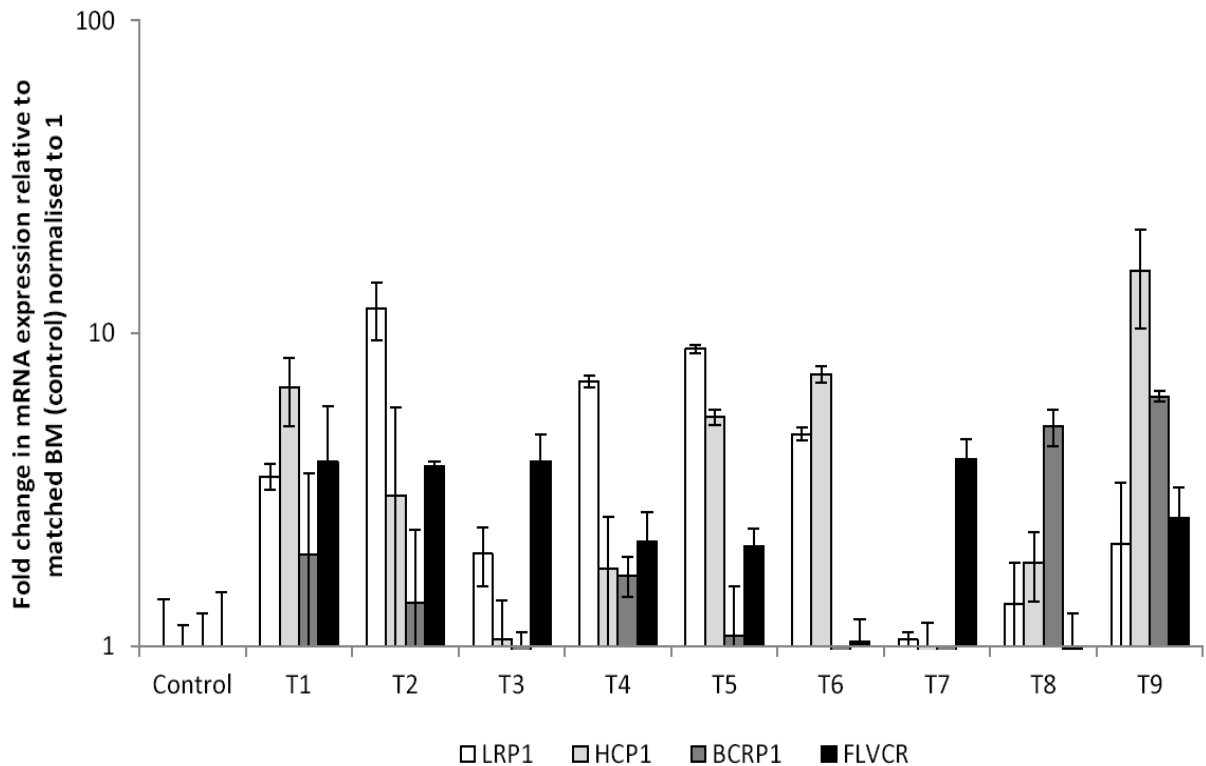


**Figure 3.2 mRNA expression for the haem transport proteins is significantly up-regulated in the malignant progression of dysplastic BM to invasive OAC**

Matched surgical resection samples of dysplastic BM and OAC (n=9) were processed for LRP1, HCP1, BCRP and FLVCR mRNA expression by qRT-PCR. Results are displayed as a fold change in mRNA expression by OAC sample compared to average dysplastic BM control. Statistically significant changes in average mRNA fold change were observed in the malignant progression of dysplastic BM to invasive OAC for LRP1, HCP1, BCRP or FLVCR ( $p=0.049$ ,  $p=0.018$ ,  $p=0.05$  and  $p=0.042$  respectively). Error bars denote  $\pm$  SEM.

### **3.3.2 Protein expression of the haem import proteins LRP1 and HCP1 and export proteins BCRP and FLVCR in the malignant progression of BM to OAC**

Fresh OAC resection specimens (n=9) matched with adjacent dysplastic BM and benign non-dysplastic BM (n=9) matched with NS, were obtained from surgical resection specimens and surveillance endoscopy. Protein expression was determined by Western blotting and densitometric scanning of the observed protein normalised to  $\beta$ -actin. Mean fold changes in LRP1, HCP1, BCRP and FLVCR protein expression were compared between matched samples: benign BM versus NS; and dysplastic BM versus OAC.

#### **3.3.2.1 Protein expression for the haem import proteins LRP1 and HCP1 in the malignant progression of OAC**

Haem import protein expression was analogous to observed changes in mRNA expression. LRP1 and HCP1 protein expression was not significantly different between benign BM and matched NS, although HCP1 tended towards up-regulation in benign BM, this failed to reach statistical significance ( $p=0.94$  and  $p=0.084$  for LRP1 and HCP1) (figure 3.3). Haem import protein expression was strongly up-regulated in OAC compared to matched dysplastic BM ( $p=0.001$  and  $p=0.03$  for LRP1 and HCP1 respectively) (figure 3.3).

#### **3.3.2.2 Protein expression for the haem export proteins BCRP and FLVCR in the malignant progression of OAC**

In accordance with mRNA, no change in BCRP or FLVCR protein expression was apparent when comparing benign BM to NS ( $p=0.71$  and  $p=0.8$  for BCRP and FLVCR) (figure 3.3). The observed increase in BCRP and FLVCR mRNA expression, on progression of dysplastic BM to invasive OAC, was supported by a corresponding significant overexpression at the translational level. Fold change in protein expression for BCRP and FLVCR was

significantly raised for OAC compared to dysplastic BM ( $p=0.001$  and  $p=0.001$  for BCRP and FLVCR) (figure 3.3).

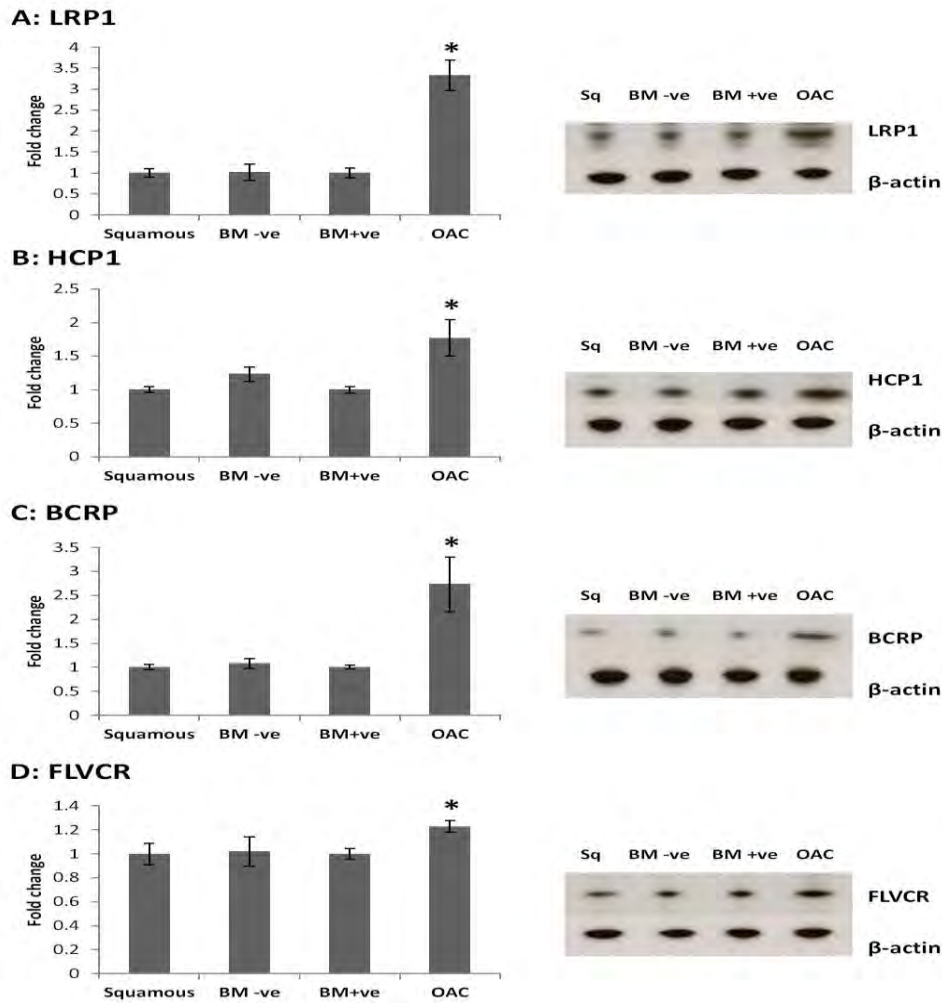


**Figure 3.3 The expression of proteins capable of haem transport is up-regulated in the malignant progression of dysplastic BM to invasive OAC**

Matched biopsy samples of NS (squamous) and benign BM (BM-ve) and resection specimens of dysplastic BM (BM+ve) and OAC were processed for LRP1, HCP1, BCRP and FLVCR protein expression by Western blotting. Results were standardised to  $\beta$ -actin and expressed as an average fold change compared to control. No significant change in expression was observed in the metaplastic replacement of NS with benign BM. However, both import and export protein expression was significantly up-regulated in the malignant progression of dysplastic BM to OAC ( $p=0.001$ ,  $p=0.03$ ,  $p=0.001$  and  $p=0.001$  for LRP1, HCP1, BCRP and FLVCR).

### **3.3.3 Immunolocalisation of the haem import proteins LRP1 and HCP1 and haem export proteins BCRP and FLVCR in the malignant progression of BM to OAC**

Semiquantitative immunohistochemistry was utilised to elucidate the cellular localisation and approximate expression levels of the haem import and export proteins in paraffin sections. Selected sections were biopsy specimens of benign BM with adjacent NS (n=26) and surgical resection specimens of OAC with associated dysplastic BM and NS (n=16). All material was screened by a consultant pathologist (PT) to confirm the samples contained the relevant tissue types. Normal liver and small bowel were utilised for positive and negative control.

#### **3.3.3.1 Semiquantitative immunolocalisation of haem import proteins LRP1 and HCP1 in the malignant progression of OAC**

LRP1 (figure 3.4): No immunoreactivity for LRP1 was observed in NS mucosa. Benign BM similarly demonstrated minimal immunoreactivity for LRP1 with no observed difference on semi-quantitative analysis ( $p=0.23$ ). Dysplastic BM associated with invasive OAC demonstrated moderate immunoreactivity, principally on the apical border with slight enhancement towards the crypts. Strong immunoreactivity for LRP1 was observed in OAC with marked pan-membranous activity. The difference in immunoreactivity between OAC and associated dysplastic BM was strongly significant ( $p=0.003$ ). Normal liver was used as a positive control where pan-membranous and cytosolic immunoreactivity was observed.

HCP1 (figure 3.5): HCP1 immunoreactivity within NS was very weak. No significant difference in immunoreactivity was noted between NS and benign BM ( $p=0.3$ ) where immunoreactivity remained weak and mainly apical. A significant difference in immunoreactive intensity was observed between OAC and associated dysplastic BM

( $p=0.001$ ). OAC associated dysplastic BM still maintained apical membrane immunoreactivity which contrasted with more generalised membranous immunoreactivity for OAC. Normal small bowel was used as a positive control and demonstrated strong HCP1 immunoreactivity evenly along the villous apical membrane.

### **3.3.3.2 Semiquantitative immunolocalisation of haem export proteins BCRP and FLVCR in the malignant progression of OAC**

BCRP (figure 3.6): Moderate BCRP immunoreactivity was noted in NS mucosa, more evident towards the basal cell layer. No significant difference was observed in the intensity of immunoreactivity between NS and benign BM ( $p=0.4$ ). In benign BM, immunoreactivity remained weak but was more clearly localised to the apical membrane. In OAC, very intense apical immunoreactivity was observed. OAC associated dysplastic BM was significantly less immunoreactive ( $p=0.001$ ) but still demonstrated apical activity. Normal liver was employed as a positive control with strong immunoreactivity in the cytoplasm and membrane. No evidence of nuclear BCRP immunoreactivity was observed.

FLVCR (figure 3.7): The most striking observation was that FLVCR immunoreactivity was exclusively nuclear in all tissue types. No statistical difference in activity was noted between NS and benign BM ( $p=0.24$ ), although the former appeared to be graduated with more intense immunoreactivity towards the basal cell-layer of the oesophagus. Nuclear immunoreactivity was markedly more pronounced in OAC compared to associated dysplastic BM ( $p=0.001$ ) and again was specifically nuclear. Small bowel was used as a positive control where again exclusively strong nuclear staining was observed.

Protein immunoreactivity	NS (n=26;mean±SE)	Benign BM (n=26;mean±SE)	BM associated with OAC (n=16;mean±SE)	OAC (n=16;mean±SE)
LRP1	0.6 ± 0.1	0.91 ± 0.31	2.45 ± 0.52	<b>7.45 ± 1.2 *</b>
HCP1	1.8 ± 0.3	2.62 ± 0.7	4.13 ± 0.85	<b>7.04 ± 0.9 *</b>
FLVCR	1.88 ± 0.1	2.33 ± 1.66	5.27 ± 0.43	<b>8.4 ± 0.83 *</b>
BCRP	0.3 ± 0.21	0.5 ± 0.16	2.35 ± 0.46	<b>6.52 ± 0.7 *</b>

**Table 3.1 Immunoreactivity score for organic iron transport proteins in the progression of NS to invasive OAC**

Immunoreactivity of the haem import (LRP1 and HCP1) and export proteins (BCRP and FLVCR) was evaluated using paraffin embedded immunohistochemistry. Selected sections: biopsy specimens of benign BM with adjacent NS (n=26) and surgical resection specimens of OAC with associated dysplastic BM and NS (n=16). Immunoreactivity was scored on a semi-quantitative basis (observers blinded to tissue and antibody identity) by three independent observers. Staining intensity was scored as a function of two factors: a scale of 0-3 (0= absent, 3=strong); and percentage of positively stained cells within microscopic view (0= no cells, 1= 1-25%, 2= 26-50%, 3= 51-75% and 4=>76%). The two scores were multiplied to give a total score 0-12 (\*p-value <0.05 benign BM compared to BM and OAC compared to OAC associated BM).

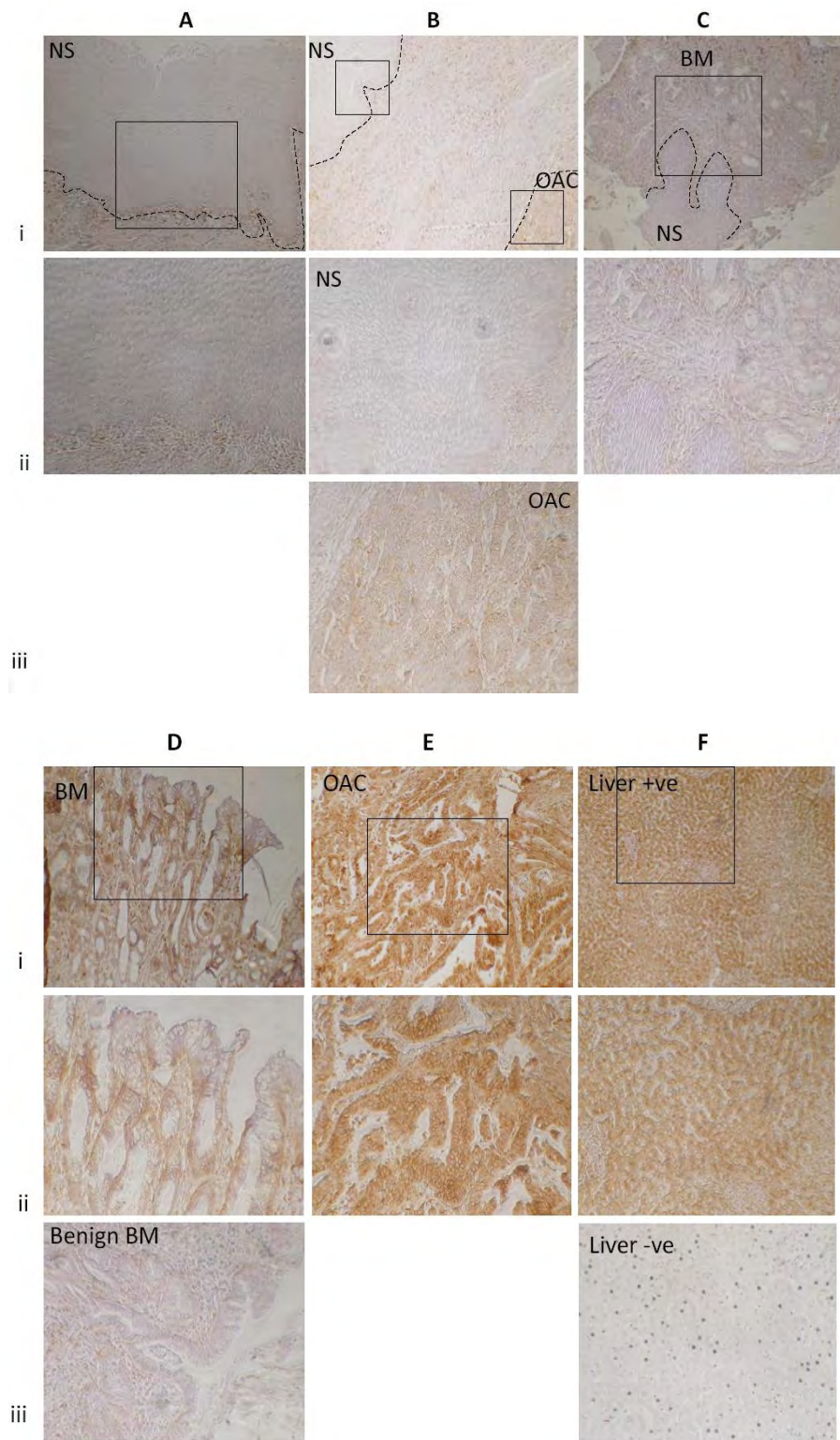


**Figure 3.4 LRP1 immunoreactivity**

Paraffin sections of NS, benign BM, BM and OAC. Liver used as a positive and negative control. Magnification x20 and boxed area extrapolated to x60. Dotted lines: Ai squamo-submucosal border; Bi squamo-submucosal border and extent of OAC invasion; Ci border between squamous mucosa and BM.

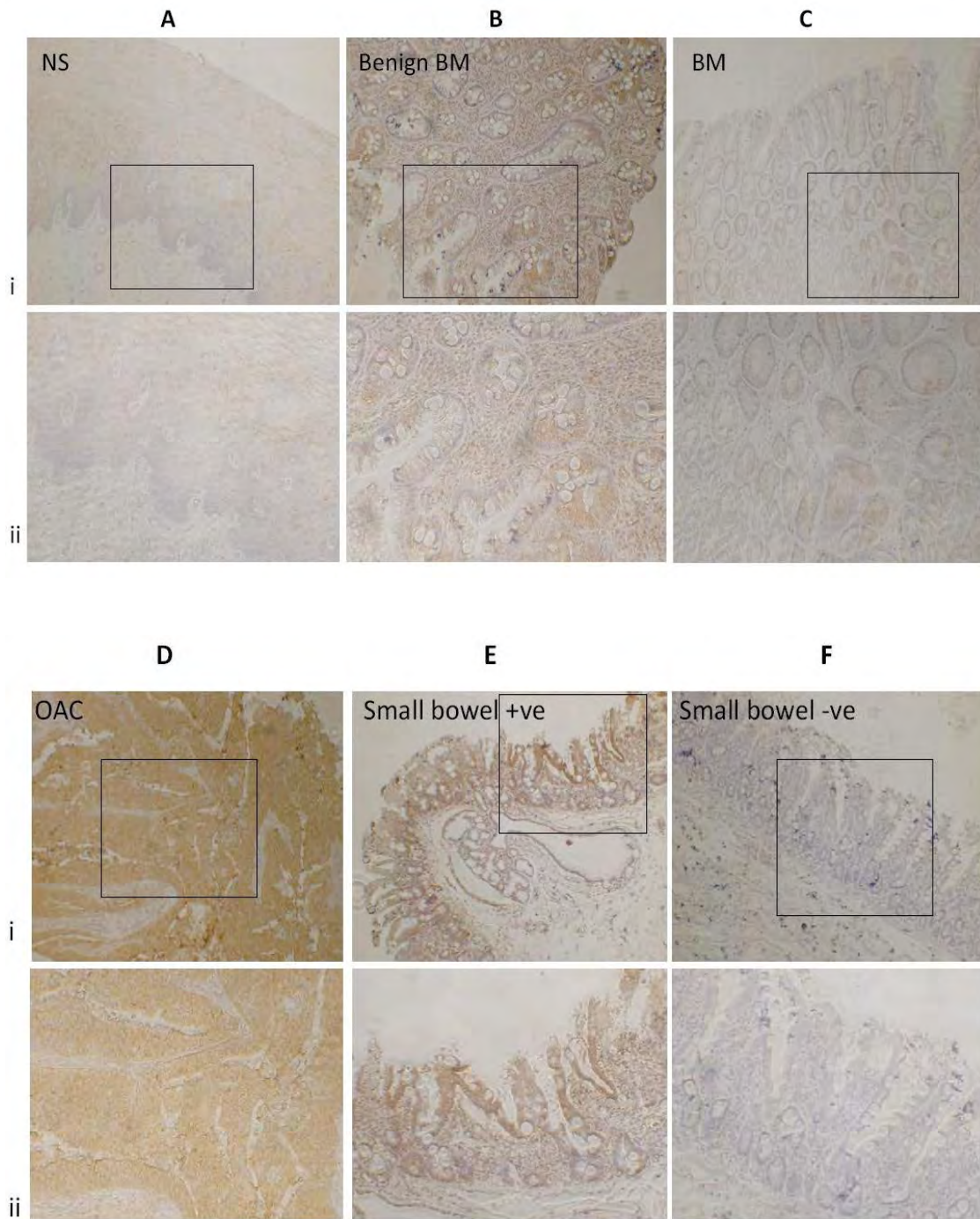


**Figure 3.5 HCP1 immunoreactivity**

Paraffin sections of NS, benign BM, BM and OAC. Small bowel used as a positive and negative control. Magnification x20 and boxed area extrapolated to x60.

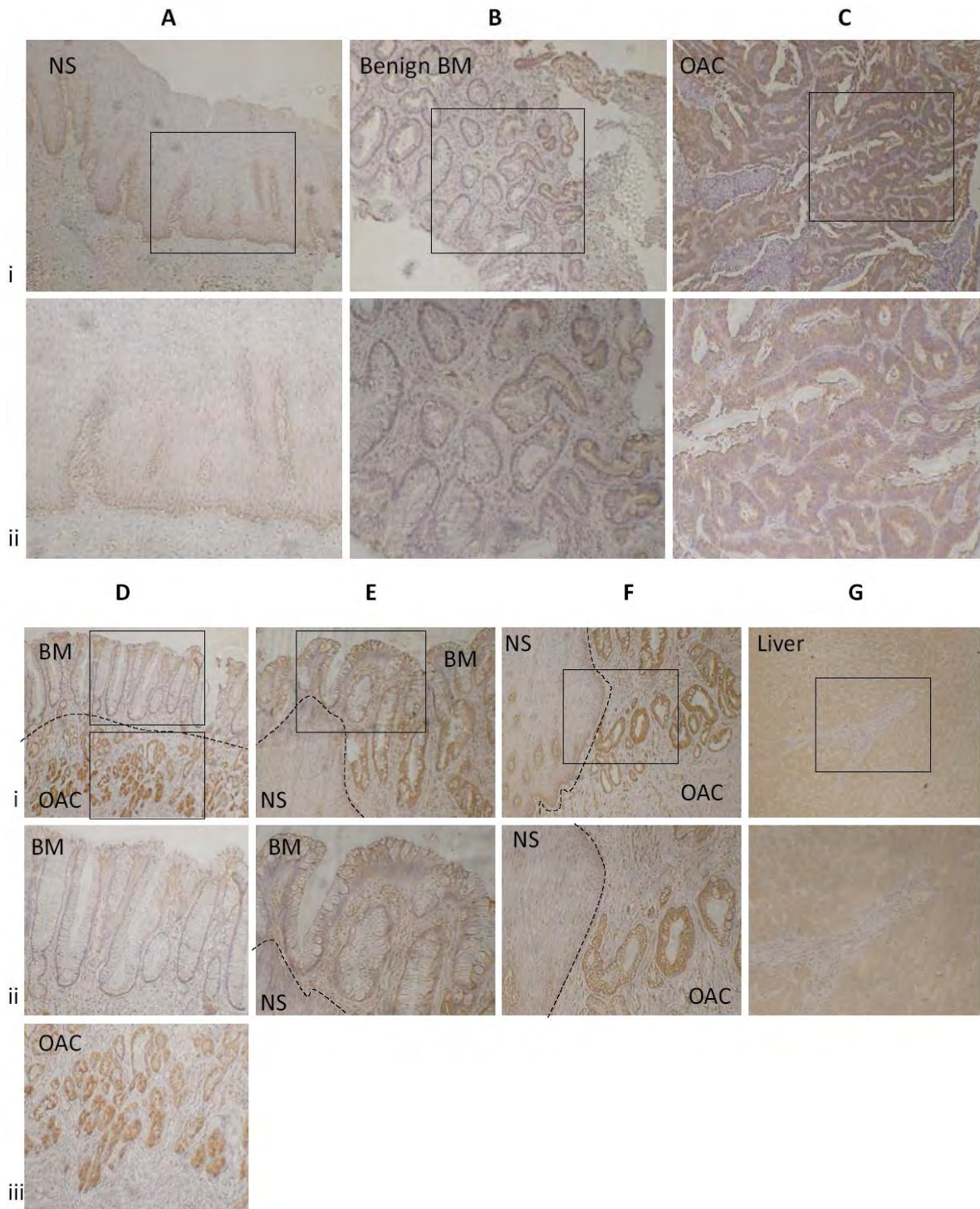


**Figure 3.6 BCRP Immunoreactivity**

Paraffin sections of NS, benign BM, BM and OAC. Liver used as a positive and negative control. Magnification x20 and boxed area extrapolated to x60. Dotted lines: Di border between BM and ADC; Ei border between BM and squamous mucosa; Fi border between squamous mucosa and OAC.

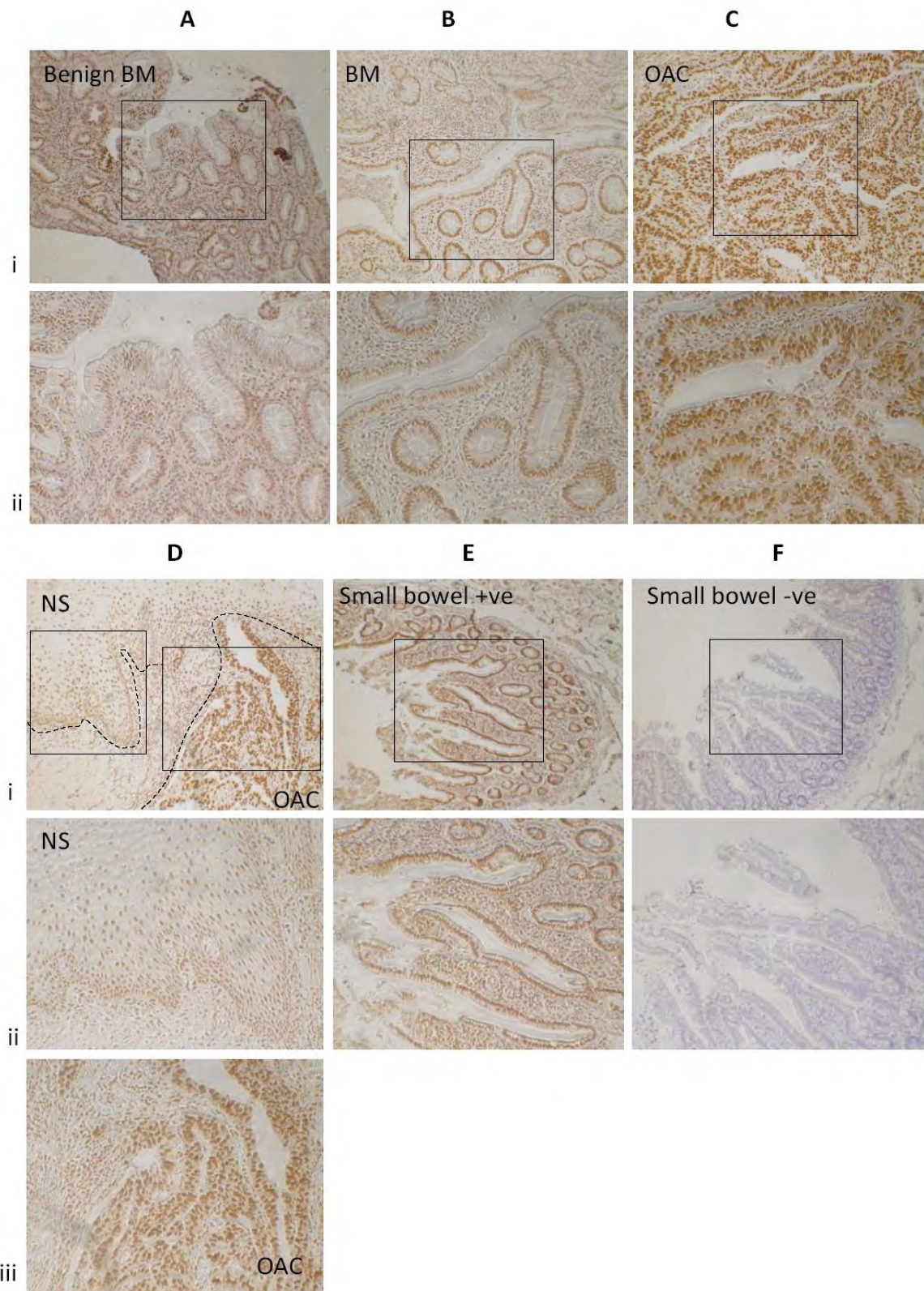


**Figure 3.7 FLVCR immunoreactivity**

Paraffin sections of NS, benign BM, BM and OAC. Small bowel used as a positive and negative control. Magnification x20 and boxed area extrapolated to x60. Dotted lines: Di extent of OAC invasion into NS.

### **3.3.4 Haem transport protein immunoreactivity stratified by tumour stage**

An OAC tissue microarray derived from surgical resection specimens (n=78) (kind gift of Dr J Bury, University of Sheffield) with known pathological staging was processed for LRP1, HCP1, BCRP and FLVCR immunohistochemistry (figure 3.8). Semiquantitative analysis was performed by three observers blinded to the targeted immunoreactivity and OAC staging (SF, CT, KR). Results were stratified by staging criteria (local infiltration T-stage 1-3, tumour differentiation and presence of nodal metastases). Despite the observed up-regulation of haem import and export proteins in the malignant progression of BM to invasive OAC, none of the import or export proteins demonstrated a significant change in immunoreactivity score with T-stage, tumour differentiation or presence of nodal metastases.

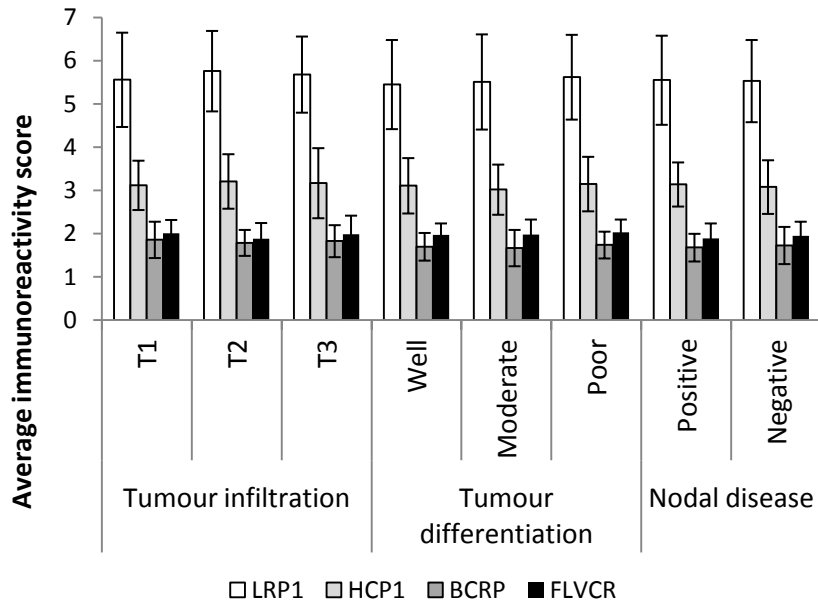


**Figure 3.8 Semi-quantitative immunohistochemistry analysis of haem transport proteins by tumour stage**

OAC tissue microarray (n=78) stratified by tumour infiltration (T-stage), differentiation and presence of nodal disease. No significant difference in immunoreactivity was observed for haem import or export proteins.

### 3.4 Conclusions

Haem transport proteins are hereby shown to be expressed in OAC and associated dysplastic BM for the first time. This novel finding is highly suggestive that haem acquisition has a significant role in contributing to the increased intracellular iron pool previously demonstrated in the malignant progression from BM to invasive OAC<sup>171</sup>. Indeed, haem import protein expression appears to be nonexistent in NS, negligible in benign BM and significantly up-regulated at both the transcription and translation levels upon malignant transformation of dysplastic BM to invasive OAC. Haem, once acquired by the cell, is metabolised and incorporated into inorganic iron processing pathways<sup>276</sup>. Iron loading of cancer cells serves as a means to drive the cell cycle, facilitate DNA synthesis, diminish cell-cell adhesion and increase the potential for further DNA aberrations through ROS generation<sup>178</sup>.

LRP1 and HCP1 mRNA transcripts and protein expression were significantly up-regulated in the malignant transition from dysplastic BM to invasive OAC. LRP1 immunoreactivity was absent in NS and benign BM but present in dysplastic BM suggesting that LRP1 overexpression is likely to be an early event in the evolution of BM associated dysplasia. Direct comparison of the expression of the haem transport proteins between benign BM and dysplastic BM was not performed as it was not possible to match samples derived from the same patient. HCP1 immunoreactivity was also weak in NS and benign BM but much more pronounced in dysplastic BM. LRP1 and HCP1 were immunolocalised to the apical border in dysplastic BM, however on progression to OAC, cellular polarity was lost with abundant LRP1 and HCP1 immunoreactivity evident in pan-membranous locations. Localisation to the cancer cell membrane is highly suggestive of a metabolically active

role for LRP1 and HCP1 supporting the hypothesis that OAC cells can acquire systemic haem either bound to haemopexin via LRP1 mediated endocytosis or free haem actively transported by HCP1. The disorganised interstitium of the tumour is likely to contain a relative abundance of haem secondary to the friable nature of tumour neovascularisation, central necrosis, ulceration and direct vessel invasion. The membranous location of HCP1 in particular is notable as the protein is post-transcriptionally regulated to the cytoplasm in iron replete states<sup>274</sup>; further evidence of the errant iron metabolism seen in OAC cells. HCP1 is also up-regulated in hypoxic conditions such as those potentially encountered within the tumour substance. The normal physiological role of HCP1 is not solely to import haem but is also strongly associated with folate transport<sup>296</sup> and as such, caution must be given when considering the exact role of HCP1 in the malignant progression of OAC. In a similar fashion, LRP1 is putatively regarded as a haem import protein as part of a larger scavenging and signalling role<sup>298</sup>, although its role in carcinogenesis is yet to be fully explored. The non-specific membranous immunolocalisation of LRP1 observed in OAC is analogous to that observed in hepatocytes for the endocytosis of haemopexin bound haem<sup>300</sup>. Although it is likely that LRP1 is actively importing haem iron, given its ubiquitous nature, it may have another, as yet, unidentified function in carcinogenesis.

Although evident in the progression of dysplastic BM to OAC, LRP1 and HCP1 were not significantly associated with advanced OAC staging on semi-quantitative immunohistochemistry suggesting that further up-regulation in an established tumour is not essential to propagation of the malignant phenotype.

The up-regulation of FLVCR mRNA and protein expression in OAC and associated dysplastic BM was an unexpected observation based on the evidence that FLVCR is able to efflux haem and therefore potentially diminish the intracellular iron pool. However, the immunolocalisation of FLVCR is exclusively nuclear and therefore unlikely to be facilitating haem export from the cancer cell. FLVCR was first identified in erythrocyte precursors as an apically located membrane haem exporter keeping cytosolic haem concentrations below critical toxicity and plays a similar role in macrophages, post-phagocytosis of senescent erythrocytes, to prevent cell death when the ability of HO1 to detoxify haem is overwhelmed<sup>305</sup>. Similarly, in the face of increased haem import from overexpression of LRP1 and HCP1, the activity of HO1 to detoxify haem within a potentially hypoxic cancer cell may not be sufficient to prevent critical toxicity, promoting the protective expression of haem efflux proteins. However, this does not explain the apparent localisation of FLVCR to the nucleus unless to facilitate haem efflux and prevent toxicity within the nucleus. FLVCR has significant receptor homology with members of the Major Facilitator Superfamily<sup>305</sup> and could have a role other than haem iron transport in the nucleus. It may be possible that the FLVCR monoclonal antibody has significant cross-reactivity with members of the Major Facilitator Superfamily erroneously identifying FLVCR as a nuclear protein in OAC. This is the first time that FLVCR has been characterised in cancer genesis; it may be that other cancers exhibit similar nuclear immunolocalisation.

The observed up-regulation of BCRP mRNA, protein expression and immunolocalisation does not aid preservation of intracellular iron. However, the findings are consistent with observations in breast cancer where overexpression of the ATP-binding cassette transport system protects cells from cytotoxic agents due to drug efflux and is a major

mechanism mediating multi-drug resistance<sup>310</sup>. All of the analysed OAC and associated dysplastic BM was taken from resection specimens pre-exposed to neoadjuvant chemotherapy. These tumours may be subject to a selection bias, as those tumours with the ability to efflux chemotherapeutic agents would potentially be less likely to be obliterated at the time of resection and therefore more prevalent for research. There are very few studies on the expression pattern of BCRP in native tumour tissues and therefore the clinical relevance of BCRP in the pathophysiology of cancer is still unknown. Increased expression of BCRP from dysplastic BM to OAC could represent preserved negative feed-back in the presence of elevated intracellular haem concentrations driven by up-regulated haem import. In this capacity, it may be advantageous to the cancer cell to regulate cytosolic haem concentration to avoid haem toxicity, especially during hypoxic stress which is regularly encountered in rapidly expanding tumours. Indeed BCRP has a hypoxia responsive element, increasing expression and translocation to the cell membrane<sup>317</sup>.

Up-regulation of the haem import proteins appears to be an early event in the evolution of OAC and supports the hypothesis that OAC cells are able to acquire systemic organic iron in a manner analogous to that of inorganic iron. The apparent increase in expression of the haem export proteins in OAC is likely to be multi-factorial; however it may be that these proteins maintain a crucial detoxifying role especially during hypoxic stress.

# CHAPTER 4: THE *IN-VITRO* AND *IN-VIVO* EFFECTS OF HAEM AND ABROGATION OF HAEM TRANSPORT PROTEINS ON OESOPHAGEAL CANCER CELLS

## 4.1 Introduction

Whole body iron stores slowly accumulate with age, as intake gradually exceeds loss<sup>165</sup>. Cohort studies have correlated a replete iron state with increased risk of cancer mortality and the genetic iron loading disorder, haemochromatosis, is strongly associated with a variety of gastrointestinal malignancies<sup>151,152,154,155,166</sup>. Excessive red meat consumption is associated with OAC and oesophageal SCC development independent of preservation and cooking methods<sup>148,149</sup>. Furthermore, animal models receiving supplementary iron demonstrate progressive epithelial proliferation, hyperplasia, inflammation and iron deposition culminating in OAC<sup>150,170</sup>.

Inorganic iron has been strongly implicated in the development of BM and progression to invasive OAC<sup>171</sup>. A sequential up-regulation of inorganic iron import proteins, together with functional loss of iron export and subsequent iron loading has been established on progression through the BM-dysplasia-OAC sequence<sup>171</sup>. *In-vitro* culture of OAC cells with supplementary iron prompts avid proliferation and gross cellular iron loading<sup>171</sup>. The mechanistic consequence of up-regulating iron import proteins is the ability of OAC cells to acquire systemic iron via TfR1 mediated endocytosis<sup>171</sup>. The iron loaded OAC cell is then able to proliferate unencumbered by the finite constraints of iron dependent processes controlling the cell cycle<sup>186-188</sup>.

Dietary haem, principally derived from red meat, is readily bio-available and actively transported across the enterocytes brush border by HCP1<sup>271,274</sup>. Iron is then liberated from haem by HO1 within the enterocytes and enters the inorganic iron metabolic pathways<sup>270,276</sup>. In addition, there exists a large systemic pool of haemopexin bound haem, predominantly derived from the turn-over of senescent erythrocytes by the reticulo-endothelial system<sup>270,274,285</sup>. The recent identification of a systemic haemopexin receptor, LRP1, led to the hypothesis that OAC cells could also acquire systemic organic iron by endocytosis of haemopexin bound haem<sup>292</sup>. In chapter 3, *ex-vivo* oesophageal tissue was utilised to establish for the first time that haem import proteins LRP1 and HCP1 are both up-regulated in the progression of BM to invasive OAC. The extent to which LRP1 and HCP1 contribute to the malignant phenotype of OAC cells and the potential to abrogate these proteins as therapeutic targets is unknown.

## 4.2 Aims

1. Characterise the influence of LRP1 and HCP1 protein abrogation on cellular iron loading and iron transport protein expression *in-vitro*
2. Determine the impact of LRP1 and HCP1 silencing on cell phenotype
3. Examine the impact of LRP1 and HCP1 silencing on cell cycle
4. Investigate the impact of LRP1 and HCP1 abrogation on tumour burden in a murine model

## **4.3 Results**

### **4.3.1 Abrogation of LRP1 and HCP1 protein expression (LRP1 and HCP1 knock-downs)**

Stable LRP1 and HCP1 knock-downs (KD) were created in OE33, OE19 and OE21 cell lines by introducing pGIPZ constructs, using a lenti-virus vector, containing specifically designed shRNA sequences for LRP1 and HCP1. A non-silencing shRNA was used as a control and a double LRP1 and HCP1 KD was created by combining the viral vectors. Successfully knocked-down cells, containing an antibiotic resistance cassette as part of the pGIPZ construct, were selected by culture with Puromycin. Successful infection and expression of the pGIPZ construct was also visually confirmed by expression of GFP under blue light excitation (figure 4.1). Interference of LRP1 and HCP1 mRNA by siRNA and subsequent protein knock-down was confirmed by Western blotting (figure 4.2).

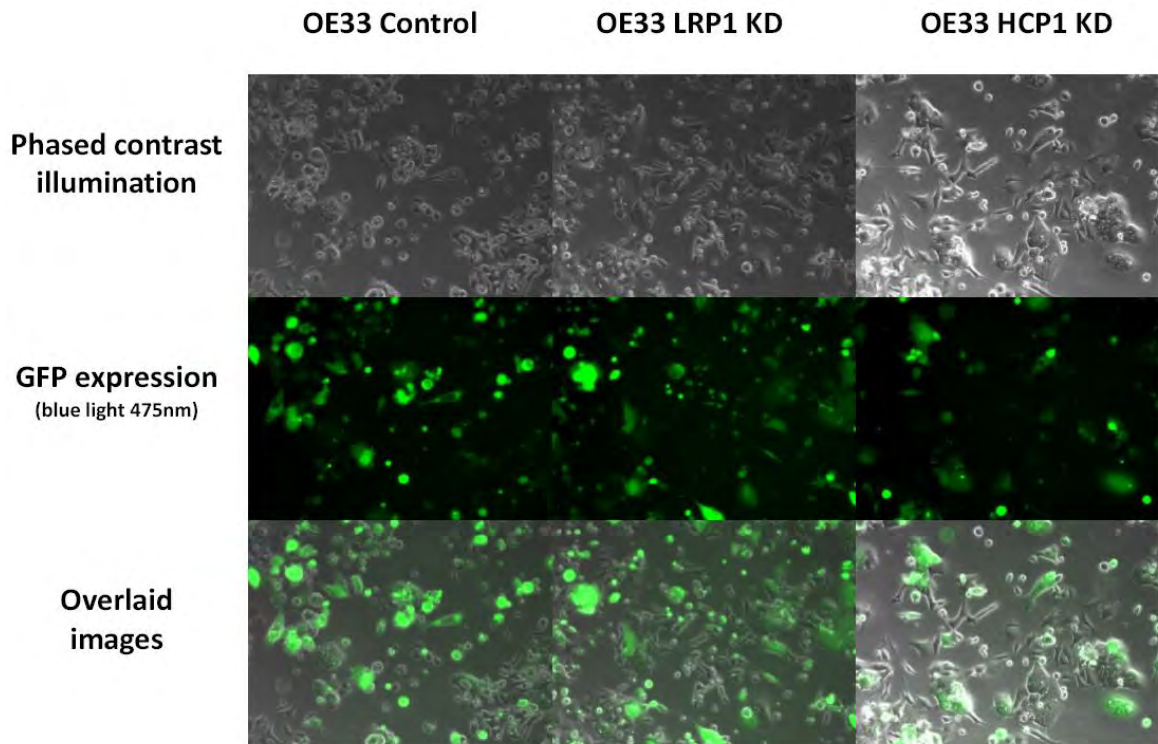


**Figure 4.1 OE33 cell line expressing GFP after successful infection with lenti-virus vector containing pGIPZ constructs and culture with Puromycin**

OE33 cell line was co-cultured with lenti-virus vector containing pGIPZ constructs specifically designed to abrogate LRP1 and HCP1 protein expression via RNAi. Each pGIPZ construct contains shRNA to LRP1, HCP1 or non-silencing control along with green fluorescent protein (GFP) expression and Puromycin resistance cassette. x60 magnification.

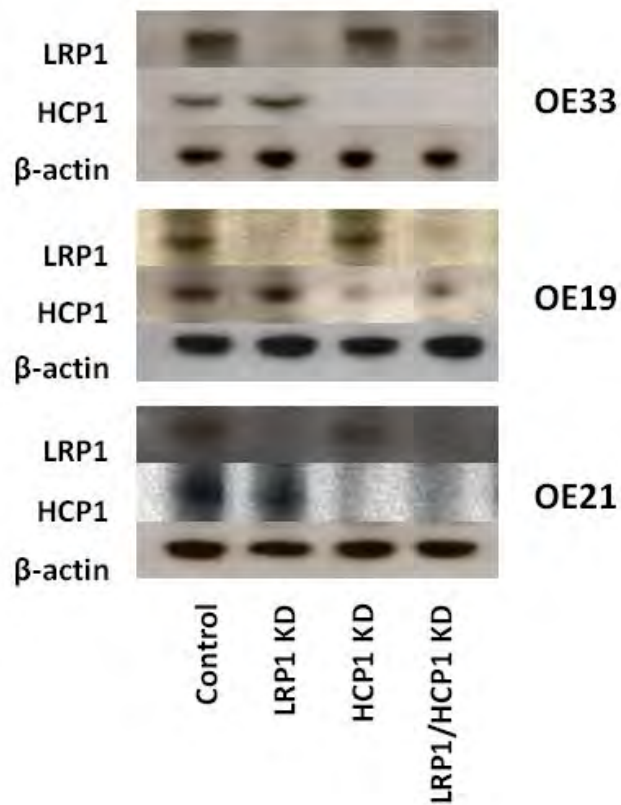


**Figure 4.2 Confirmation of successful silencing of LRP1 and HCP1 protein expression in OE33, OE19 and OE21 cell line knock-downs**

OE33, OE19 and OE21 cell line knock-downs (KD) were co-cultured with lenti-virus vector containing pGIPZ constructs specifically designed to abrogate LRP1 and HCP1 protein expression via RNAi. Successful silencing of LRP1 and HCP1 protein expression was confirmed by Western blotting.  $\beta$ -actin used as an internal protein loading control.

### **4.3.2 Characterisation of the influence of LRP1 and HCP1 protein abrogation on cellular iron loading and iron transport protein expression *in-vitro***

#### **4.3.2.1 LRP1 and HCP1 knock-down suppresses cellular ability to acquire haem to augment the intracellular iron pool compared to control**

To determine if the abrogation of haem importing proteins, LRP1 and HCP1, has an effect on intracellular iron concentration, OE33, OE19 and OE21 cell line knock-downs (non-silencing control, LRP1, HCP1 and LRP1/HCP1 knock-downs) were cultured in control or haem loaded media (20 $\mu$ M) for 48 hours prior to ferrozine assay (figure 4.3).

After 48 hours of culture in plain media, there was no significant difference in cellular iron concentration between non-silenced control and LRP1, HCP1 and combined knock-downs in any cell line. A significant difference was seen between non-silenced controls cultured in control media and haem loaded media ( $p=0.001$  for all cell lines). This significance was lost when LRP1, HCP1 and LRP1/HCP1 knock-downs, across all cell lines, were cultured in haem loaded media.

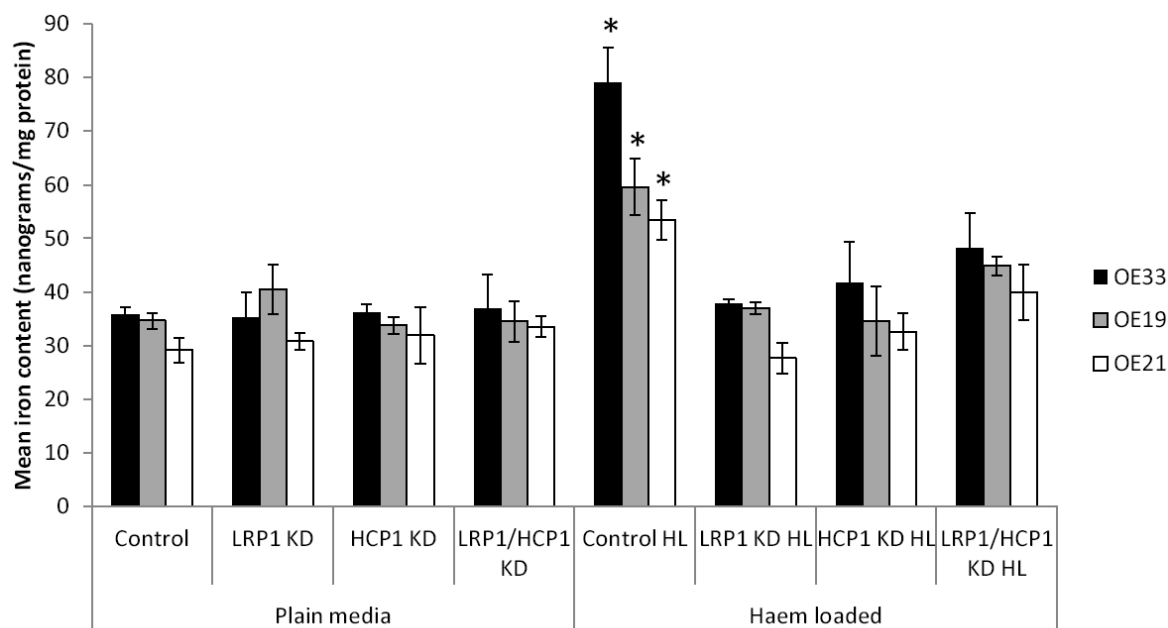


**Figure 4.3 LRP1 and HCP1 knock-down suppresses cellular ability to acquire haem to augment the intracellular iron pool compared to control**

OE33, OE19 and OE21 cell line knock-downs were cultured with or without 20 $\mu$ M haem for 48 hours and processed for a ferrozine assay. No significant difference in intracellular iron was seen between non-silenced control and knock-downs when cultured in media alone. Non-silenced control cells, across all three lines, demonstrated a significant increase in intracellular iron (\* $p=0.001$ ) when cultured with haem. However, knock-down of LRP1 and HCP1 suppressed cellular ability to acquire haem, even in the presence of haem loaded media, there was no significant difference in intracellular iron concentration when compared to non-silenced controls grown in media alone. Control: non-silenced control; HL: haem loaded; KD: knock-down. N=3 for each regime. Error bars denote  $\pm$  SEM.

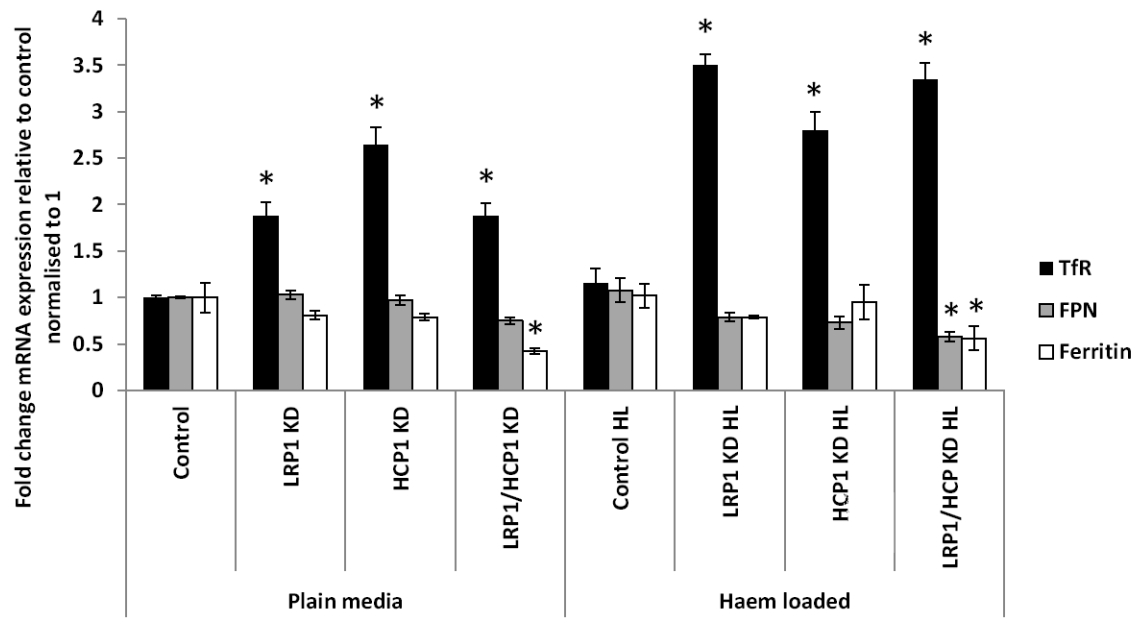
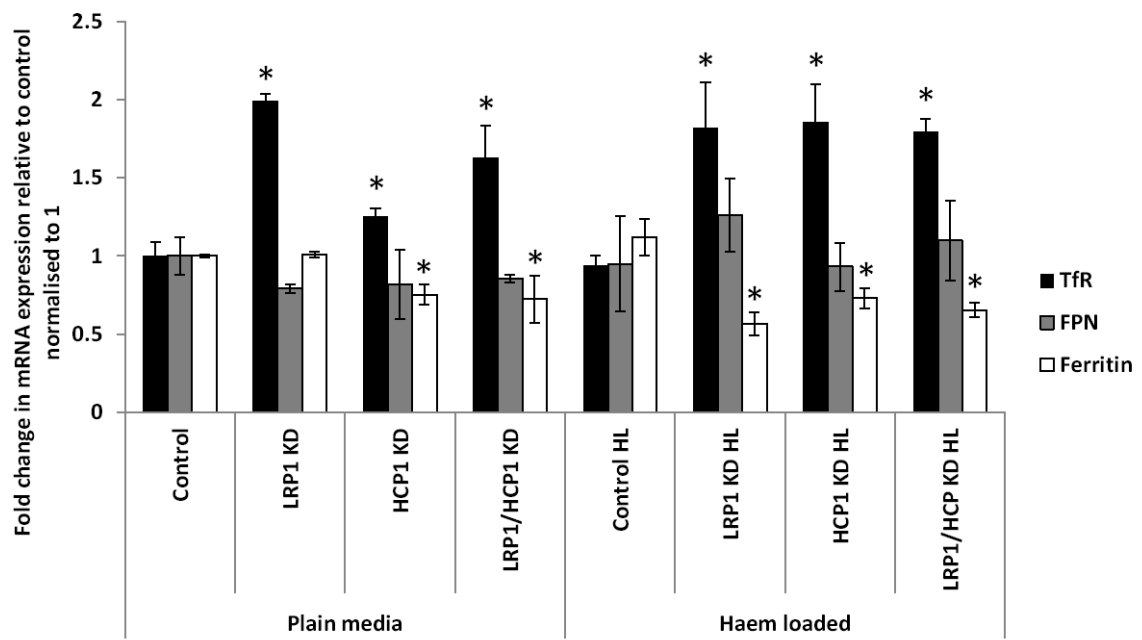
#### **4.3.2.2 Knock-down of LRP1 and HCP1 proteins in oesophageal cancer cells influences mRNA of iron transport proteins**

OE33, OE19 and OE21 cell line knock-downs were cultured with or without 20 $\mu$ M haem for 48 hours. Cells were then harvested and mRNA expression for TfR1, FPN and ferritin determined using qRT-PCR (figure 4.4).

TfR1 mRNA expression was significantly increased, compared to control, in LRP1 and HCP1 knock-down cells cultured with or without supplementary haem. Up-regulation of TfR1 mRNA was preserved across all three cell lines (all  $p < 0.05$ ). No difference in TfR1 mRNA expression was seen between non-silenced cells cultured with or without haem.

Overall, FPN mRNA expression in knock-down cells trended towards a decrease in fold change in the presence or absence of supplementary haem, reaching significance in a number of cases: OE33 LRP1/HCP1 KD haem loaded  $0.75 \pm 0.05$   $p = 0.05$ ; OE21 HCP1 KD  $0.69 \pm 0.13$   $p = 0.048$ ; OE21 LRP1 KD and HCP1 KD haem loaded  $0.5 \pm 0.12$ ,  $0.43 \pm 0.02$   $p = 0.04$  and  $0.01$  respectively.

Ferritin mRNA expression was significantly repressed in the majority of knock-downs compared to non-silenced control in the presence or absence of haem loading. Fold change in ferritin mRNA was most marked in the OE19 cell line (all  $p$ -values  $\leq 0.05$  except LRP1 KD which showed no change in ferritin mRNA expression). Again, no change in mRNA expression was noted when non-silenced controls were cultured with supplementary haem.

**A****B**

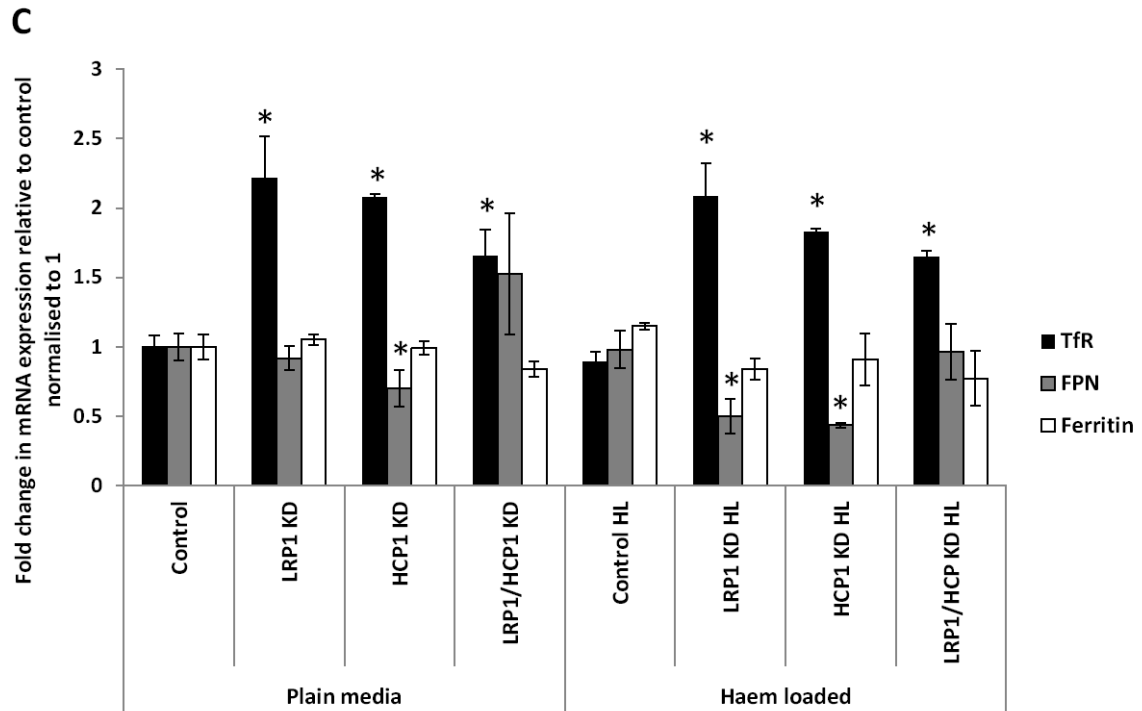


**Figure 4.4 Knock-down of LRP1 or HCP1 proteins alters TfR1, FPN and ferritin mRNA expression**

Figure A: OE33, Figure B: OE19 and Figure C: OE21 knock-downs were cultured with or without 20µM haem for 48 hours. Control: non-silenced control; KD: knock-down; HL: haem loaded. (\*p=<0.05 compared to non-silenced control cultured in plain media). Error bars denote ± SEM.

#### **4.3.2.3 Knock-down of LRP1 and HCP1 proteins in oesophageal cancer cells influences iron transport protein expression**

OE33, OE19 and OE21 cell line knock-downs were cultured with or without 20 $\mu$ M haem for 48 hours. Cells were then harvested and protein expression for TfR1, FPN and ferritin determined by Western blotting (figure 4.5: OE33, figure 4.6: OE19 and figure 4.7: OE21).

TfR1 protein expression was significantly elevated in LRP1 and HCP1 knock-downs compared to non-silenced control across all three cell lines with changes most marked in the SCC OE21 cell line (all  $p < 0.05$ ). No change in TfR1 protein expression was seen when non-silenced control cells were cultured in plain or haem loaded media.

FPN protein expression varied across the cell lines. OE33 LRP1 and HCP1 knock-downs demonstrated significant decreases in FPN protein expression when cultured in either plain or haem loaded media, broadly in keeping with changes seen at the mRNA level (all  $p$ -values  $< 0.05$ ). OE19 and OE21 cell line knock-downs showed no significant change or slight elevation in FPN protein expression when cultured with haem loaded media. No change in FPN protein expression was demonstrated between non-silenced controls cultured in plain or haem loaded media in any cell line.

Ferritin protein expression was suppressed in OE33 and OE19 LRP1 and HCP1 knock-downs cultured in plain media compared to non-silenced controls. When cultured with haem loaded media, ferritin expression in the OE19 and OE21 cell line knock-downs tended towards a marginal elevation reaching significance in a minority. In all knock-downs demonstrating increased ferritin protein expression, none were higher than their respective haem loaded non-silenced controls. OE19 and OE21 cell lines demonstrated

significant increases in ferritin protein expression in non-silenced haem loaded controls compared to non-silenced controls cultured in plain media (OE19:  $1.43 \pm 0.24$   $p=0.01$  and OE21:  $1.96 \pm 0.34$   $p=0.02$ ).

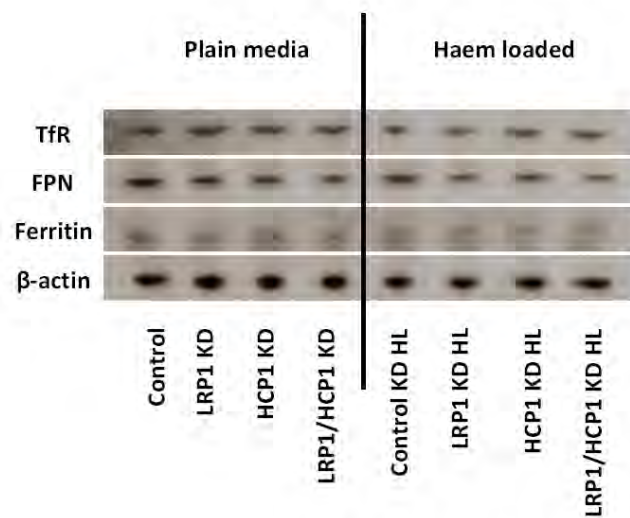
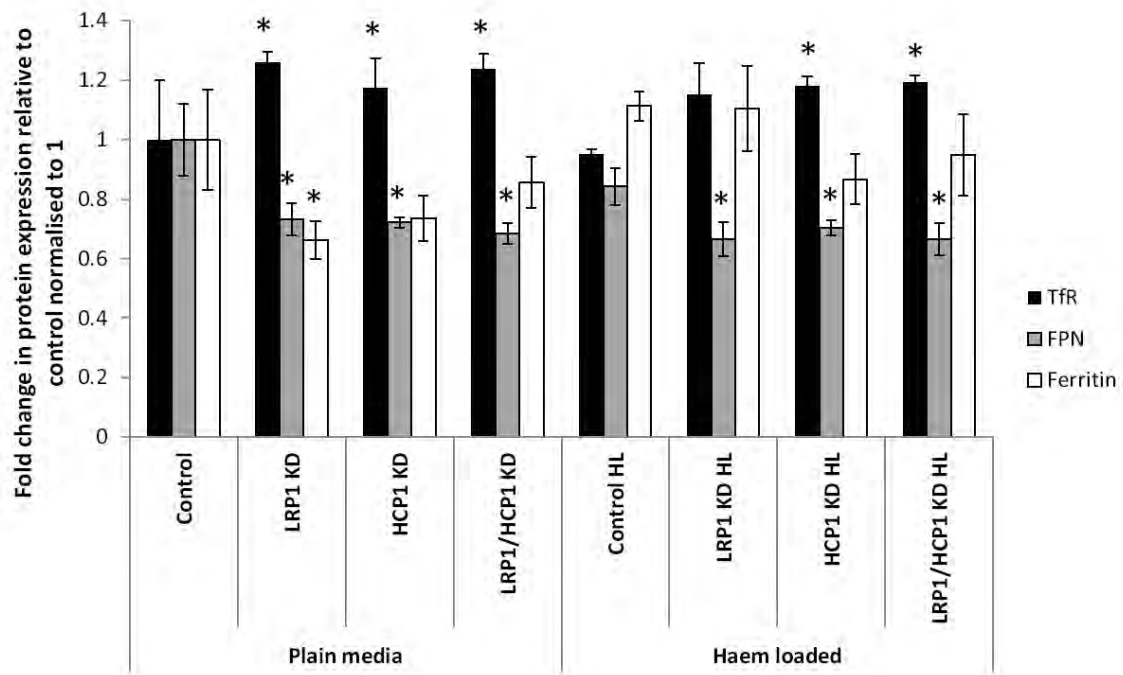


**Figure 4.5 Knock-down of LRP1 and HCP1 proteins in the OE33 cell line alters TfR1, FPN and ferritin protein expression**

OE33 cell line knock-downs cultured with or without 20µM haem for 48 hours. Control: non-silenced control; KD: knock-down; HL: haem loaded. (\*p<0.05 fold change in protein expression compared to non-silenced control cultured in plain media). Error bars denote ± SEM.

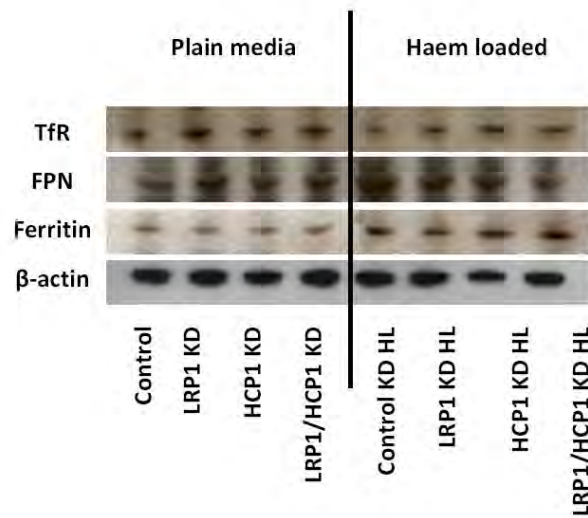
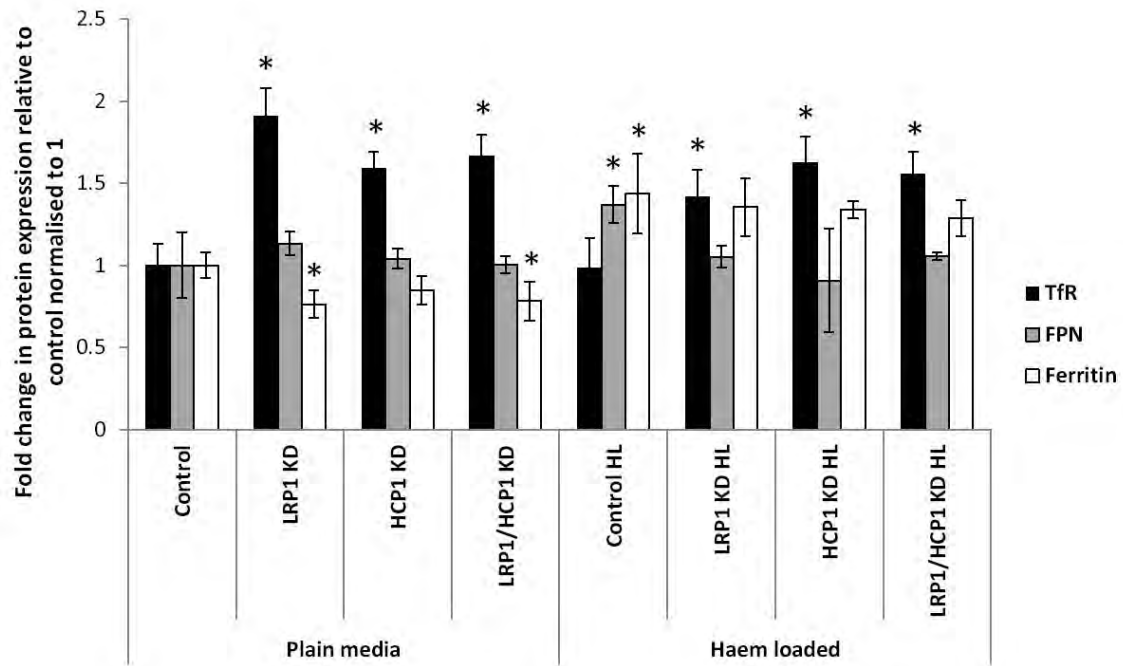


**Figure 4.6 Knock-down of LRP1 and HCP1 proteins in the OE19 cell line alters TfR1, FPN and ferritin protein expression**

OE19 cell line knock-downs cultured with or without 20µM haem for 48 hours. Control: non-silenced control; KD: knock-down; HL: haem loaded. (\*p<0.05 fold change in protein expression compared to non-silenced control cultured in plain media). Error bars denote ± SEM.

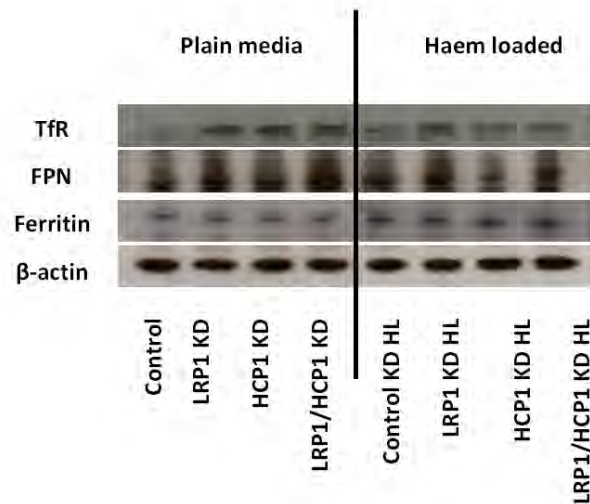
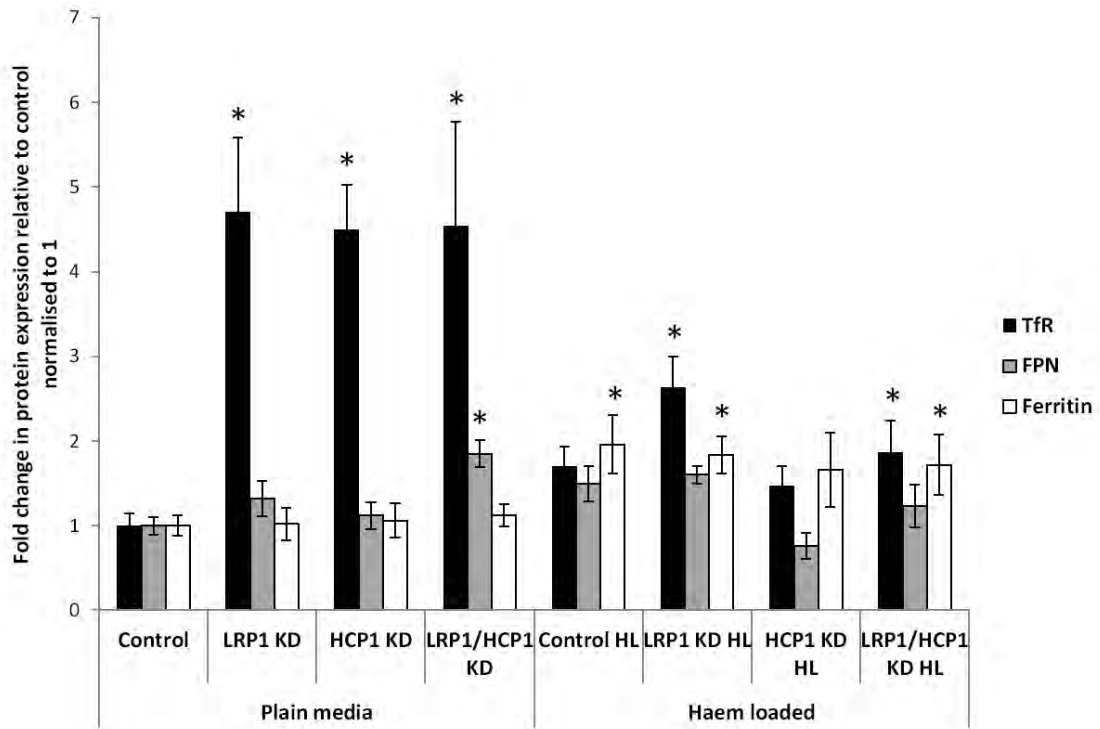


**Figure 4.7 Knock-down of LRP1 and HCP1 proteins in the OE21 cell line alters TfR1, FPN and ferritin protein expression**

OE21 cell line knock-downs cultured with or without 20µM haem for 48 hours. Control: non-silenced control; KD: knock-down; HL: haem loaded. (\* $p < 0.05$  fold change in protein expression compared to non-silenced control cultured in plain media). Error bars denote  $\pm$  SEM.

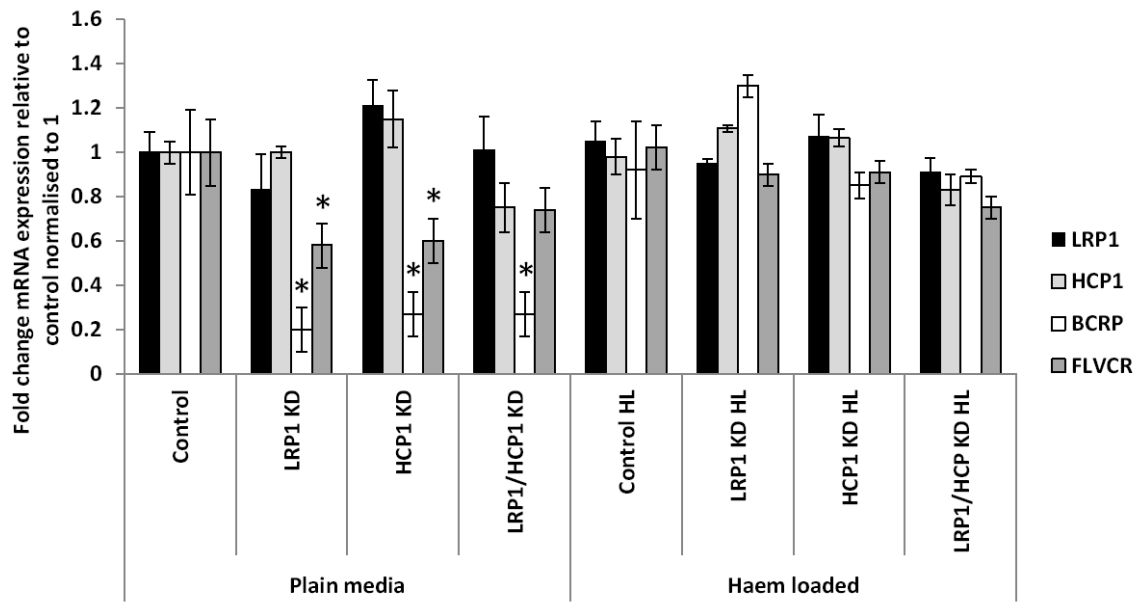
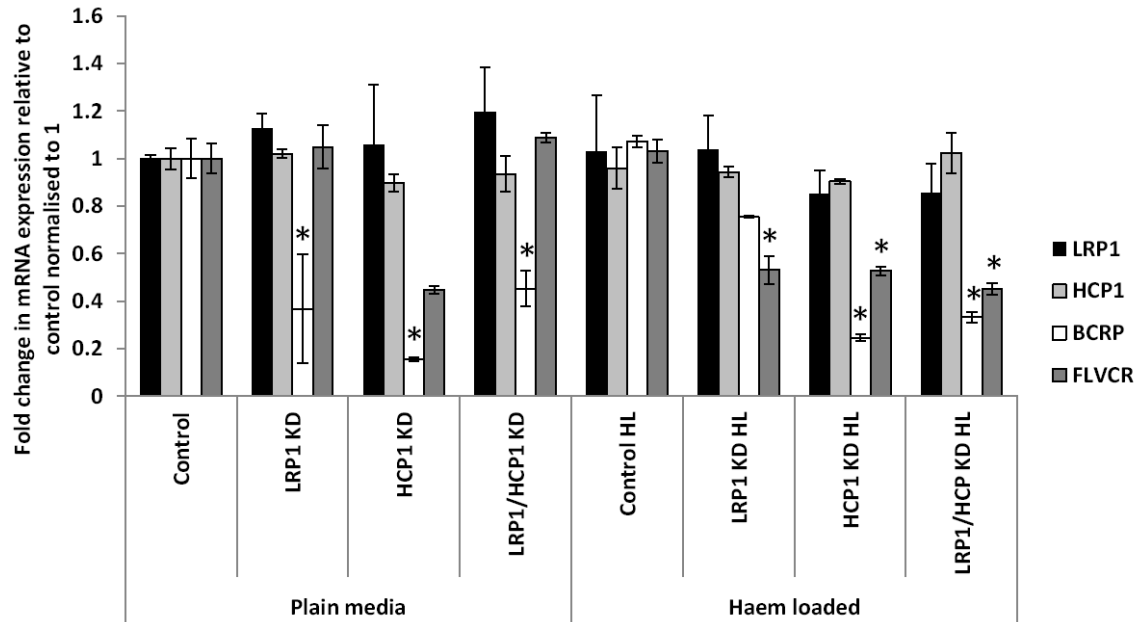
#### **4.3.2.4 Knock-down of LRP1 and HCP1 proteins in oesophageal cancer cells alters mRNA expression of haem transporting proteins**

OE33, OE19 and OE21 cell line knock-downs were cultured with or without 20 $\mu$ M haem for 48 hours. Cells were then harvested and mRNA expression for LRP1, HCP1, BCRP and FLVCR determined using qRT-PCR (figure 4.8 A: OE33, B: OE19 and C: OE21).

Haem importing proteins LRP1 and HCP1 were targets for RNAi. Loss of LRP1 protein expression did not influence HCP1 mRNA expression. This observation held true across all cell lines; in the presence or absence of haem loading. Conversely the loss of HCP1 protein expression showed a significant increase in LRP1 mRNA expression in the OE21 cell line but no change in the OAC lines, OE33 and OE19 ( $1.58\pm 0.24$ ,  $p=0.024$  and  $1.36\pm 0.31$ ,  $p=0.048$  for OE21 HCP1 KD plain media and haem loaded media respectively).

mRNA expression for the haem effluxing proteins BCRP and FLVCR generally demonstrated a significant decrease in the presence of LRP1 and HCP1 knock-downs. However, this observation was not consistent across the panel of cell lines. Both BCRP and FLVCR mRNA expression was suppressed in OE33 knock-downs cultured in plain but not haem loaded media. BCRP mRNA expression was significantly reduced in OE19 knock-downs cultured in plain media and both BCRP and FLVCR mRNA expression was suppressed with the presence of haem loading. OE21 knock-downs exhibited significantly repressed BCRP mRNA expression in plain media but little difference compared to non-silenced control with the addition of haem loading. Conversely, OE21 knock-downs showed a significant decrease in FLVCR mRNA expression in haem loaded media but no change in expression compared to non-silenced control in plain media. Interestingly, no

significant difference in either BCRP or FLVCR mRNA expression was noted between non-silenced controls cultured in plain or haem loaded media across the three cell lines.

**A****B**

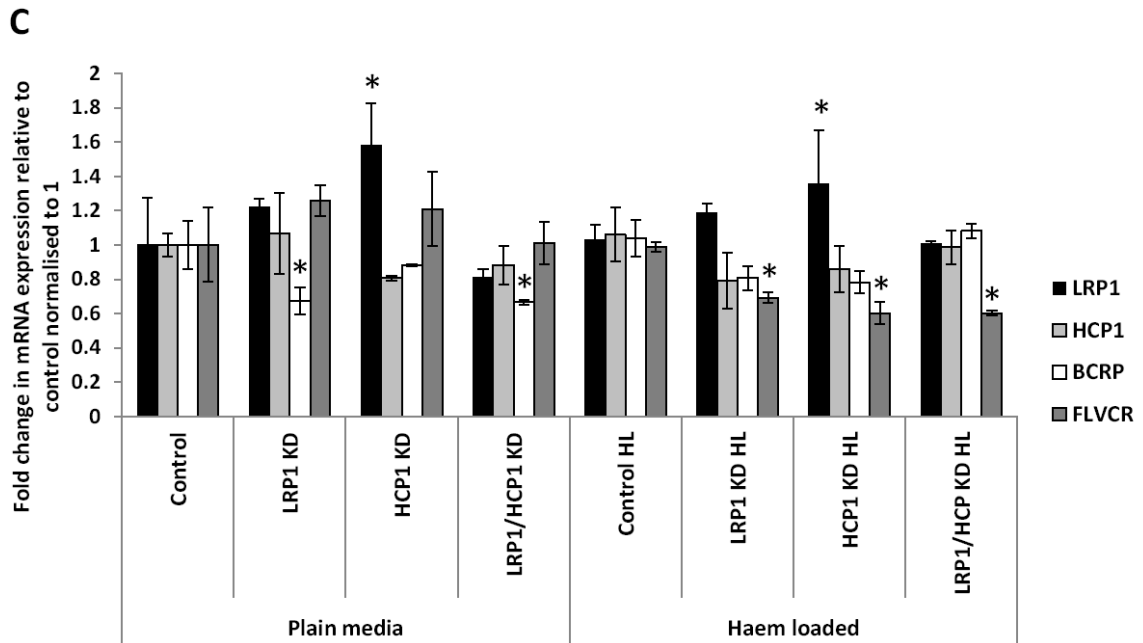


**Figure 4.8 Knock-down of LRP1 or HCP1 proteins alters mRNA expression of haem transport proteins**

Figure A: OE33, figure B: OE19 and figure C: OE21. OE33, OE19 and OE21 LRP1, HCP1 and combined knock-downs were cultured with or without 20 $\mu$ M haem for 48 hours. Control: non-silenced control; KD: knock-down; HL: haem loaded. (\* $p < 0.05$  compared to non-silenced control cultured in plain media). Error bars denote  $\pm$  SEM.

#### **4.3.2.5 Knock-down of LRP1 and HCP1 proteins in oesophageal cancer cells influences haem transport protein expression**

OE33, OE19 and OE21 cell line knock-downs were cultured with or without 20 $\mu$ M haem for 48 hours. Cells were then harvested and protein expression for LRP1, HCP1, BCRP and FLVCR determined by Western blotting (figure 4.9: OE33, figure 4.10: OE19 and figure 4.11: OE21).

LRP1 and HCP1 proteins were successfully knocked-down with negligible protein expression seen on Western blotting. As previously noted with mRNA expression, there was very little interplay between expression of the haem import proteins with no compensatory increase in HCP1 protein expression on knock-down of LRP1 and vice-versa, no up-regulation of LRP1 in the absence of HCP1 protein expression. One exception was the OE21 LRP1 knock-down cultured in haem loaded media that demonstrated a significant increase in HCP1 protein expression ( $1.57\pm 0.35$ ,  $p=0.001$ ).

Expression of the haem efflux protein BCRP was significantly reduced in all knock-downs of the OE33 and OE21 cell lines but did not alter those of OE19 cell line origin.

FLVCR expression was affected to a much lesser degree with suppression seen in the OE19 cell line knock-downs cultured in plain media only (OE19 fold changes:  $0.66\pm 0.03$ ,  $0.57\pm 0.04$  and  $0.63\pm 0.02$  for LRP1 KD, HCP1 KD and LRP1/HCP1 KD respectively). On comparison of the non-silenced controls, OE19 controls alone exhibited a significant increase in BCRP expression when cultured in haem loaded media. No change was observed for FLVCR expression across the cell panel.

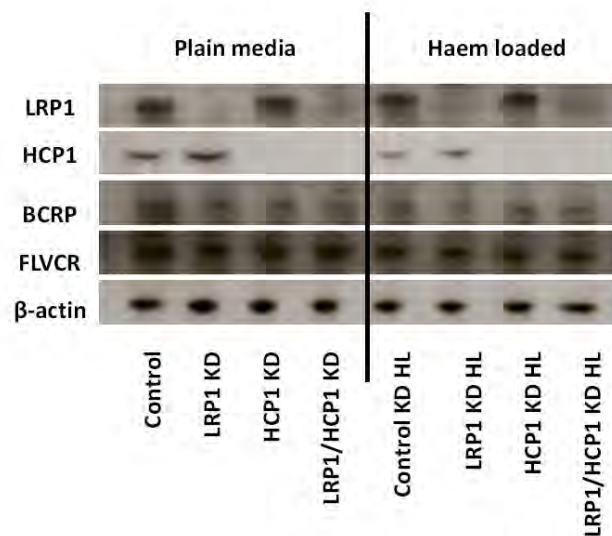
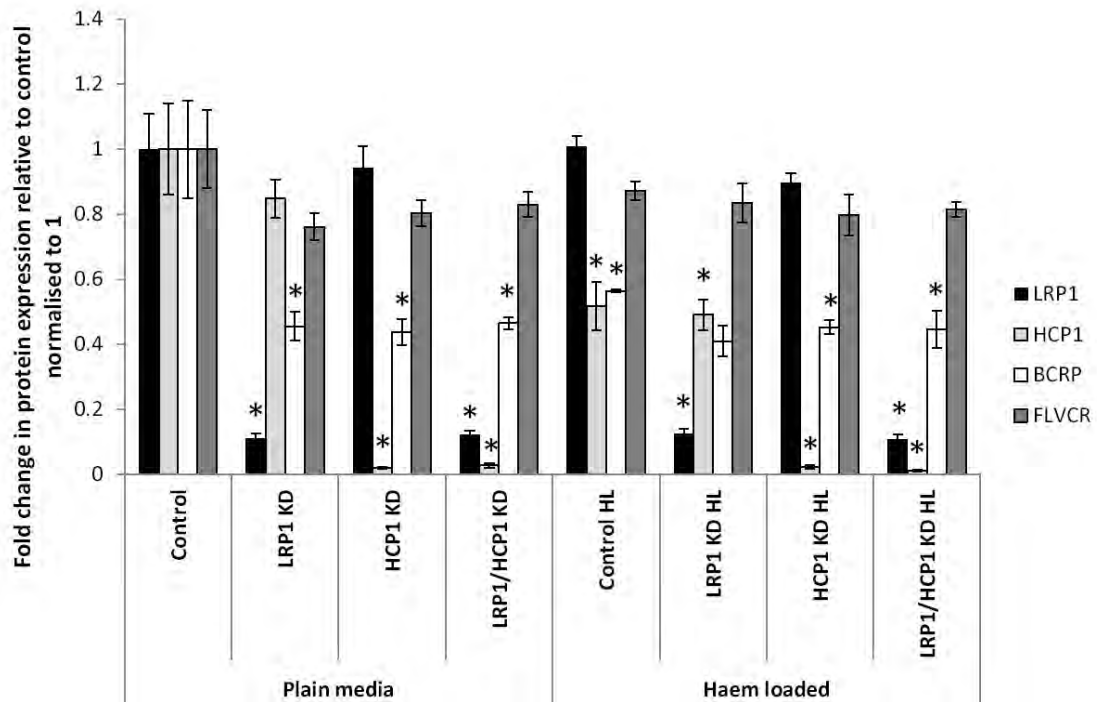


**Figure 4.9 Confirmation of knock-down of LRP1 and HCP1 proteins in OE33 cell line and altered expression of haem transporting proteins**

OE33 cell line knock-downs cultured with or without 20µM haem for 48 hours. Control: non-silenced control; KD: knock-down; HL: haem loaded. (\*p<0.05 fold change in protein expression compared to non-silenced control cultured in plain media). Error bars denote ± SEM.

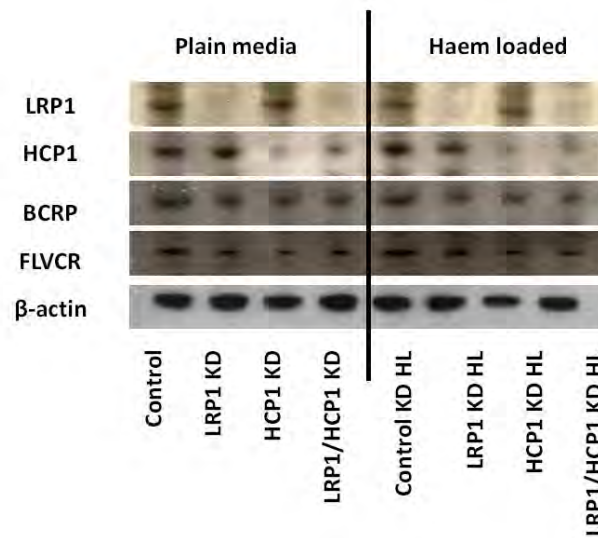
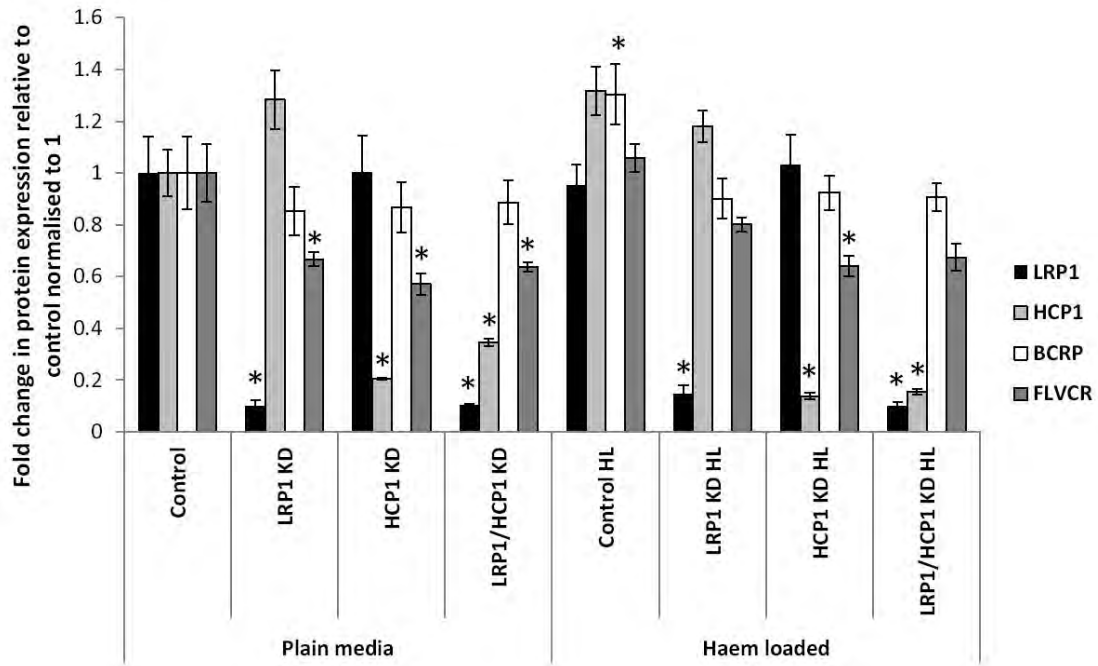


**Figure 4.10 Confirmation of knock-down of LRP1 and HCP1 proteins in OE19 cell line and altered expression of haem transporting proteins**

OE19 cell line knock-downs cultured with or without 20µM haem for 48 hours. Control: non-silenced control; KD: knock-down; HL: haem loaded. (\*p<0.05 fold change in protein expression compared to non-silenced control cultured in plain media). Error bars denote ± SEM.

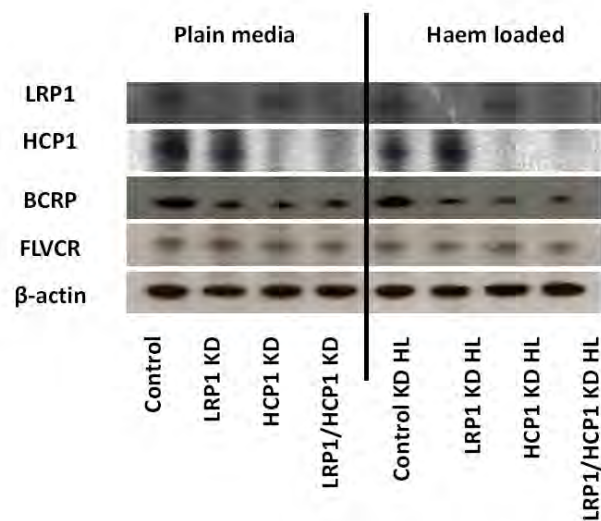
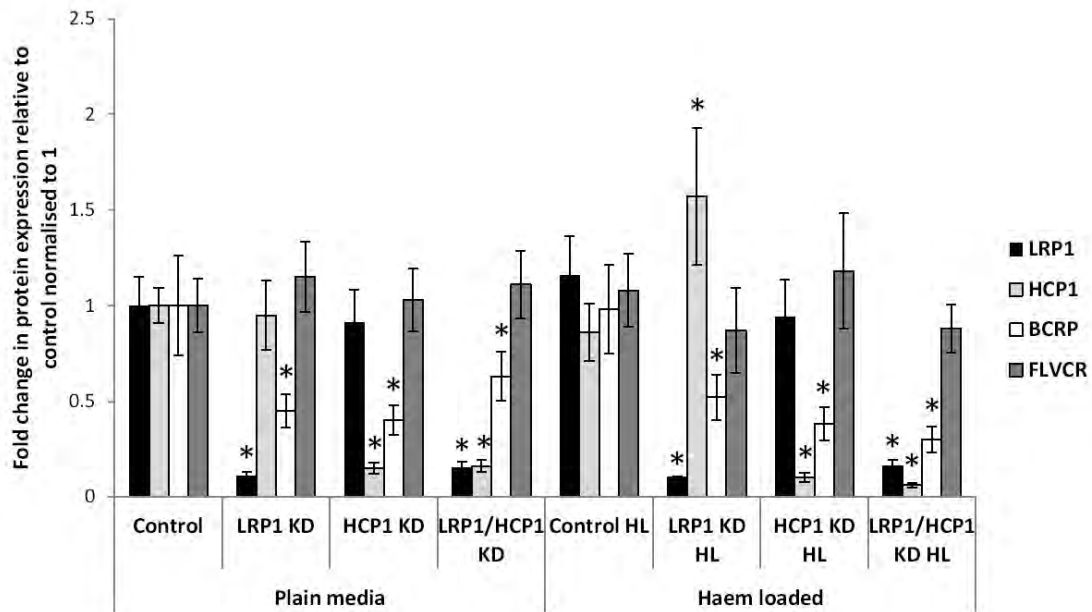


**Figure 4.11 Confirmation of knock-down of LRP1 and HCP1 proteins in OE21 cell line and altered expression of haem transporting proteins**

OE21 cell line knock-downs cultured with or without 20µM haem for 48 hours. Control: non-silenced control; KD: knock-down; HL: haem loaded. (\*p<0.05 fold change in protein expression compared to non-silenced control cultured in plain media). Error bars denote ± SEM.

### **4.3.3 Determination of the impact of LRP1 and HCP1 silencing on cell viability, proliferation and phenotype**

An increase in intracellular iron increases cellular viability, proliferation and creates a more aggressive phenotype. Up-regulation of the haem importing proteins LRP1 and HCP1 in *ex-vivo* OAC samples suggests that OAC cells are able to acquire circulating haem by scavenging free haem or capturing haemopexin bound haem to augment the intracellular iron pool. Abrogation of the active haem import proteins should therefore have an impact on cellular viability, proliferation and phenotype.

#### **4.3.3.1 LRP1 and HCP1 knock-down reduces oesophageal cancer cell viability and proliferation and neutralises the stimulatory effect of supplementary haem**

OE33, OE19 and OE21 cell line LRP1 and HCP1 knock-downs were cultured with or without supplementary haem (20 $\mu$ M) for 48 hours. Cells were then assessed for differences in cellular viability and proliferation with MTT and BrdU assays respectively (Figure 4.12).

When cultured with plain media, LRP1 and HCP1 knock-downs derived from the OAC line OE33 did not demonstrate any change in either viability or proliferation. However, when cultured in the presence of supplementary haem, the viability and proliferation of the non-silenced control was significantly enhanced ( $p=0.007$  and  $p=0.0039$ ) compared to culture in plain media alone. The increase in viability and proliferation induced by supplementary haem was lost in the LRP1 and HCP1 knock-downs. This observation was consistent across all three cell lines. OE19 knock-downs, cultured in plain media, demonstrated significantly reduced viability compared to non-silenced control in both

LRP1 and HCP1 knock-downs but the double LRP1/HCP1 knock-down missed significance ( $p=0.0052$ ,  $p=0.034$  and  $p=0.14$  respectively). OE19 knock-down proliferation was not significantly different from control in plain media. Supplementary haem enhanced viability and proliferation in the non-silenced OE19 control ( $p=0.05$  and  $p=0.02$ ) which was again lost in the LRP1 and HCP1 knock-downs that were no different to plain media control. The most marked changes in viability and proliferation were determined in the oesophageal SCC cell line OE21. HCP1 and the double LRP1/HCP1 knock-down both demonstrated significantly reduced viability compared to non-silenced control ( $p=0.006$  and  $p=0.016$ ). Proliferation was reduced in all three OE21 knock downs cultured in plain media ( $p=0.0046$ ,  $p=0.012$  and  $p=0.0005$  for HCP1, LRP1 and LRP1/HCP1 KDs respectively). OE21 non-silenced controls cultured with supplementary haem exhibited an expected increase in viability and proliferation ( $p=0.012$ ,  $p=0.05$ ) compared to plain media alone. OE21 knock-downs continued the observed trend in lacking any enhanced viability in the presence of supplementary haem and actually showed a decrease in proliferation compared to non-silenced plain media control ( $p=0.01$ ,  $p=0.6$  and  $p=0.05$  for HCP1, LRP1 and LRP1/HCP1 KD respectively).

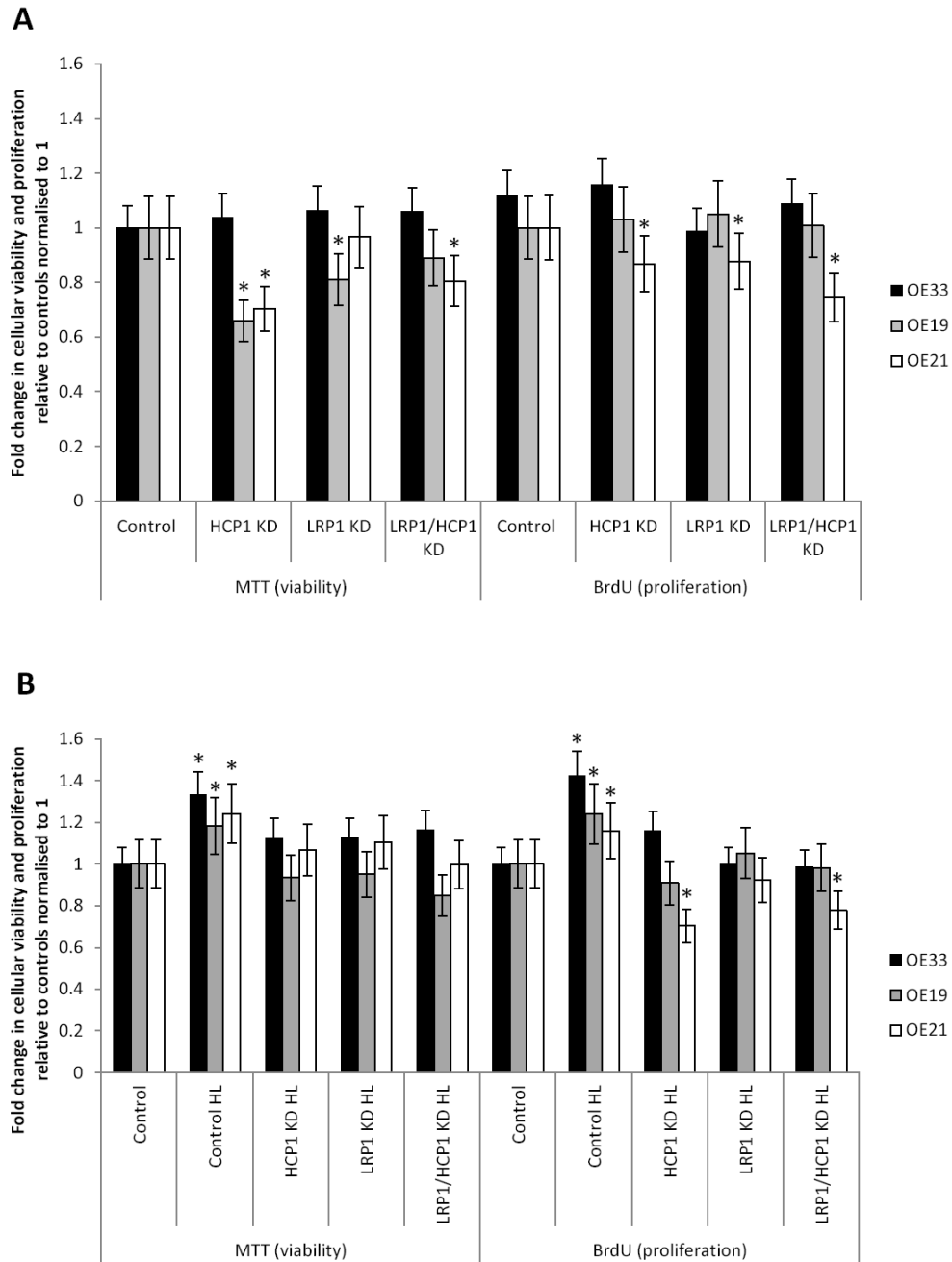
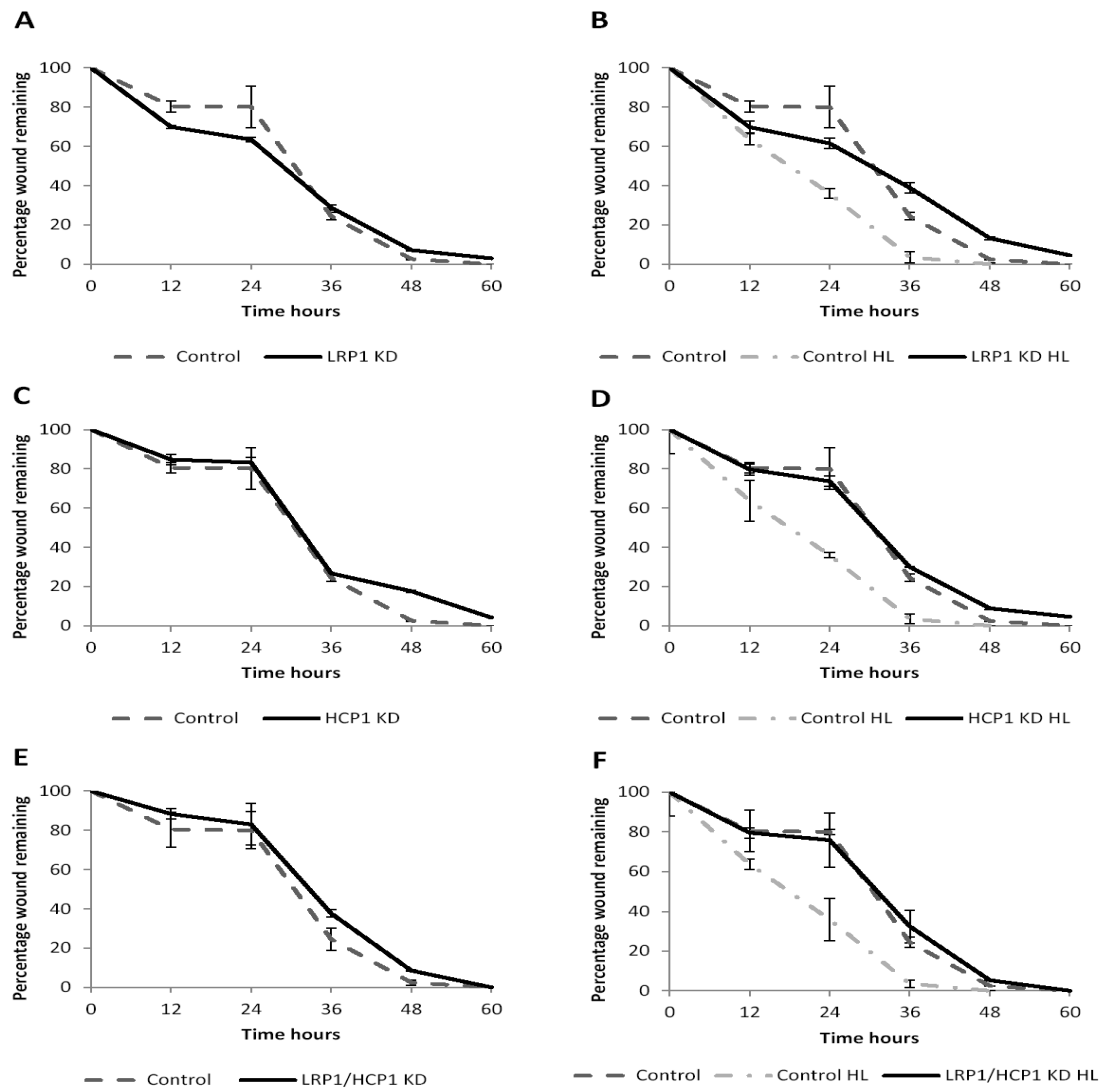


**Figure 4.12 LRP1 and HCP1 knock-down reduces oesophageal cancer cell viability and proliferation and neutralises the stimulatory effect of supplementary haem**

OE33, OE19 and OE21 cell line knock-downs cultured in plain media (figure A) or 20µM haem (figure B) for 48 hours. Control: non-silenced control; KD: knock-down; HL: haem loaded. (\* $p < 0.05$  fold change in viability or proliferation compared to non-silenced control cultured in plain media).

#### **4.3.3.2 LRP1 and HCP1 knock-down prevents the stimulatory effect of supplementary haem on oesophageal cancer cell migration**

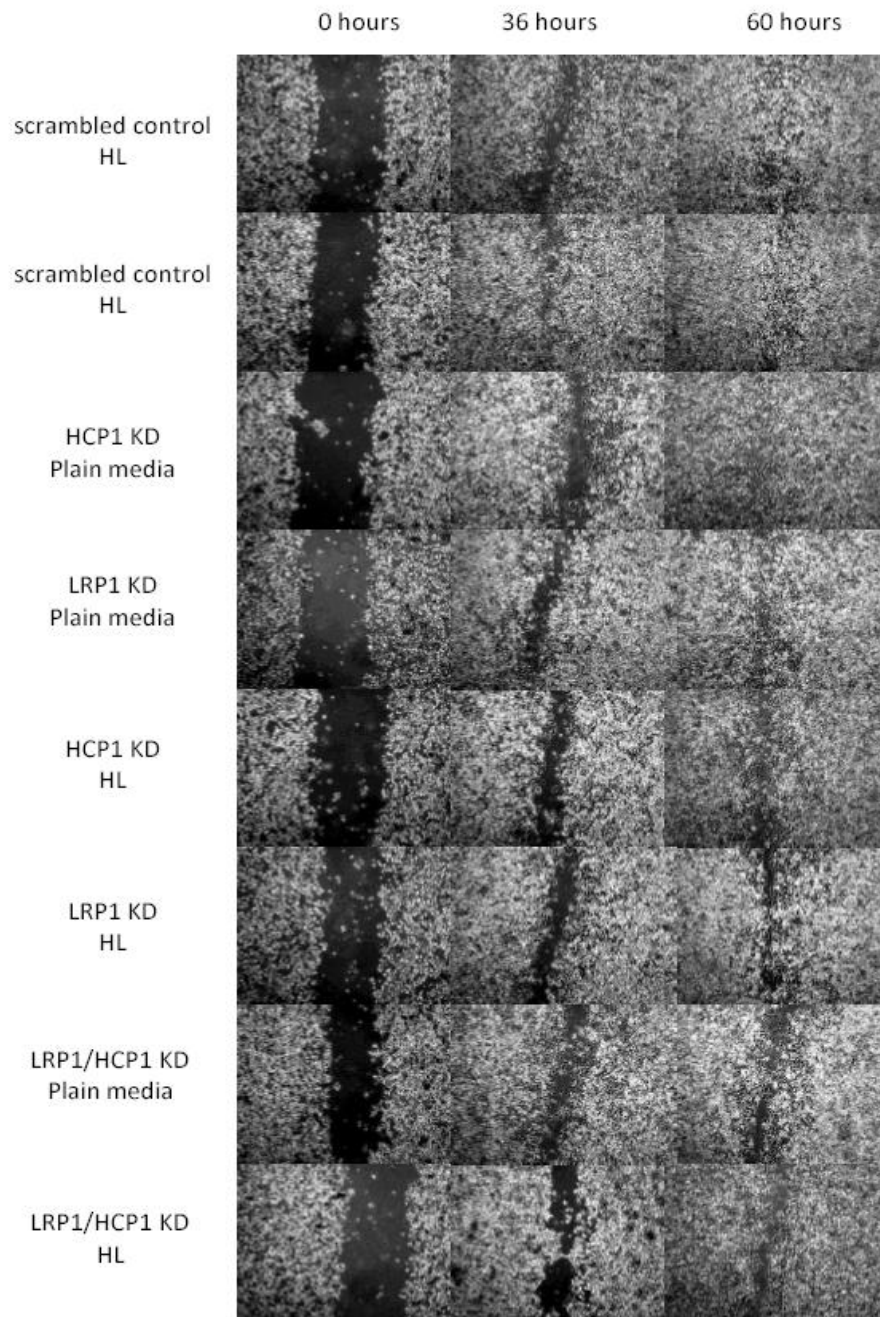
OE33, OE19 and OE21 cell line LRP1 and HCP1 knock-downs were cultured until 100 percent confluent. The cellular monolayer was then scratched to create a “wound” and media substituted for either fresh plain media (control) or media supplemented with 20µM haem. Cellular migration across the wound was visually recorded at 12 hourly intervals and expressed as a percentage of wound remaining (figures 4.13 and 4.14: OE33, figures 4.15 and 4.16: OE19 and figures 4.17 and 4.18: OE21). After 60 hours of observation the majority of scratch wounds had healed. No significant difference was noted in cell migration rate between non-silenced controls and LRP1 or HCP1 knock-downs cultured in plain media. OE19 and OE21 double LRP1/HCP1 knock-downs cultured in plain media did show a significant reduction in overall wound healing compared to control ( $p=0.032$  and  $p=0.001$  for OE19 and OE21 LRP1/HCP1 KD). In all three cell lines the addition of supplementary haem to the culture media of non-silenced controls led to a significant increase in the rate of overall wound closure (non-silenced control plain media vs. non-silenced control haem supplemented media  $p=0.001$ ,  $p=0.04$  and  $p=0.05$  for OE33, OE19 and OE21 respectively). The stimulatory effect of supplementary haem on non-silenced control was lost upon knock-down of either LRP1 or HCP1 in all three cell lines with no significant difference in cell migration compared to plain media control. Again, the double LRP1/HCP1 knock-downs of OE19 and OE21 demonstrated reduced cellular migration with significantly inhibited overall wound closure rates compared to plain media control ( $p=0.02$  and  $p=0.0001$  for OE19 and OE21). OE33 double LRP1/HCP1 knock-down it not show a significant reduction in migratory ability compared to non-silenced control cultured in plain or haem supplemented media.



**Figure 4.13 LRP1 and HCP1 knock-down prevents the stimulatory effect of supplementary haem on OE33 cell line migration**

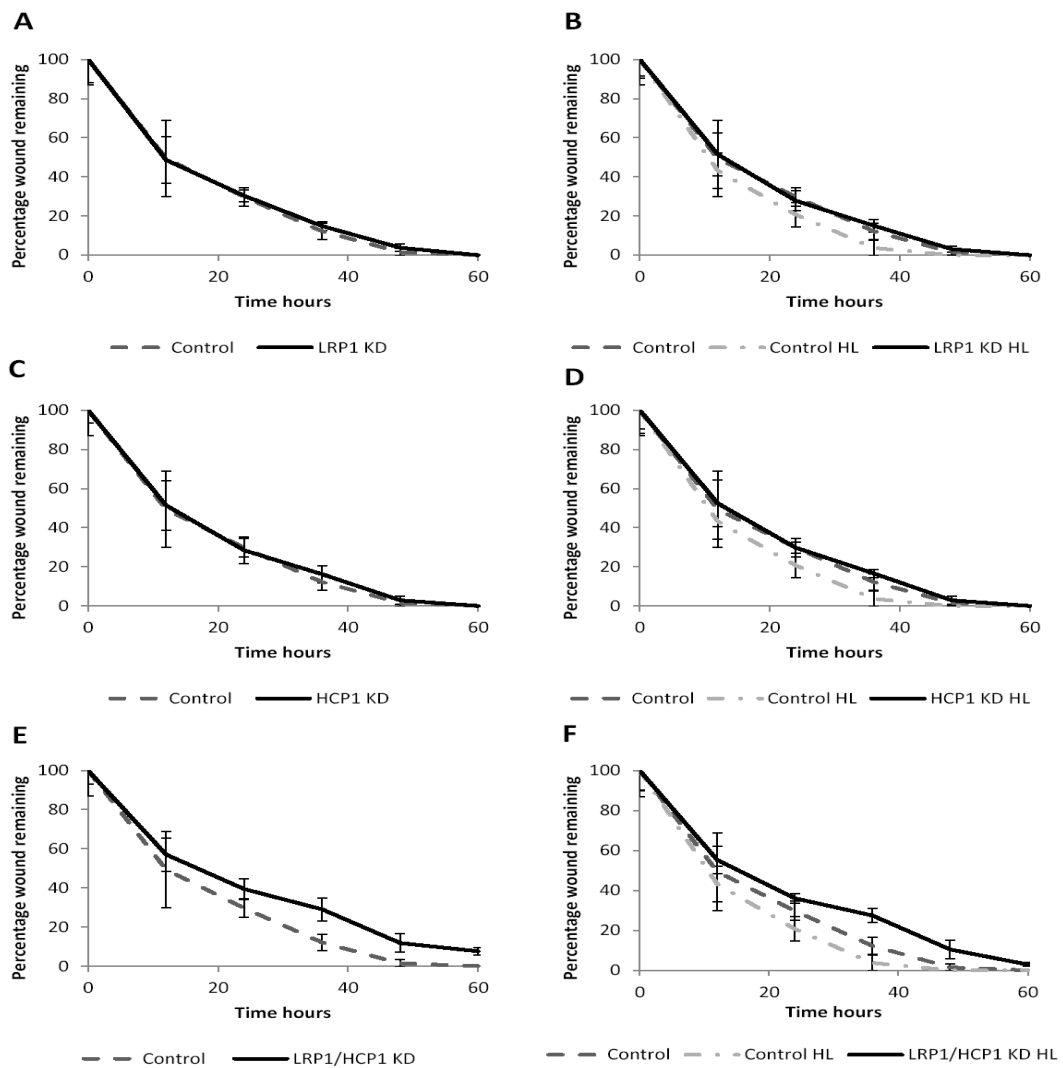
OE33 cell line knock-downs cultured in plain media or 20 $\mu$ M haem loaded media (n=9).

Figure A: non-silenced control vs. LRP1 KD, figure B: non-silenced control plain and HL media vs. LRP1 KD HL, figure C: non-silenced control vs. HCP1 KD, figure D: non-silenced control plain and HL media vs. HCP1 KD HL, figure E: non-silenced control vs. double LRP1/HCP1 KD and figure F: non-silenced control plain and HL media vs. double LRP1/HCP1 KD HL. Control: non-silenced control; KD: knock-down; HL: haem loaded. Error bars denote  $\pm$  SEM.



**Figure 4.14 LRP1 and HCP1 knock-down prevents the stimulatory effect of supplementary haem on OE33 cell line migration**

Representative images of OE33 cell line knock-downs cultured in plain and 20 $\mu$ M haem supplemented media over 60 hours. Scrambled: non-silenced control; KD: knock-down; HL: haem loaded.



**Figure 4.15 LRP1 and HCP1 knock-down prevents the stimulatory effect of supplementary haem on OE19 cell line migration**

OE19 cell line knock-downs cultured in plain media or 20 $\mu$ M haem loaded media (n=9). Figure A: non-silenced control vs. LRP1 KD, figure B: non-silenced control plain and HL media vs. LRP1 KD HL, figure C: non-silenced control vs. HCP1 KD, figure D: non-silenced control plain and HL media vs. HCP1 KD HL, figure E: non-silenced control vs. double LRP1/HCP1 KD and figure F: non-silenced control plain and HL media vs. double LRP1/HCP1 KD HL. Control: non-silenced control; KD: knock-down; HL: haem loaded. Error bars denote  $\pm$  SEM.

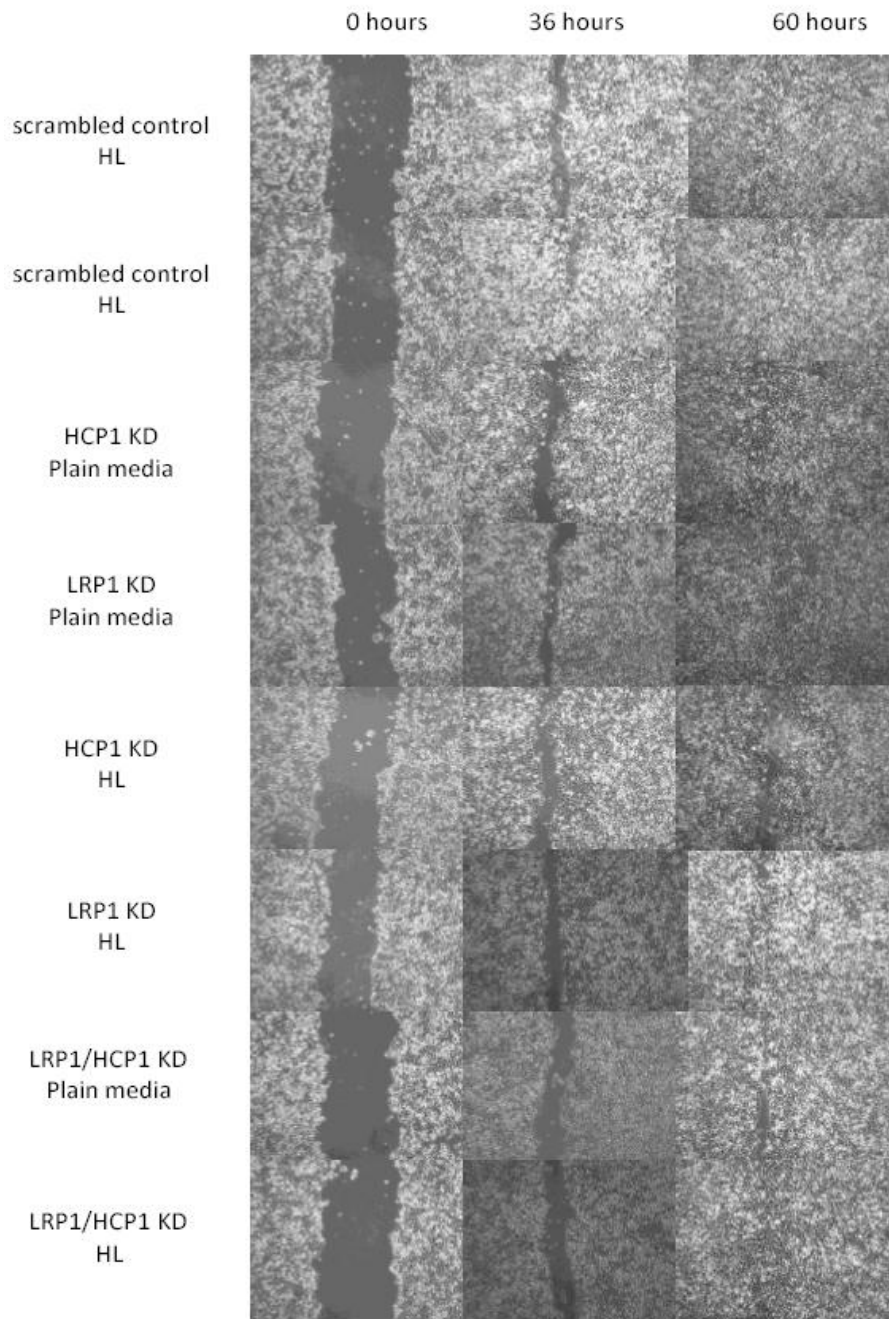


**Figure 4.16 LRP1 and HCP1 knock-down prevents the stimulatory effect of supplementary haem on OE19 cell line migration**

Representative images of OE19 cell line knock-downs cultured in plain and 20 $\mu$ M haem supplemented media over 60 hours. Scrambled: non-silenced control; KD: knock-down; HL: haem loaded.

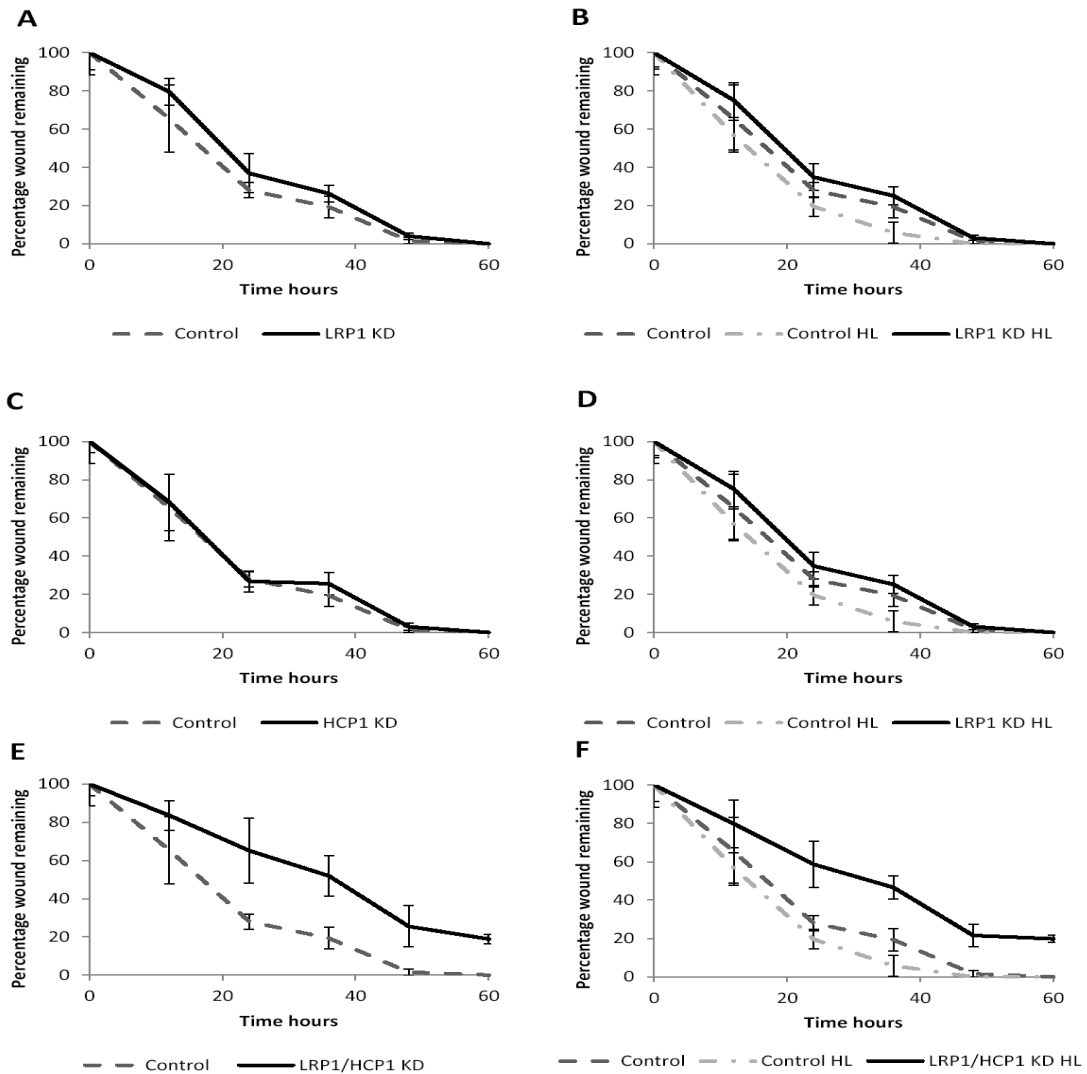


**Figure 4.17 LRP1 and HCP1 knock-down prevents the stimulatory effect of supplementary haem on OE21 cell line migration**

OE21 cell line knock-downs cultured in plain media or 20 $\mu$ M haem loaded media (n=9).

Figure A: non-silenced control vs. LRP1 KD, figure B: non-silenced control plain and HL media vs. LRP1 KD HL, figure C: non-silenced control vs. HCP1 KD, figure D: non-silenced control plain and HL media vs. HCP1 KD HL, figure E: non-silenced control vs. double LRP1/HCP1 KD and figure F: non-silenced control plain and HL media vs. double LRP1/HCP1 KD HL. Control: non-silenced control; KD: knock-down; HL: haem loaded. Error bars denote  $\pm$  SEM.

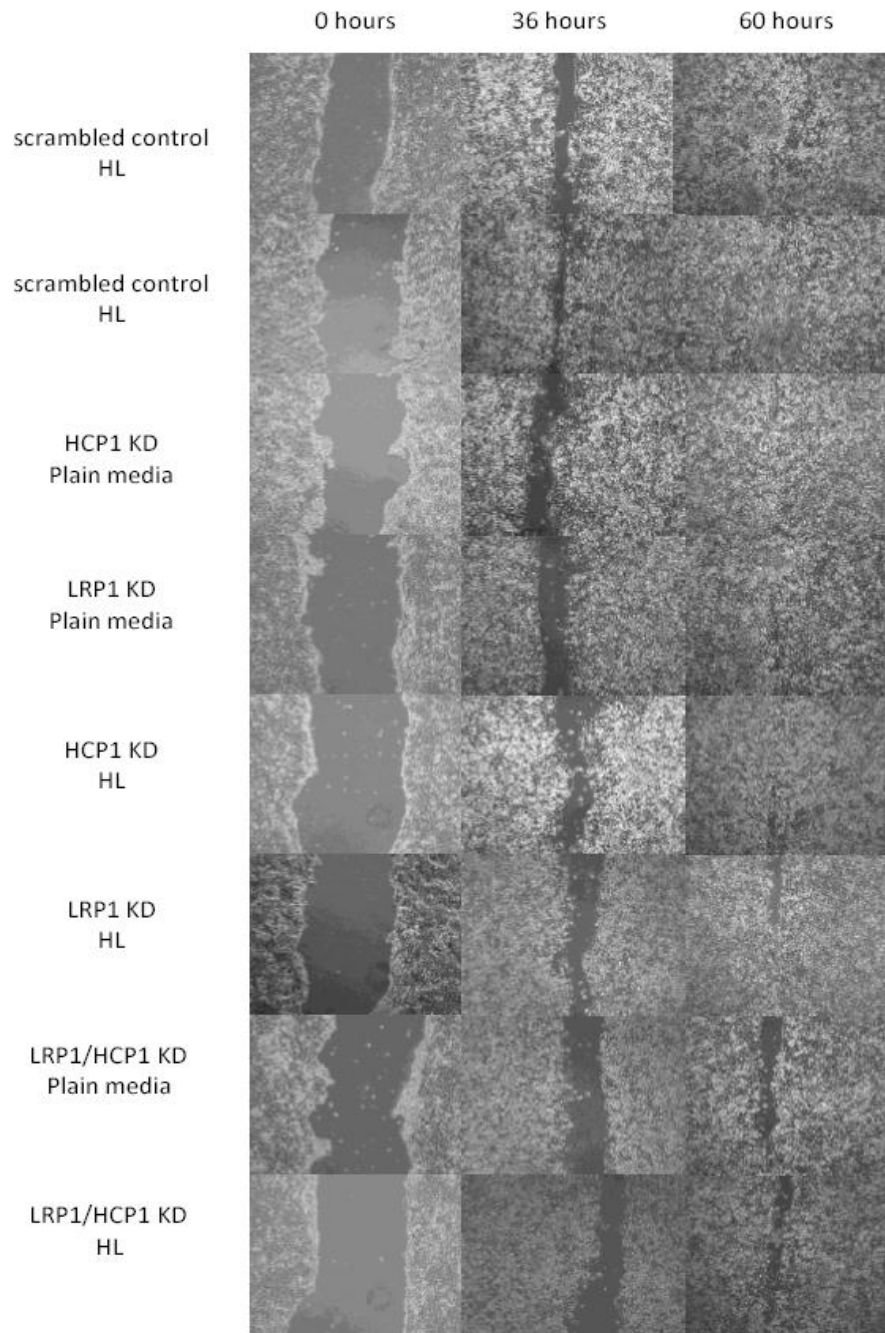


**Figure 4.18 LRP1 and HCP1 knock-down prevents the stimulatory effect of supplementary haem on OE21 cell line migration**

Representative images of OE21 cell line knock-downs cultured in plain and 20 $\mu$ M haem supplemented media over 60 hours. Scrambled: non-silenced control; KD: knock-down; HL: haem loaded.

#### **4.3.3.3 LRP1 and HCP1 knock-down suppresses independent colony formation with or without supplementary haem**

OE33, OE19 and OE21 cell line knock-downs were seeded as a single cell suspension in agar containing plain media or spiked with 20 $\mu$ M haem. After two weeks of incubation, the average colony size was calculated in pixels<sup>2</sup> (figure 4.19: OE33, figure 4.20: OE19 and figure 4.21: OE21).

All cell line knock-downs formed colonies. Similar observations in the range of average colony size were made from OE33, OE19 and OE21 cell line knock-downs. Compared to non-silenced controls, abrogation of LRP1 and HCP1 protein expression significantly impaired average colony size (OE33: p=0.01, p=0.05 and p=0.001; OE19: p=0.05, p=0.04 and p=0.001; OE21: p=0.022, p=0.02 and p=0.001 for LRP1, HCP1 and LRP1/HCP1 knock-downs respectively). Non-silenced control colonies, incubated in agar spiked with haem, demonstrated significantly larger average colony sizes compared to non-silenced controls, grown in agar containing plain media. This observation was identified in all cell lines (p=0.001, p=0.01 and p=0.048 for OE33, OE19 and OE21 lines). In a similar fashion to changes seen with viability, proliferation and migration, the stimulatory effect of additional haem on colony formation was entirely lost with the silencing of LRP1 and HCP1 proteins. In fact, even when incubated in supplementary haem, knock-downs from each cell line still demonstrated reduced average colony size compared to non-silenced controls grown in agar containing plain media alone (OE33: p=0.05, p=0.04 and p=0.02; OE19: p=0.05, p=0.04 and p=0.001; OE21: p=0.01, p=0.008 and p=0.0001 for LRP1, HCP1 and LRP1/HCP1 knock-downs respectively).

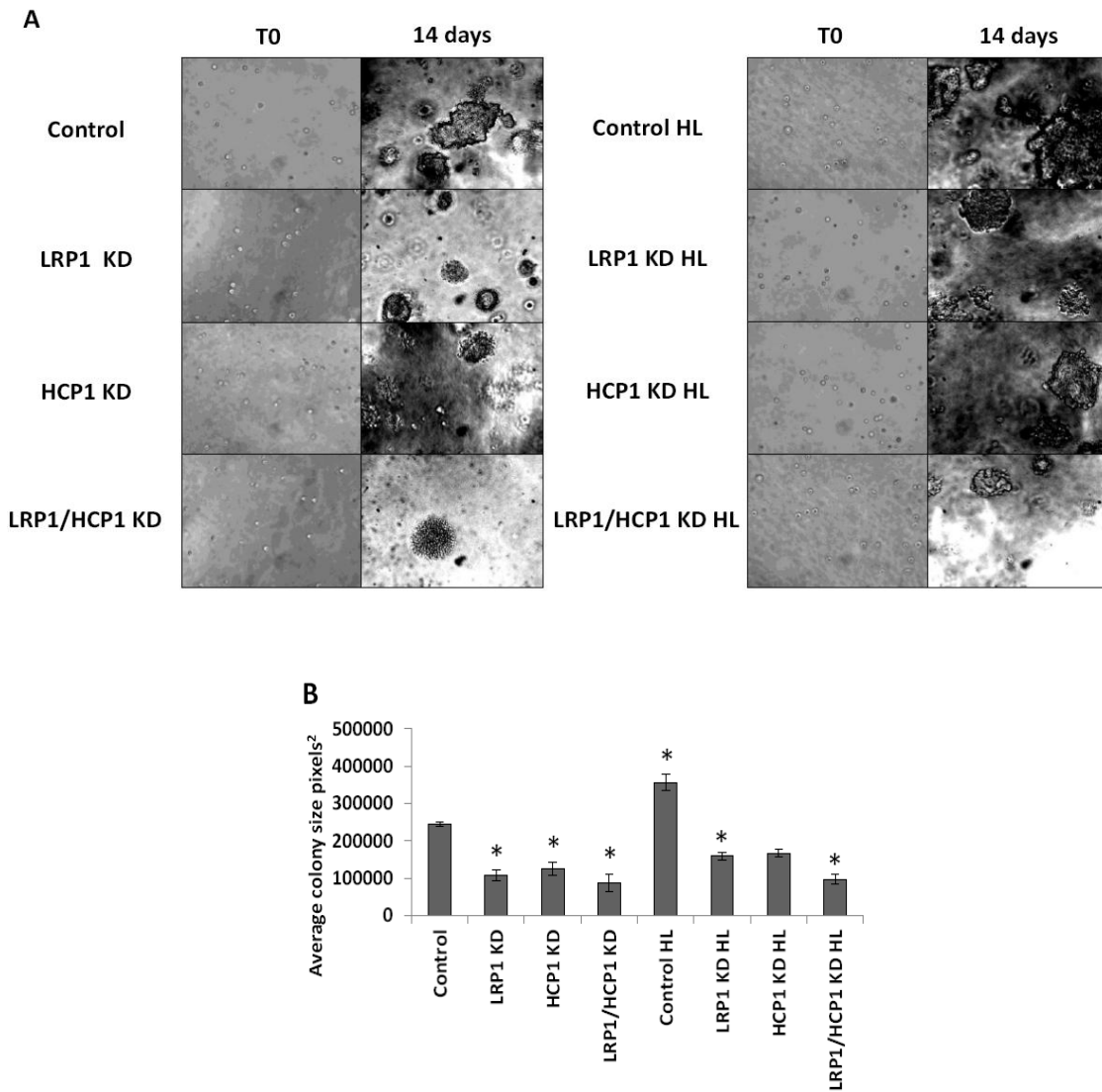


**Figure 4.19 LRP1 and HCP1 knock-down suppresses independent colony formation with or without supplementary haem in OE33 cell line**

OE33 cell line LRP1 and HCP1 knock-downs were seeded as a single cell suspension in agar containing plain or media spiked with 20 $\mu$ M haem. After two weeks of incubation, the average colony size was calculated in pixels<sup>2</sup>. Figure A: images of initial seeding (T0) and at 14 days. Figure B: average colony sizes at 14 days. Control: non-silenced control; KD: knock-down; HL: haem loaded. (\* $p < 0.05$  significant change in average colony size compared to non-silenced control cultured in plain media,  $n=9$ ).

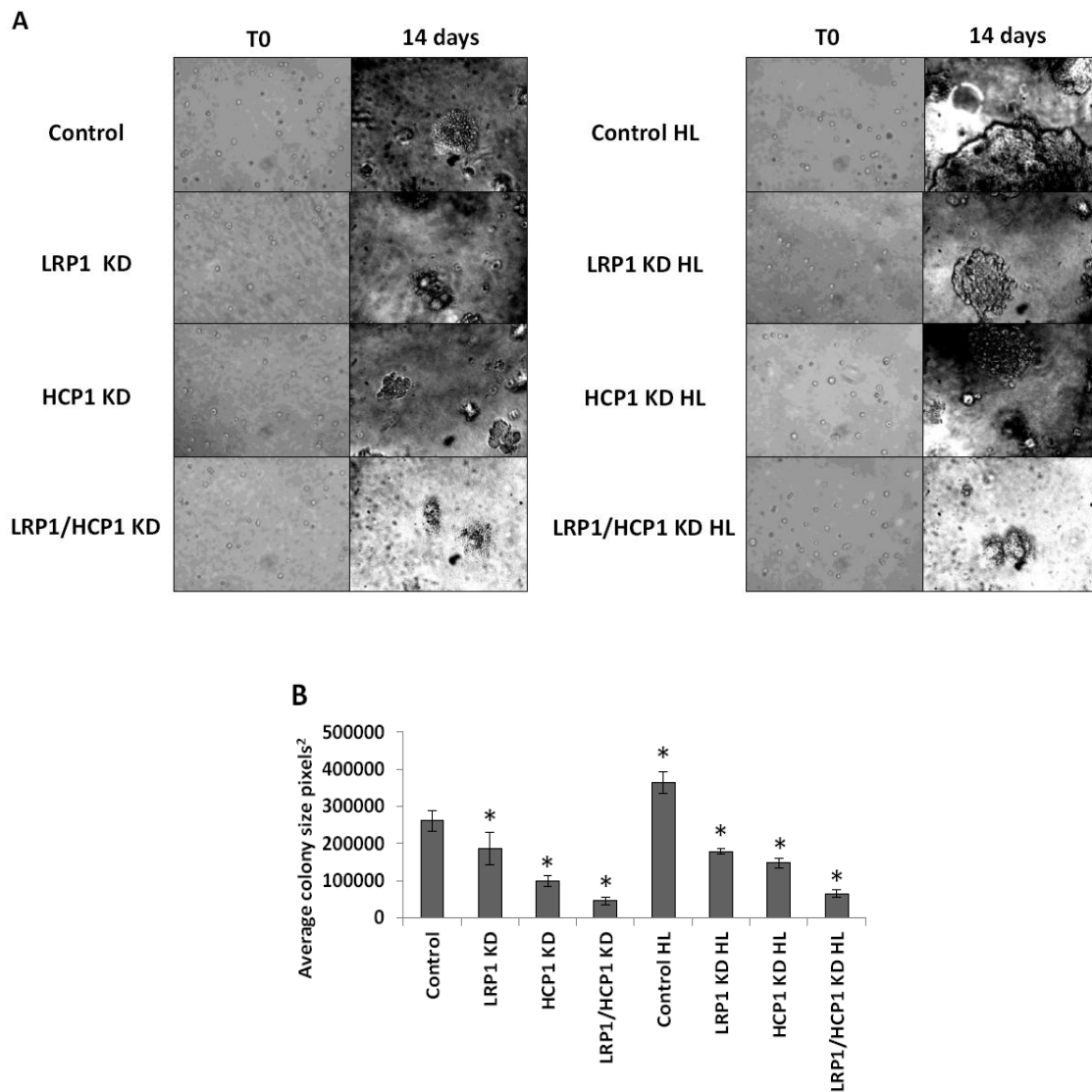


**Figure 4.20 LRP1 and HCP1 knock-down suppresses independent colony formation with or without supplementary haem in OE19 cell line**

OE19 cell line LRP1 and HCP1 knock-downs were seeded as a single cell suspension in agar containing plain or media spiked with 20 $\mu$ M haem. After two weeks of incubation, the average colony size was calculated in pixels<sup>2</sup>. Figure A: images of initial seeding (T0) and at 14 days. Figure B: average colony sizes at 14 days. Control: non-silenced control; KD: knock-down; HL: haem loaded. (\* $p < 0.05$  significant change in average colony size compared to non-silenced control cultured in plain media,  $n=9$ ).

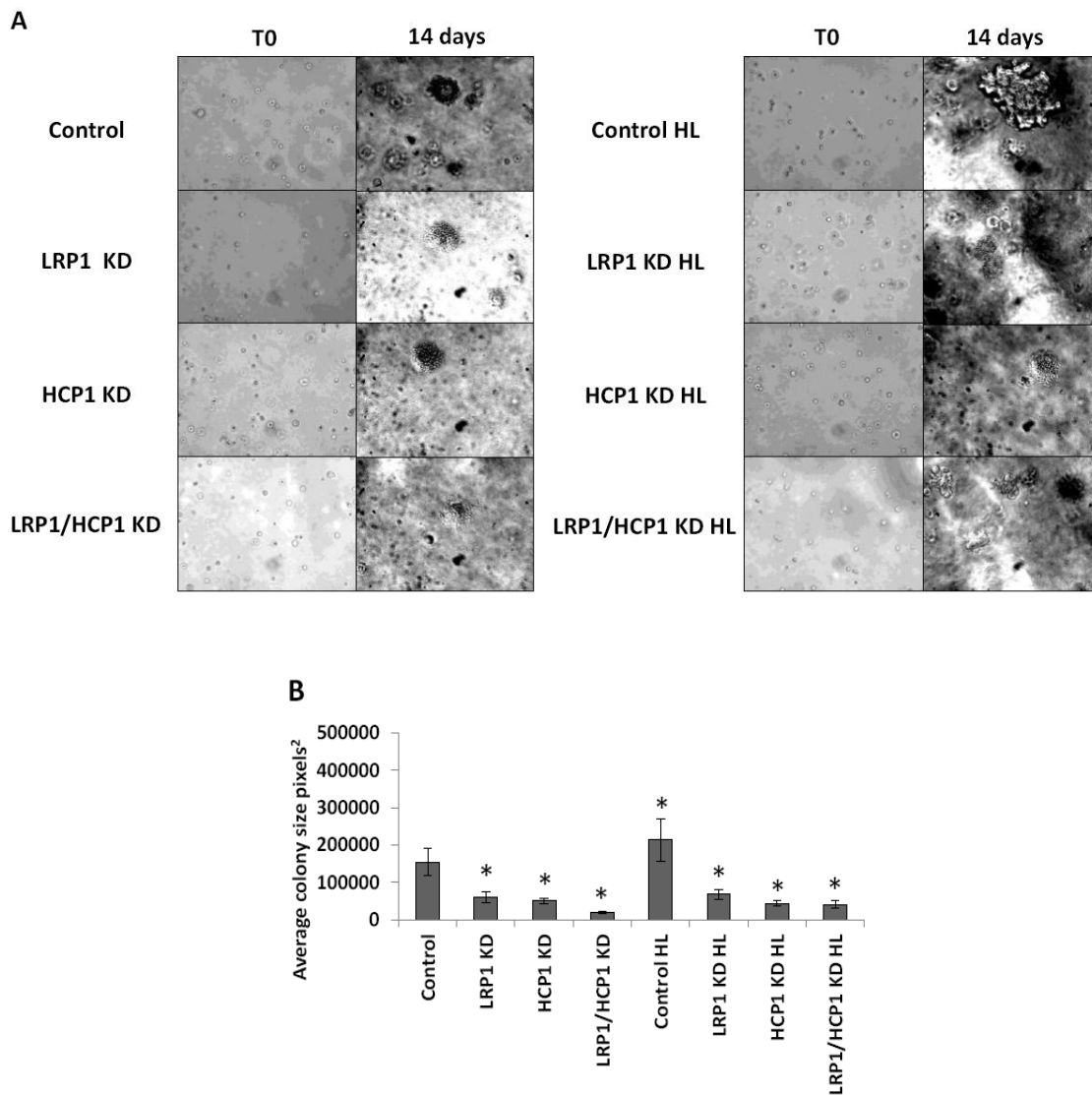


**Figure 4.21 LRP1 and HCP1 knock-down suppresses independent colony formation with or without supplementary haem in OE21 cell line**

OE21 cell line LRP1 and HCP1 knock-downs were seeded as a single cell suspension in agar containing plain or media spiked with 20 $\mu$ M haem. After two weeks of incubation, the average colony size was calculated in pixels<sup>2</sup>. Figure A: images of initial seeding (T0) and at 14 days. Figure B: average colony sizes at 14 days. Control: non-silenced control; KD: knock-down; HL: haem loaded. (\* $p < 0.05$  significant change in average colony size compared to non-silenced control cultured in plain media,  $n=9$ ).

#### **4.3.4 The impact of LRP1 and HCP1 silencing on OE33, OE19 and OE21 cell cycle *in-vitro***

To assess the impact of LRP1 and HCP1 silencing on cell cycle, OE33, OE19 and OE21 cell line knock-downs were cultured in plain or haem loaded media (20 $\mu$ M haem) for 48 hours. Cells were then harvested and processed for propidium iodide FACS analysis of the cell cycle (figure 4.22).

##### **4.3.4.1 LRP1 and HCP1 protein knock-down neutralises the stimulatory effect of supplementary haem on the cycle cell**

Cell cycle was assessed using propidium iodide FACS analysis and represented as the average percentage of cells in G<sub>0</sub>/G<sub>1</sub>, S or G<sub>2</sub>/M phases of the cycle. The distribution of cells in the cycle was not significantly different between non-silenced controls and LRP1 and HCP1 knock-downs cultured in plain media. A predicted stimulatory effect of supplementary haem was demonstrated by a significant decrease in the percentage of cells in the G<sub>0</sub>/G<sub>1</sub> phase, and a significant increase in S-phase and G<sub>2</sub>/M phases in non-silenced haem loaded controls, compared to those cultured in plain media (OE33: G<sub>0</sub>/G<sub>1</sub> p=0.01, S p=0.001 and G<sub>2</sub>/M p=0.09; OE19: G<sub>0</sub>/G<sub>1</sub> p=0.01, S p=0.001 and G<sub>2</sub>/M p=0.05; OE21: G<sub>0</sub>/G<sub>1</sub> p=0.012, S p=0.001 and G<sub>2</sub>/M p=0.044). Abrogation of LRP1 and HCP1 removed the stimulatory effect of haem in knock-down cells cultured with haem showing no change in the distribution of cells in any phase of the cell cycle. These observations were constant across the three cell lines.

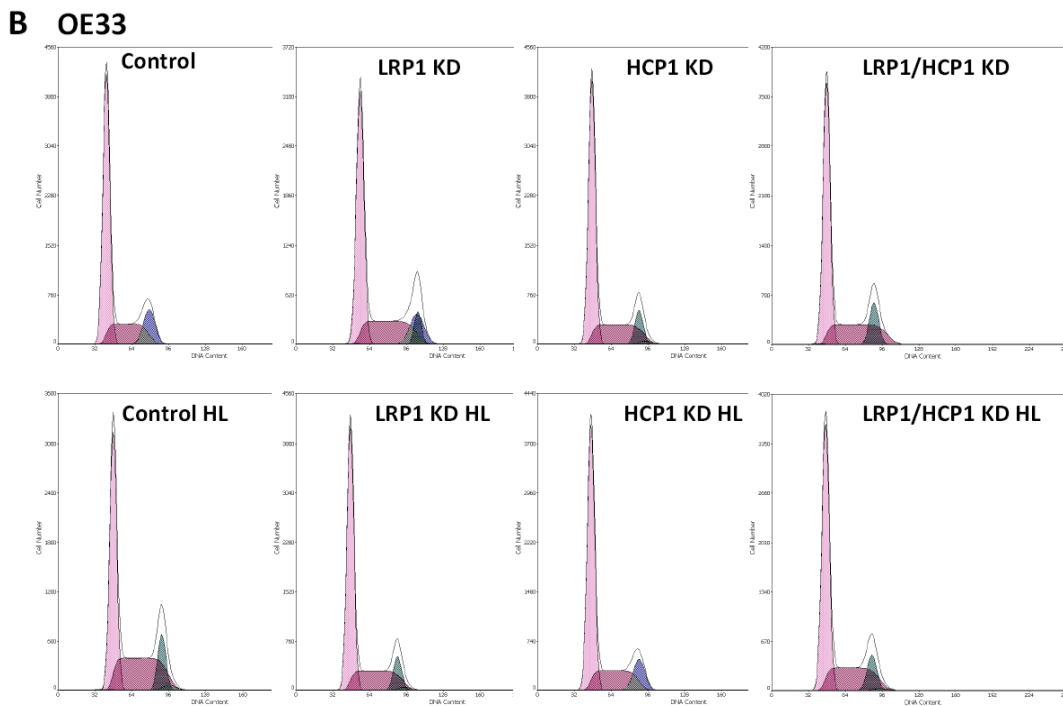
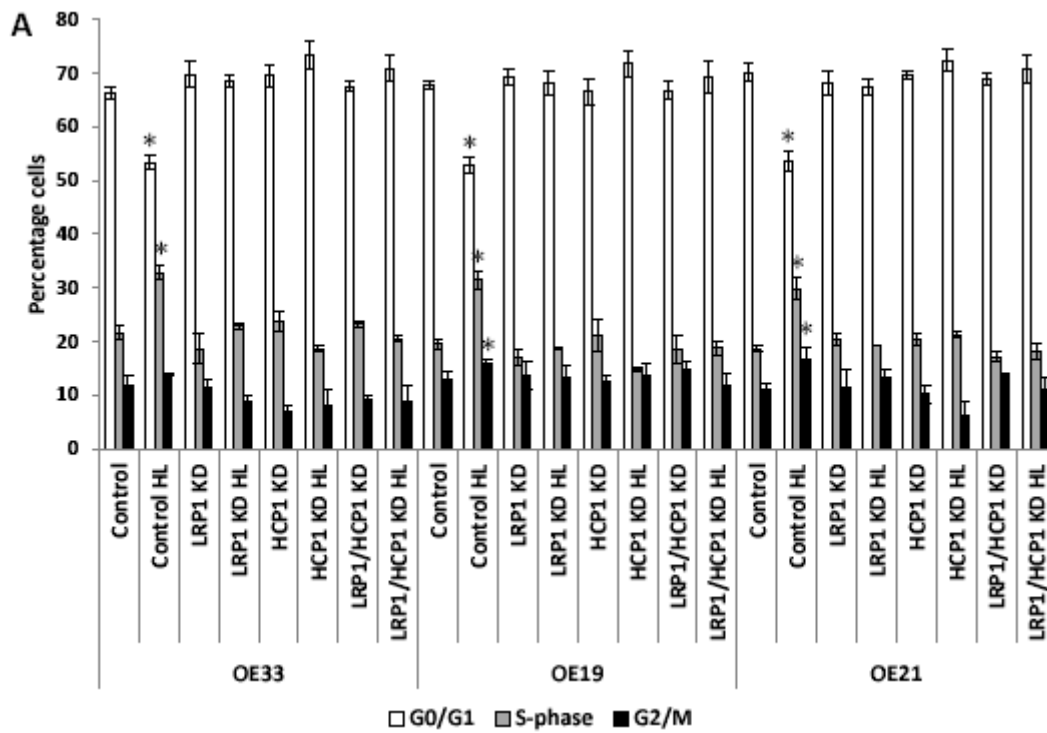


**Figure 4.22** LRP1 and HCP1 protein knock-down neutralises the stimulatory effect of supplementary haem on the cycle cell

OE33, OE19 and OE21 cell line knock-downs were cultured in plain or haem loaded media (20 $\mu$ M) for 48 hours. Cells were then harvested and processed for propidium iodide FACS analysis of the cell cycle presented as the average percentage of cells in G<sub>0</sub>/G<sub>1</sub>, S or G<sub>2</sub>/M phases. Figure A: percentage of cells in each phase of the cell cycle for OE33, OE19 and OE21 cell line knock-downs. Figure B: graphical representation of OE33 cell line knock-downs by DNA content (x-axis) and number of cells (y-axis), first peak: G<sub>0</sub>/G<sub>1</sub>, second plateau peak: S-phase and final peak: G<sub>2</sub>/M. Control: non-silenced control; KD: knock-down; HL: haem loaded. (\*p=<0.05 significant change in percentage distribution within the cell cycle compared to non-silenced control cultured in plain media, n=9).

#### **4.3.5 *In-vivo* effects of LRP1 and HCP1 protein silencing**

Silencing of the haem import proteins, LRP1 and HCP1 is detrimental to oesophageal cancer cell viability, proliferation, migration and independent colony forming. In addition, loss of LRP1 and HCP1 alters expression of iron transport proteins, cell cycle and eliminates the stimulatory effects of supplementary haem on cell phenotype. To see if these *in-vitro* observations would influence tumour burden *in-vivo*, OE33 cell line knock-downs were xenografted into a NOD-SCID mouse model and allowed to establish. After a period of 24 days the mice were culled and xenografts harvested, weighed and processed for immunohistochemistry and mRNA analysis.

##### **4.3.5.1 Silencing of LRP1 and HCP1 in the OE33 cell line significantly reduces xenograft tumour burden in NOD-SCID mice**

OE33 cell line knock-downs ( $1 \times 10^6$  cells) were injected in the left flank, subcutaneous tissue plane of NOD-SCID mice (n=5). After 24 days xenografts had established and developed in 100 percent of mouse models. Mice were culled and the xenografts harvested and weighed. Significant differences in average xenograft weight (mg) were recorded between LRP1 and HCP1 knock-downs and non-silenced control (figure 4.23). The most dramatic difference was observed in the LRP1 knock-down with a 70% reduction in tumour burden (LRP1 KD  $29.9 \pm 5.5$  vs. control  $100.9 \pm 23.1$ ,  $p=0.014$ ). Loss of HCP1 also resulted in a significant decrease in tumour burden of 58% (HCP1 KD  $42.0 \pm 10.5$ ,  $p=0.043$ ). The combined knock-down of LRP1 and HCP1 had the least, but still significant effect on tumour burden with a reduction of 51% (LRP1/HCP1 KD  $49.1 \pm 3.31$ ,  $p=0.05$ ).

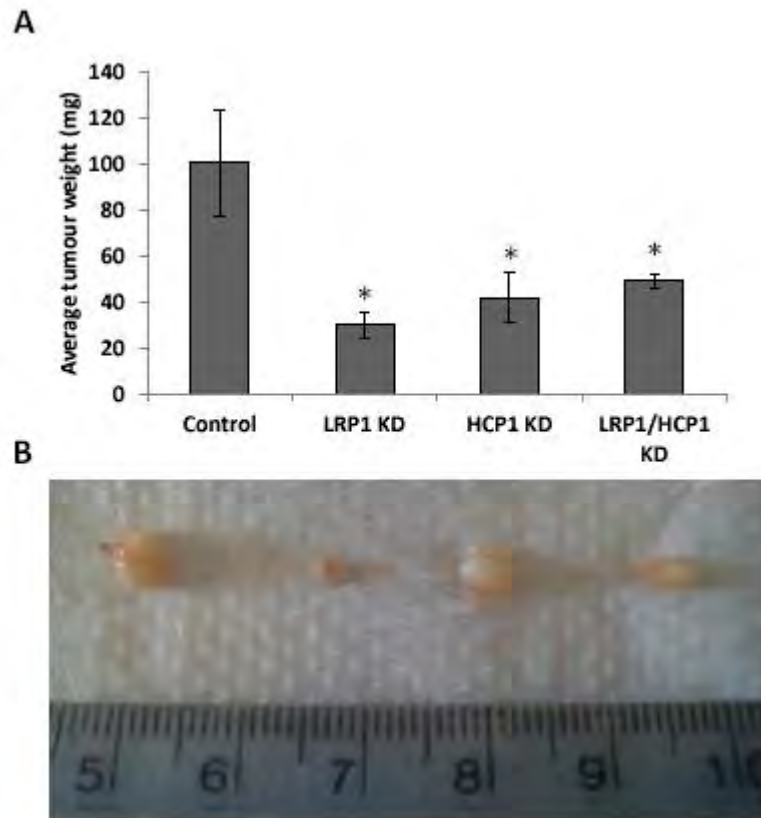


**Figure 4.23 Silencing of LRP1 and HCP1 in OE33 cell line xenografts significantly reduced tumour burden in a murine model**

OE33 cell line LRP1 and HCP1 knock-downs were xenografted into a NOD-SCID mouse model and allowed to develop for 24 days. Mice were then culled and average xenograft weight (mg) recorded and compared to non-silenced control (LRP1 KD 70% reduction in tumour burden,  $p=0.014$ ; HCP1 KD 58% reduction,  $p=0.043$ ; LRP1/HCP1 KD 51% reduction,  $p=0.05$ ). Control: non-silenced control; KD: knock-down. (\* $p<0.05$  significant change in mean xenograft weight compared to non-silenced control,  $n=5$ ). Error bars denote  $\pm$  SEM.

#### 4.3.5.2 Silencing of LRP1 and HCP1 in OE33 cell line xenografts significantly alters mRNA expression of iron and haem transport proteins

OE33 LRP1 and HCP1 knock-down xenografts were harvested after 24 days of growth in a NOD-SCID mouse model. A representative fragment of xenograft tissue was snap frozen and processed for mRNA expression (figure 4.24).

IRE-IRP regulated mRNA expression was significantly altered; most notably, a marked increase in TfR1 expression in LRP1 and HCP1 knock-downs compared to control (fold change in TfR1 mRNA: LRP1 KD  $2.42 \pm 0.44$ ,  $p=0.05$ ; HCP1 KD  $2.41 \pm 0.48$ ,  $p=0.035$ ; LRP1/HCP1 KD  $7.94 \pm 2.01$ ,  $p=0.001$ ). FPN mRNA expression was significantly repressed in the HCP1 and combined LRP1 and HCP1 knock-downs compared to non-silenced control (fold change in FPN mRNA expression: HCP1 KD  $0.53 \pm 0.08$ ,  $p=0.005$ ; LRP1/HCP1 KD  $0.57 \pm 0.08$ ,  $p=0.022$ ). LRP1 knock-down demonstrated reduced FPN mRNA expression but this narrowly missed statistical significance  $0.83 \pm 0.17$ ,  $p=0.082$ . Similarly a marked reduction in ferritin mRNA expression was observed in all knock-down xenografts compared to non-silenced control (fold change in ferritin mRNA expression: LRP1 KD  $0.53 \pm 0.04$ ,  $p=0.0001$ ; HCP1 KD  $0.42 \pm 0.08$ ,  $p=0.0001$ ; LRP1/HCP1 KD  $0.65 \pm 0.024$ ,  $p=0.01$ ).

Very little difference in mRNA expression of the haem transporting proteins was demonstrated in xenografted knock-downs compared to control. There was no apparent change in HCP1 expression in LRP1 knockdowns and conversely no interplay between silencing of HCP1 and LRP1 mRNA expression. In contrast to the *in-vitro* behaviour of haem effluxing protein mRNA expression, where suppression was seen, no fold change in BCRP or FLVCR mRNA expression was noted, with the exception of BCRP in the combined LRP1/HCP1 knock-down ( $0.52 \pm 0.09$ ,  $p=0.022$ ).

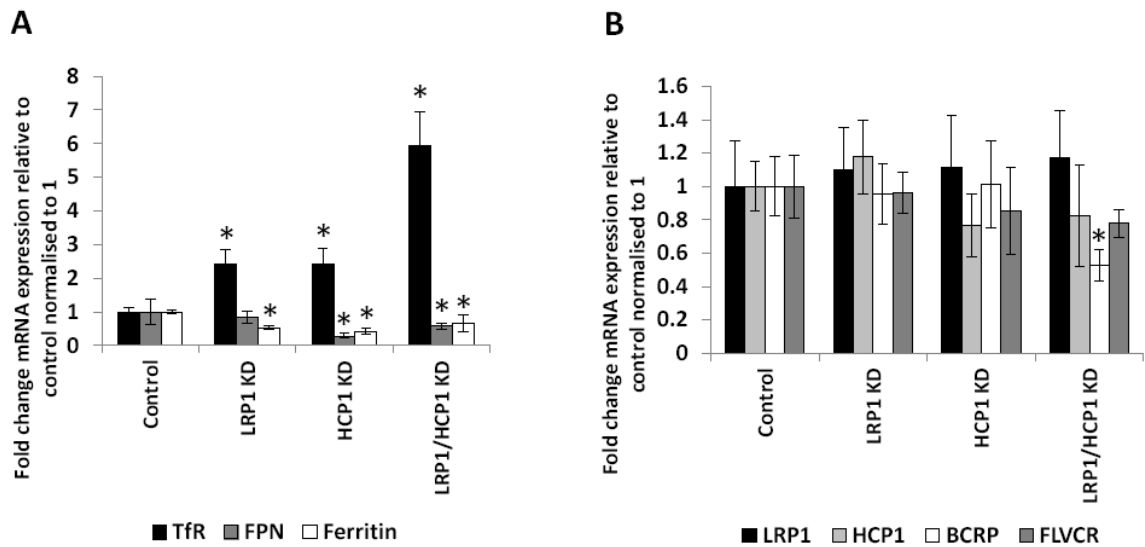


**Figure 4.24 Silencing of LRP1 and HCP1 in OE33 cell line xenografts significantly alters mRNA expression of iron transport proteins but has little impact on haem transport mRNA expression**

Figure A: mRNA expression for the iron transport proteins and figure B: mRNA for haem transport proteins in OE33 cell line LRP1 and HCP1 knock-down xenografts. Control: non-silenced control; KD: knock-down; (\* $p < 0.05$  significant change in mRNA expression fold change compared to non-silenced control,  $n=5$ ).

#### **4.3.5.3 Silencing of LRP1 and HCP1 in OE33 cell line xenografts is maintained and confirmed by immunohistochemistry**

OE33 LRP1 and HCP1 knock-down xenografts were harvested after 24 days of growth in the NOD-SCID mouse model. Xenografts were fixed in formalin, blocked in paraffin and mounted on slides. Slides were then subjected to immunohistochemistry and immunoreactivity scored as described in section 2.2.2.

LRP1 and HCP1 silencing was maintained with minimal immunoreactivity in the corresponding xenograft tissue (figure 2.25) (LRP1: LRP1 KD  $p=0.001$ ; HCP1 KD  $p=0.6$ ; LRP1/HCP1 KD  $p=0.001$ ) (HCP1: LRP1 KD  $p=0.56$ ; HCP1 KD  $p=0.0006$ ; LRP1/HCP1 KD  $p=0.001$ ).

As previously noted, there was no compensatory increase in the intensity of immunoreactivity for either HCP1 or LRP1 on silencing of LRP1 or HCP1, respectively.

LRP1 immunoreactivity was intense and principally membranous with weak cytoplasmic staining evident in the non-silenced control and HCP1 knock-down. Near complete absence of LRP1 immunoreactivity was observed in the LRP1 and double LRP1/HCP1 knock-downs (figure 4.26).

HCP1 immunoreactivity was also intense and strongly membranous in the non-silenced control and LRP1 knock-down. HCP1 reactivity was absent in the HCP1 and combined LRP1/HCP1 knock-downs. Normal human small bowel was used as a positive control for HCP1 where specific apical immunoreactivity was clearly evident (figure 4.26).

#### **4.3.5.4 Silencing of LRP1 and HCP1 in OE33 cell line xenografts significantly increases TfR1 and decreases ferritin immunoreactivity**

Silencing of LRP1 and HCP1 significantly increases the expression of TfR1 as evidenced by the marked increase in TfR1 immunoreactivity in LRP1 and HCP1 knock-downs compared to non-silenced control (immunoreactivity scoring for TfR1: LRP1 KD  $8.5\pm 0.5$ ,  $p=0.0004$ ; HCP1 KD  $8.33\pm 0.49$ ,  $p=0.0005$ ; LRP1/HCP1 KD  $8.33\pm 0.49$ ,  $p=0.0005$ ; non-silenced control  $5\pm 0.44$ ) (figure 4.25).

TfR1 immunoreactivity was mainly membranous with some weak cytosolic reactivity. The increase in TfR1 immunoreactivity seen on silencing of LRP1 and HCP1 was intense and predominantly membranous (figure 4.27).

In contrast to the increase in TfR1 immunoreactivity, silencing of LRP1 and HCP1 caused a significant suppression of ferritin reactivity compared to non-silenced control (immunoreactivity scoring for ferritin: LRP1 KD  $4\pm 0.44$ ,  $p=0.0015$ ; HCP1 KD  $5.33\pm 0.42$ ,  $p=0.021$ ; LRP1/HCP1 KD  $3.8\pm 0.4$ ,  $p=0.0012$ ; non-silenced control  $7.5\pm 0.67$ ) (figure 4.25).

Ferritin immunoreactivity was cytosolic in all cases, although as reflected in the immunoreactivity scoring, intensity was markedly decreased on silencing of the haem importing proteins LRP1 and HCP1 (figure 4.27).

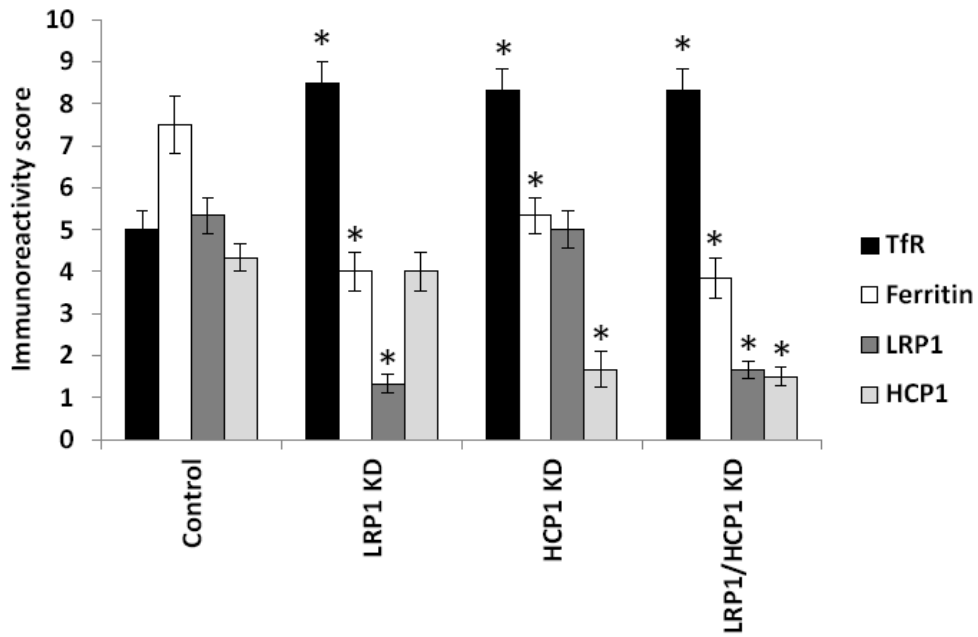


**Figure 4.25 Semi-quantitative immunoreactivity scoring - silencing of LRP1 and HCP1 in OE33 cell line xenografts is maintained and significantly increases TfR1 and decreases ferritin immunoreactivity**

OE33 cell line knock-down xenograft tissue was processed for immunohistochemistry and scored for immunoreactivity as described in section 2.2.2. Error bars denote  $\pm$  SEM.

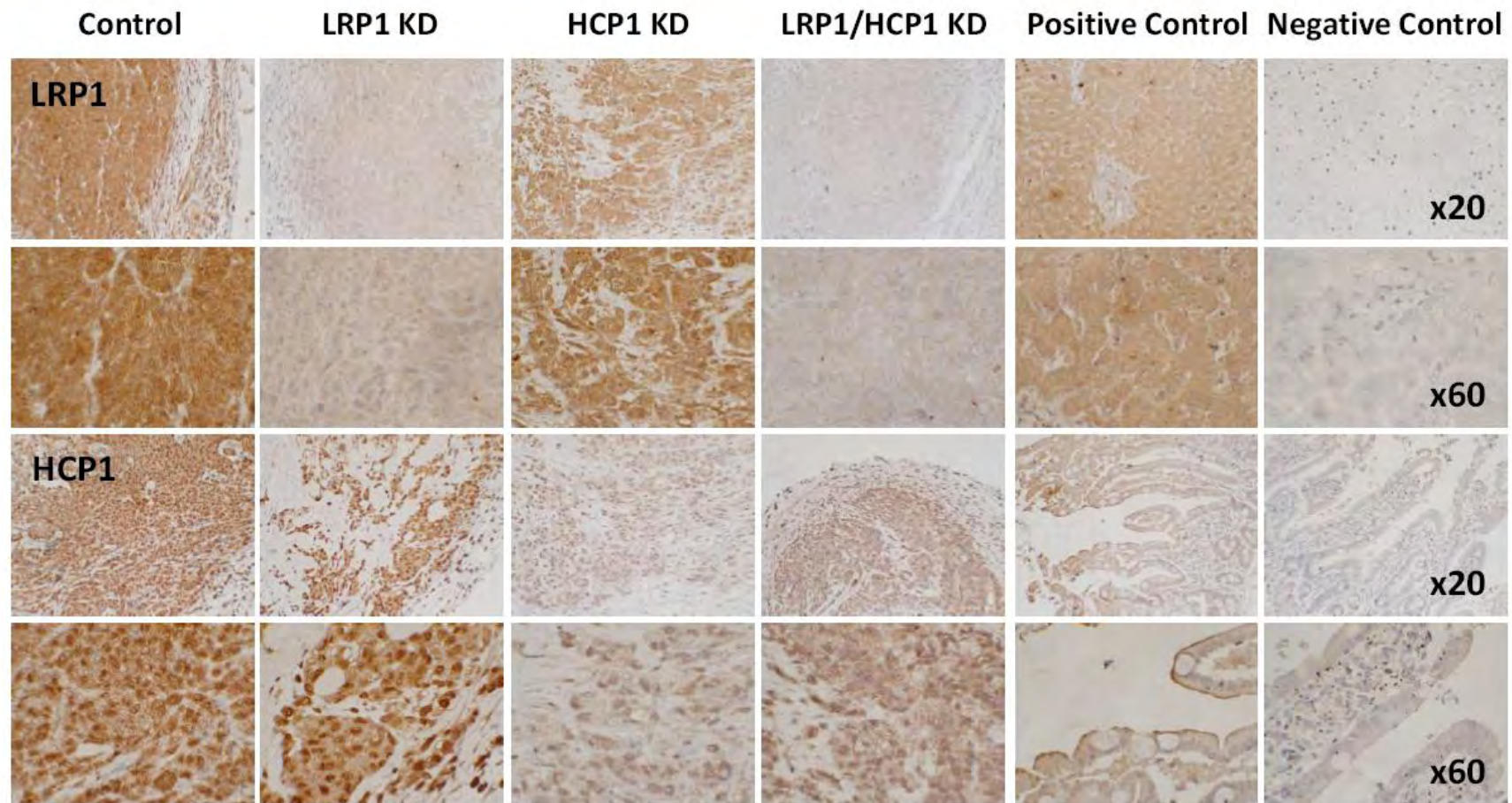


**Figure 4.26 Representative immunolocalisation of LRP1 and HCP1 for OE33 LRP1 and HCP1 knock-down xenografts**

Controls: Liver for LRP1 and small bowel for HCP1. Antibody omitted for negative control. Magnification x20 and x60.

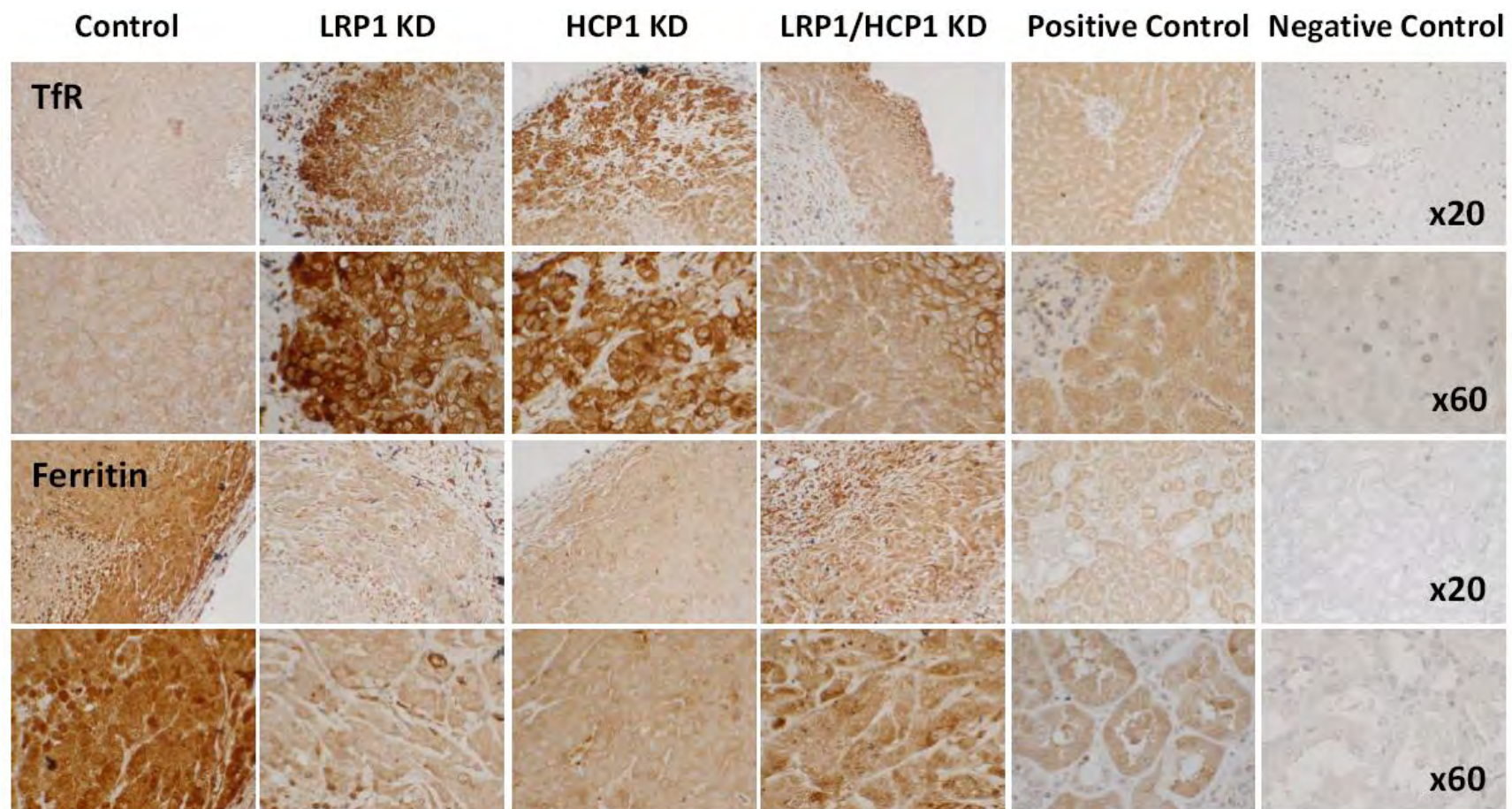


**Figure 4.27 Representative immunolocalisation of TfR1 and ferritin for OE33 LRP1 and HCP1 knock-down xenografts**

Controls: Liver for TfR and kidney for ferritin. Antibody omitted for negative control. Magnification x20 and x60.

#### 4.4 Conclusions

Abrogation of LRP1 and HCP1 was successful in all three cell lines, confirmed by Western blotting, GFP expression and immunohistochemistry.

Loss of LRP1 and HCP1 functionality in the presence of plain media had little effect on gross cell iron content suggesting that with no exogenous haem supplementation, active haem import has little overall contribution to cell iron status or that the cell can adequately compensate for lack of haem import by increasing inorganic iron acquisition. In the presence of supplementary haem, gross iron concentration was significantly increased in non-silenced controls, in-keeping with the hypothesis that oesophageal cancer cells are able to acquire haem iron when physiologically available. Culture with supplementary haem did not significantly alter gross cell iron content in the absence of LRP1 and HCP1, indicating that these import proteins are necessary for active haem import and that iron loading, in the presence of supplementary haem, cannot simply be explained by passive diffusion.

The effect of LRP1 and HCP1 abrogation on expression of the IRE-IRP responsive iron transport proteins (TfR1, ferritin and FPN) was consistent across OE33, OE19 and OE21 cell lines. Changes in mRNA expression generally tallied with those of protein expression, in keeping with IRE-IRP regulation at the level of transcription. Changes in TfR1 mRNA and protein expression were most striking with significant increases in fold change seen in LRP1 and HCP1 knock-downs in the presence or absence of supplementary haem. Increased TfR1 expression, in the absence of active haem import, is likely to be compensatory in order to boost inorganic iron endocytosis and maintain cellular iron

homeostasis under the influence of the IRE-IRP system. Compensatory increases in TfR1 expression explains the retained uniformity of cellular iron content observed in the background loss of active haem import. No difference in TfR1 expression was demonstrated between non-silenced controls cultured in plain or haem loaded media; such an observation was unexpected as cell iron loading, through haem supplementation, may be expected to decrease TfR1 expression by the IRE-IRP system. However, cultured oesophageal cancer cells may have depleted basal levels of intracellular iron, precluding suppression of TfR1 expression, even in the presence of relative haem abundance. An alternative explanation may be that experimental cell lines have acquired an aberrant IRE-IRP system, akin to that observed in colorectal adenocarcinoma cells lines, exhibiting paradoxical TfR1 overexpression in the face of intracellular iron loading<sup>175,176</sup>. Indeed, TfR1 overexpression and relative intracellular iron loading, is associated sequentially with progression of the BM-dysplasia-OAC paradigm<sup>171</sup>. Changes in FPN and ferritin expression largely conformed to those predicted by IRE-IRP regulation: decreased expression of the iron efflux protein FPN and decreased ferritin mediated iron storage capacity<sup>248</sup>. However, these changes were not uniformly seen across all three cell lines and only reached significance in the OE33 OAC line.

Very little interplay between the expression of LRP1 and HCP1 was noted on silencing suggesting that the expression of LRP1 has little bearing on the expression of HCP1 or vice-versa. This is not an unexpected observation as HCP1 is post-translationally mediated by redistribution between the cytosolic compartment and cell membrane depending on iron status; expression is insensitive to intracellular iron concentration but is hypoxia mediated<sup>274,285,295</sup>. The control of LRP1 expression has not yet been elucidated;

however it appears that gross intracellular iron concentration and free haem are not potent regulators.

Loss of active haem import had a heterogeneous effect on mRNA and protein expression of the haem export proteins. BCRP expression demonstrated the most consistent response across all three cell lines with significant suppression at the transcription level with corresponding reduction of protein synthesis in LRP1 and HCP1 knock-downs. It would follow that in the absence of haem import the detoxifying action of BCRP is less crucial to cellular protection from ROS formation, however no significant difference in BCRP expression was noted between control cells in plain or haem loaded media, implying that even in the presence of supplementary haem, cell lines *in-vitro* do not acquire enough haem to overwhelm HO1 levels and induce cellular toxicity. FLVCR mRNA and protein expression were not significantly altered by loss of haem import, drawing a potential explanation that the expression of proteins capable of exporting cellular haem are more likely to be regulated by cellular hypoxia, possibly potentiated by intracellular haem concentration. The significantly elevated expression of BCRP and FLVCR seen in *ex-vivo* OAC samples, presented in chapter three, adds credence to this observation.

Non-silenced controls cultured with supplementary haem exhibited significantly enhanced viability and proliferation across all three cell lines. This is the first time that haem has been demonstrated to have a stimulatory effect on oesophageal cancer cell phenotype and adds further to the hypothesis that cancer cells are able to acquire haem to affect cellular iron loading in a manner akin to that demonstrated with inorganic iron in oesophageal and colorectal adenocarcinomas<sup>171,175</sup>. Further evidence of the contribution of haem to oesophageal cancer cell viability and proliferation is highlighted

by a significant reduction in these parameters when LRP1 and HCP1 are abrogated, even with the compensatory increase in inorganic iron acquisition inferred by up-regulation of TfR1 when active haem import is lost. The stimulatory effect of supplementary haem was attenuated in the LRP1 and HCP1 knock-downs compared to non-silenced controls, again demonstrating that the acquisition of available haem lends a survival advantage to oesophageal cancer cells.

Analysis of the surrogate indicators of migratory capacity and ability to form viable metastatic tumours (wound healing and independent colony forming assays) affords further evaluation of the effect of haem on oesophageal cancer cell phenotype. Supplementary haem significantly enhanced the ability of oesophageal cancer cells to migrate and form independent colonies, whereas abrogation of active haem import attenuated this response. Such an observation is entirely consistent with previous reports detailing the positive effects of inorganic iron supplementation on OAC cell phenotype *in-vitro*; potentially mediated through the iron dependent down-regulation of the cell-cell adhesion molecule E-cadherin<sup>128,171</sup>.

Control of the cell cycle is regulated by many factors, not least the iron dependent protein RNR<sup>187,188</sup>. The mitogenic effect of supplementary haem on the cell cycle was apparent with a significant reduction in the percentage of cells resting in G<sub>0</sub>/G<sub>1</sub> and subsequent significant increase in cells entering S phase through to G<sub>2</sub>/M. This observation was consistently observed in both OAC and SCC lines. The stimulatory effect of supplementary haem on the cell cycle was reduced with the abrogation of active haem import, strongly implicating haem derived cell iron loading as the driving mechanism.

The effect of impeding active haem import in the OE33 cell line was assessed *in-vivo*, utilising a murine xenograft model. A dramatic effect on tumour burden was recorded with reductions in mean xenograft weight of seventy percent for LRP1 knock-down and fifty-eight percent for HCP1. The combined knock-down of LRP1 and HCP1 did not demonstrate an additive or synergistic effect on xenograft weight. These striking results implicate systemic haem as a major source of intracellular iron loading in OAC especially as knock-down xenografted cells still have access to transferrin bound inorganic iron. Haem, both free and bound to haemopexin, is likely to be relatively abundant in the substance of the xenograft due to implantation trauma, low grade immunogenic reaction, friable neovascularisation, direct vessel invasion and ulceration; a situation comparable to that encountered within the substance of *in-vivo* native oesophageal cancers. In a similar manner to observations *in-vitro*, proteins regulated by the IRE-IRP system demonstrated significant changes in mRNA expression to suggest compensatory acquisition of inorganic iron in the LRP1 and HCP1 knock-down xenografts; TfR1 was significantly up-regulated and ferritin and FPN down-regulated. Semi-quantitative immunohistochemistry was again strongly suggestive of the up-regulation of inorganic iron acquisition through TfR1 mediated endocytosis in LRP1 and HCP1 knock-down xenografts. TfR1 immunoreactivity was apparent on the cell membrane suggesting biological activity. In addition, ferritin immunoreactivity was significantly lower in the knock-down xenografts inferring reduced requirement for cellular iron storage. The immunoreactivity of LRP1 and HCP1 in their respective xenografts was negligible, confirming continued successful abrogation of haem import. It must be stressed, however, that despite the circumstantial evidence of alterations in cellular iron biology to indicate relative iron depletion, in the face of loss of active haem import, LRP1 and HCP1

are not solely haem importers. The ubiquitously expressed LRP1 protein interacts with extracellular metalloproteinases, potentially limiting the ability of the xenograft to expand and invade the extracellular matrix when function of LRP1 is lost<sup>298,304,432</sup>. HCP1 is also a folate transporter and could in theory limit tumourigenic activity due to relative folate deficiency within the xenograft<sup>296</sup>. Unfortunately, the volume of xenografted material was not sufficient to allow for accurate assessment of gross iron content and therefore a more complete argument in favour of relative iron deprivation as the major factor responsible for the observed differences in tumour burden.

This chapter has demonstrated that oesophageal cancer cells can acquire both organic and inorganic iron by the action of several transport proteins which helps explain why targeting TfR1 alone with monoclonal antibodies fails to produce a robust anti-neoplastic effect in a variety of malignant lineages<sup>208</sup>. LRP1 and HCP1 could be considered as novel targets for therapeutic monoclonal antibodies in the treatment of oesophageal malignancy; however the simultaneous functional blockade of multiple targets is not practical and likely to be prohibitively expensive and unpredictable. An alternative would be to deprive the cancer cell of iron by use of a chelating agent. The effect of iron chelators as a potential therapeutic modality has not been explored in oesophageal cancer and is the subject of chapter five of this thesis.

## CHAPTER 5: THE *IN-VITRO* AND *IN-VIVO* ANTI-NEOPLASTIC ACTIVITY OF IRON CHELATORS IN OESOPHAGEAL CANCER

### 5.1 Introduction

The incidence of oesophageal adenocarcinoma has dramatically increased over the last 25 years and is now rising faster than any other malignant disease in Western nations<sup>8,9,24</sup>. Oesophageal cancer is a devastating condition associated with an extremely poor overall five-year survival of just 10%<sup>2</sup>. Surgical resection is the only curative treatment for OAC, however, the majority of patients present with advanced disease or are unsuitable for radical intervention<sup>3</sup>. Of the minority that undergo surgery, the outlook remains bleak with only 20-30% surviving two years<sup>3</sup>. Locally advanced disease and undiagnosed metastatic spread greatly contribute to failure of treatment with curative intent<sup>3</sup>. High rates of loco-regional and distant recurrence has led to much interest in pre-operative (neoadjuvant) combination chemotherapy with response rates of up to 30-40%<sup>3,7</sup>. Cisplatin, 5-FU and Epirubicin based chemotherapy, combined with surgery, increases overall survival by 6% at five years, compared to surgery alone<sup>7</sup>. Despite the addition of neoadjuvant chemotherapy and refinement of surgical technique, the vast majority of patients still die from overwhelming malignant disease progression. It would appear that further advances in treatment will be governed by understanding of the molecular events involved in oesophageal cancer evolution and the development of novel therapeutic strategies where side effects, complications and mortality associated with existing forms of treatment can be minimised.

The transition from BM to invasive OAC is associated with progressive overexpression of proteins involved in cellular iron acquisition, coupled with loss of iron efflux<sup>171</sup>. Chapter four of this thesis established the potential for oesophageal cancer cells to actively acquire haem, in addition to transferrin bound inorganic iron. Deregulation of iron metabolism explains the increase in cellular iron deposition observed in oesophageal cancer tissue that is likely to be driving a multitude of iron dependent cellular processes, including oxidative phosphorylation, DNA synthesis and the cell cycle<sup>171,191,319,433</sup>. Rapidly proliferating cancer cells are particularly susceptible to iron deprivation, mainly due to the expression of the iron dependent enzymes such as RNR, promoting iron chelation as an attractive potential anti-neoplastic strategy<sup>191,319,433</sup>. However, considering the number and complexity of cellular iron dependent processes and structural variations in iron chelating compounds, differences in the mode of action are highly likely to be observed.

A series of experimental iron chelators, most notably Dp44mT, have been developed that exhibit potent anti-neoplastic properties<sup>323,415</sup>. Dp44mT aggressively suppresses tumour growth in a range of murine xenograft models and is able to overcome chemo-resistance in an array of malignant cells *in-vitro*<sup>323</sup>. The major obstacle to clinical application of such agents is the associated systemic toxicity, manifested by myocardial fibrosis in murine models<sup>323</sup>. Encouragingly, systemic stripping of iron is not apparent and *in-vitro* data consistently supports cancer specific targeting of cytotoxicity<sup>323,325,328</sup>.

However, a number of iron chelators with excellent post-licensing safety records and side-effect profiles are regularly used in clinical practice in patients with iron overload disorders. The archetypal iron chelator for clinical use is DFO, which despite its

disadvantage of poor lipid solubility, has been shown to induce cytotoxicity in a number of *in-vitro* studies and appears to have at least some potential in the treatment of neuroblastoma<sup>325,328,359,360,362</sup>. The relatively new iron chelator Deferasirox is easily administered as an oral preparation and has high lipid solubility<sup>374,375</sup>. A limited number of case reports serendipitously noted that commencing Deferasirox treatment for iron overload was associated with remission in some patients with haematological malignancies<sup>383-385</sup>. Recently a number of *in-vitro* studies have demonstrated the cytotoxic potential of Deferasirox against leukaemia and hepatoma cell lines, surpassing the action of more traditional experimental chelators<sup>385-387</sup>.

To date, the potential anti-neoplastic action of iron chelators on gastrointestinal cancers is unknown. The hypothesis that iron chelation therapy could be of benefit in the treatment of oesophageal cancer is particularly appealing considering the potential for an iron mediated malignant phenotype and the dire need to improve survival outcomes.

## 5.2 Aims

1. Determine the ability of iron chelators to block iron up-take and mobilise iron from oesophageal cancer cells
2. Characterise the *in-vitro* effect of iron chelation on iron and haem transport protein expression
3. Determine the *in-vitro* effect of iron chelation on oesophageal cancer cell phenotype and cell cycle
4. Establish the influence of iron chelators on tumour burden and cellular iron metabolism in a murine xenograft model and calibrate potential systemic side effects and toxicity
5. Characterise the *in-vivo* effects of iron chelation on xenograft iron content and describe alterations in iron transport proteins
6. Explore the anti-neoplastic potential of iron chelators in combination with standard chemotherapeutic agents for oesophageal cancer treatment and possible action on chemoresistant cell lines

## 5.3 Results

### 5.3.1 Cell lines and iron chelators

Cell lines OE33, OE19 and OE21 were utilised for *in-vitro* experimentation and *in-vivo* xenograft murine models. Cell lines were cultured using standard media and were co-cultured with iron chelators at predetermined IC50 concentrations, unless specified otherwise. Two clinically established iron chelators, DFO and Deferasirox, were routinely studied for potential anti-neoplastic action. The experimental iron chelator, Dp44mT, was included in the majority of investigations for academic interest.

### 5.3.2 Generation of IC50 values

Iron chelator IC50 values (half-maximal inhibitory concentration) were derived by plotting a dose-response curve for each chelator. Dose response curves were drawn for both cellular viability (MTT assay) and proliferation (BrdU assay) for all three cell lines (data not shown). Very little variability in IC50 values was noted between lineages and the following values were used for all cell lines to avoid unnecessarily complicating experiments for the sake of minute variations in exact IC50 values. IC50 values: Deferasirox 20 $\mu$ M, DFO 10 $\mu$ M and Dp44mT 1 $\mu$ M.

### **5.3.3 Determine the ability of iron chelators to block iron up-take and extract iron from oesophageal cancer cells**

To determine the ability of each iron chelator to prevent the up-take of iron from culture media and extract intracellular iron from oesophageal cancer cell lines, gamma emitting  $^{59}\text{Fe}$  bound to transferrin was utilised (Kind gift of Professor Des Richardson, Sydney, Australia), as previously described<sup>323</sup>.

#### **5.3.3.1 Iron chelators can block the up-take of $^{59}\text{Fe}$ -Tf by oesophageal cancer cells *in-vitro***

OE33, OE19 and OE21 cell lines were cultured in media spiked with  $^{59}\text{Fe}$ -Tf and increasing concentrations of iron chelators.  $^{59}\text{Fe}$ -Tf spiked media alone was used as a control. After three hours, the amount of  $^{59}\text{Fe}$ -Tf taken up by the cells was measured using a gamma counter and expressed as a percentage of control up-take (figure 5.1).

Dp44mT was consistently the most effective agent at blocking iron up-take across the three cell lines; reaching a plateau blocking effect at its IC50 value (1 $\mu\text{M}$ ) of approximately 80%. Higher concentrations of Dp44mT did not further increase the amount of iron up-take blocked by the agent. Deferasirox was the next most effective agent at blocking iron-uptake. In contrast to Dp44mT, a steady increase in the ability of Deferasirox to block iron up-take was observed with increasing concentration, although the relationship between concentration and blocking effect was not linear. The majority of the blocking effect was achieved at a concentration of 1 $\mu\text{M}$  (50% up-take blocked) and then it increased in a steady fashion to its IC50 concentration (20 $\mu\text{M}$ , at the top end of the concentration range assessed) to achieve up-take blocking of 58%, 75% and 77% on OE33, OE19 and OE21 cell lines respectively. DFO was the least effective agent at blocking

up-take with the relationship between concentration and up-take blocking similar to that of Deferasirox (IC50 10 $\mu$ M blocked 20%, 32% and 30% of iron up-take for OE33, OE19 and OE21 cell lines respectively).

### **5.3.3.2 Iron chelators can extract (efflux) $^{59}\text{Fe}$ -Tf from oesophageal cancer cells *in-vitro***

Cell lines OE33, OE19 and OE21 were cultured in media spiked with  $^{59}\text{Fe}$ -Tf. After 3 hours,  $^{59}\text{Fe}$ -Tf media was replaced with media containing increasing concentrations of iron chelators, DFO, Deferasirox and Dp44mT. After a further 3 hours of incubation, cellular and media fractions were subject to gamma counting and results expressed by the media fraction as a percentage of the combined media and cellular fractions (i.e. total  $^{59}\text{Fe}$  taken up) (figure 5.2).

Dp44mT was the most effective agent at mobilising intracellular  $^{59}\text{Fe}$ , extracting 74%, 63% and 68% of internalised  $^{59}\text{Fe}$  at its IC50 value of 1 $\mu$ M for OE33, OE19 and OE21 lines respectively. Any further increase in Dp44mT concentration did not translate to improved  $^{59}\text{Fe}$  extraction. Deferasirox and DFO had similar profiles of extraction ability, exhibiting a gradual increase in the amount of  $^{59}\text{Fe}$  mobilised with increasing chelator concentration. At IC50 values, Deferasirox effluxed 65%, 48% and 54% for OE33, OE19 and OE21 cell lines respectively and DFO extracted 41%, 42% and 38% of internalised  $^{59}\text{Fe}$ .

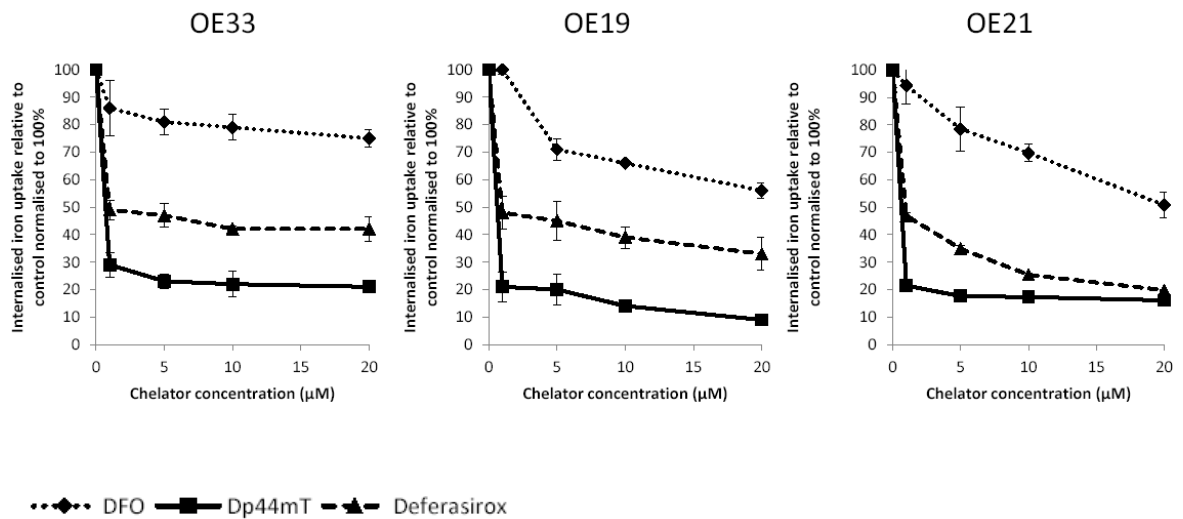


**Figure 5.1 Iron chelators DFO, Deferasirox and Dp44mT can block the up-take of  $^{59}\text{Fe-Tf}$  by oesophageal cancer cells *in-vitro***

Cell lines OE33, OE19 and OE21 cultured in media spiked with  $^{59}\text{Fe-Tf}$  and various iron chelators for three hours. Up-take of  $^{59}\text{Fe-Tf}$  assessed using a gamma counter and expressed as a percentage of  $^{59}\text{Fe-Tf}$  up-take alone. Error bars denote  $\pm$  SEM.

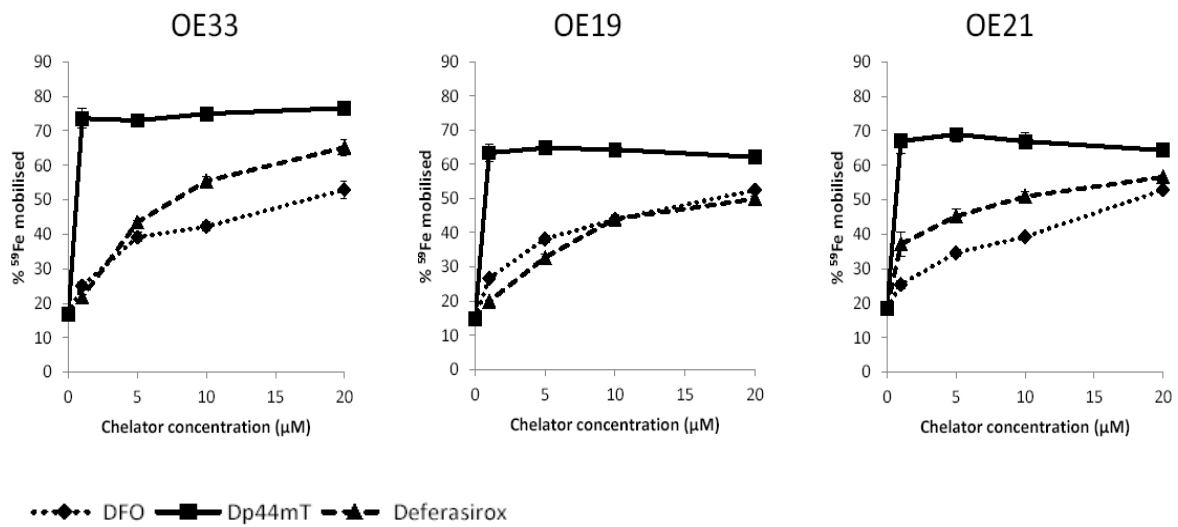


**Figure 5.2 Iron chelators DFO, Deferasirox and Dp44mT can efflux iron from oesophageal cancer cells *in-vitro***

Cell lines OE33, OE19 and OE21 cultured in media spiked with <sup>59</sup>Fe-Tf for 3 hours and then substituted for media containing iron chelators DFO, Deferasirox or Dp44mT for a further 3 hours. Results expressed by the media fraction gamma count as a percentage of the combined media and cellular fractions. Error bars denote ± SEM.

### **5.3.4 The *in-vitro* effects of iron chelation on iron and haem transport protein expression in oesophageal cancer cells**

To determine the effect of iron chelation on the expression of iron and haem transport proteins OE33, OE19 and OE21 cell lines were cultured for 48 hours with DFO or Deferasirox at IC50 value concentrations (10 and 20 $\mu$ M respectively). The cellular monolayer was then harvested and processed for mRNA and protein expression.

#### **5.3.4.1 Iron chelators influence mRNA expression of the iron transport proteins *in-vitro***

OE33, OE19 and OE21 cell lines were cultured with DFO or Deferasirox for 48 hours. Cells were then harvested and processed for TfR1, FPN and ferritin mRNA expression and presented as a fold change relative to control media alone (figure 5.3).

Culture with either Deferasirox or DFO induced a dramatic fold change in TfR1 mRNA expression in all cell lines. TfR1 mRNA induction was especially marked in the OE33 OAC line and the magnitude of change was similar for both chelators ( $p=0.0094$ ,  $p=0.01$  and  $p=0.005$  for Deferasirox OE33, OE19 and OE21 lines respectively, and  $p=0.033$ ,  $p=0.02$  and  $p=0.0001$  for DFO) (figure 5.3A).

The changes in ferritin mRNA expression were less pronounced than TfR1 with borderline significant reductions in mRNA fold change in the OE33 and OE21 cell lines cultured with DFO ( $p=0.05$  and  $p=0.02$ ). No significant mRNA changes were induced within the OE19 cell line and Deferasirox tended to slightly increase ferritin mRNA expression, although no changes were statistically significant (figure 5.3B).

Overall, culture with Deferasirox or DFO reduced FPN mRNA expression, although this was not consistently statistically significant. No statistically significant changes were

observed in the OE33 cell line ( $p=0.27$  and  $p=0.91$  for Deferasirox and DFO respectively). Deferasirox induced a significant reduction in FPN mRNA fold change in OE19 cells ( $p=0.05$ ) and DFO produced a more pronounced reduction in the squamous OE21 cell line ( $p=0.0025$ ) (figure 5.3C).

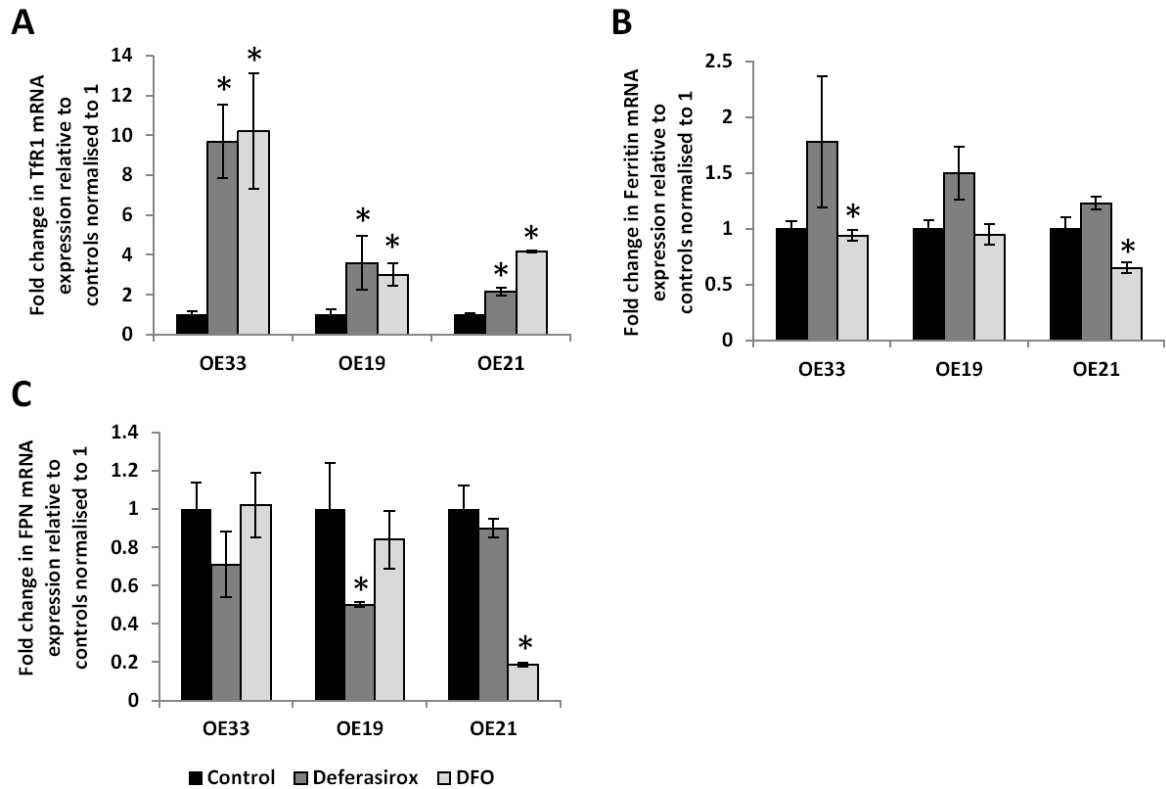


**Figure 5.3 Culture with iron chelators Deferasirox and DFO alters mRNA expression of iron transport proteins *in-vitro***

Figure A: Tfr1, figure B: ferritin and figure C: FPN mRNA expression for cell lines OE33, OE19, and OE21 after 48 hours culture with iron chelators Deferasirox or DFO. (\* $p < 0.05$  fold change in mRNA expression compared to plain media control and normalised to 1). Error bars denote  $\pm$  SEM.

#### 5.3.4.2 Iron chelators influence iron transport protein expression *in-vitro*

OE33, OE19 and OE21 cell lines were cultured with DFO or Deferasirox for 48 hours. Cells were then harvested and protein lysates subjected to Western blotting for TfR1, FPN and ferritin protein expression. Subsequent optical densities were normalised to  $\beta$ -actin and presented as a fold change relative to control media alone (figure 5.4).

Changes in TfR protein expression mirrored those of mRNA with significant induction across all three cell lines. The iron chelating action of Deferasirox and DFO induced changes of a similar magnitude ( $1.92 \pm 0.14$   $p=0.0015$ ,  $1.42 \pm 0.08$   $p=0.0024$  and  $2.03 \pm 0.06$   $p=0.0001$  for Deferasirox OE33, OE19 and OE21 lines respectively and  $1.89 \pm 0.07$   $p=0.0001$ ,  $1.33 \pm 0.12$   $p=0.01$  and  $1.57 \pm 0.1$   $p=0.0007$  for DFO) (figure 5.4A).

Ferritin protein expression was significantly reduced in the OE33 cell line ( $0.53 \pm 0.04$   $p=0.0009$  and  $0.51 \pm 0.03$   $p=0.0009$  for Deferasirox and DFO respectively). Neither the junctional adenocarcinoma cell line OE19 or squamous carcinoma OE21 line demonstrated any significant change in ferritin protein expression with either chelator (figure 5.4B).

FPN protein expression was consistently down in response to iron chelator exposure. No difference in degree of reduction was noted between chelators ( $0.63 \pm 0.03$   $p=0.0006$ ,  $0.62 \pm 0.05$   $p=0.0001$  and  $0.84 \pm 0.05$   $p=0.0029$  for Deferasirox OE33, OE19 and OE21 lines respectively and  $0.69 \pm 0.05$   $p=0.0022$ ,  $0.55 \pm 0.06$   $p=0.0001$  and  $0.73 \pm 0.08$   $p=0.0001$  for DFO) (figure 5.4C).

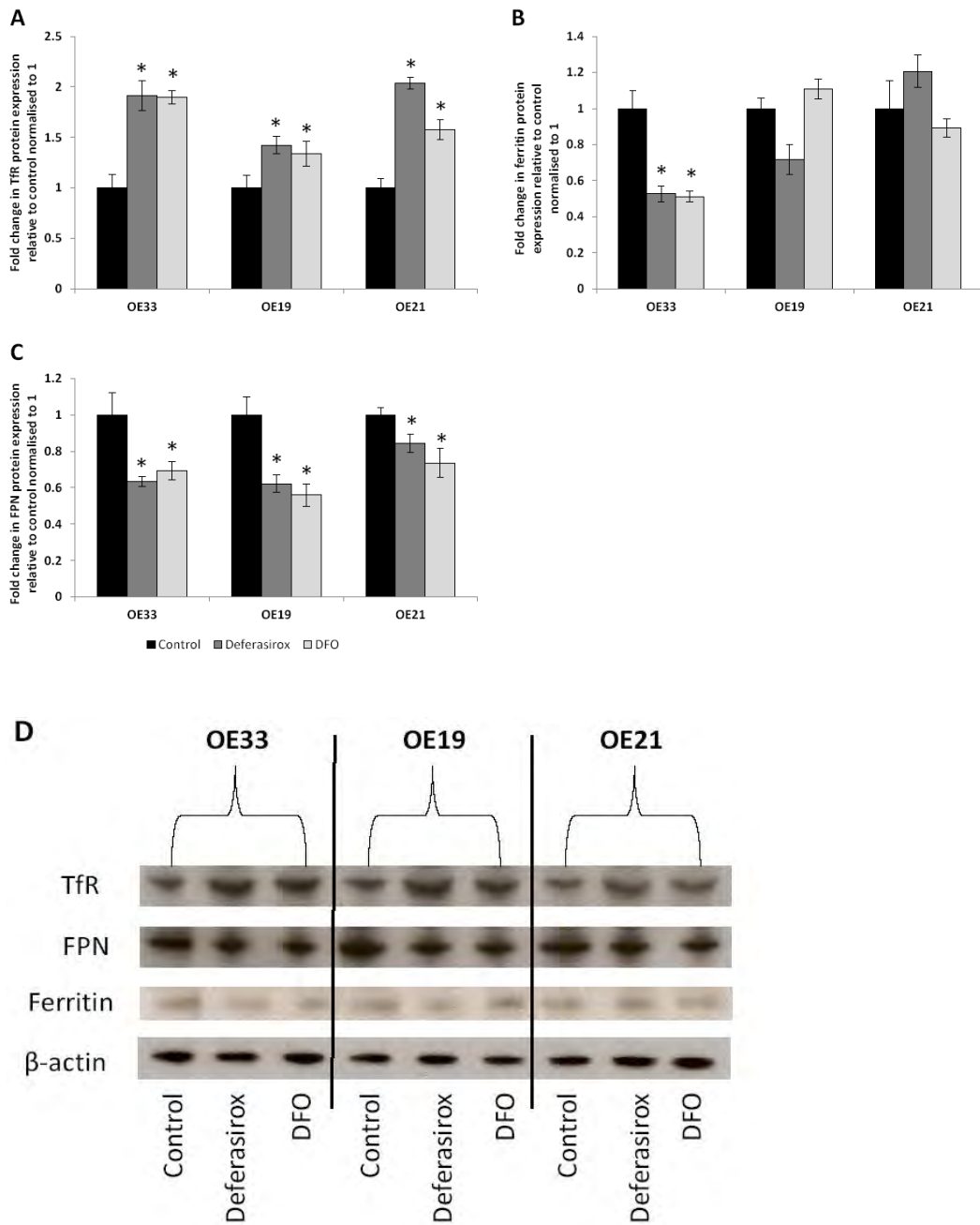


**Figure 5.4 Culture with iron chelators Deferasirox and DFO alters iron transport protein expression *in-vitro***

Figure A: Tfr1, figure B: ferritin and figure C: FPN protein expression for cell lines OE33, OE19, and OE21 after 48 hours culture with iron chelators Deferasirox or DFO. Figure D: Western blots for Tfr1, ferritin and FPN protein expression. (\* $p < 0.05$  fold change in protein expression compared to plain media control and normalised to 1).

#### 5.3.4.3 Iron chelators influence the mRNA expression of haem transport proteins *in-vitro*

OE33, OE19 and OE21 cell lines were cultured with DFO or Deferasirox for 48 hours. Cells were then harvested and processed for LRP1, HCP1, BCRP and FLVCR mRNA expression and presented as a fold change relative to control media alone (figure 5.5).

LRP1 mRNA expression was elevated across all cell lines in response to Deferasirox and DFO exposure. However, only the OE21 cell line cultured with Deferasirox exhibited a statistically significant increase in expression ( $2.54 \pm 0.54$   $p=0.049$ ) (figure 5.5A).

mRNA expression for the haem import protein HCP1, in a similar fashion to LRP1, was raised but did not reach statistical significance. The OE19 cell line showed no change in HCP1 mRNA expression after culture with chelators compared to control (figure 5.5B).

BCRP mRNA expression in the OE33 cell line remained unchanged after culture with either chelator ( $1.26 \pm 0.15$   $p=0.19$  and  $1.07 \pm 0.03$   $p=0.41$  for Deferasirox and DFO respectively). However, in contrast, both the OE19 and OE21 cell lines exhibited marked repression in BCRP mRNA expression compared to control ( $0.1 \pm 0.018$   $p=0.003$ ,  $0.26 \pm 0.03$   $p=0.05$  for Deferasirox exposed OE19 and OE21 lines respectively and  $0.1 \pm 0.03$   $p=0.0082$ ,  $0.39 \pm 0.1$   $p=0.15$  for DFO) (figure 5.5C).

Changes in the haem effluxing protein FLVCR mRNA expression were very similar to BCRP. Culture with Deferasirox or DFO failed to elicit an expression change in OE33 cells ( $0.73 \pm 0.17$   $p=0.2$  and  $1.17 \pm 0.06$   $p=0.12$  for Deferasirox and DFO respectively). Both OE19 and OE21 cell lines responded to iron chelation by suppressing FLVCR mRNA expression

( $0.22 \pm 0.02$   $p=0.015$ ,  $0.17 \pm 0.04$   $p=0.02$  for Deferasirox exposed OE19 and OE21 cell lines respectively and  $0.28 \pm 0.04$   $p=0.0026$ ,  $0.46 \pm 0.04$   $p=0.05$  for DFO) (figure 5.5D).

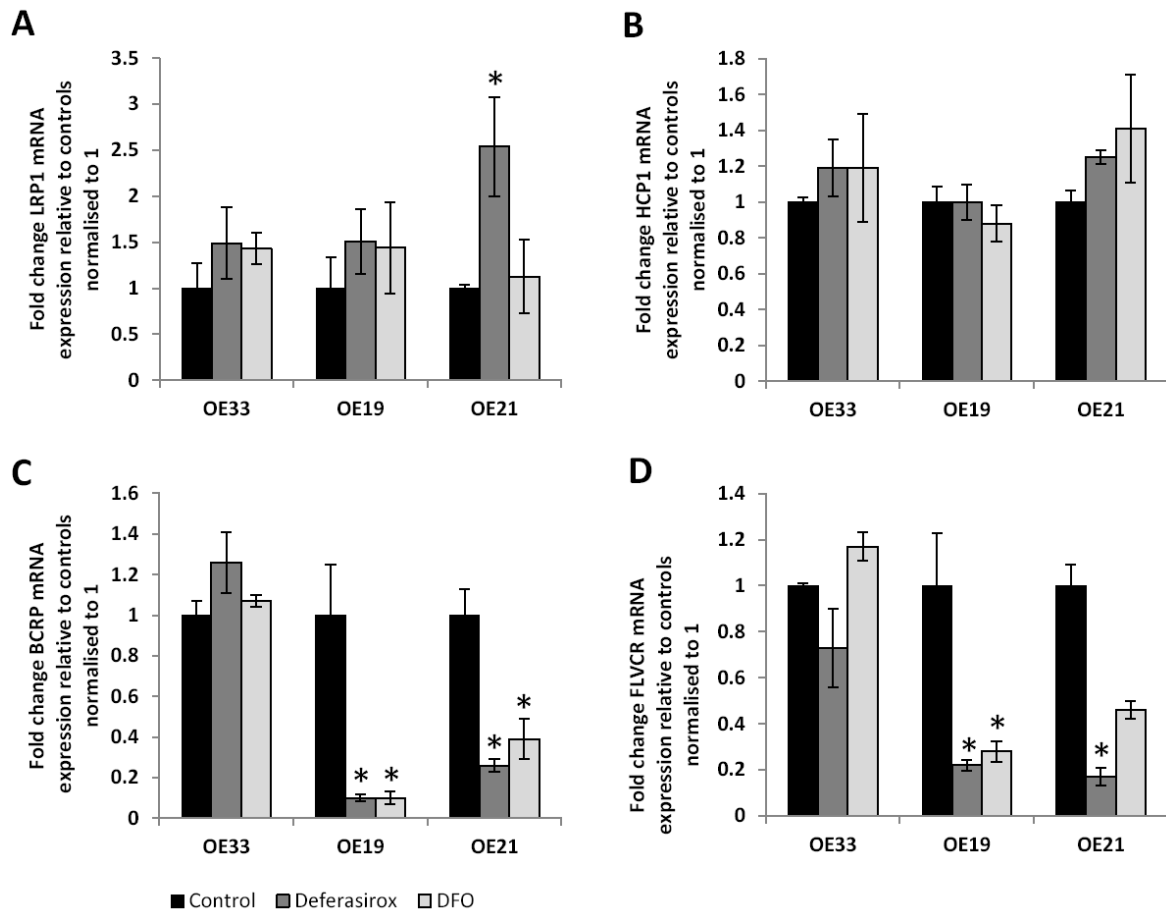


**Figure 5.5 Culture with iron chelators Deferasirox and DFO influences mRNA expression of haem transport proteins *in-vitro***

Figure A: LRP1, figure B: HCP1, figure C: BCRP and figure D: FLVCR mRNA expression for cell lines OE33, OE19, and OE21 after 48 hours culture with iron chelators Deferasirox or DFO. (\* $p < 0.05$  fold change in mRNA expression compared to plain media control and normalised to 1). Error bars denote  $\pm$  SEM.

#### 5.3.4.4 Iron chelators influence haem transport protein expression *in-vitro*

OE33, OE19 and OE21 cell lines were cultured with DFO or Deferasirox for 48 hours. Cells were then harvested and protein lysates utilised for Western blotting for LRP1, HCP1, BCRP and FLVCR protein expression. Subsequent optical densities were normalised to  $\beta$ -actin and presented as a fold change relative to control media alone (figure 5.6).

LRP1 protein expression was significantly raised in response to culture with Deferasirox or DFO in OE33 and OE21 cell lines ( $2.08 \pm 0.09$   $p=0.0004$ ,  $1.69 \pm 0.08$   $p=0.0001$  for OE33 and OE21 cell lines cultured with Deferasirox respectively and  $1.47 \pm 0.07$   $p=0.0019$ ,  $1.4 \pm 0.06$   $p=0.0005$  for DFO. OE19 cells exhibited minor elevation in LRP1 protein expression which narrowly missed statistical significance ( $1.11 \pm 0.05$   $p=0.091$  and  $1.19 \pm 0.04$   $p=0.056$  for Deferasirox and DFO respectively) (figure 5.6A).

HCP1 protein expression, in response to culture with iron chelators, was near identical to mRNA observations. OE33 cells exhibited an increase in expression without reaching statistical significance ( $1.32 \pm 0.06$   $p=0.062$ ,  $1.13 \pm 0.09$   $p=0.12$  for Deferasirox and DFO respectively), OE19 cells offered no change ( $0.99 \pm 0.06$   $p=0.67$ ,  $1.01 \pm 0.1$   $p=0.66$  for Deferasirox and DFO respectively) and OE21 determined a significant rise in HCP1 protein expression compared to control ( $1.73 \pm 0.08$   $p=0.0002$ ,  $1.45 \pm 0.07$   $p=0.0003$  for Deferasirox and DFO respectively) (figure 5.6B).

The suppression in BCRP mRNA expression reflected a marked reduction in protein expression in OE19 and OE21 cell lines for both Deferasirox and DFO ( $0.47 \pm 0.11$   $p=0.0001$ ,  $0.67 \pm 0.05$   $p=0.0001$  for OE19 and OE21 cultured with Deferasirox and  $0.46 \pm 0.06$   $p=0.0001$ ,  $0.60 \pm 0.09$   $p=0.0001$  for DFO). OE33 cells did not demonstrate a

difference in BCRP protein fold change compared to control ( $0.9\pm 0.1$   $p=0.3$ ,  $0.97\pm 0.13$   $p=0.63$  for Deferasirox and DFO respectively) (figure 5.6C).

In accordance with suppressed mRNA expression, the OE19 cell line exhibited reduced FLVCR protein production in response to both chelators ( $0.62\pm 0.11$   $p=0.0001$ ,  $0.53\pm 0.1$   $p=0.0001$  for Deferasirox and DFO respectively). Iron chelators induced no change in FLVCR protein fold change in OE33 cells ( $0.84\pm 0.07$   $p=0.12$ ,  $0.9\pm 0.08$   $p=0.22$ ) or the OE21 cell line, despite the latter demonstrating a significant suppression of FLVCR mRNA ( $1.06\pm 0.07$   $p=0.86$ ,  $0.9\pm 0.08$   $p=0.2$ ) (figure 5.6D).

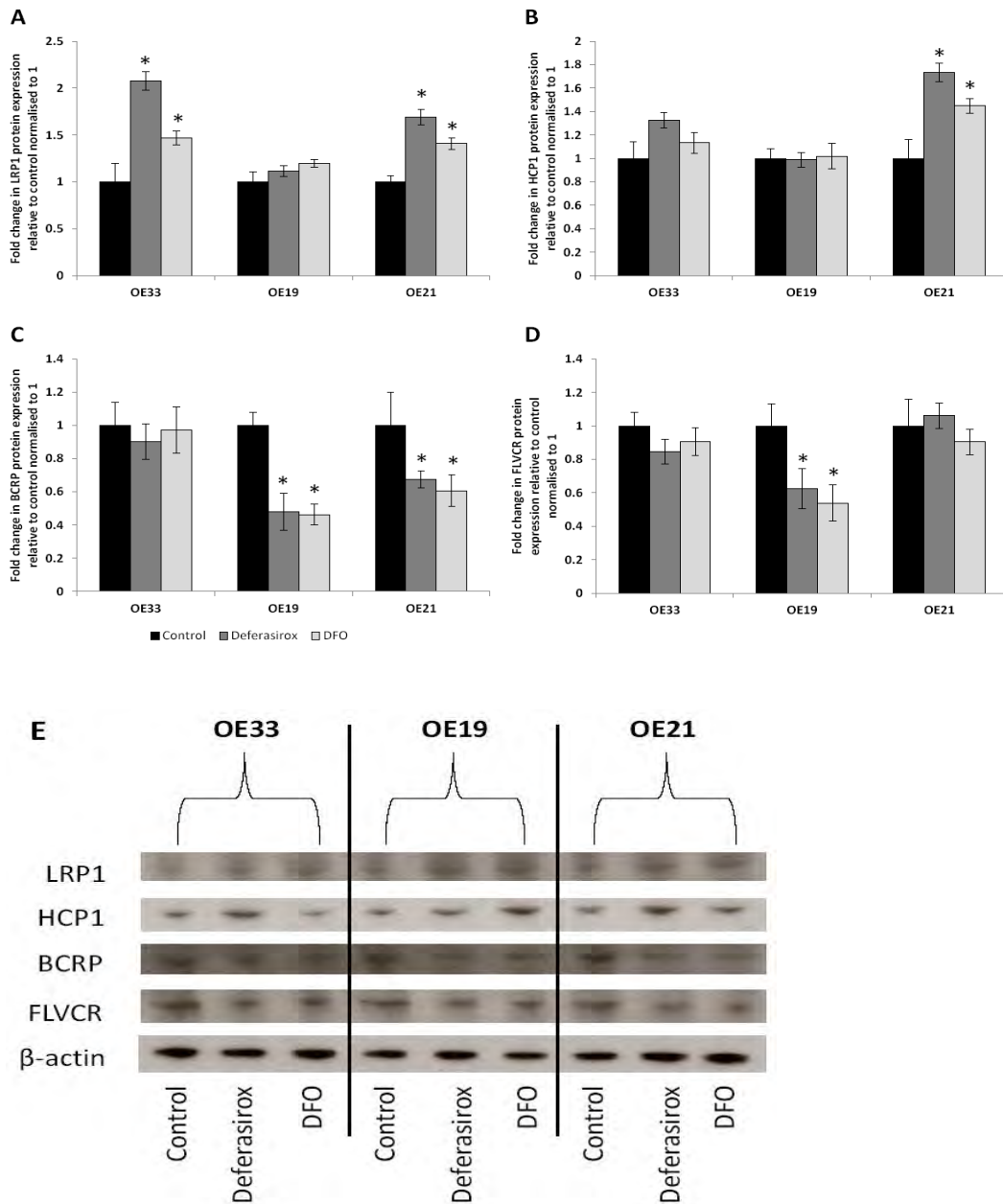


**Figure 5.6 Culture with iron chelators Deferasirox and DFO influences haem transport protein expression *in-vitro***

Figure A: LRP1, figure B: HCP1, figure C: BCRP and figure D: FLVCR protein expression for cell lines OE33, OE19, and OE21 after 48 hours culture with iron chelators Deferasirox or DFO. Figure E: Western blots for LRP1, HCP1, BCRP and FLVCR protein expression. (\* $p < 0.05$  fold change in protein expression compared to plain media control and normalised to 1).

### **5.3.5 The *in-vitro* effect of iron chelation on oesophageal cancer cell phenotype**

OE33, OE19 and OE21 cell lines were utilised to assess the effect of iron chelation on cellular phenotype *in-vitro*. Iron chelators were used at IC50 values (Deferasirox 20  $\mu$ M, DFO 10  $\mu$ M and Dp44mT 1  $\mu$ M). Iron 100 $\mu$ M and plain media alone were used as positive and negative controls respectively. Changes in cellular phenotype were assessed with MTT assay (viability), BrdU assay (proliferation), colony forming assay (ability to form independent colonies) and scratch assay (migration).

#### **5.3.5.1 Iron chelators Deferasirox and DFO inhibit oesophageal cancer cell viability and proliferation *in-vitro***

OE33, OE19 and OE21 cell lines were cultured in the presence of Deferasirox or DFO +/- iron or haem (Deferasirox 20 $\mu$ M, DFO 10 $\mu$ M, iron 100 $\mu$ M and haem 50 $\mu$ M). After 48 hours of culture, cells were assessed for viability and proliferation relative to control media (figures 5.7 and 5.8).

Observations were consistent between OE33 and OE19 OAC lines and the SCC line, OE21. Supplementary iron and haem induced significant increases in viability and proliferation, compared to control media alone. Deferasirox and DFO reduced viability and proliferation by approximately 50%, in line with observations expected with both agents used at IC50 concentrations. Supplementary iron or haem co-cultured with Deferasirox or DFO failed to completely rescue the cells from the inhibitory effect of chelation. Deferasirox and haem appeared to decrease viability and proliferation compared to Deferasirox alone, whereas additional haem partially reversed the effects of DFO.

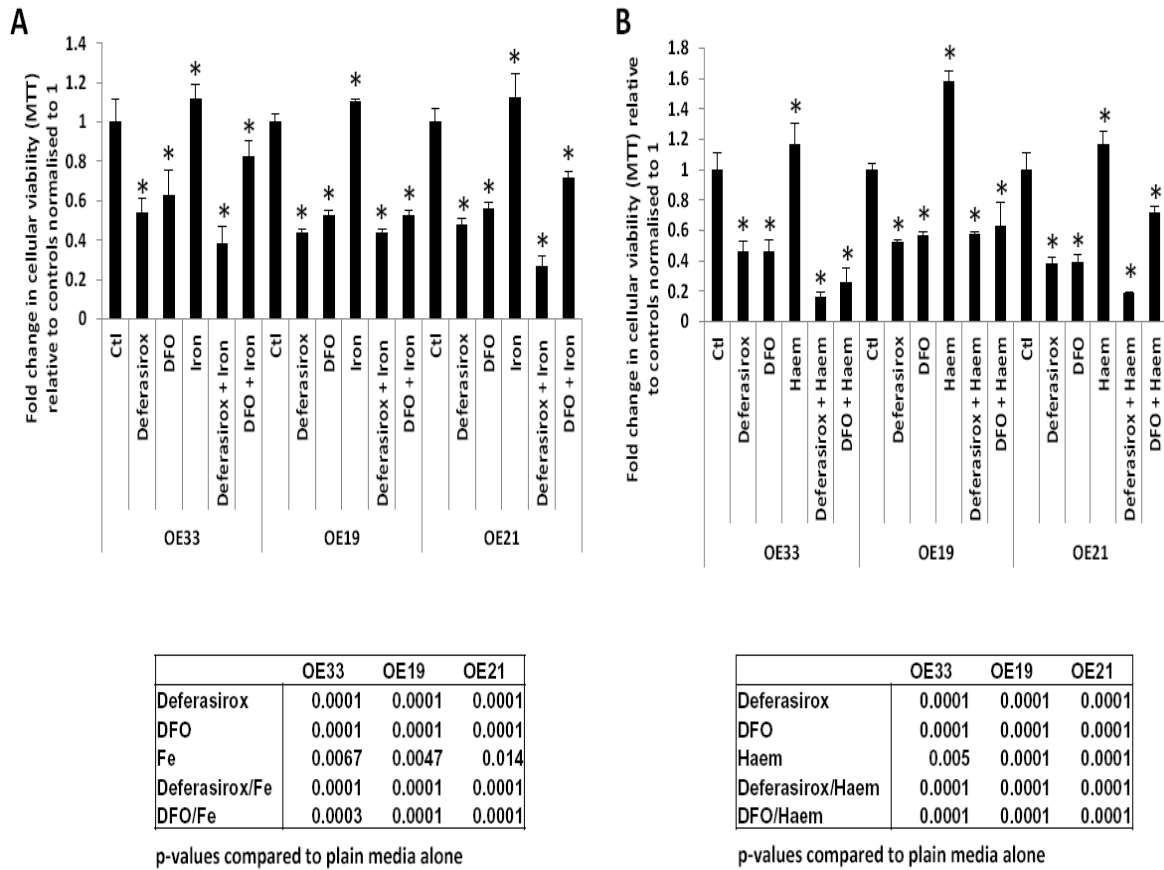


**Figure 5.7 Iron chelators Deferasirox and DFO inhibit oesophageal cancer cell viability**

OE33, OE19 and OE21 cell lines cultured for 48 hours in the presence of Deferasirox or DFO +/- iron (figure A) or haem (figure B) (Deferasirox 20µM, DFO 10µM, iron 100µM haem 50µM). Viability presented relative to plain control media and normalised to 1. Associated p-values given in table beneath figures. (\*p<0.05 fold change in viability or proliferation compared to control and normalised to 1). Error bars denote ± SEM.

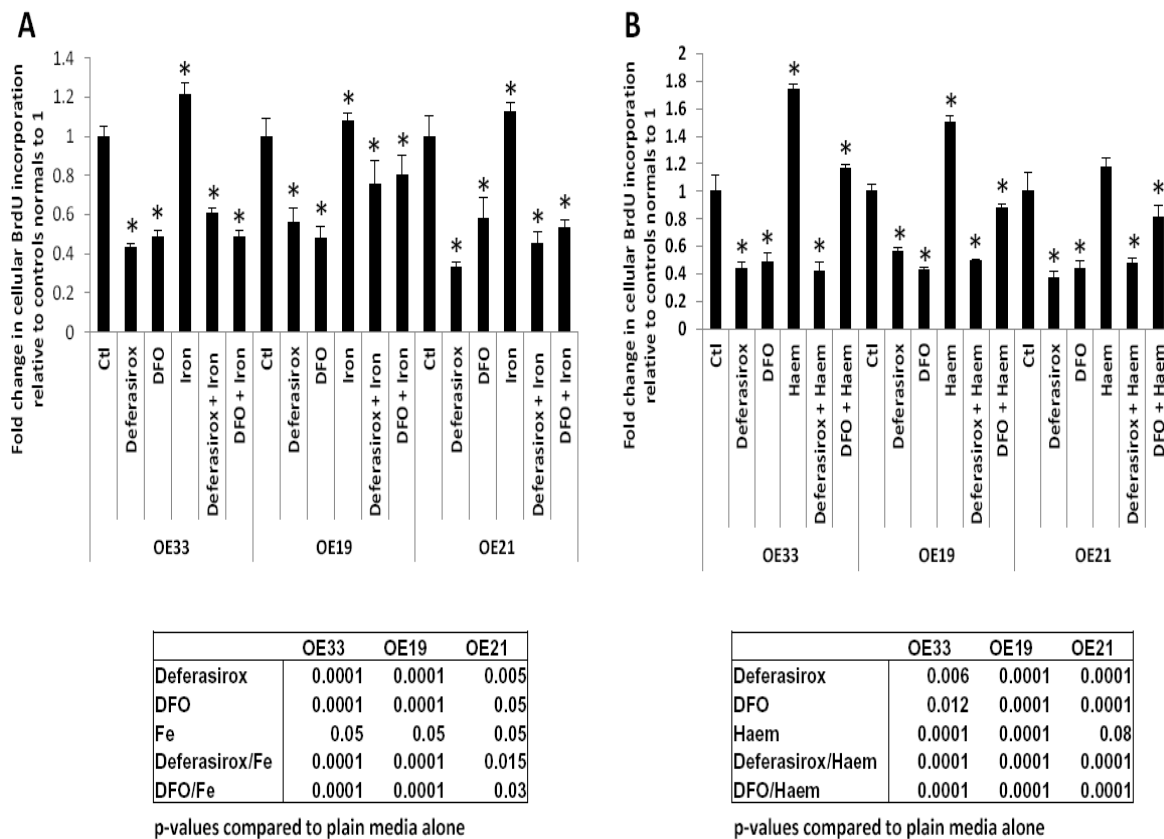


**Figure 5.8 Iron chelators Deferasirox and DFO inhibit oesophageal cancer cell proliferation**

OE33, OE19 and OE21 cell lines cultured for 48 hours in the presence of Deferasirox or DFO +/- iron (figure A) or haem (figure B) (Deferasirox 20µM, DFO 10µM, iron 100µM haem 50µM). Proliferation presented relative to plain control media and normalised to 1. Associated p-values given in table beneath figures. (\*p<0.05 fold change in viability or proliferation compared to control and normalised to 1). Error bars denote ± SEM.

#### **5.3.5.2 Dp44mT inhibits oesophageal cancer cell viability and proliferation *in-vitro***

OE33, OE19 and OE21 cell lines were cultured in the presence of Dp44mT 1 $\mu$ M or Dp2mT 1 $\mu$ M (negative control) with or without Fe (100 $\mu$ M) (positive control). After 48 hours of culture cells were assessed for viability and proliferation relative to plain control media and normalised to 1 (figure 5.9).

Results were again consistent across all three cell lines with iron in combination with Dp2mT inducing significant increases in viability and proliferation compared to Dp2mT alone. Dp44mT significantly reduced viability and proliferation by approximately 50% in line with use at the predetermined IC50 value of 1 $\mu$ M. The addition of iron to Dp44mT containing media did not rescue the exposed cell lines from the effects Dp44mT with viability and proliferation remaining at values seen with Dp44mT alone.

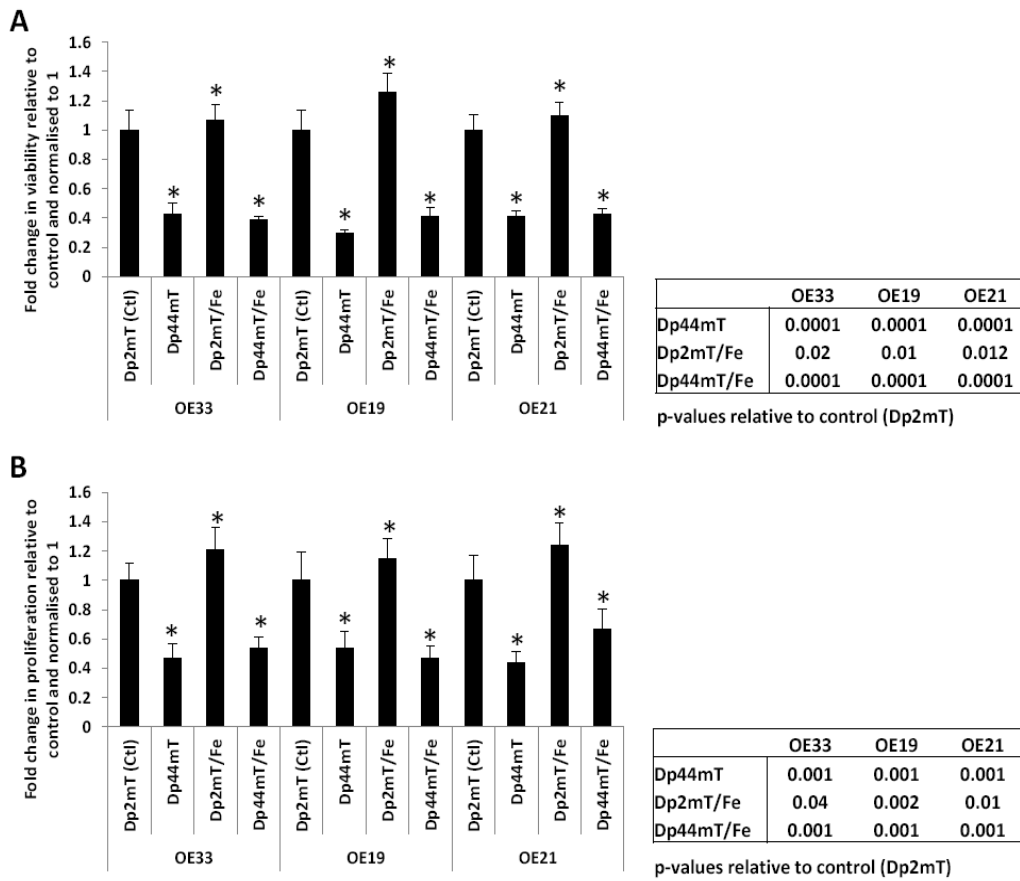


**Figure 5.9 Dp44mT inhibits oesophageal cancer cell viability and proliferation *in-vitro***

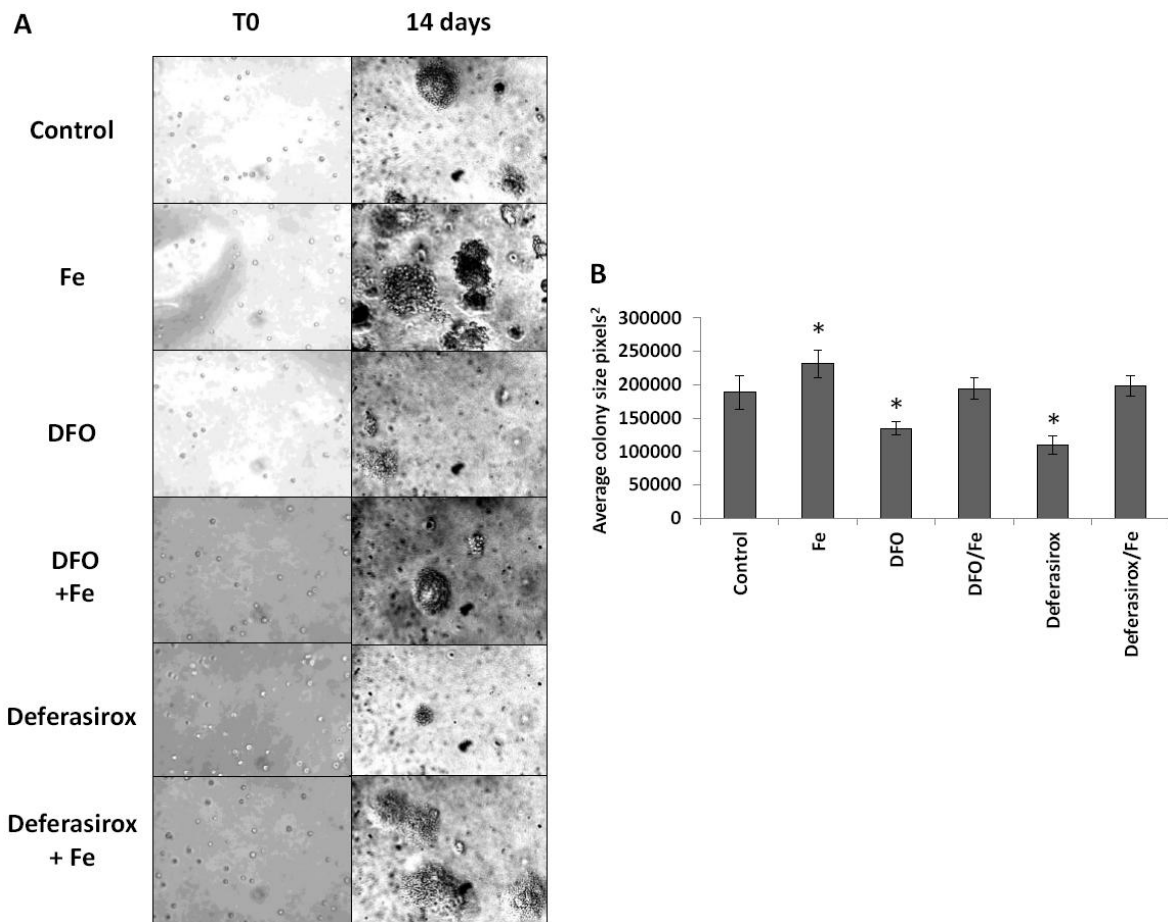
OE33, OE19 and OE21 cell lines were cultured in the presence of Dp44mT 1 $\mu$ M or Dp2mT 1 $\mu$ M (negative control) with or without Fe 100 $\mu$ M (positive control). After 48 hours of culture cells were assessed for viability (figure A) and proliferation (figure B) relative to plain control media and normalised to 1. (\* $p < 0.05$  fold change in viability or proliferation compared to control and normalised to 1). Error bars denote  $\pm$  SEM.

### 5.3.5.3 Iron chelators inhibit oesophageal cancer cell anchorage independent growth

OE33, OE19 and OE21 cell lines were seeded as a single cell suspension in agar containing plain media or media with iron chelators at IC50 concentrations (Deferasirox 20 $\mu$ M, DFO 10 $\mu$ M and Dp44mT 1 $\mu$ M). Iron (100 $\mu$ M) was used as a positive control or in combination with iron chelators. After two weeks of incubation, the average colony size was calculated in pixels<sup>2</sup> (figures 5.10: OE33, 5.11: OE19 and 5.12: OE21).

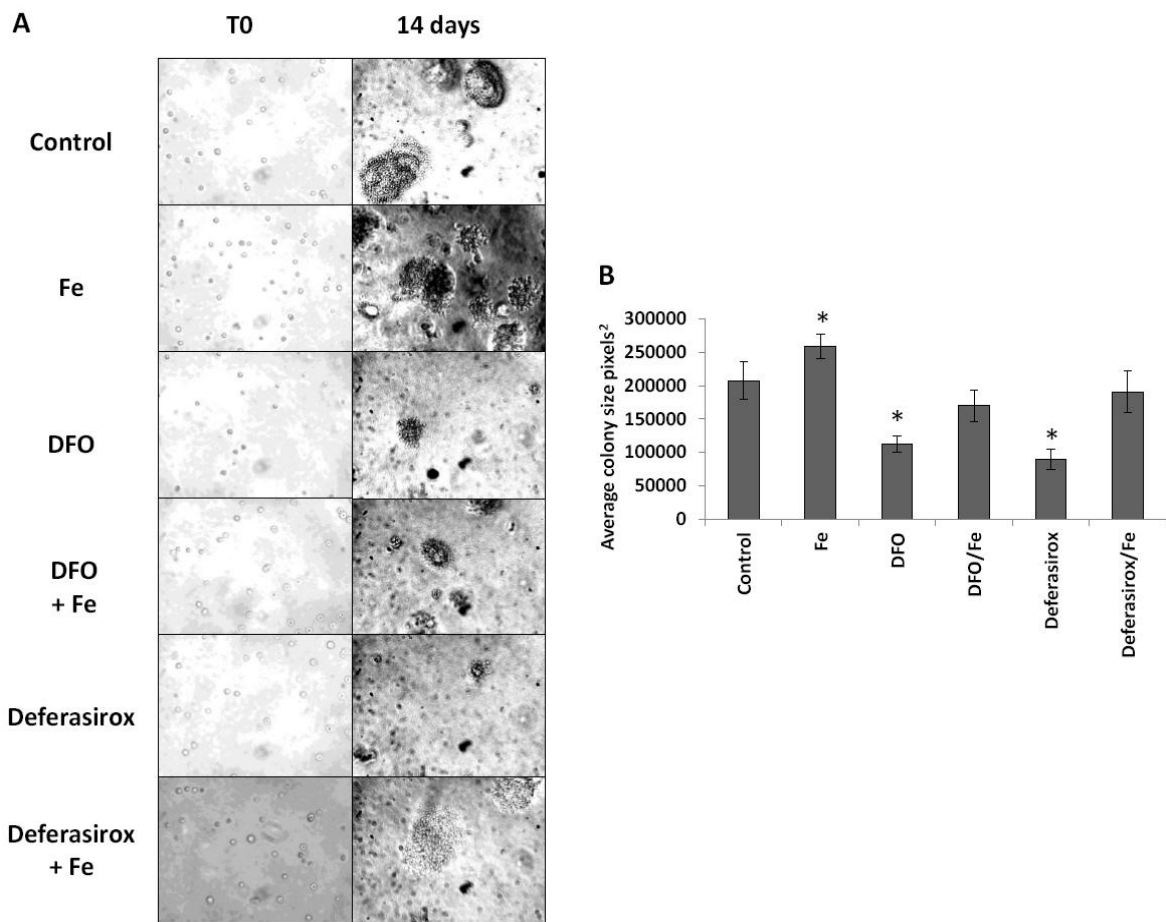
Observations were consistent across all three cell lines. The addition of iron to agar growing media significantly enhanced the average colony size ( $p=0.01$ ,  $p=0.038$  and  $p=0.032$  for OE33, OE19 and OE21 cell lines respectively). In the absence of supplementary iron, Deferasirox and DFO significantly retarded colony size with the former agent exhibiting a slightly superior inhibitory effect ( $p=0.0054$ ,  $p=0.0019$  and  $p=0.005$  for OE33, OE19 and OE21 cell lines exposed to Deferasirox and  $p=0.017$ ,  $p=0.0036$  and  $p=0.0019$  for DFO). The addition of supplementary iron to growing media containing Deferasirox or DFO neutralised the inhibitory effect of the iron chelators.

In the presence of Dp44mT (compared to growing media containing Dp2mT as a non-iron chelating control) no viable colonies formed in any cell line ( $p<0.0001$  for all lines). The addition of iron to Dp2mT control media invoked a significantly increased colony size ( $p=0.0002$ ,  $p=0.001$  and  $p=0.001$  for OE33, OE19 and OE21 cell lines respectively). In marked contrast to Deferasirox and DFO, the addition of supplementary iron to Dp44mT containing growth media failed to reverse the inhibitory effect of Dp44mT alone (figures 5.13: OE33, 5.14: OE19 and 5.15: OE21).



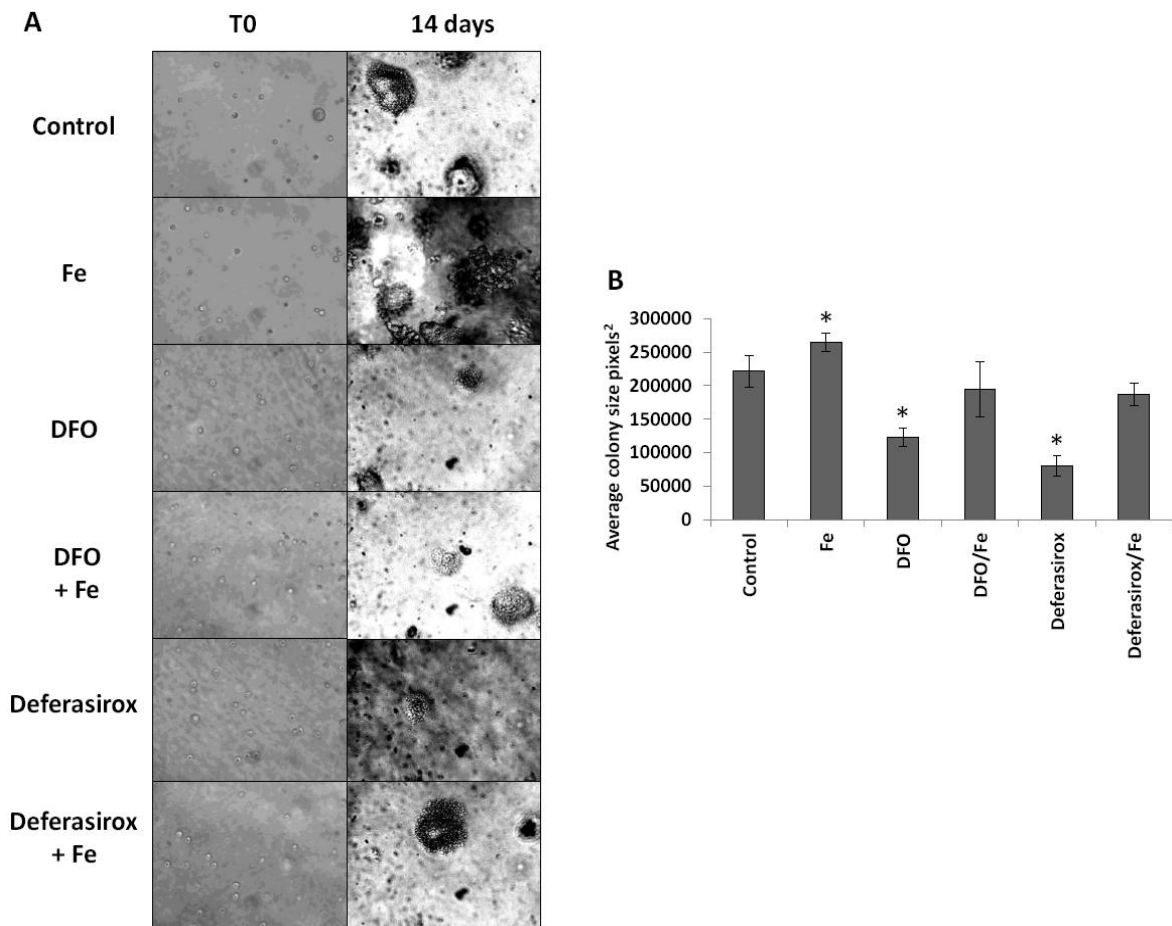
**Figure 5.10 Iron chelators inhibit OE33 cell line anchorage independent growth**

Figure A: OE33 OAC cell line seeded as a single cell suspension in agar containing plain media or media with iron chelators at IC50 concentrations (Deferasirox 20 $\mu$ M and DFO 10 $\mu$ M) (n=9). Iron 100 $\mu$ M was used as a positive control or in combination with iron chelators. Figure B: after 14 days of incubation, the average colony size was calculated in pixels<sup>2</sup>. (\*p<0.05 significant change in average colony size compared to plain media control). Error bars denote  $\pm$  SEM.



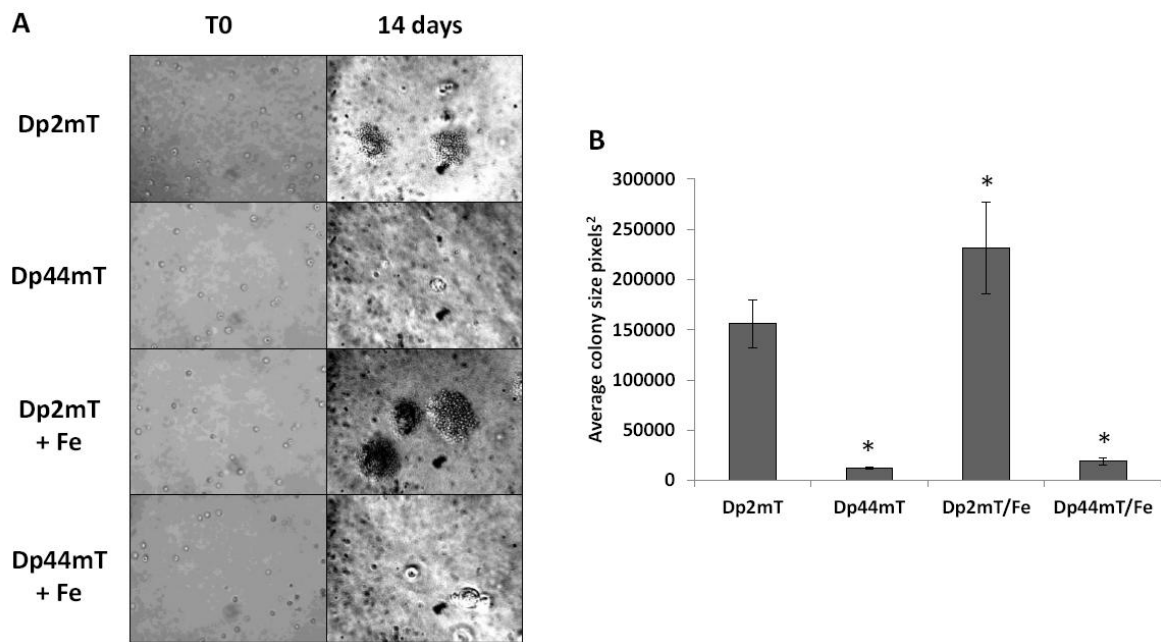
**Figure 5.11 Iron chelators inhibit OE19 cell line anchorage independent growth**

Figure A: OE19 junctional OAC cell line seeded as a single cell suspension in agar containing plain media or media with iron chelators at IC50 concentrations (Deferasirox 20 $\mu$ M and DFO 10 $\mu$ M) (n=9). Iron 100 $\mu$ M was used as a positive control or in combination with iron chelators. Figure B: after 14 days of incubation, the average colony size was calculated in pixels<sup>2</sup>. (\*p<0.05 significant change in average colony size compared to plain media control). Error bars denote  $\pm$  SEM.



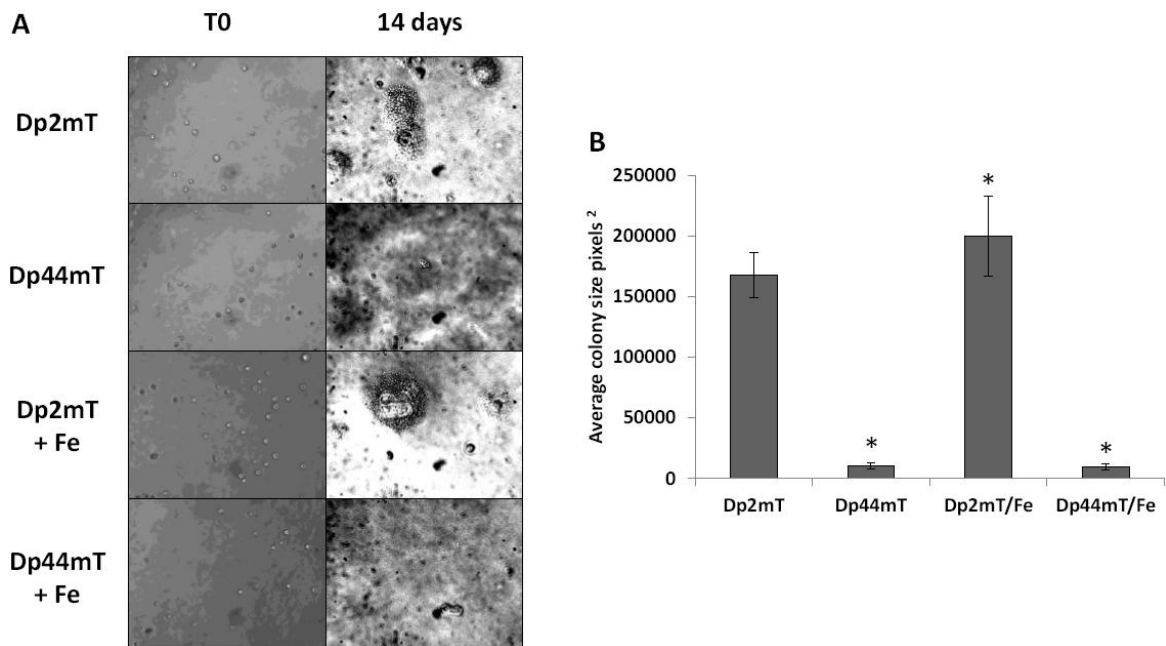
**Figure 5.12 Iron chelators inhibit OE21 cell line anchorage independent growth**

Figure A: OE21 oesophageal SCC line seeded as a single cell suspension in agar containing plain media or media with iron chelators at IC<sub>50</sub> concentrations (Deferasirox 20 $\mu$ M and DFO 10 $\mu$ M) (n=9). Iron 100 $\mu$ M was used as a positive control or in combination with iron chelators. Figure B: after 14 days of incubation, the average colony size was calculated in pixels<sup>2</sup>. (\*p<0.05 significant change in average colony size compared to plain media control). Error bars denote  $\pm$  SEM.



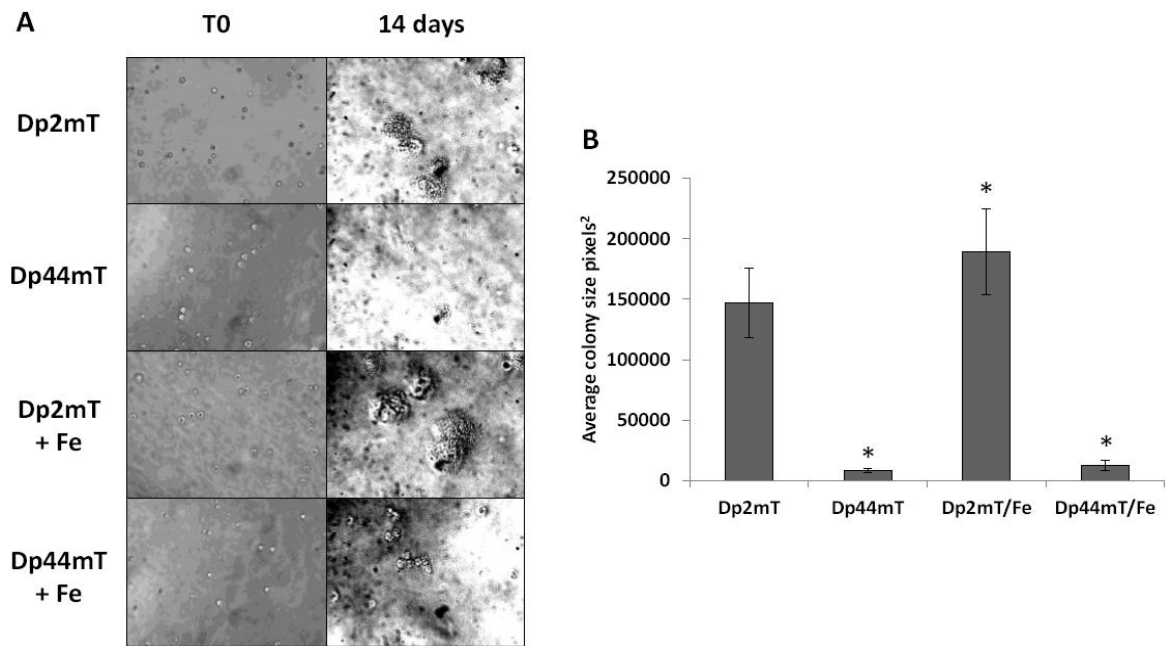
**Figure 5.13 Iron chelator Dp44mT inhibits OE33 cell line anchorage independent growth**

Figure A: OE33 cell line seeded as a single cell suspension in agar containing control media (1 $\mu$ M Dp2mT) or Dp44mT 1 $\mu$ M (n=9). Fe 100 $\mu$ M used as a positive control (with Dp2mT) or in combination with Dp44mT. Figure B: after 14 days of incubation, the average colony size was calculated in pixels<sup>2</sup>. (\*p<0.05 significant change in average colony size compared to plain media control). Error bars denote  $\pm$  SEM.



**Figure 5.14 Iron chelator Dp44mT inhibits OE19 cell line anchorage independent growth**

Figure A: OE19 cell line seeded as a single cell suspension in agar containing control media (1 $\mu$ M Dp2mT) or Dp44mT 1 $\mu$ M (n=9). Fe 100 $\mu$ M used as a positive control (with Dp2mT) or in combination with Dp44mT. Figure B: after 14 days of incubation, the average colony size was calculated in pixels<sup>2</sup> (Fig B). (\*p<0.05 significant change in average colony size compared to plain media control). Error bars denote  $\pm$  SEM.



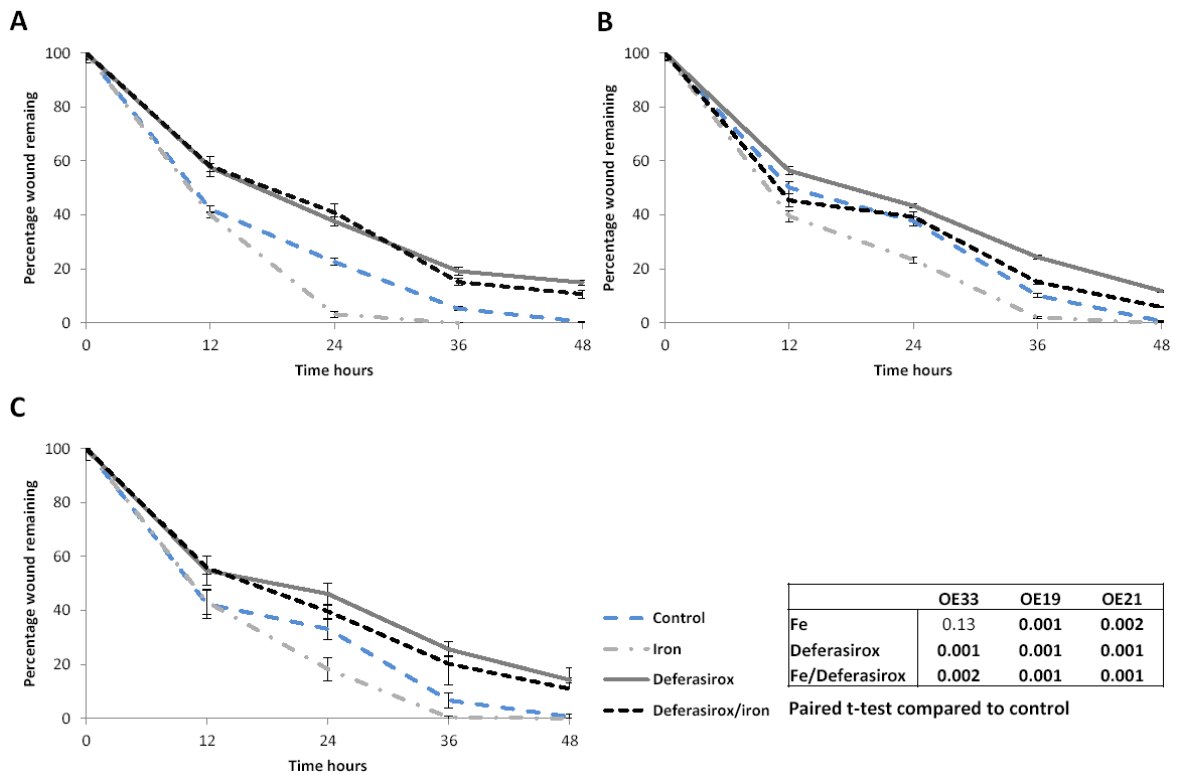
**Figure 5.15 Iron chelator Dp44mT inhibits OE21 cell line anchorage independent growth**

Figure A: OE21 cell line seeded as a single cell suspension in agar containing control media (1 $\mu$ M Dp2mT) or Dp44mT 1 $\mu$ M (n=9). Fe 100 $\mu$ M used as a positive control (with Dp2mT) or in combination with Dp44mT. Figure B after 14 days of incubation, the average colony size was calculated in pixels<sup>2</sup>. (\*p<0.05 significant change in average colony size compared to plain media control). Error bars denote  $\pm$  SEM.

#### **5.3.5.4 Iron chelators inhibit oesophageal cancer cell migration *in-vitro***

OE33, OE19 and OE21 cell lines were cultured in plain media and allowed to form a monolayer. The cell monolayer was then scratched (wounded) and plain media substituted for media spiked with iron chelators at IC50 concentrations (Deferasirox 20 $\mu$ M, DFO 10 $\mu$ M and Dp44mT 1 $\mu$ M). Iron 100 $\mu$ M was used as a positive control or in combination with iron chelators. The degree to which the wound healed was described as a percentage of wound remaining as a function of time and compared to control media alone (figures 5.16 and 5.17 for Deferasirox; figure 5.18 for DFO and figures 5.19 and 5.20 for Dp44mT).

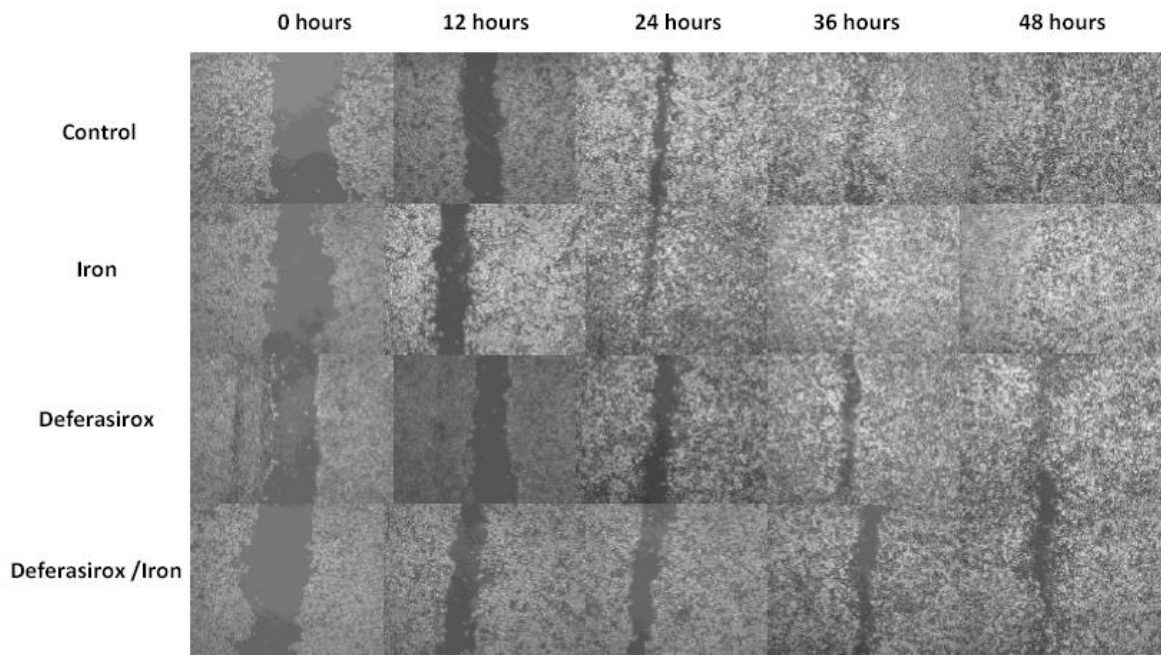
Observations were consistent across the three cell lineages. Addition of iron to the culture media was associated with significantly more rapid wound closure compared to control. In the presence of Deferasirox, DFO or Dp44mT wound closure was significantly retarded compared to control. Deferasirox and DFO demonstrated similar inhibitory effects with Dp44mT exhibiting a very potent anti-migratory action. In contrast to previous observations, where the addition of supplementary iron reverses the inhibitory effects of Deferasirox and DFO, additional iron did not prevent the chelators impeding cellular migration. Dp44mT retained its potent inhibition of migration with supplementary iron, in accordance with previous observations of colony forming, viability and proliferation.



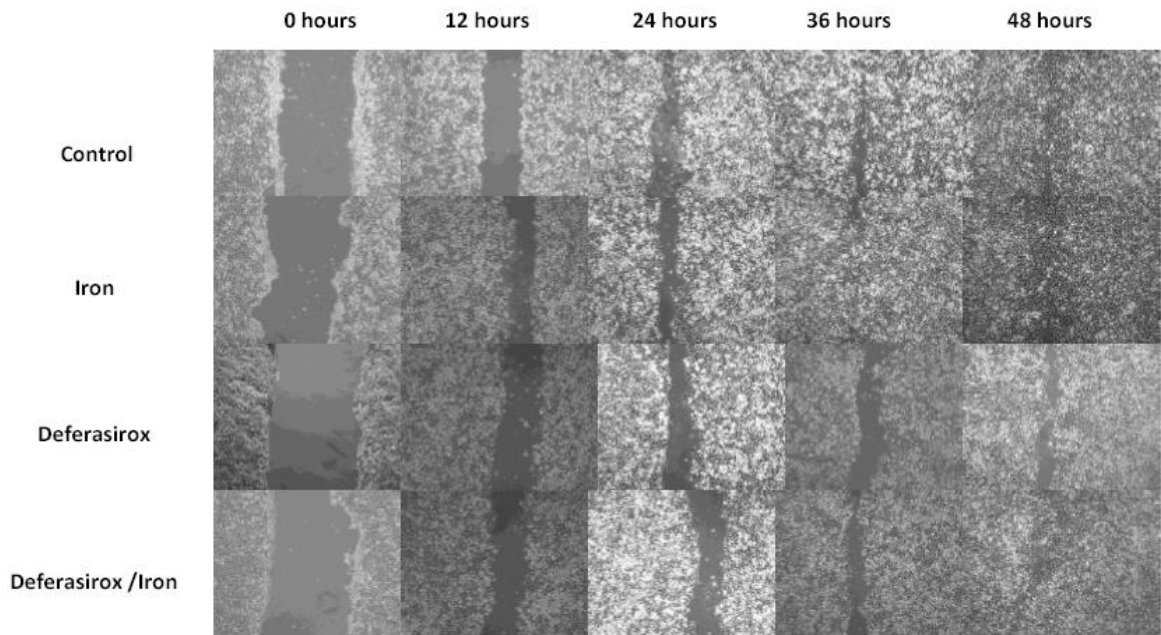
**Figure 5.16 Deferasirox inhibits oesophageal cancer cell migration *in-vitro***

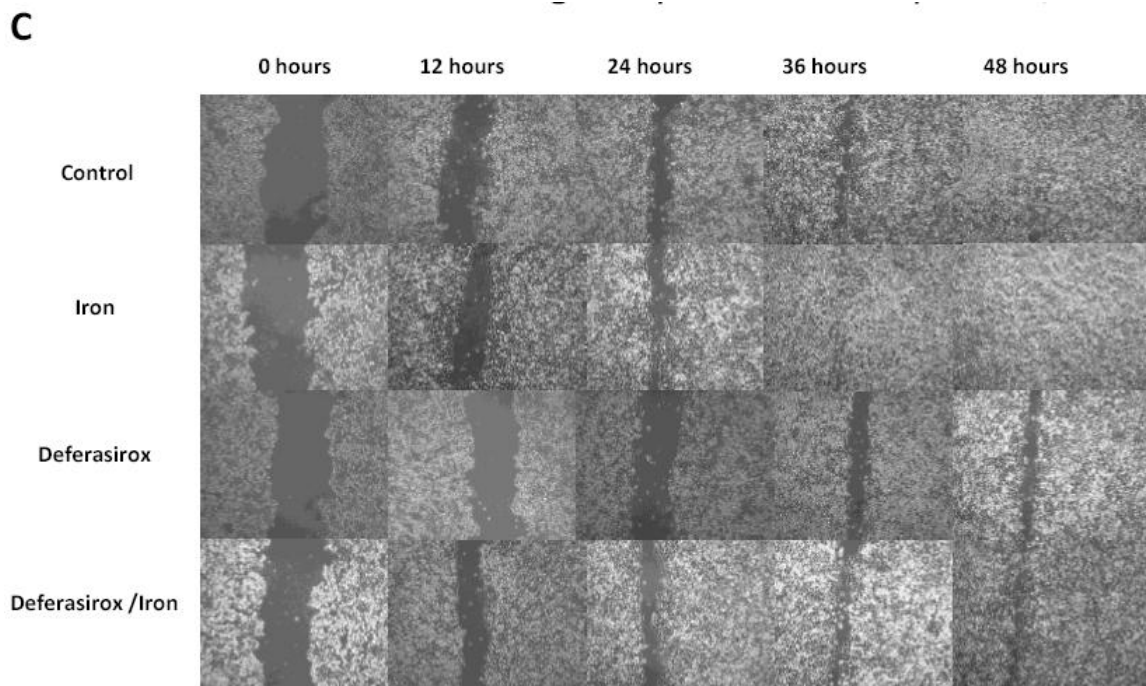
Figure A: OE33, figure B: OE19 and figure C: OE21 cell lines were cultured in plain media and allowed to form a monolayer. The cell monolayer was then scratched (wounded) and plain media substituted for media spiked with Deferasirox 20 $\mu$ M. Iron 100 $\mu$ M was used as a positive control or in combination with Deferasirox. The degree to which the wound healed was described as a percentage of wound remaining as a function of time and compared to control media alone. Error bars denote  $\pm$  SEM.

**A**



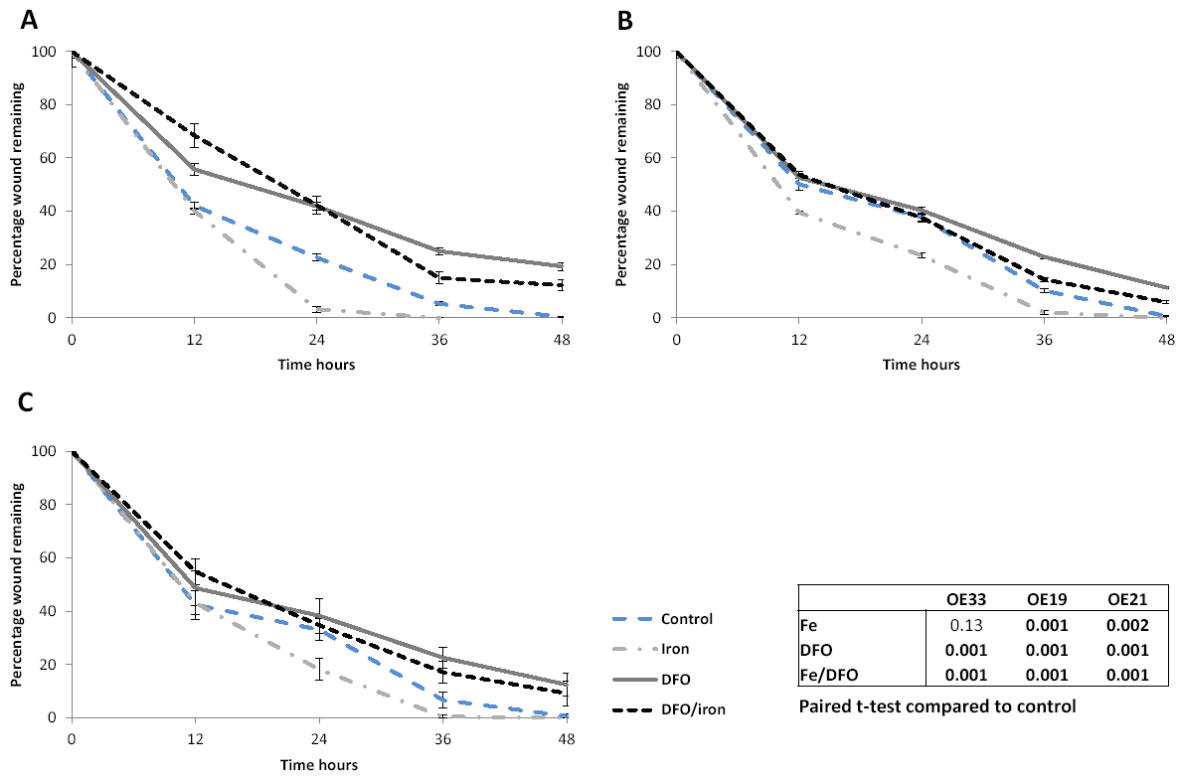
**B**





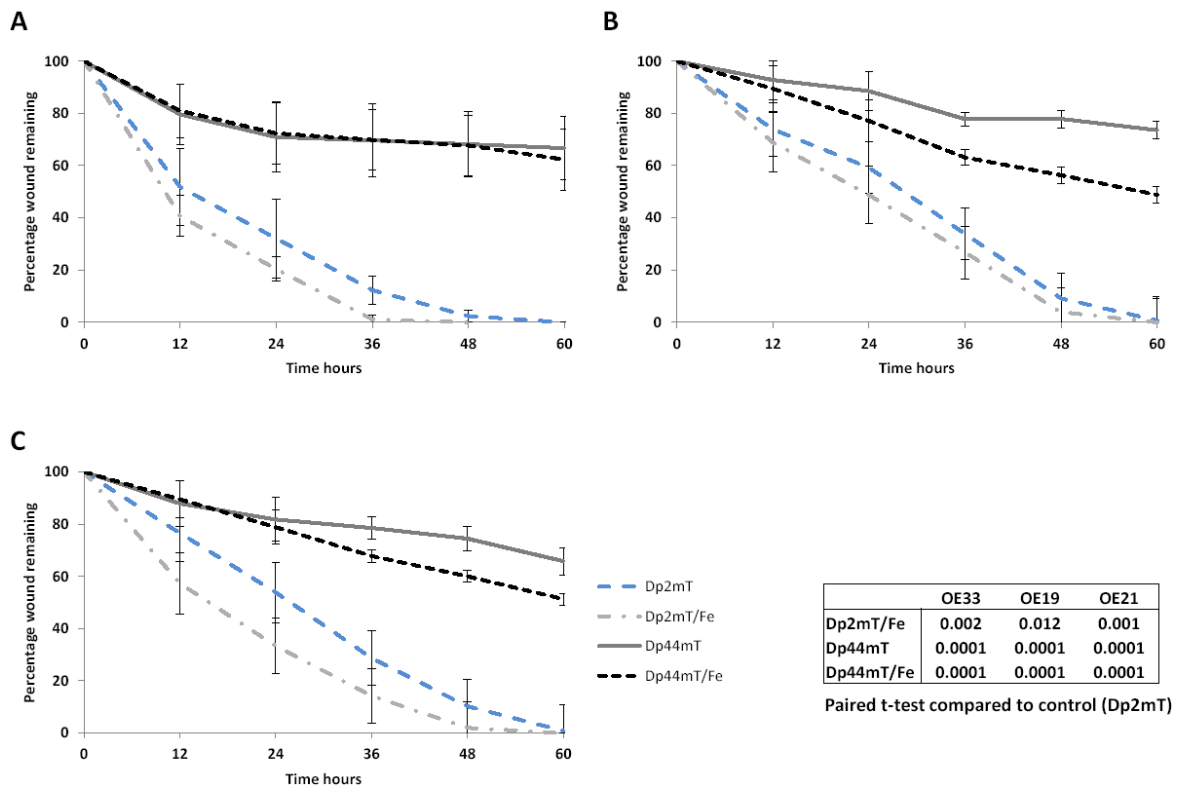
**Figure 5.17 Deferasirox inhibits oesophageal cancer cell migration *in-vitro***

Figure A: OE33, figure B: OE19 and figure C: OE21 cell lines were cultured in plain media and allowed to form a monolayer (n=9). The cell monolayer was then scratched (wounded) and plain media substituted for media spiked with Deferasirox 20 $\mu$ M. Fe 100 $\mu$ M was used as a positive control alone or a combination of Deferasirox. Representative images of wound closure over 48 hours; 20 x magnification.



**Figure 5.18 DFO inhibits oesophageal cancer cell migration *in-vitro***

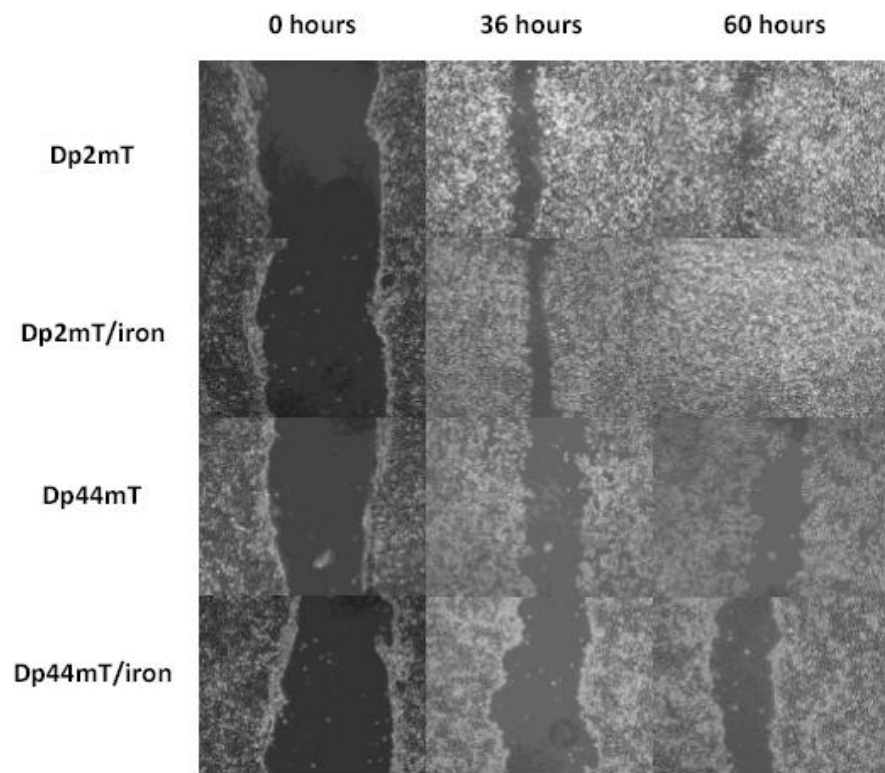
Figure A: OE33, figure B: OE19 and figure C: OE21 cell lines were cultured in plain media and allowed to form a monolayer (n=9). The cell monolayer was then scratched (wounded) and plain media substituted for media spiked with DFO 10 $\mu$ M. Fe 100 $\mu$ M was used as a positive control alone or a combination of DFO. The degree to which the wound healed was described as a percentage of wound remaining as a function of time and compared to control media alone. Error bars denote  $\pm$  SEM.



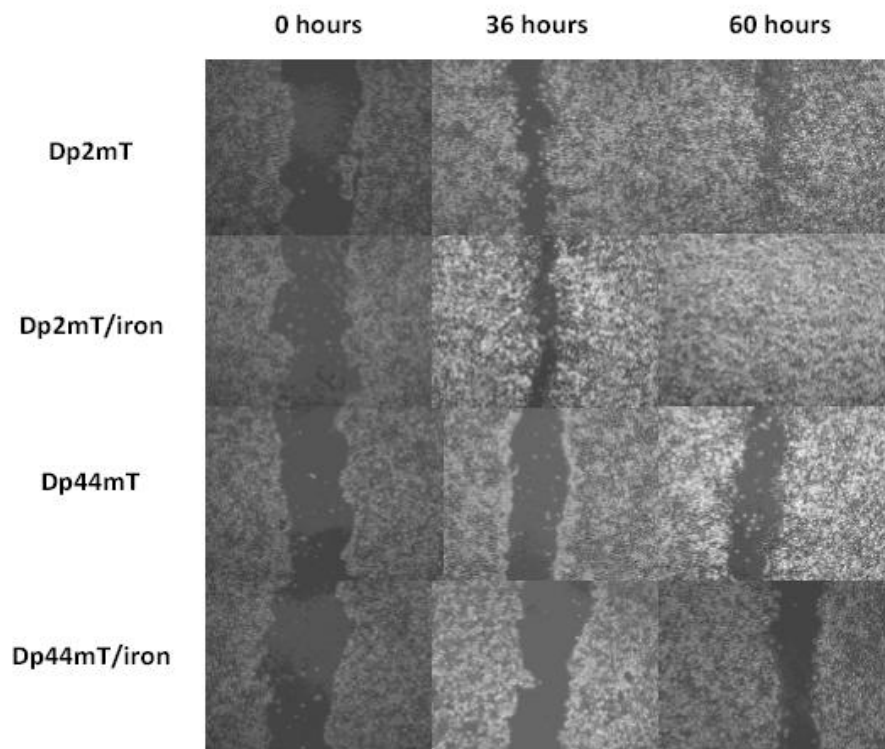
**Figure 5.19 Dp44mT inhibits oesophageal cancer cell migration *in-vitro***

Figure A: OE33, figure B: OE19 and figure C: OE21 cell lines were cultured in plain media and allowed to form a monolayer (n=9). The cell monolayer was then scratched (wounded) and plain media substituted for media spiked with Dp44mT 1 $\mu$ M (Dp2mT 1  $\mu$ M as negative control). Fe 100 $\mu$ M was used as a positive control alone or in combination with Dp44mT or Dp2mT. The degree to which the wound healed was described as a percentage of wound remaining as a function of time and compared to control media alone. Error bars denote  $\pm$  SEM.

**A**



**B**



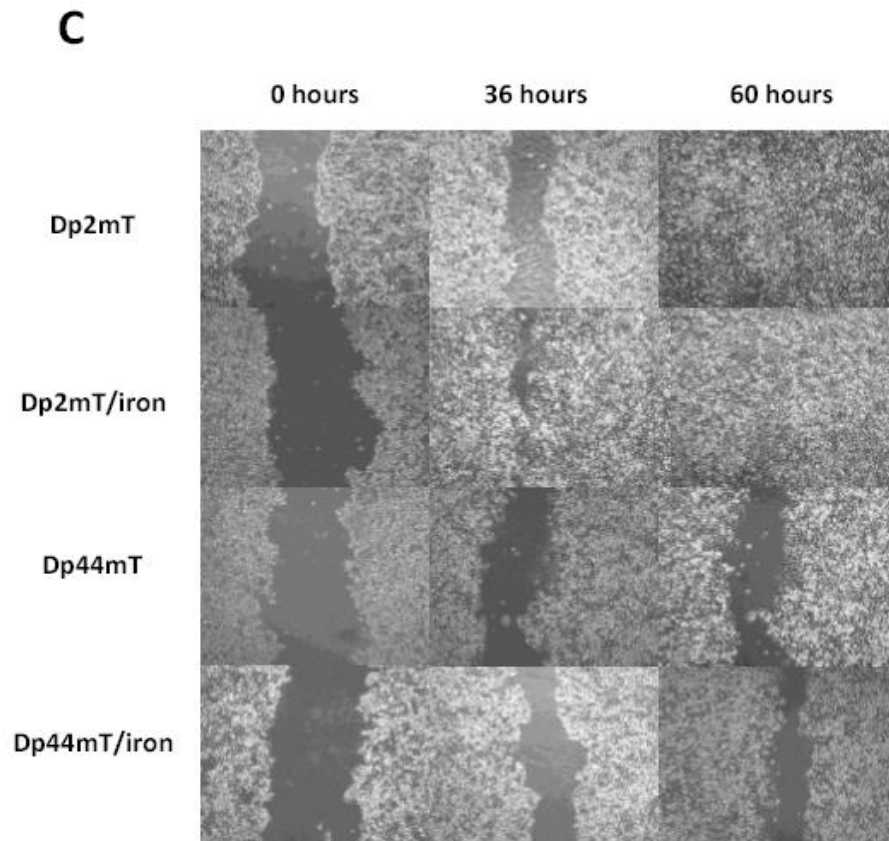


**Figure 5.20 Dp44mT inhibits oesophageal cancer cell migration *in-vitro***

Figure A: OE33, figure B: OE19 and figure C: OE21 cell lines were cultured in plain media and allowed to form a monolayer (n=9). The cell monolayer was then scratched (wounded) and plain media substituted for media spiked with Dp44mT 1 $\mu$ M (Dp2mT 1  $\mu$ M as negative control). Fe 100 $\mu$ M was used as a positive control alone or in combination with Dp44mT or Dp2mT. Representative images of wound closure over 60 hours; 20 x magnification.

### **5.3.6 Characterisation of the *in-vitro* effect of iron chelation on oesophageal cancer cell cycle**

Culture of oesophageal cancer cells with supplementary iron and haem stimulates proliferation compared to standard media alone. The addition of an iron chelator attenuates the stimulatory effect of supplementary iron. The effect of iron chelation on the cell cycle of oesophageal cancer cells was determined using FACS with propidium iodide labelling. OE33, OE19 and OE21 cell lines were cultured with or without Deferasirox, DFO and Dp44mT +/- supplementary iron or haem for 48 hours before propidium iodide staining and FACS analysis. Results were expressed as a percentage of cells in G<sub>0</sub>/G<sub>1</sub>, S or G<sub>2</sub>/M phases of the cell cycle and compared to control media alone (figure 5.21A: OE33, 5.21B: OE19 and 5.21C: OE21).

#### **5.3.6.1 Iron chelation significantly inhibits oesophageal cancer cell cycle**

Culture with supplementary iron significantly altered the percentage of cells in each phase of the cell cycle implying an increase in proliferation. OE33, OE19 and OE21 cell lines all decreased the percentage of cells in G<sub>0</sub>/G<sub>1</sub> (p=0.05, p=0.0055 and p=0.007 for OE33, OE19 and OE21 respectively) and significantly increased percentage in S phase (p=0.05, p=0.0008 and p=0.005) which followed into a significant increase in G<sub>2</sub>/M (p=0.092, p=0.05 and p=0.015). Similar but less pronounced changes were observed with supplementary haem with a trend towards a decreased percentage of cells in G<sub>0</sub>/G<sub>1</sub> and an increase in S and G<sub>2</sub>/M phases, but changes reached statistical significance in the OE19 cell line only (p=0.003, p=0.0011 and p=0.0071 for G<sub>0</sub>/G<sub>1</sub>, S and G<sub>2</sub>/M). The most dramatic change in cell cycle composition was seen in the presence of Deferasirox. Deferasirox dramatically increased the percentage of cells in S phase (all p= <0.001 for G<sub>0</sub>/G<sub>1</sub>, S and

G<sub>2</sub>/M) at the expense of the proportion of cells in G<sub>0</sub>/G<sub>1</sub>, across all three cell lines (all p=0.001). The exceptionally large percentage of cells in S phase was not seen to be translated into an increase in G<sub>2</sub>/M (p=0.77, p=0.9 and p=0.045), suggesting that Deferasirox had arrested oesophageal cancer cells in S phase. Culture with DFO failed to demonstrate a discernable change in cell cycle composition in any cell line. The addition of Deferasirox to culture media containing supplementary iron returned the distribution of cells in each phase of the cycle to those of control media alone, eliminating the stimulatory effect of iron and the inhibitory changes seen with Deferasirox alone. The addition of Deferasirox to media supplemented with haem had a similar effect, with the loss of accumulation of cells in S phase, except in the OE21 line where some features of Deferasirox inhibition persisted. Changes in cell cycle composition were inconsistent when DFO was added to media spiked with supplementary iron or haem. The stimulatory effect of iron or haem was only partially reversed by the addition of DFO in the OE33 and OE19 cell lines and similar to control in the OE21 line.

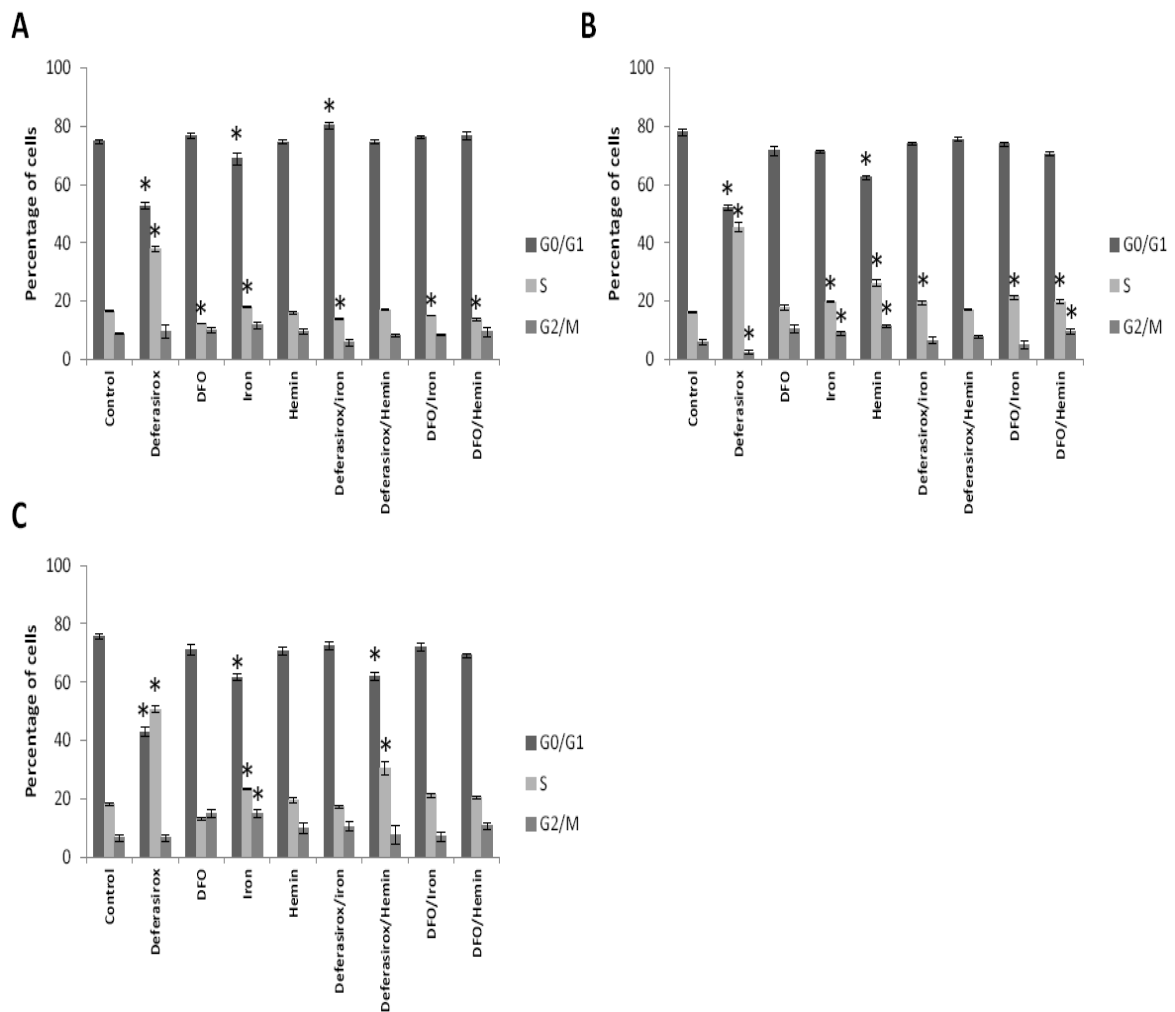


**Figure 5.21 Iron chelation significantly inhibits the oesophageal cancer cell cycle**

Propidium iodide FACS analysis of oesophageal cancer cell lines. Figure A: OE33, figure B: OE19 and figure C: OE21 after 48 hours culture with or without Deferasirox and DFO at IC50 concentrations +/- supplementary 100µM iron or haem 20µM. Deferasirox arrests oesophageal cancer cells in S phase and prevents the stimulatory effect of supplementary iron and haem. (\*p<0.05 significant change in percentage of cells in given cell cycle phase compared to plain media control). Error bars denote ± SEM.

### **5.3.6.2 Deferasirox increases expression of the cell cycle related nuclear protein CDC45L in oesophageal cancer cells**

Deferasirox appears to arrest the cell cycle of oesophageal cancer cells in S phase when the iron dependent, cell cycle regulatory protein RNR is normally active. Inactivation of RNR activity, secondary iron chelation, may account for cell arrest in S phase. To add credence to this argument, a proxy marker of S phase suspension, CDC45L accumulation was utilised<sup>434,435</sup>. Cell lines OE33, OE19 and OE21 were cultured with or without Deferasirox 20 $\mu$ M +/- iron 100 $\mu$ M. Hydroxyurea (HU) 2mM, a potent inhibitor of RNR, and plain media were included as positive and negative controls respectively. After 48 hours cells were harvested and the nuclear fraction isolated and processed for CDC45L Western blotting. Protein loading was standardised to the highly expressed nuclear protein SP-1 (figure 5.22).

In all three cell lines, HU exposure induced a highly significant rise in CDC45L protein expression (all  $p < 0.0001$ ). Media spiked with Deferasirox demonstrated a similar but slightly less pronounced induction of CDC45L. Deferasirox induced CDC45L expression was statistically significant in all, but most evident in, the OE21 cell line (fold change  $1.64 \pm 0.07$   $p = 0.001$ ,  $2.46 \pm 0.25$   $p = 0.002$  and  $2.62 \pm 0.21$   $p = 0.0001$  for OE33, OE19 and OE21 respectively). The addition of supplementary iron to Deferasirox containing media nullified the increase in CDC45L expression to levels consistent with control media alone ( $0.95 \pm 0.06$   $p = 0.9$ ,  $1.12 \pm 0.09$   $p = 0.42$  and  $1.21 \pm 0.06$   $p = 0.14$  for OE33, OE19 and OE21 respectively). Supplementary iron alone increased CDC45L protein expression in all cell lines, reaching statistical significance in OE19 and OE21 cells ( $1.36 \pm 0.07$   $p = 0.012$ ,  $1.53 \pm 0.15$   $p = 0.05$  and  $2.1 \pm 0.16$   $p = 0.012$  for OE33, OE19 and OE21 cell lines).

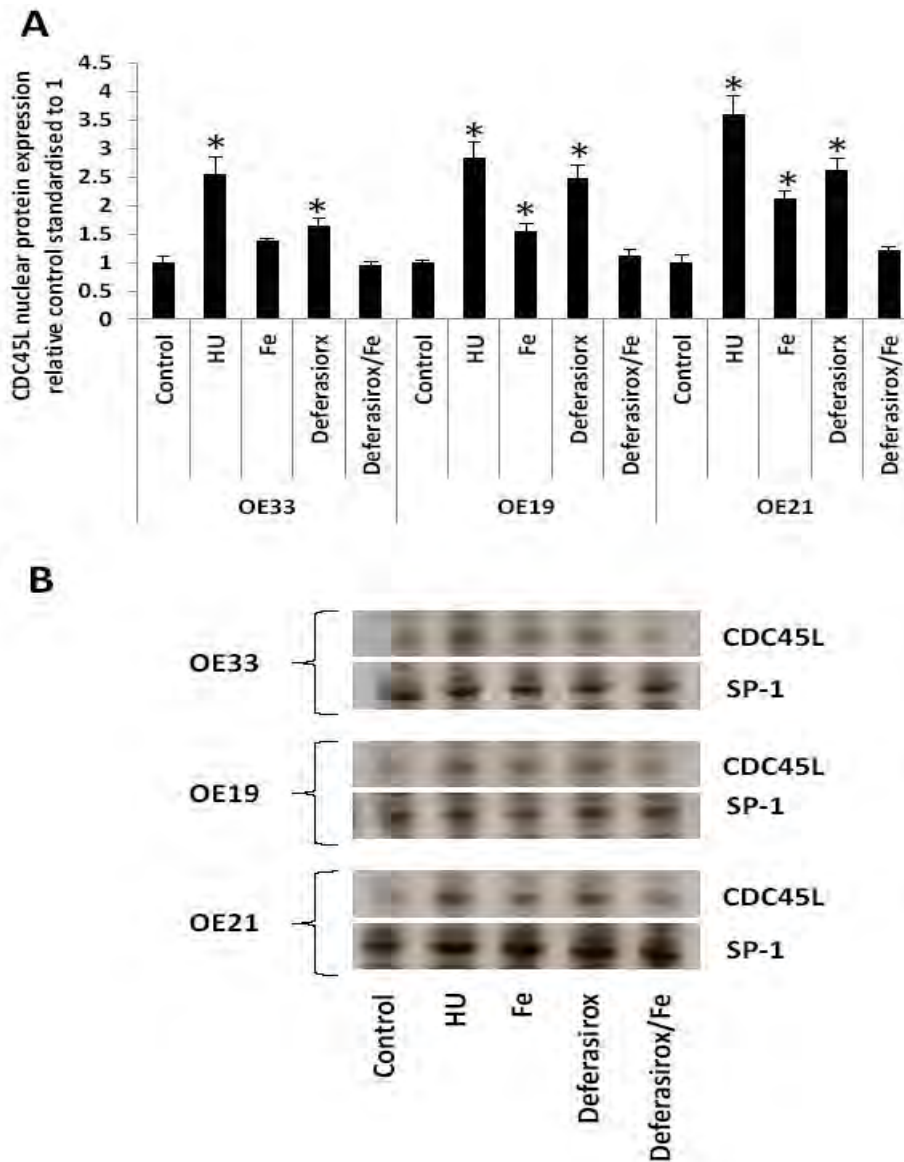


**Figure 5.22 Deferasirox increases expression of the cell cycle related nuclear protein CDC45L in oesophageal cancer cells**

Cell lines OE33, OE19 and OE21 were cultured with or without Deferasirox 20 $\mu$ M +/- iron 100 $\mu$ M. Hydroxyurea (HU) 2mM, a potent inhibitor of RNR, and plain media were included as positive and negative controls respectively. After 48 hours cells were harvested and the nuclear fraction isolated and processed for CDC45L Western blotting. Protein loading was standardised to the highly expressed nuclear protein SP-1. (\* $p$ <0.05 significant change in CDC45L protein expression relative to control and normalised to 1).

### **5.3.7 The *in-vivo* activity of oral Deferasirox on tumour burden in murine xenograft models of oesophageal cancer and quantification of systemic toxicity**

OE33, OE19 and OE21 cell lines, mixed 50/50 v/v with freshly thawed Matrigel, were injected into the subcutaneous plane of NOD-SCID mice ( $1 \times 10^6$ ) and allowed to establish mature xenografts. The mice were then gavaged with Deferasirox (20mg/Kg) or vehicle alone on alternate days for 3 weeks. The mice were culled and xenografts, organs and blood harvested for analysis (xenograft weight, haematological and biochemical parameters, gross xenograft iron content, xenograft tissue for qRT-PCR and immunohistochemistry).

#### **5.3.7.1 Oral Deferasirox significantly reduces xenograft tumour burden in murine models of oesophageal cancer**

OE33, OE19 and OE21 cell xenografts were harvested after a 21 day period of orally gavaged Deferasirox. Oral Deferasirox significantly reduced average xenograft weight in the OAC and SCC xenografts compared to control vehicle alone (OE33: control n=14,  $409 \pm 52$ mg; Deferasirox n= 12,  $232 \pm 17.9$ mg,  $p=0.061$ ; OE19: control n=8,  $344 \pm 45$ mg; Deferasirox n=5,  $199 \pm 40$ mg,  $p=0.05$ ; OE21: control n=5,  $426 \pm 70$ mg; Deferasirox n=5,  $217 \pm 29$ mg,  $p=0.025$ ). Deferasirox reduced overall tumour burden by 43%, 42% and 37% for OE33, OE19 and OE21 xenografts compared to control (figure 5.23).

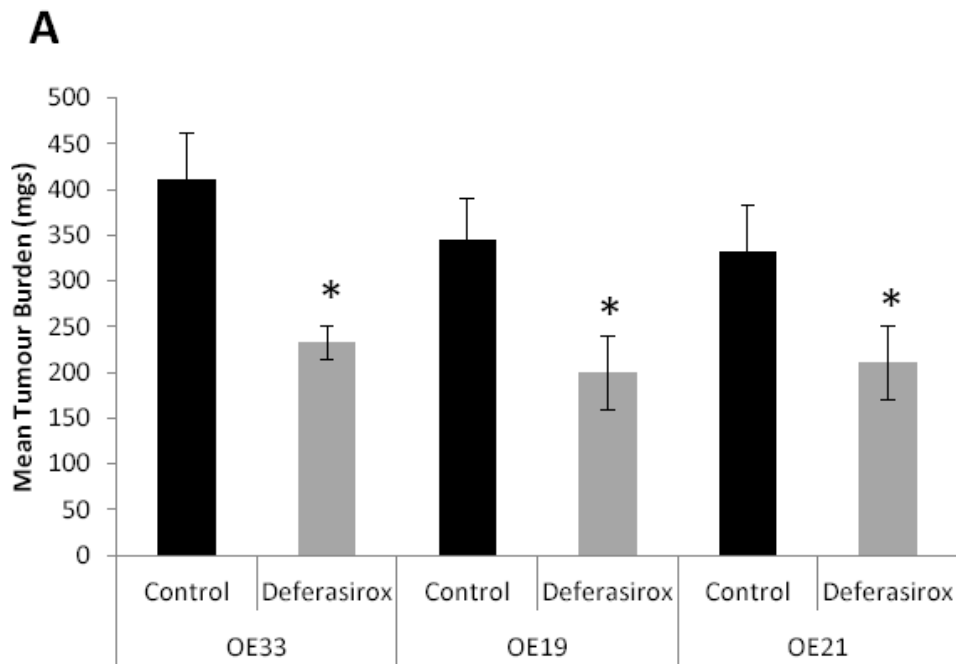


**Figure 5.23 Oral Deferasirox significantly reduces xenograft tumour burden in a murine model of oesophageal cancer**

Mean OE33, OE19 and OE21 cell line xenograft weight (Figure A) and representative images (Figure B) after orally administered Deferasirox (20mg/Kg) on alternate days for three weeks compared to vehicle alone. (\* $p=0.0061$ ,  $p=0.05$  and  $p=0.025$  for OE33, OE19 and OE21 respectively). Error bars denote  $\pm$  SEM.

### 5.3.7.2 Oral administration of Deferasirox (20mg/Kg) does not adversely affect mouse weight

Mouse weight, as a proxy of well being and general physiological condition was monitored over the three week period of oral Deferasirox administration<sup>436</sup>.

Oral Deferasirox did not show a statistical difference, in average mouse weight, compared to vehicle alone ( $p=0.8$ ) (figure 5.24).

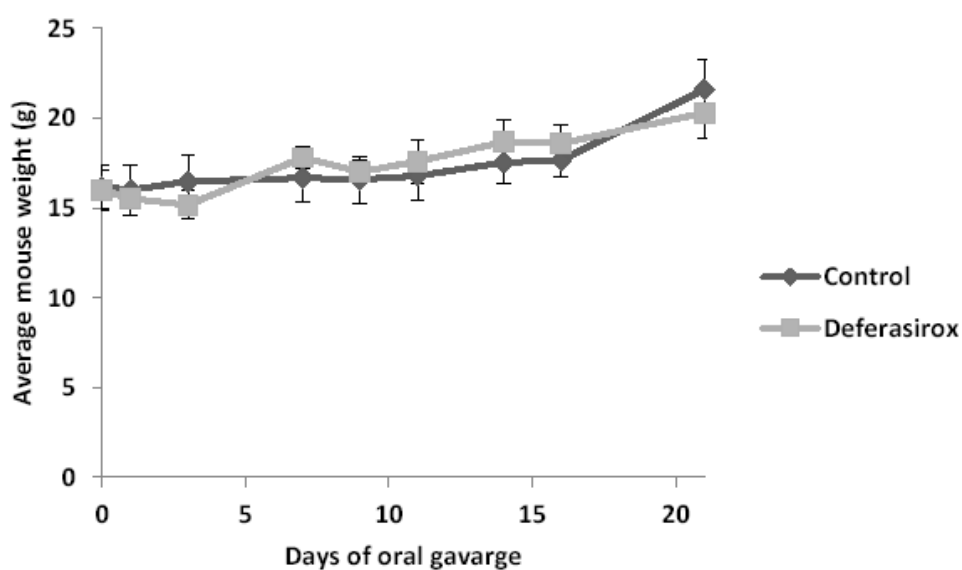


**Figure 5.24 Oral administration of Deferasirox (20mg/Kg) does not adversely affect mouse weight**

Mice were gavaged with either Deferasirox 20mg/Kg or vehicle alone for 21 days. No difference in average weight was observed between the control and treatment cohorts ( $p=0.08$ ). Control  $n=33$ ; Deferasirox  $n=27$ . Error bars denote  $\pm$  SEM.

### **5.3.7.3 Oral administration of Deferasirox (20mg/Kg) does not impact on murine systemic haematological and biochemical indices**

Mice were gavaged with either Deferasirox 20mg/Kg or vehicle alone for 21 days. Blood samples were obtained by direct cardiac puncture, at the time of culling, for FBC and biochemical analysis (urea, creatinine, ALT, AST, albumin, total bilirubin, serum iron, and total iron binding capacity).

No statistically significant difference was noted between the haematological and biochemical indices of vehicle alone and Deferasirox treated murine cohorts. Orally administered Deferasirox (20mg/Kg over 21 days) does not appear to cause significant systemic iron stripping or derange liver or renal function in mice. Unfortunately, serum samples were not large enough for creatinine and AST calculation and therefore could not be analysed (table 5.1).

A		B			
	Control	Deferasirox		Control	Deferasirox
		154.25 ±			
Hb(g/L)	153 ± 0.57	1.75	Serum iron (µmol/L)	33.8 ± 1.1	35.054 ± 5.7
HCT(%)	48.4 ± 0.25	47.7 ± 0.60	TIBC (µmol/L)	57.5 ± 0.6	56.2 ± 0.7
MCV(fL)	47.63 ± 0.28	46.5 ± 0.24	ALP (U/L)	139.8 ± 5.9	159.5 ± 3.3
MCH(pg)	15.1 ± 0.07	15.1 ± 0.09	ALT (U/L)	30.9 ± 3	34.4 ± 3.9
MCHC(g/L)	316.2 ± 1.01	323.5 ± 1.0	ALB (g/L)	32.5 ± 0.89	31.7 ± 0.7
PLT(10 <sup>9</sup> /L)	929.5 ± 102	1457.25 ± 74	TP (g/L)	55.1 ± 1.7	53.4 ± 1.4
WBC(10 <sup>9</sup> /L)	6.65 ± 0.37	6.05 ± 0.76	Urea (mmol/L)	7.9 ± 0.2	7.9 ± 0.25
RET(10 <sup>12</sup> /L)	0.59 ± 0.03	0.58 ± 0.02			
NEUT(%)	19.4 ± 2.1	23.75 ± 2.3			

**Table 5.1 Oral administration of Deferasirox (20mg/Kg) does not impact on systemic haematological and biochemical indices in murine models**

Mice were gavaged with either Deferasirox 20mg/Kg or vehicle alone for 21 days. Deferasirox treatment does not impact on haematological (Table A) or biochemical (Table B) parameters with no evidence of systemic iron stripping or derangement of liver and renal function. (Hb: haemoglobin; HCT: haematocrit; MCV: mean cell volume; MCH: mean cell haemoglobin; MCHC: mean cell haemoglobin concentration; PLT: platelets; WBC: total white cell count; RET: reticulocyte count; NEUT: neutrophil count; TIBC: total iron binding capacity; ALP: alkaline phosphatase; ALT: alanine transferase; ALB: albumin; TP: total protein). (All p-values >0.5).

#### **5.3.7.4 Oral administration of Deferasirox (20mg/Kg) does not alter major organ weight or iron content in murine models**

Mice were gavaged with either Deferasirox 20mg/Kg or vehicle alone for 21 days. After culling, major organs (liver, spleen and heart) were harvested and average weights compared between the control and treatment cohorts. No significant difference in average liver, spleen or heart weight was noted between the treatment groups.

Harvested organs (liver, spleen and heart) were then processed to derive gross iron content (ferrozine assay). No significant difference in average iron content was observed between the Deferasirox treated cohort and vehicle alone controls (figure 5.25).

	<b>Control</b>	<b>Deferasirox</b>
<b>Liver</b>	<b>923 ± 47</b>	<b>1057 ± 53</b>
<b>Spleen</b>	<b>94 ± 10</b>	<b>103 ± 5</b>
<b>Heart</b>	<b>89 ± 5</b>	<b>93 ± 3</b>

**Table 5.2 Oral administration of Deferasirox (20mg/Kg) does not alter major organ weights in murine models**

Mice were gavaged with either Deferasirox 20mg/Kg or vehicle alone for 21 days. Major organs (liver, spleen and heart) were harvested and average weights (mg) compared (all p-values >0.5)

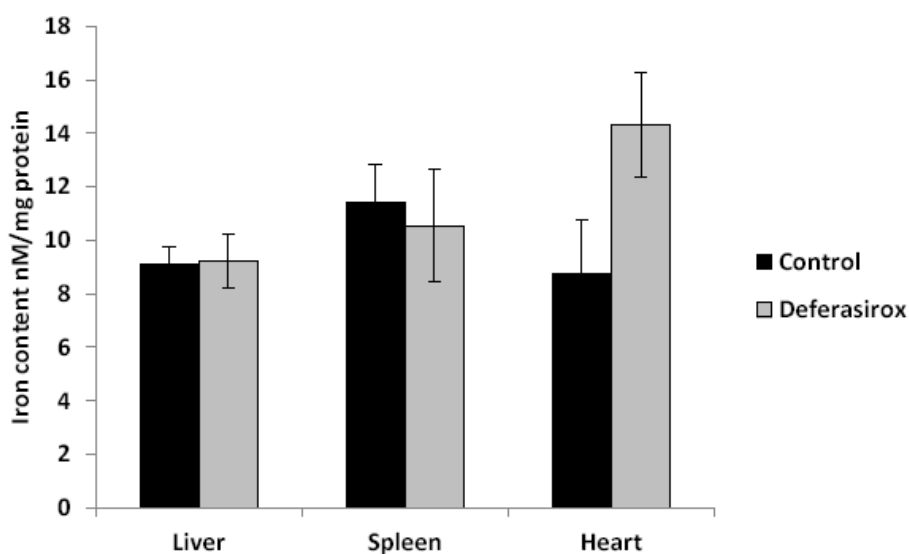


**Figure 5.25 Oral administration of Deferasirox (20mg/Kg) does not alter major organ iron content in murine models**

Mice were gavaged with either Deferasirox 20mg/Kg or vehicle alone for 21 days. Major organs (liver, spleen and heart) were harvested and average iron content (nM/mg protein) compared (all p-values >0.5). Error bars denote  $\pm$  SEM.

**5.3.7.5 Oral administration of Deferasirox (20mg/Kg) does not alter iron transport protein immunoreactivity in murine major organs (liver, spleen and heart)**

Mice were gavaged with either Deferasirox 20mg/Kg or vehicle alone for 21 days. Major organs (liver, spleen and heart) were harvested and processed for TfR1, ferritin and FPN immunohistochemistry. No difference in immunoreactivity was observed for TfR1, ferritin or FPN in any organ after Deferasirox administration when compared to vehicle alone controls (figure 5.26).

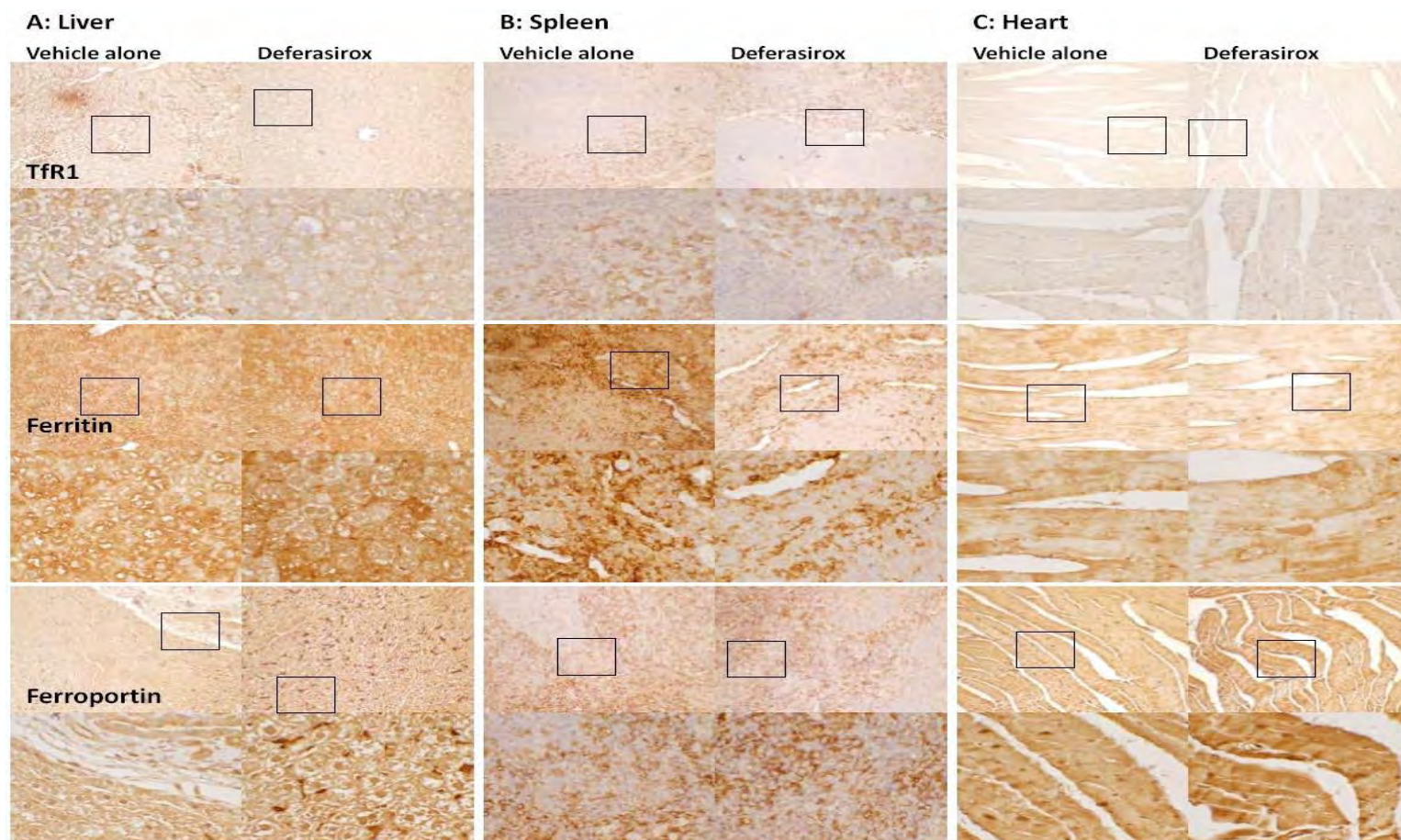


**Figure 5.26 Representative images of major organ immunoreactivity following oral administration of Deferasirox or control vehicle alone**

NOD-SCID mice were gavaged with Deferasirox (20mg/Kg) or vehicle alone for 21 days. Immunoreactivity for TfR1, ferritin and FPN in liver, spleen and heart (magnification x20; inset box extrapolated to x60).

#### **5.3.7.6 Characterisation of the *in-vivo* effects of iron chelation on xenograft iron content and alterations in iron transport proteins**

OE33, OE19 and OE21 cell xenografts were harvested after a 21-day period of orally gavaged Deferasirox and compared to vehicle alone controls. Harvested xenograft material was divided and processed for iron transport protein mRNA expression, immunohistochemistry and iron content.

#### **5.3.7.7 Oral administration of Deferasirox (20mg/Kg) for 21 days significantly reduces iron content in oesophageal cancer xenografts**

OE33, OE19 and OE21 xenografts were harvested at the time of culling after 21 days of oral Deferasirox or vehicle alone. Xenograft tissue was processed for gross iron content, utilising the ferrozine assay, and expressed as nM/mg protein. In contrast to the native major intra-abdominal organs, xenograft tissue from mice receiving Deferasirox showed marked and statistically significant reductions in iron content when compared to control. This observation was consistent across all three cell lines (OE33:  $p=0.0046$ ; OE19:  $p=0.05$ ; OE21:  $p=0.048$ ) (figure 5.27).

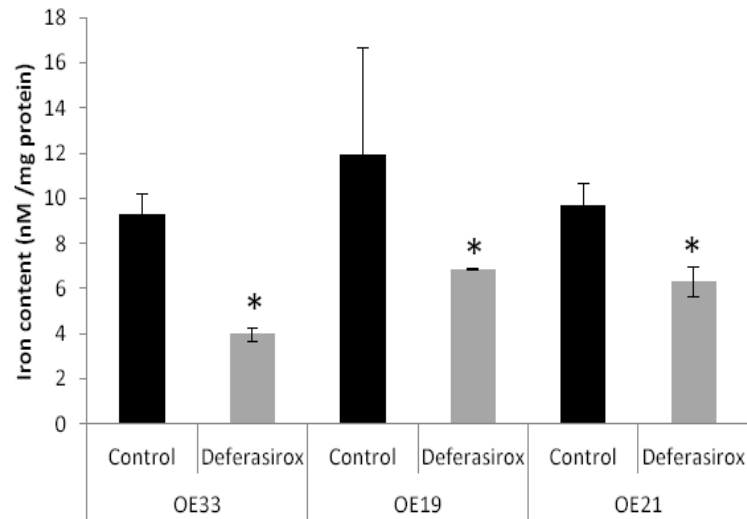


**Figure 5.27 Oral administration of Deferasirox (20mg/Kg) for 21 days significantly reduces iron content in oesophageal cancer xenografts**

Gross iron content (nM/mg protein) of xenografted oesophageal cell lines after orally administered Deferasirox or control vehicle alone. A significant reduction in average iron content was evident in the Deferasirox cohort compared to control. (\* $p=0.0046$ ,  $p=0.05$  and  $p=0.048$  for OE33, OE19 and OE21 cell lines respectively). Error bars denote  $\pm$  SEM.

#### **5.3.7.8 Oral administration of Deferasirox (20mg/Kg) for 21 days significantly alters mRNA expression of iron transport proteins in oesophageal cancer xenografts**

NOD-SCID mice bearing OE33, OE19 and OE21 xenografts were subject to oral Deferasirox (20mg/Kg) or control vehicle alone for 21 days. Upon culling, xenograft tissue was analysed for TfR1, ferritin and FPN mRNA expression using qRT-PCR (figure 5.28).

Marked up-regulation of TfR1 mRNA expression was observed in the xenograft tissue exposed to Deferasirox, compared to control, across all lineages (fold change:  $4.26 \pm 0.95$   $p=0.0012$ ;  $2.04 \pm 0.3$   $p=0.048$ ;  $3.61 \pm 0.89$   $p=0.041$  for OE33, OE19 and OE21 cell lines, respectively). mRNA of the iron storage protein ferritin, was significantly reduced in the Deferasirox cohort, compared to control and again was consistent across the cell lines ( $0.79 \pm 0.2$   $p=0.05$ ;  $0.64 \pm 0.1$   $p=0.006$ ;  $0.74 \pm 0.08$   $p=0.05$  for OE33, OE19 and OE21 cell lines respectively). FPN mRNA expression was similarly significantly reduced in all cell lines ( $0.32 \pm 0.12$   $p=0.021$ ;  $0.57 \pm 0.04$   $p=0.05$ ;  $0.38 \pm 0.08$   $p=0.041$  for OE33, OE19 and OE21, respectively).

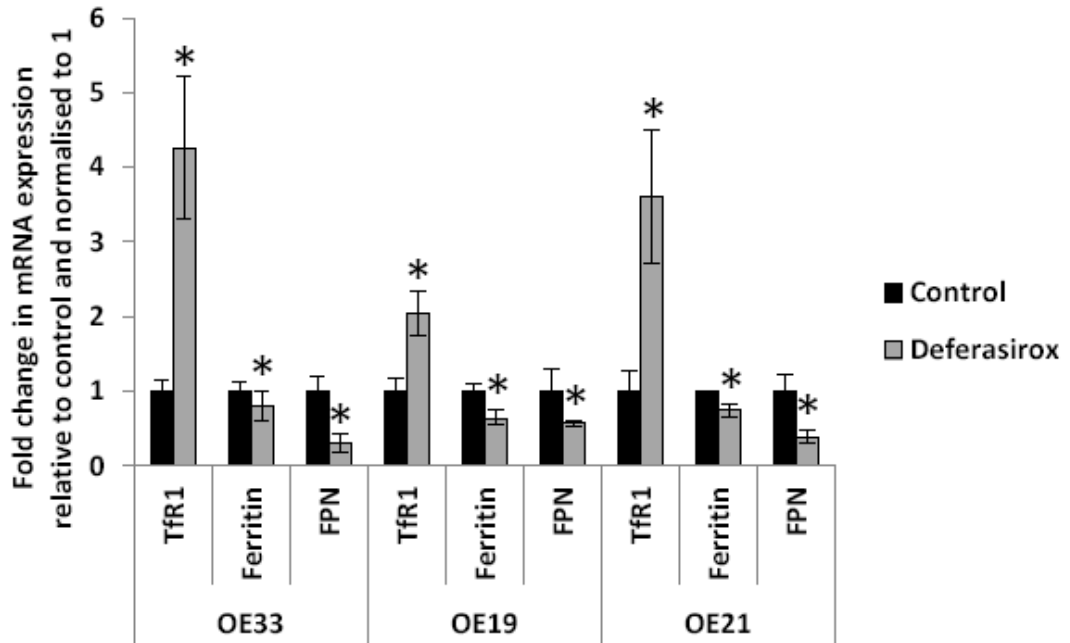


**Figure 5.28 Oral administration of Deferasirox significantly alters mRNA expression of the iron transport proteins in oesophageal cancer xenografts**

NOD-SCID mice bearing OE33, OE19 and OE21 xenografts were subjected to oral Deferasirox (20mg/Kg) or control vehicle alone for 21 days. Upon culling, xenograft tissue was analysed for TfR1, ferritin and FPN mRNA expression using qRT-PCR (\*p<0.05 fold change compared to vehicle alone).

### **5.3.7.9 Oral administration of Deferasirox (20mg/Kg) for 21 days significantly alters iron transport protein expression (immunohistochemistry) in oesophageal cancer xenografts**

Mice bearing OE33, OE19 and OE21 xenografts were subjected to oral Deferasirox (20mg/Kg) or control vehicle alone for 21 days. Immediately after culling, xenograft tissue was analysed for TfR1, ferritin and FPN protein localisation and semi-quantitative expression utilising immunohistochemistry as previously described (2.2.2) (figures 5.29 and 5.30).

Changes in immunohistochemistry reactivity scores for TfR1, ferritin and FPN mirrored observed changes in mRNA expression. TfR1 immunoreactivity was significantly elevated in the Deferasirox exposed cohort for all three cell lines (OE33:  $2.66 \pm 0.33$  vs  $10 \pm 1$ ,  $p=0.0022$ ; OE19:  $2.66 \pm 0.33$  vs  $11 \pm 1.0$ ,  $p=0.0014$ ; OE21:  $3.33 \pm 0.33$  vs  $11 \pm 1.0$ ,  $p=0.0019$  for control and Deferasirox cohorts respectively). TfR1 immunoreactivity appeared principally to be membranous with a degree of cytoplasmic reactivity. Similar TfR1 protein localisation was noted between cell lines, varying only in immunoreactivity intensity between control and Deferasirox cohorts (figure 5.30). Xenograft ferritin immunoreactivity was significantly reduced in mice gavaged with Deferasirox compared to vehicle alone (OE33:  $8.0 \pm 1.0$  vs  $4.66 \pm 0.66$ ,  $p=0.05$ ; OE19:  $10 \pm 1.0$  vs  $2.66 \pm 0.33$ ,  $p=0.0022$ ; OE21:  $9.66 \pm 1.2$  vs  $3.33 \pm 0.33$ ,  $p=0.0017$  for control and Deferasirox cohorts respectively). Ferritin localisation was cytoplasmic in both Deferasirox and control cohorts across all cell lines (figure 5.30). FPN immunoreactivity was significantly reduced in xenografts exposed to Deferasirox compared to vehicle alone (OE33:  $5.33 \pm 0.66$  vs  $2.33 \pm 0.33$ ,  $p=0.016$ ; OE19:  $8.66 \pm 0.33$  vs  $2.66 \pm 0.33$ ,  $p=0.0022$ ; OE21:  $8.33 \pm 0.33$  vs  $3.33 \pm 0.33$ ,  $p=0.0004$  for control and Deferasirox cohorts respectively). FPN localisation

varied little between treatment cohorts and cell lines with immunoreactivity presenting mixed cytoplasmic and membranous distributions (figure 5.30).

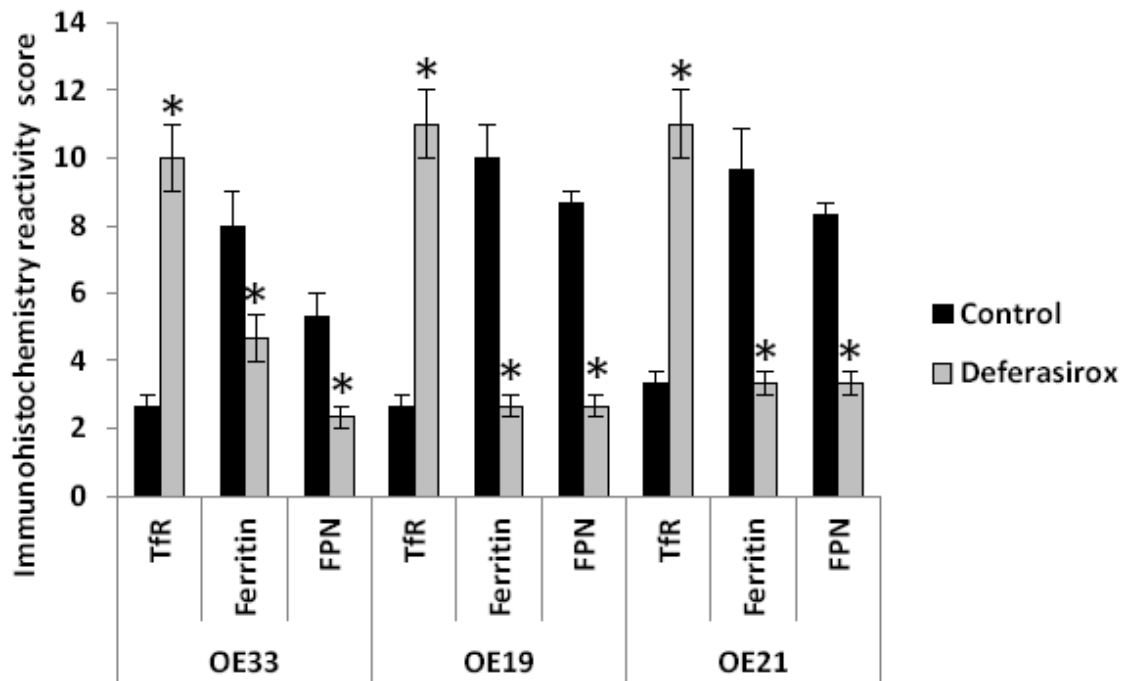


**Figure 5.29 Oral administration of Deferasirox alters iron transport protein expression (immunohistochemistry) in oesophageal cancer xenografts**

NOD-SCID mice bearing OE33, OE19 and OE21 cell line xenografts were gavaged with Deferasirox (20mg/Kg) or vehicle alone for 21 days. Immunoreactivity for TfR1, ferritin and FPN was analysed with a semi-quantitative technique. (\* $p < 0.05$  compared to vehicle alone). Error bars denote  $\pm$  SEM.

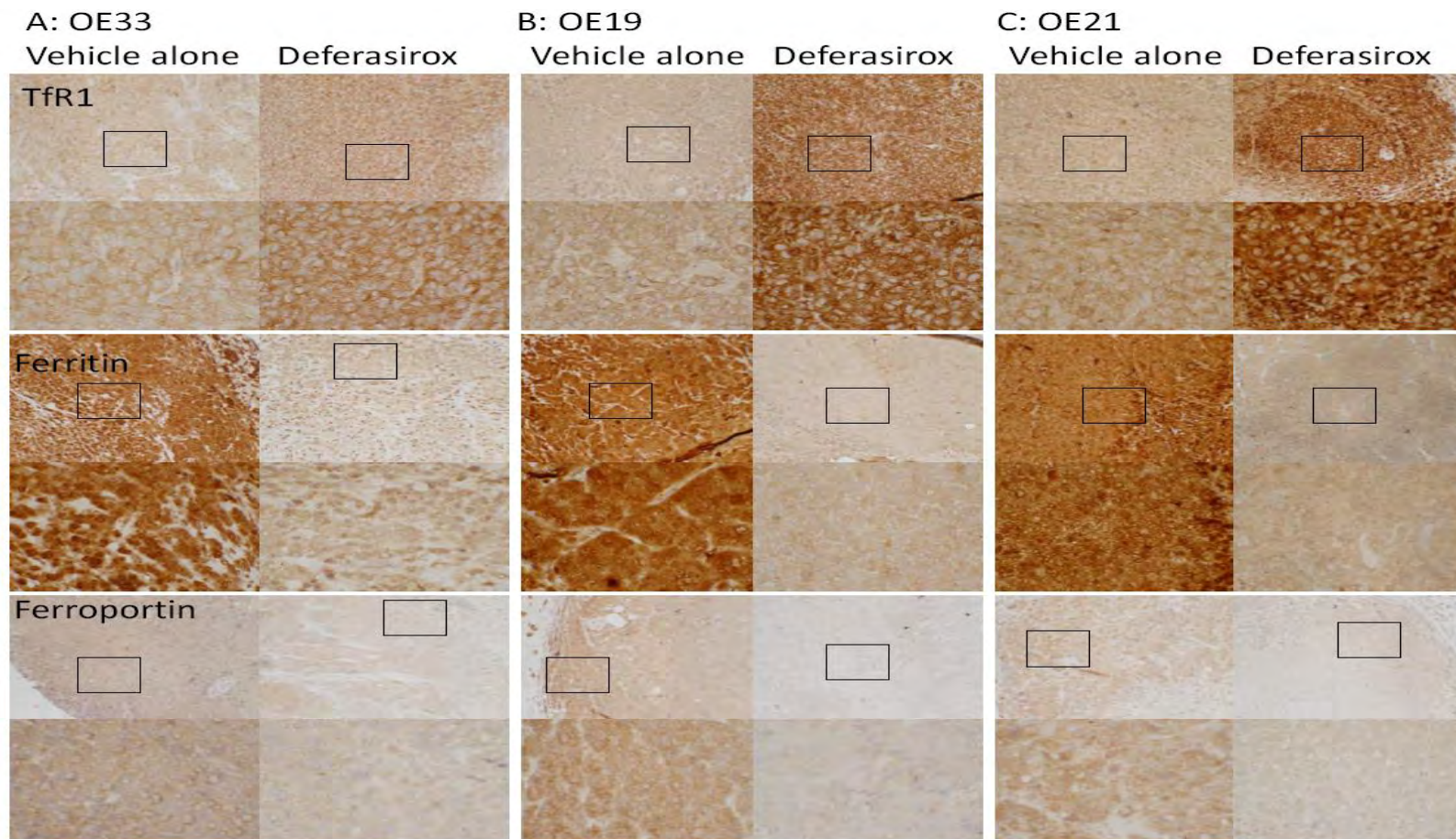


**Figure 5.30 Representative images of xenograft immunoreactivity following oral administration of Deferasirox or control vehicle alone**

NOD-SCID mice bearing OE33, OE19 and OE21 cell line xenografts were gavaged with Deferasirox (20mg/Kg) or vehicle alone for 21 days. Immunoreactivity for TfR1, ferritin and FPN (magnification x20; inset box extrapolated to x60).

### **5.3.8 Exploration of the anti-neoplastic potential of iron chelators in combination with standard chemotherapeutic agents for oesophageal cancer treatment and possible action on chemoresistant lineages**

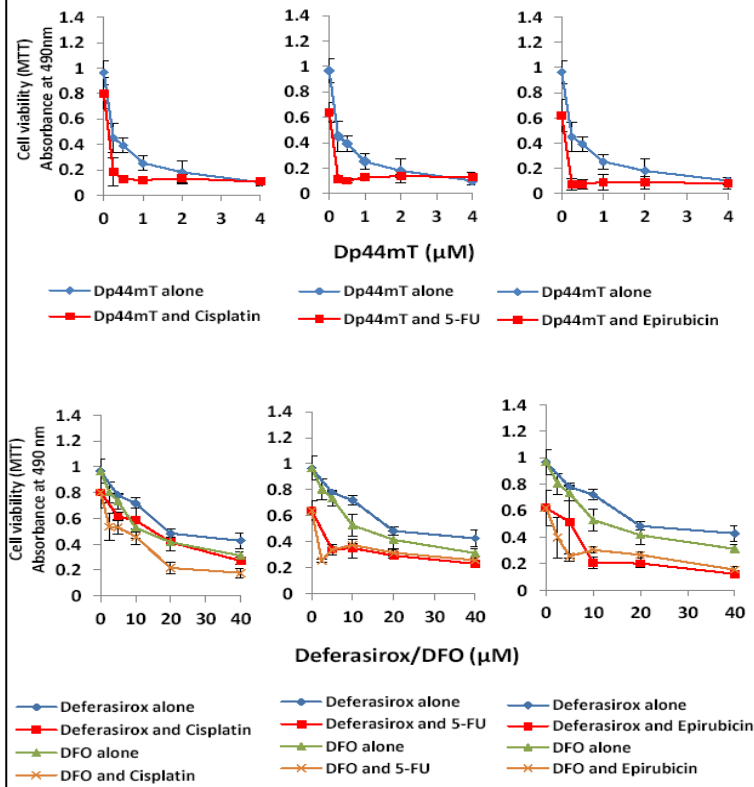
The current standard chemotherapeutic regime for the treatment of OAC and SCC is a combination of Cisplatin, 5-FU and Epirubicin (ECF)<sup>437</sup>. In order to assess the potential of iron chelators to enhance the response to standard chemotherapy, OE33, OE19 and OE21 cell lines were cultured with Cisplatin, 5-FU or Epirubicin, at IC50 concentration and challenged with titrated doses of Dp44mT, Deferasirox or DFO. The effect on cellular viability and proliferation was assessed by MTT and BrdU assays after 48 hours of incubation under experimental conditions. IC50 values for chemotherapy agents were derived by viability (MTT) and proliferation (BrdU) assays and determined as: Cisplatin 8 $\mu$ M, 5-FU 8 $\mu$ M and Epirubicin 1 $\mu$ M.

#### **5.3.8.1 Iron chelators confer additive anti-neoplastic action in combination with standard chemotherapeutic agents on oesophageal cancers**

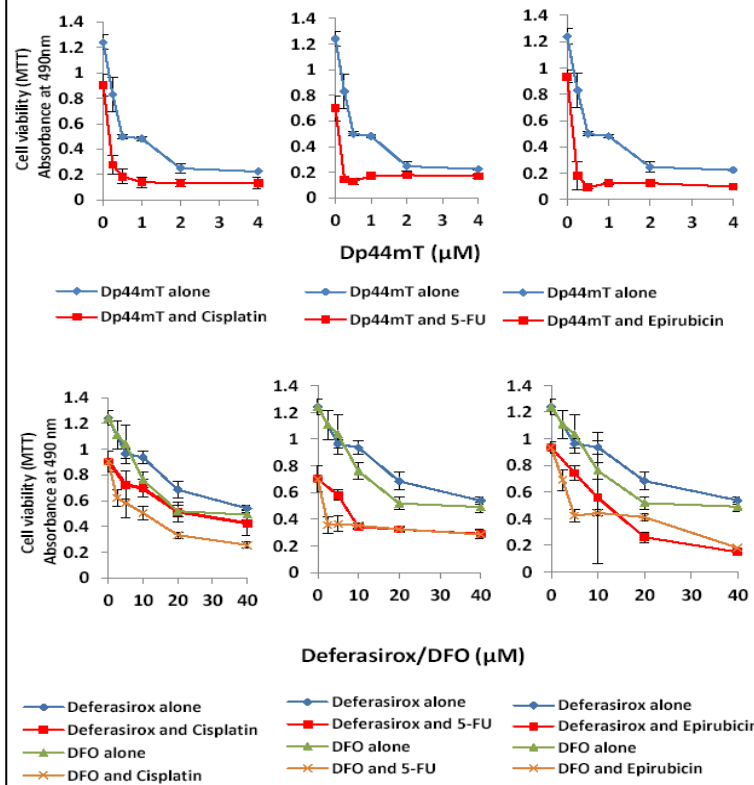
Results were consistent across all three cell lineages representing OAC and SCC malignancies. Even at low doses (0.25 $\mu$ M) Dp44mT could markedly suppress the level of viability and proliferation in the presence of Cisplatin, 5-FU or Epirubicin. Suppression of viability and proliferation was also evident for the clinically established chelators DFO and Deferasirox in combination with any of the three chemotherapeutic agents. In the majority of Deferasirox, DFO and chemotherapy agent combinations, additional chelator induced cytotoxic action occurred at concentrations below calculated IC50 values (figures 5.31 and 5.32). Furthermore, irrespective of the iron chelator and chemotherapy agent

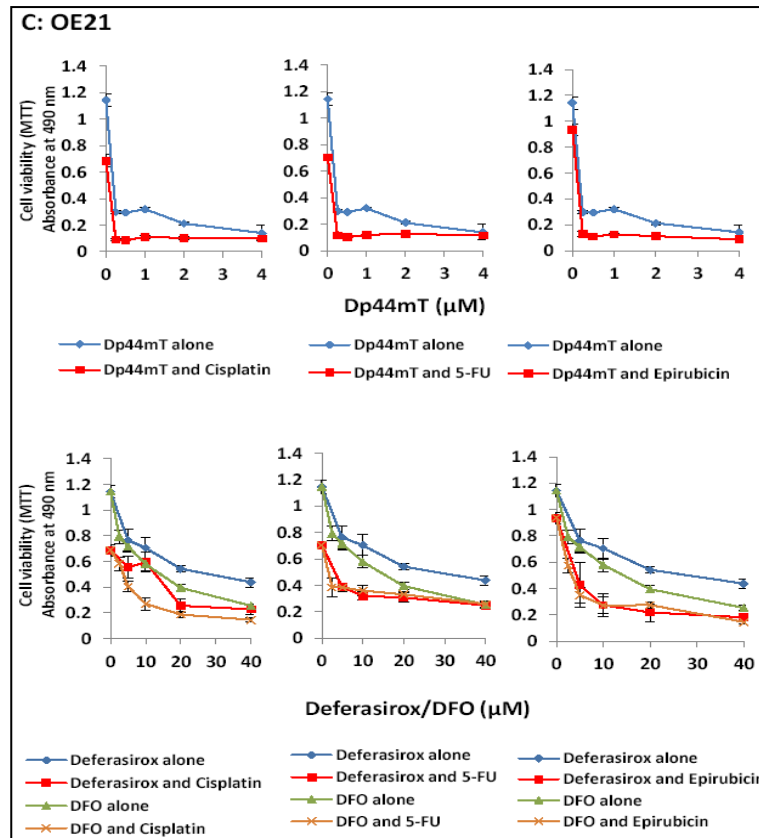
used, the effect of combining these two classes of drugs was significantly more cytotoxic than that expected with one agent alone. This positive interaction appeared to be chelator and concentration dependent in all cases (table 5.3 and 5.4).

**A: OE33**



**B: OE19**

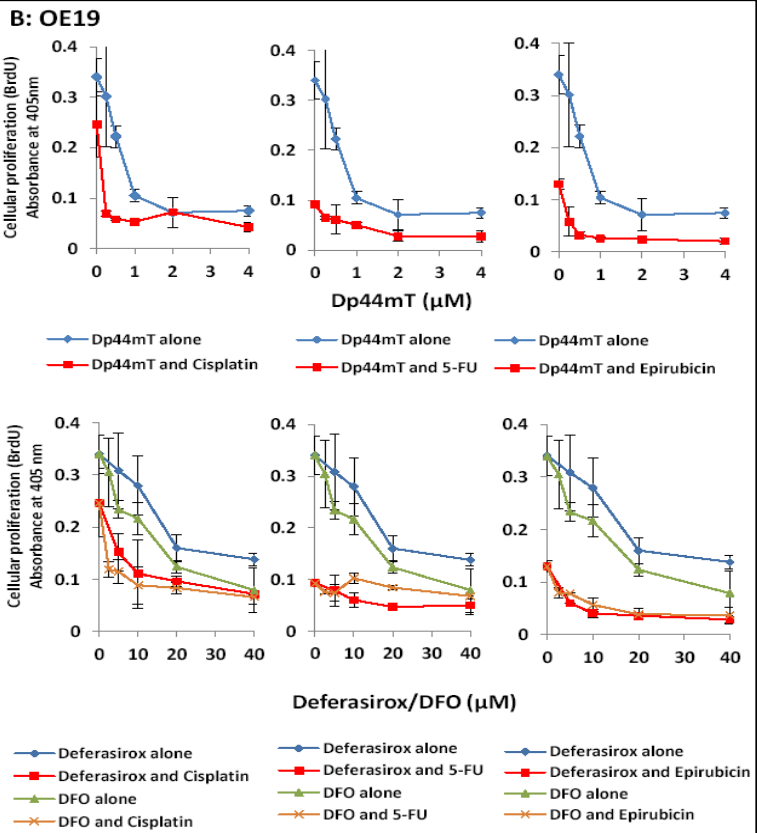
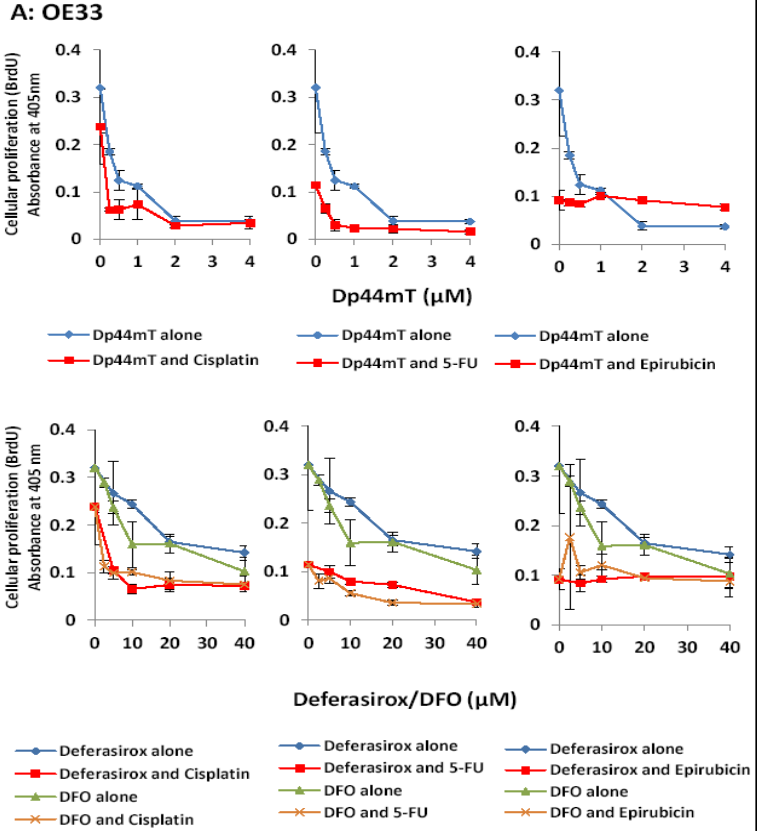




**Figure 5.31 Effect of iron chelators and standard chemotherapeutic agents on oesophageal cancer cellular viability**

Figure A: OE33, figure B: OE19 and figure C: OE21.

Cellular viability was assessed in OE33, OE19 and OE21 cell lines following 48 hours of incubation with a titrated dose of Dp44mT, Deferasirox and DFO alone or in the presence of Cisplatin ( $8 \mu\text{M}$ ), 5-FU ( $8 \mu\text{M}$ ) or Epirubicin ( $1 \mu\text{M}$ ). Error bars denote  $\pm$  SEM.



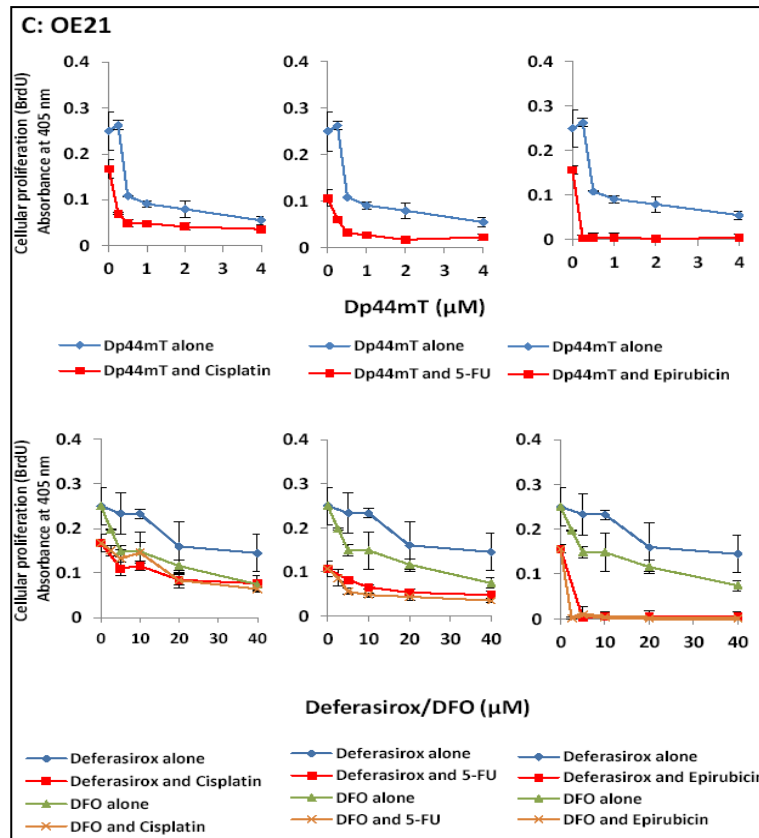


**Figure 5.32 Effect of iron chelators and standard chemotherapeutic agents on oesophageal cancer cellular proliferation**

Figure A: OE33, figure B: OE19 and figure C: OE21.

Cellular proliferation was assessed in OE33, OE19 and OE21 cell lines following 48 hours of incubation with a titrated dose of Dp44mT, Deferasirox and DFO alone or in the presence of Cisplatin (8  $\mu$ M), 5-FU (8  $\mu$ M) or Epirubicin (1  $\mu$ M). Error bars denote  $\pm$  SEM.

Cell Line	Iron Chelator	Chemotherapeutic agent	p-value	
			Viability	Proliferation
OE33	Deferasirox	Cisplatin	0.002	0.005
		5-FU	0.004	0.002
		Epirubicin	0.003	0.022
	DFO	Cisplatin	0.002	0.008
		5-FU	0.020	0.001
		Epirubicin	0.003	0.026
	Dp44mT	Cisplatin	0.024	0.036
		5-FU	0.036	0.024
		Epirubicin	0.016	0.317
OE19	Deferasirox	Cisplatin	0.001	0.008
		5-FU	0.001	0.006
		Epirubicin	<0.001	0.004
	DFO	Cisplatin	0.001	0.013
		5-FU	0.005	0.020
		Epirubicin	0.004	0.004
	Dp44mT	Cisplatin	0.008	0.045
		5-FU	0.021	0.020
		Epirubicin	0.009	0.012
OE21	Deferasirox	Cisplatin	0.007	0.002
		5-FU	0.004	<0.001
		Epirubicin	0.002	0.002
	DFO	Cisplatin	0.003	0.046
		5-FU	0.023	0.001
		Epirubicin	0.003	<0.001
	Dp44mT	Cisplatin	0.015	0.037
		5-FU	0.024	0.014
		Epirubicin	0.002	0.015

**Table 5.3 Assessment of the statistical significance of treating oesophageal cancer cell lines with chelator alone compared to a combination of chelator and standard chemotherapeutic agent**

OE33, OE19 and OE21 cell lines were challenged with a titrated dose of Dp44mT, Deferasirox or DFO in the presence or absence of Cisplatin (8  $\mu$ M), 5-FU (8  $\mu$ M) or Epirubicin (1  $\mu$ M) for 48 hours and assessed for viability and proliferation. Mean cell counts were then assessed across each regimen and statistical analysis performed between different regimes and p-values derived (Kindly calculated by statistician Dr Roger Holder – see statistical methods 2.2.18).

Cell line	Chelating Agent	5-Fu	Cisplatin	Epirubicin
OE19	Deferasirox	10 $\mu$ M	5-10 $\mu$ M	5-80 $\mu$ M
	DFO	2.5-5 $\mu$ M	2.5-10 $\mu$ M	2.5-40 $\mu$ M
	Dp44MT	0.25 $\mu$ M	0.25 $\mu$ M-1 $\mu$ M	0.25-1 $\mu$ M
OE21	Deferasirox	5-10 $\mu$ M	5-10 $\mu$ M	5-40 $\mu$ M
	DFO	nil	nil	2.5-20 $\mu$ M
	Dp44MT	0.25 $\mu$ M	0.25 $\mu$ M	0.25-0.5 $\mu$ M
OE33	Deferasirox	5-10 $\mu$ M	5-20 $\mu$ M	10 $\mu$ M
	DFO	2.5-5 $\mu$ M	2.5-5 $\mu$ M -20 $\mu$ M	2.5-5 $\mu$ M
	Dp44MT	0.25 $\mu$ M	0.25-0.5 $\mu$ M	0.25 $\mu$ M

**Table 5.4 Concentration/range of iron chelators indicating a chemo-sensitising potential in the presence of standard chemotherapeutic agents**

Concentration ranges were derived by MTT and or BrdU assays (kindly calculated by statistician Dr Roger Holder) for OE19, OE33 and OE21 cell lines and iron chelators Dp44mT, Deferasirox or DFO in the presence of chemotherapeutic agents 5-FU (8 $\mu$ M), Cisplatin (8 $\mu$ M) or Epirubicin (1 $\mu$ M).

### **5.3.8.2 Deferasirox and DFO can overcome Cisplatin chemo-resistance *in-vitro***

To further investigate the action of Deferasirox and DFO to enhance chemotherapeutic effects and potentially overcome chemo-resistance, the oesophageal SCC Cisplatin-resistant cell line TE-4 was utilised<sup>438</sup>. As expected there was no loss in cellular viability when culturing TE-4 cells with 2µM Cisplatin relative to untreated controls. However, culturing TE-4 cells with even a very low concentration of Deferasirox (5µM) together with 2µM Cisplatin resulted in a significant decrease in cellular viability compared to Cisplatin alone ( $p < 0.05$ ). Notably, the same low concentration of Deferasirox did not induce any loss of viability compared to untreated control cells when used in isolation. Similarly when DFO was used at a non-toxic concentration (2.5 µM) and co-cultured with Cisplatin, a marked suppression of cellular viability compared to Cisplatin alone was observed (figure 5.33).

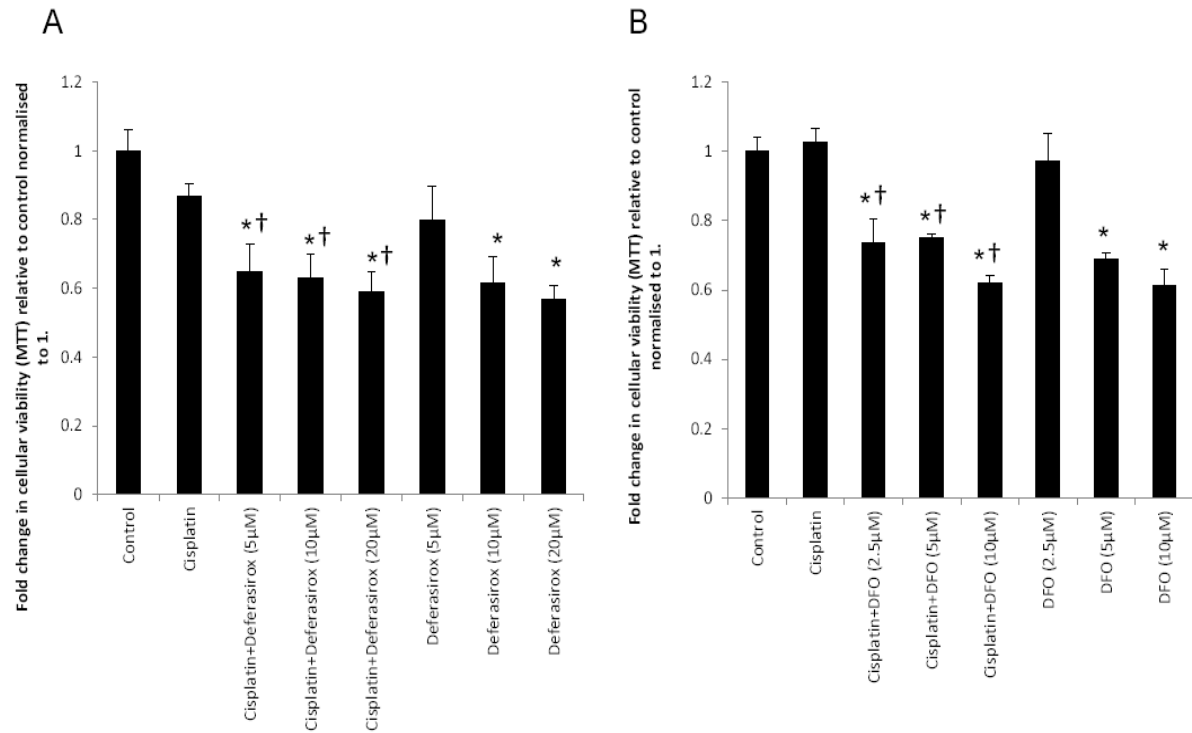


**Figure 5.33 The effect of iron chelators on TE-4 cellular viability**

TE-4 cells were challenged with Cisplatin (2 $\mu$ M) in the presence or absence of Deferasirox (figure A; 5-20 $\mu$ M) or DFO (figure B; 2.5-10 $\mu$ M) and cellular viability assessed utilising an MTT assay. (\* $p$ <0.05 compared to control unchallenged cells;  $\dagger$  Denotes  $p$ <0.05 compared to Cisplatin alone). Error bars denote  $\pm$  SEM.

## 5.4 Conclusions

This study is the first to provide evidence that iron chelators may be of use in the treatment of oesophageal cancer.

Deferasirox was the most effective clinically established agent in blocking up-take and extraction of iron from the panel of oesophageal cancer cells *in-vitro*. The promising experimental chelator Dp44mT is vastly superior to Deferasirox and DFO in chelating iron, however, it is too toxic to be trialled in humans in its present form. Interestingly, both Deferasirox and DFO delivered significant chelating capability at a fraction of the calculated IC50 values suggesting that *in-vivo* activity could still be achieved at relatively low doses.

The chelating action of Deferasirox and DFO, on intracellular iron, resulted in a classical IRE-IRP mediated response to iron deprivation<sup>250</sup>. TfR1 was consistently up-regulated at the mRNA and protein levels, reflecting the increase in inorganic iron endocytosis. Correspondingly, iron storage capacity and efflux were curtailed. Proteins capable of haem import or export generally responded in a manner expected of a cell depleted of iron. However, the responses were not consistent or statistically significant in all cell lineages. LRP1 protein was significantly elevated in OAC cells but not the squamous OE21 line. Conversely, HCP1 was not significantly elevated in OAC lines but was in OE21 cells. Logically, elevated expression of the haem importing protein LRP1 would fit with an increased need for cellular iron. However in chapter four, it was apparent that LRP1 did not seem to be regulated by intracellular iron concentration, although the exact mechanism of expression is yet to be elucidated. mRNA and protein expression of HCP1 may not reflect iron requirements of the cell as HCP1 is post-translationally regulated by

intracellular iron concentration, shuffling between the cytosolic and membranous compartments as required<sup>274,285,295</sup>. The expression of haem export proteins, BCRP and FLVCR, was generally down at the mRNA and protein levels, most likely reflecting the reduced levels of oxidative stress in the iron depleted cell as part of a detoxifying role rather than responding directly to intracellular iron concentration.

Cellular iron deprivation, induced by exposure to Deferasirox and DFO, had a significant impact on cellular viability and proliferation. Viability and proliferation were both reduced by approximately fifty percent, in line with application at their respective predetermined IC50 concentrations. Supplementary iron sulphate and haem induced significant increases in viability and proliferation as previously observed in chapter four. The addition of iron chelators to media spiked with either inorganic or haem nullified the mitogenic action of supplementary iron. The anti-proliferative effect of iron chelators, in the presence of both inorganic and organic iron, is particularly encouraging given the recognised contribution of haem to the intracellular iron pool of oesophageal cancer cells. Importantly, these *in-vitro* effects were observed across all three oesophageal cell lines (OAC and SCC lines), suggesting that the effect of modulating cellular iron levels is not cell lineage dependent. Indeed, the indiscriminate action of iron chelators on malignant cell lineages is consistent with the existing literature involving experimental chelators<sup>323,325,439-441</sup>. In this study, the experimental chelator Dp44mT demonstrated aggressive *in-vitro* anti-neoplastic effects which were not reversed by the addition of iron. This interesting observation is likely to be mediated by the novel mechanism of action of Dp44mT. Dp44mT is capable of prolific ROS generation by free radical cycling with iron and subsequent induction of pro-apoptotic pathways<sup>323,400</sup>.

Further evidence of the anti-neoplastic effects of iron chelators on cellular phenotype was demonstrated by the impaired ability of all three cell lines to form viable independent colonies (as a surrogate for metastatic potential) and inhibit cell migration. Deferasirox and DFO significantly reduced colony formation and migratory potential which was subsequently reversed by the addition of supplementary iron. Again, Dp44mT demonstrated marked impairment of the malignant activities of colony formation and migration which was robustly maintained with the addition of supplementary iron. As expected, iron alone significantly enhanced colony formation and migratory activity, potentially mediated by iron-induced down-regulation of the adhesion molecule E-cadherin. Dp44mT is also known to up-regulate expression of the tumour growth and metastasis suppressor, Ndr1 in pancreatic cancer cells and may mediate the same effects in malignant oesophageal lineages<sup>408</sup>.

Cell cycle analysis demonstrated a clear stimulatory effect of supplementary iron in all cell lines, significantly decreasing the percentage of cells in G<sub>0</sub>/G<sub>1</sub> and boosting percentages passing through S and into G<sub>2</sub>/M. A similar effect was seen with supplementary haem, although the response was more muted and reached statistical significance in the OE19 cell line only. The most startling changes were observed in the presence of Deferasirox which appeared to arrest the cell cycle in S phase. S phase arrest of the cell cycle was an unexpected finding as iron chelators have classically been observed to cause cycle arrest at the G<sub>1</sub>/S interface. The action of DFO has been studied in great detail in other malignant lineages and conforms to the expected G<sub>1</sub>/S arrest, mediated by a series of complex interactions which culminate in a decrease of the hyperphosphorylated form of pRb and G<sub>1</sub>/S arrest<sup>189,194,371</sup>. DFO does not appear to directly inhibit the iron dependent

enzyme RNR, or it at least mediates cell cycle arrest before this becomes significantly important<sup>371</sup>. DFO failed to consistently alter the cell cycle in oesophageal cancer cells although it did show statistically significant evidence of G<sub>1</sub>/S hold-up in the OE33 cell line. Deferasirox mediated cell cycle arrest in S phase is likely to represent functional loss of RNR through iron deprivation, preventing the cell from completing the task of DNA replication, rather than disrupting G<sub>1</sub>/S. The potential inhibition of RNR by Deferasirox was further investigated by Western blotting for nuclear levels of CDC45L protein, as a proxy marker of cellular arrest in S phase<sup>434,435</sup>. CDC45L protein levels were significantly higher in cells exposed to Deferasirox and comparable to the degree of CDC45L protein accumulation seen with the application of HU to formally block RNR activity. Co-culture of iron with Deferasirox returned CDC45L levels back to those of control. Recently published data detailing the anti-neoplastic effects of Deferasirox on human hepatoma cells has also shown blockade of the cell cycle in S phase, potentially attributed to iron depletion and reduced polyamine metabolism<sup>387</sup>. Iron chelators are likely to interact in subtly different ways with the complex control mechanisms of the cell cycle and clearly an in-depth evaluation of the effects of Deferasirox on the cell cycle is required.

A murine xenograft model of human oesophageal cancer was developed to assess the *in-vivo* anti-neoplastic effects of Deferasirox as the agent of choice in a future clinical trial. Over a three week period, oral Deferasirox administration had a remarkable impact on xenograft tumour burden, reducing the mean average xenograft weight by approximately forty percent for OAC and SCC lineages. Such a reduction is on a par with the actions of experimental iron chelators in other non-gastrointestinal xenografts<sup>323</sup>. The average gross iron content of the xenografts exposed to Deferasirox was significantly reduced compared

to control, strongly supporting iron deprivation as an important mechanism of anti-neoplastic action. Furthermore, the mice tolerated Deferasirox treatment extremely well maintaining a normal growth trajectory and organ weight compared to control. Despite extracting iron from the xenograft, importantly, there was no evidence of systemic and solid organ iron stripping or biochemical derangement. Changes seen in IRE-IRP responsive iron transport proteins were more consistent and marked than those observed *in-vitro*. Xenografts exposed to Deferasirox uniformly demonstrated significant up-regulation of TfR1 mRNA expression in response to iron deprivation to increase inorganic iron endocytosis. Similarly, iron storage capacity and efflux was reduced with significant suppression of ferritin and FPN mRNA expression in response to Deferasirox. Semi-quantitative immunohistochemistry was again concordant with xenograft iron deprivation. No changes in IRE-IRP responsive iron transport proteins were observed in the solid organs of mice administered Deferasirox, further supporting the tumour specific action of Deferasirox; at least at this low dose and relatively short duration. Deferasirox was administered at the standard starting dose for patients treated for iron overload (20mg/Kg). Even considering the differences between human and mouse biochemistry and pharmacodynamics, 20mg/Kg is a low dose and may reflect the ability of Deferasirox to chelate the majority of iron from malignant cells at very low concentrations, as seen *in-vitro*. The apparent sparing of healthy benign cells has been noted in all studies assessing the potential anti-neoplastic effects of iron chelators<sup>323,325,328</sup>. This fascinating observation may represent the relative sensitivity of malignant cells to iron deprivation or subtle changes in the metabolism of iron by cancer cells rendering them more accessible to chelation. One such mechanism may be inhibition of the canonical Wnt/ $\beta$ -catenin oncogenic signalling pathway which is well known to be active in gastrointestinal

epithelial cancers<sup>176</sup>. DFO and Deferasirox are both potent iron dependent inhibitors of Wnt signalling in malignant colorectal lineages<sup>331</sup>. However, it is likely that iron chelators mediate cytotoxic activity by several pathways that may not be iron dependent. Indeed, the cytotoxic action of Deferasirox in myelodysplastic syndromes may be mediated through inhibition of the NF- $\kappa$ B pathway, which was not influenced by the addition of iron and is highly active in oesophageal cancers<sup>386,442</sup>. In addition, Deferasirox may mediate anti-proliferative effects on myeloid leukaemia cells by suppression of signalling through the mTOR pathway, which is again active in oesophageal malignancy<sup>396,443</sup>.

Chemotherapy is the key to enhancing overall survival and prolonging life in patients receiving palliative care for oesophageal malignancy<sup>444</sup>. Perhaps the most encouraging aspect of the anti-neoplastic effects of DFO and Deferasirox are their apparent chemosensitising properties in combination with the standard chemotherapeutic agents currently utilised in the treatment of oesophageal malignancies. The combination of chelators and chemotherapy agents demonstrated significantly greater cytotoxicity than observed with one agent alone in both OAC and SCC lineages. Pertinently for potential translation into clinical trials, Deferasirox and DFO showed marked additional cytotoxic action at doses well below IC50 values when in combination with chemotherapeutic agents, affording the possibility of dose reduction to minimise toxicity. The chemosensitising action of Deferasirox and DFO was further highlighted when applied to the Cisplatin-resistant cell line TE-4, which became responsive to Cisplatin in the background of small doses of Deferasirox or DFO. These observations are consistent with other studies utilising the experimental iron chelator Dp44mT, which has been shown to overcome both etoposide and vinblastine resistance<sup>323</sup>. Similar data has been generated

in a leukaemic cell line, K562, where pre-incubation of cells with Deferasirox and subsequent incubation with etoposide, led to increased apoptosis above that expected with either agent alone<sup>396</sup>. Chemo-resistance is of major concern in the treatment OAC and many patients with non-responsive tumours are subject to unnecessary chemotherapy induced toxicity and subsequent delay in oesophagectomy<sup>445,446</sup>. At the present time, it is not possible to identify subtle differences in tumour biology that could robustly guide more selective treatment, therefore the introduction of a chemo-sensitising agent that possesses independent anti-neoplastic properties is likely to benefit the majority of patients.

Iron chelators show potential as anti-neoplastic and chemo-sensitising agents. This chapter provides a platform for assessing the utility of clinically established agents, such as Deferasirox, in the treatment of patients with oesophageal cancer.

## CHAPTER 6: DISCUSSION

### 6.1 Conclusions

The cumulative evidence implicating iron in the pathogenesis and propagation of oesophageal malignancy is compelling. Understanding of the regulatory and metabolic pathways controlling iron homeostasis is now largely established and this knowledge can now be applied to delineate the pathological derangement in iron metabolism seen in malignancy.

*Ex-vivo* samples of OAC are iron loaded in a progressive manner from benign BM to dysplastic BM and finally malignant transformation<sup>171</sup>. This continuing iron acquisition in oesophageal malignancies is paradoxical, given the high intracellular iron levels, and is clearly demonstrated by the ability of OAC cells to sequester more iron, through up-regulation of TfR1 mediated endocytosis of transferrin bound iron and functional loss of iron export processes, in the background of an iron replete state<sup>171</sup>. The elegant and finely tuned homeostatic mechanism for controlling intracellular iron concentration, based on the IRE-IRP system, appears to have been abandoned at some point in the evolutionary paradigm of oesophageal carcinogenesis<sup>120,248,249</sup>. The exact trigger for this phenomenon remains elusive, although, it has been postulated that increased expression of the oncogene c-Myc induces inappropriate up-regulation of TfR1 in the background loss of APC function<sup>176</sup>.

However, there exists a pool of systemic haem that is constantly re-cycled in the process of erythrocyte regeneration, which is potentially available to cancer cells as a major source of iron accumulation<sup>270,290</sup>. This thesis provides, for the first time, evidence that both OAC and oesophageal SCC are able to capture haem in a manner akin to inorganic iron acquisition<sup>171</sup>. *Ex-vivo* OAC resection specimens, matched with adjacent dysplastic BM, demonstrate progressive up-regulation of the two recently discovered haem importing proteins LRP1 and HCP1. The membranous location of LRP1 and HCP1, demonstrated by immunohistochemistry in oesophageal cancer specimens, is highly suggestive of a functional role in capturing systemic haem. Haem, both free and bound to haemopexin, is likely to be relatively abundant in the substance of the tumour due to friable neovascularisation, direct vessel invasion and ulceration. Once within the cell, iron is liberated from haem and enters a common inorganic iron metabolic pathway to create a more aggressive cellular phenotype<sup>171,270</sup>. Supplementary haem significantly enhances cellular proliferation, viability, migration and colony forming ability *in-vitro* compared to control. Abrogation of LRP1 or HCP1 expression reverses the stimulatory action of supplementary haem and induces a compensatory overexpression of TfR1, potentially mediated by the IRE-IRP regulatory mechanism in response to relative iron deprivation. The dramatic *in-vivo* contribution of LRP1 and HCP1 to tumourigenicity was highlighted here for the first time in a xenograft model of OAC where tumour burden was significantly reduced by up to seventy percent after loss of LRP1 or HCP1 expression.

Intriguingly, the expression of haem exporting proteins, FLVCR and BCRP, was significantly up-regulated in OAC compared to adjacent dysplastic BM. These proteins are known to protect developing erythrocytes from excessive haem toxicity and enterocytes

from dietary derived toxins<sup>273,279</sup>. It is probable that the overexpression of FLVCR and BCRP in OAC could protect cancer cells from haem induced oxidative stress, especially within the hypoxic environment encountered in fast growing tumours<sup>285</sup>.

LRP1 and HCP1 should be considered as novel targets for therapeutic monoclonal antibodies in the treatment of oesophageal malignancy. However, neither LRP1 nor HCP1 are solely importers of haem. LRP1 is ubiquitously expressed as a general scavenger receptor with multiple ligands and HCP1 is putatively regarded to actively transport folate as well as haem<sup>296,298</sup>. With this in mind, the mechanism of anti-neoplastic action of blocking LRP1 or HCP1 could be multi-factorial and currently clinically unpredictable.

The outcome from oesophageal cancer is notoriously dismal with an overall five-year-survival figure quoted at just ten percent<sup>2,3</sup>. Despite the addition of neoadjuvant chemotherapy and refinement of surgical technique, the vast majority of patients still die from overwhelming malignant disease progression<sup>3</sup>. Oesophageal cancer cells have now been shown to acquire both organic and inorganic iron by the action of several transport proteins which helps explain why targeting TfR1 alone with monoclonal antibodies fails to produce a robust anti-neoplastic effect in a variety of malignant lineages<sup>208</sup>. Clearly simultaneous therapeutic functional blockade of multiple targets is not practical and likely to be prohibitively expensive and unpredictable. An alternative would be to deprive the cancer cell of iron by use of a chelating agent. This approach is particularly appealing as iron chelators have shown considerable anti-neoplastic properties in other malignancies and appear to exhibit cancer specific action without systemic iron stripping<sup>319,322,323,325,328</sup>. In addition, a number of iron chelators, including DFO and

Deferasirox are already in clinical use for the treatment of iron overload disorders and have excellent safety profiles<sup>357,379</sup>.

This thesis details for the first time that iron chelators show potent anti-neoplastic action on OAC and oesophageal SCC both *in-vitro* and *in-vivo*. Experimental and clinically established iron chelators are able to extract significant amounts of iron from oesophageal cancer cells and prevent the up-take of ambient iron. The action of iron chelators significantly reduces proliferation, viability, migration and colony forming *in-vitro* and reverses the stimulatory effect of supplementary iron. The experimental iron chelator Dp44mT displays the most aggressive anti-neoplastic action, however its potential systemic toxicity prohibits clinical application at the present time. Excitingly, the clinically established and orally administered iron chelator Deferasirox exhibited potent anti-cancer properties *in-vitro* and was taken forward to assess *in-vivo* performance in a mouse xenograft model. Orally administered Deferasirox significantly inhibited oesophageal cancer xenograft growth by up to forty percent and was extremely well tolerated without evidence of systemic or visceral iron stripping. The observed anti-neoplastic action of Deferasirox is directly translatable into clinical research and should be considered for clinical trials in oesophageal cancer patients. Furthermore, iron chelators including Deferasirox, demonstrated an additive anti-neoplastic action in combination with current standard chemotherapy agents used in the treatment of oesophageal malignancy and were able to overcome chemo-resistance at very low concentrations. Chemo-resistance is of major concern in the treatment of OAC and many patients with non-responsive tumours are subject to unnecessary chemotherapy induced toxicity and subsequent delay in oesophagectomy<sup>445,446</sup>. At the present time, it is not

possible to identify subtle differences in tumour biology that could robustly guide more selective treatment; therefore the introduction of a chemo-sensitising agent that possesses independent anti-neoplastic properties is likely to benefit the majority of patients<sup>445</sup>.

Oesophageal adenocarcinoma incidence is increasing at an alarming rate in Western populations and is principally associated with obesity, gastro-oesophageal reflux and Barrett's metaplasia<sup>1,42,45,46,55,58,120</sup>. Understanding the genetic and molecular events involved in the development of this disease is paramount to improving survival. This thesis contributes to the growing evidence implicating iron in the pathogenesis of oesophageal cancer and provides a platform to assess the utility of iron chelators as clinically therapeutic agents.

## **6.2 Future work**

### **6.2.1 Laboratory experimental work**

Current understanding of the complex nature of systemic and cellular iron acquisition is not at a stage where targeted therapy, in the form of monoclonal antibodies to iron and haem transporting proteins, could be attempted in clinical trials. Regulatory interplay between LRP1 and HCP1 and cellular iron status is not clear and the ubiquitous expression of LRP1 in particular, creates an element of uncertainty as to the likely clinical effect of blocking these receptors<sup>298</sup>.

In contrast, iron chelation therapy, as an adjunct to current clinical management of patients with oesophageal malignancies, represents a far safer, cheaper, and more achievable alternative. The clinically licensed, well tolerated and orally administered chelator Deferasirox is the obvious agent of choice. Although there is little doubt that the principal mode of action of this drug is the chelation of iron, the exact pathways through which the cytotoxic action is mediated remain to be clarified. A reasonable place to start would be the NF- $\kappa$ B, mTOR and canonical Wnt/ $\beta$ -catenin signalling pathways that appear to be inhibited by Deferasirox in other cell lineages and are known to be active in oesophageal malignancies<sup>176,331,386,396,442,443</sup>. A more comprehensive assessment of the interplay between the complex mechanisms controlling the cell cycle and the action of Deferasirox would be appropriate especially considering the apparent induced cell cycle arrest in S phase, rather than G<sub>1</sub>/S more classically associated with iron chelators<sup>189,371</sup>.

The exciting *in-vitro* evidence of the chemo-sensitising capabilities of Deferasirox should be further explored and validated in murine models using a combination of chelator, standard chemotherapy agents and multiple cell lineages. Furthermore, the dose and timing of Deferasirox administration, as a pre-sensitising dose or in combination with chemotherapy agents, needs to be addressed.

### **6.2.2 Clinical experimental work**

Work is currently underway to design and obtain funding and ethical approval for the assessment of Deferasirox in human clinical trials. In the first instance, safety, tolerability and proof of concept are paramount. Assuming murine studies are successful in validating the *in-vitro* evidence of the chemo-sensitising action of Deferasirox and provide

guidance on the most appropriate dosing regimen, these data can be used to finalise the proposed protocol for the application of Deferasirox in patients receiving palliative chemotherapy. The ultimate goal would be to combine Deferasirox with neoadjuvant chemotherapy in patients deemed potentially curable with a view to improving overall survival and prolonging life in the palliative setting.

## REFERENCES

1. Parker SL, Tong T, Bolden S, Wingo PA. Cancer statistics, 1997. *CA Cancer J Clin* 1997; 47: 5-27.
2. Holmes RS, Vaughan TL. Epidemiology and pathogenesis of esophageal cancer. *Semin Radiat Oncol* 2007; 17: 2-9.
3. Surgical resection with or without preoperative chemotherapy in oesophageal cancer: a randomised controlled trial. *Lancet* 2002; 359: 1727-33.
4. Blot WJ, Devesa SS, Kneller RW, Fraumeni JF, Jr. Rising incidence of adenocarcinoma of the esophagus and gastric cardia. *JAMA* 1991; 265: 1287-9.
5. Bird-Lieberman EL, Fitzgerald RC. Early diagnosis of oesophageal cancer. *Br J Cancer* 2009; 101: 1-6.
6. Djarv T, Lagergren J, Blazeby JM, Lagergren P. Long-term health-related quality of life following surgery for oesophageal cancer. *Br J Surg* 2008; 95: 1121-6.
7. Allum WH, Stenning SP, Bancewicz J, Clark PI, Langley RE. Long-term results of a randomized trial of surgery with or without preoperative chemotherapy in esophageal cancer. *J Clin Oncol* 2009; 27: 5062-7.
8. Blot WJ, Fraumeni JF, Jr. Trends in esophageal cancer mortality among US blacks and whites. *Am J Public Health* 1987; 77: 296-8.
9. Devesa SS, Blot WJ, Fraumeni JF, Jr. Changing patterns in the incidence of esophageal and gastric carcinoma in the United States. *Cancer* 1998; 83: 2049-53.
10. El Serag HB, Mason AC, Petersen N, Key CR. Epidemiological differences between adenocarcinoma of the oesophagus and adenocarcinoma of the gastric cardia in the USA. *Gut* 2002; 50: 368-72.
11. Brown LM, Devesa SS. Epidemiologic trends in esophageal and gastric cancer in the United States. *Surg Oncol Clin N Am* 2002; 11: 235-56.
12. Brown LM, Devesa SS, Chow WH. Incidence of adenocarcinoma of the esophagus among white Americans by sex, stage, and age. *J Natl Cancer Inst* 2008; 100: 1184-7.
13. Pohl H, Welch HG. The role of overdiagnosis and reclassification in the marked increase of esophageal adenocarcinoma incidence. *J Natl Cancer Inst* 2005; 97: 142-6.

14. Pohl H, Sirovich B, Welch HG. Esophageal adenocarcinoma incidence: are we reaching the peak? *Cancer Epidemiol Biomarkers Prev* 2010; 19: 1468-70.
15. Pera M, Manterola C, Vidal O, Grande L. Epidemiology of esophageal adenocarcinoma. *J Surg Oncol* 2005; 92: 151-9.
16. Bosch A, Frias Z, Caldwell WL. Adenocarcinoma of the esophagus. *Cancer* 1979; 43: 1557-61.
17. Puestow CB, Gillesby WJ, Guynn VL. Cancer of the esophagus. *AMA Arch Surg* 1955; 70: 662-71.
18. Turnbull AD, Goodner JT. Primary adenocarcinoma of the esophagus. *Cancer* 1968; 22: 915-8.
19. Webb JN, Busuttill A. Adenocarcinoma of the oesophagus and of the oesophagogastric junction. *Br J Surg* 1978; 65: 475-9.
20. Pera M, Cameron AJ, Trastek VF, Carpenter HA, Zinsmeister AR. Increasing incidence of adenocarcinoma of the esophagus and esophagogastric junction. *Gastroenterology* 1993; 104: 510-3.
21. Powell J, McConkey CC. The rising trend in oesophageal adenocarcinoma and gastric cardia. *Eur J Cancer Prev* 1992; 1: 265-9.
22. Levi F, La Vecchia C. Adenocarcinoma of the esophagus in Switzerland. *JAMA* 1991; 265: 2960.
23. Lord RV et al. Rising incidence of oesophageal adenocarcinoma in men in Australia. *J Gastroenterol Hepatol* 1998; 13: 356-62.
24. El Serag HB. The epidemic of esophageal adenocarcinoma. *Gastroenterol Clin North Am* 2002; 31: 421-40, viii.
25. Wei JT, Shaheen N. The changing epidemiology of esophageal adenocarcinoma. *Semin Gastrointest Dis* 2003; 14: 112-27.
26. Macfarlane GJ, Boyle P. The epidemiology of oesophageal cancer in the UK and other European countries. *J R Soc Med* 1994; 87: 334-7.
27. Law S, Wong J. Changing disease burden and management issues for esophageal cancer in the Asia-Pacific region. *J Gastroenterol Hepatol* 2002; 17: 374-81.
28. Ribeiro U, Jr., Posner MC, Safatle-Ribeiro AV, Reynolds JC. Risk factors for squamous cell carcinoma of the oesophagus. *Br J Surg* 1996; 83: 1174-85.
29. Yang CS. Research on esophageal cancer in China: a review. *Cancer Res* 1980; 40: 2633-44.

30. Schottenfeld D. Epidemiology of cancer of the esophagus. *Semin Oncol* 1984; 11: 92-100.
31. Chalasani N, Wo JM, Waring JP. Racial differences in the histology, location, and risk factors of esophageal cancer. *J Clin Gastroenterol* 1998; 26: 11-3.
32. Chalasani N, Wo JM, Hunter JG, Waring JP. Significance of intestinal metaplasia in different areas of esophagus including esophagogastric junction. *Dig Dis Sci* 1997; 42: 603-7.
33. Blot WJ. Esophageal cancer trends and risk factors. *Semin Oncol* 1994; 21: 403-10.
34. Blot WJ, McLaughlin JK. The changing epidemiology of esophageal cancer. *Semin Oncol* 1999; 26: 2-8.
35. Zhang ZF et al. Adenocarcinomas of the esophagus and gastric cardia: medical conditions, tobacco, alcohol, and socioeconomic factors. *Cancer Epidemiol Biomarkers Prev* 1996; 5: 761-8.
36. Heath EI, Limburg PJ, Hawk ET, Forastiere AA. Adenocarcinoma of the esophagus: risk factors and prevention. *Oncology (Williston Park)* 2000; 14: 507-14.
37. Cheng KK, Day NE. Nutrition and esophageal cancer. *Cancer Causes Control* 1996; 7: 33-40.
38. Wahrendorf J et al. Blood, retinol and zinc riboflavin status in relation to precancerous lesions of the esophagus: findings from a vitamin intervention trial in the People's Republic of China. *Cancer Res* 1988; 48: 2280-3.
39. Ghadirian P. Thermal irritation and esophageal cancer in northern Iran. *Cancer* 1987; 60: 1909-14.
40. Gao YT et al. Reduced risk of esophageal cancer associated with green tea consumption. *J Natl Cancer Inst* 1994; 86: 855-8.
41. Cheng KK. The etiology of esophageal cancer in Chinese. *Semin Oncol* 1994; 21: 411-5.
42. Calle EE, Kaaks R. Overweight, obesity and cancer: epidemiological evidence and proposed mechanisms. *Nat Rev Cancer* 2004; 4: 579-91.
43. Nilsson M, Johnsen R, Ye W, Hveem K, Lagergren J. Obesity and estrogen as risk factors for gastroesophageal reflux symptoms. *JAMA* 2003; 290: 66-72.
44. Wu AH, Wan P, Bernstein L. A multiethnic population-based study of smoking, alcohol and body size and risk of adenocarcinomas of the stomach and esophagus (United States). *Cancer Causes Control* 2001; 12: 721-32.

45. Lagergren J, Bergstrom R, Nyren O. Association between body mass and adenocarcinoma of the esophagus and gastric cardia. *Ann Intern Med* 1999; 130: 883-90.
46. Reid BJ, Li X, Galipeau PC, Vaughan TL. Barrett's oesophagus and oesophageal adenocarcinoma: time for a new synthesis. *Nat Rev Cancer* 2010; 10: 87-101.
47. Kendall BJ et al. Leptin and the risk of Barrett's oesophagus. *Gut* 2008; 57: 448-54.
48. Islami F, Kamangar F. Helicobacter pylori and esophageal cancer risk: a meta-analysis. *Cancer Prev Res (Phila)* 2008; 1: 329-38.
49. Suerbaum S, Michetti P. Helicobacter pylori infection. *N Engl J Med* 2002; 347: 1175-86.
50. Kamangar F, Dores GM, Anderson WF. Patterns of cancer incidence, mortality, and prevalence across five continents: defining priorities to reduce cancer disparities in different geographic regions of the world. *J Clin Oncol* 2006; 24: 2137-50.
51. Kamangar F et al. Opposing risks of gastric cardia and noncardia gastric adenocarcinomas associated with Helicobacter pylori seropositivity. *J Natl Cancer Inst* 2006; 98: 1445-52.
52. Chow WH et al. An inverse relation between cagA+ strains of Helicobacter pylori infection and risk of esophageal and gastric cardia adenocarcinoma. *Cancer Res* 1998; 58: 588-90.
53. Barrett NR. Chronic peptic ulcer of the oesophagus and 'oesophagitis'. *Br J Surg* 1950; 38: 175-82.
54. Ishizuka I et al. Immunohistochemical analysis of short-segment Barrett's esophagus. *J Gastroenterol Hepatol* 2004; 19: 1410-6.
55. Lagergren J, Bergstrom R, Lindgren A, Nyren O. Symptomatic gastroesophageal reflux as a risk factor for esophageal adenocarcinoma. *N Engl J Med* 1999; 340: 825-31.
56. O'Riordan JM, Byrne PJ, Ravi N, Keeling PW, Reynolds JV. Long-term clinical and pathologic response of Barrett's esophagus after antireflux surgery. *Am J Surg* 2004; 188: 27-33.
57. Cameron AJ, Ott BJ, Payne WS. The incidence of adenocarcinoma in columnar-lined (Barrett's) esophagus. *N Engl J Med* 1985; 313: 857-9.
58. Miros M, Kerlin P, Walker N. Only patients with dysplasia progress to adenocarcinoma in Barrett's oesophagus. *Gut* 1991; 32: 1441-6.

59. Ackroyd R et al. Photodynamic therapy for dysplastic Barrett's oesophagus: a prospective, double blind, randomised, placebo controlled trial. *Gut* 2000; 47: 612-7.
60. Reid BJ et al. Flow-cytometric and histological progression to malignancy in Barrett's esophagus: prospective endoscopic surveillance of a cohort. *Gastroenterology* 1992; 102: 1212-9.
61. Locke GR, III, Talley NJ, Fett SL, Zinsmeister AR, Melton LJ, III. Prevalence and clinical spectrum of gastroesophageal reflux: a population-based study in Olmsted County, Minnesota. *Gastroenterology* 1997; 112: 1448-56.
62. Spechler SJ, Zeroogian JM, Antonioli DA, Wang HH, Goyal RK. Prevalence of metaplasia at the gastro-oesophageal junction. *Lancet* 1994; 344: 1533-6.
63. Drewitz DJ, Sampliner RE, Garewal HS. The incidence of adenocarcinoma in Barrett's esophagus: a prospective study of 170 patients followed 4.8 years. *Am J Gastroenterol* 1997; 92: 212-5.
64. O'Connor JB, Falk GW, Richter JE. The incidence of adenocarcinoma and dysplasia in Barrett's esophagus: report on the Cleveland Clinic Barrett's Esophagus Registry. *Am J Gastroenterol* 1999; 94: 2037-42.
65. Spechler SJ et al. Long-term outcome of medical and surgical therapies for gastroesophageal reflux disease: follow-up of a randomized controlled trial. *JAMA* 2001; 285: 2331-8.
66. Shaheen NJ, Crosby MA, Bozymski EM, Sandler RS. Is there publication bias in the reporting of cancer risk in Barrett's esophagus? *Gastroenterology* 2000; 119: 333-8.
67. Chow WH et al. The relation of gastroesophageal reflux disease and its treatment to adenocarcinomas of the esophagus and gastric cardia. *JAMA* 1995; 274: 474-7.
68. Farrow DC et al. Gastroesophageal reflux disease, use of H2 receptor antagonists, and risk of esophageal and gastric cancer. *Cancer Causes Control* 2000; 11: 231-8.
69. Peters JH et al. Outcome of adenocarcinoma arising in Barrett's esophagus in endoscopically surveyed and nonsurveyed patients. *J Thorac Cardiovasc Surg* 1994; 108: 813-21.
70. Falk GW, Ours TM, Richter JE. Practice patterns for surveillance of Barrett's esophagus in the united states. *Gastrointest Endosc* 2000; 52: 197-203.
71. Reid BJ et al. Observer variation in the diagnosis of dysplasia in Barrett's esophagus. *Hum Pathol* 1988; 19: 166-78.
72. Fearon ER, Vogelstein B. A genetic model for colorectal tumorigenesis. *Cell* 1990; 61: 759-67.

73. Jankowski JA et al. Molecular evolution of the metaplasia-dysplasia-adenocarcinoma sequence in the esophagus. *Am J Pathol* 1999; 154: 965-73.
74. Shaheen NJ. Advances in Barrett's esophagus and esophageal adenocarcinoma. *Gastroenterology* 2005; 128: 1554-66.
75. Falk GW, Rice TW, Goldblum JR, Richter JE. Jumbo biopsy forceps protocol still misses unsuspected cancer in Barrett's esophagus with high-grade dysplasia. *Gastrointest Endosc* 1999; 49: 170-6.
76. Heitmiller RF, Redmond M, Hamilton SR. Barrett's esophagus with high-grade dysplasia. An indication for prophylactic esophagectomy. *Ann Surg* 1996; 224: 66-71.
77. Schnell TG et al. Long-term nonsurgical management of Barrett's esophagus with high-grade dysplasia. *Gastroenterology* 2001; 120: 1607-19.
78. Skacel M et al. The diagnosis of low-grade dysplasia in Barrett's esophagus and its implications for disease progression. *Am J Gastroenterol* 2000; 95: 3383-7.
79. Buttar NS et al. Extent of high-grade dysplasia in Barrett's esophagus correlates with risk of adenocarcinoma. *Gastroenterology* 2001; 120: 1630-9.
80. Swisher SG et al. Effect of operative volume on morbidity, mortality, and hospital use after esophagectomy for cancer. *J Thorac Cardiovasc Surg* 2000; 119: 1126-32.
81. Beilstein M, Silberg D. Cellular and molecular mechanisms responsible for progression of Barrett's metaplasia to esophageal carcinoma. *Gastroenterol Clin North Am* 2002; 31: 461-79, ix.
82. Ahmadi A, Draganov P. Endoscopic mucosal resection in the upper gastrointestinal tract. *World J Gastroenterol* 2008; 14: 1984-9.
83. Ganz RA et al. Circumferential ablation of Barrett's esophagus that contains high-grade dysplasia: a U.S. Multicenter Registry. *Gastrointest Endosc* 2008; 68: 35-40.
84. Barr H et al. Rapid endoscopic identification and destruction of degenerating Barrett's mucosal neoplasia. *Surgeon* 2011; 9: 119-23.
85. DeSal G, Loda M, Pagano M. Cell cycle and cancer: critical events at the G1 restriction point. *Crit Rev Oncog* 1996; 7: 127-42.
86. Hardie LJ et al. p16 expression in Barrett's esophagus and esophageal adenocarcinoma: association with genetic and epigenetic alterations. *Cancer Lett* 2005; 217: 221-30.
87. Shields HM et al. Prospective evaluation of multilayered epithelium in Barrett's esophagus. *Am J Gastroenterol* 2001; 96: 3268-73.

88. Sarosi G et al. Bone marrow progenitor cells contribute to esophageal regeneration and metaplasia in a rat model of Barrett's esophagus. *Dis Esophagus* 2008; 21: 43-50.
89. Jenkins GJ et al. Genetic pathways involved in the progression of Barrett's metaplasia to adenocarcinoma. *Br J Surg* 2002; 89: 824-37.
90. Sherr CJ. Cancer cell cycles. *Science* 1996; 274: 1672-7.
91. Xiong Y, Zhang H, Beach D. Subunit rearrangement of the cyclin-dependent kinases is associated with cellular transformation. *Genes Dev* 1993; 7: 1572-83.
92. Klump B, Hsieh CJ, Holzmann K, Gregor M, Porschen R. Hypermethylation of the CDKN2/p16 promoter during neoplastic progression in Barrett's esophagus. *Gastroenterology* 1998; 115: 1381-6.
93. Maley CC, Reid BJ. Natural selection in neoplastic progression of Barrett's esophagus. *Semin Cancer Biol* 2005; 15: 474-83.
94. Clement G, Braunschweig R, Pasquier N, Bosman FT, Benhattar J. Alterations of the Wnt signaling pathway during the neoplastic progression of Barrett's esophagus. *Oncogene* 2006; 25: 3084-92.
95. Schneikert J, Behrens J. The canonical Wnt signalling pathway and its APC partner in colon cancer development. *Gut* 2007; 56: 417-25.
96. Zumbunn J, Kinoshita K, Hyman AA, Nathke IS. Binding of the adenomatous polyposis coli protein to microtubules increases microtubule stability and is regulated by GSK3 beta phosphorylation. *Curr Biol* 2001; 11: 44-9.
97. Kawakami K et al. Hypermethylated APC DNA in plasma and prognosis of patients with esophageal adenocarcinoma. *J Natl Cancer Inst* 2000; 92: 1805-11.
98. Eads CA et al. Fields of aberrant CpG island hypermethylation in Barrett's esophagus and associated adenocarcinoma. *Cancer Res* 2000; 60: 5021-6.
99. Casson AG, Kerkvliet N, O'Malley F, Inculet R, Troster M. p53 immunoreactivity in carcinosarcoma of the esophagus. *J Surg Oncol* 1994; 56: 132-5.
100. Harris CC. Structure and function of the p53 tumor suppressor gene: clues for rational cancer therapeutic strategies. *J Natl Cancer Inst* 1996; 88: 1442-55.
101. Kokontis JM, Wagner AJ, O'Leary M, Liao S, Hay N. A transcriptional activation function of p53 is dispensable for and inhibitory of its apoptotic function. *Oncogene* 2001; 20: 659-68.
102. Schneider PM et al. Mutations of p53 in Barrett's esophagus and Barrett's cancer: a prospective study of ninety-eight cases. *J Thorac Cardiovasc Surg* 1996; 111: 323-31.

103. Hollstein MC, Metcalf RA, Welsh JA, Montesano R, Harris CC. Frequent mutation of the p53 gene in human esophageal cancer. *Proc Natl Acad Sci U S A* 1990; 87: 9958-61.
104. Hollstein M, Sidransky D, Vogelstein B, Harris CC. p53 mutations in human cancers. *Science* 1991; 253: 49-53.
105. Maley CC et al. Selectively advantageous mutations and hitchhikers in neoplasms: p16 lesions are selected in Barrett's esophagus. *Cancer Res* 2004; 64: 3414-27.
106. Wagata T et al. Loss of 17p, mutation of the p53 gene, and overexpression of p53 protein in esophageal squamous cell carcinomas. *Cancer Res* 1993; 53: 846-50.
107. Singh SP et al. Loss or altered subcellular localization of p27 in Barrett's associated adenocarcinoma. *Cancer Res* 1998; 58: 1730-5.
108. Loda M et al. Increased proteasome-dependent degradation of the cyclin-dependent kinase inhibitor p27 in aggressive colorectal carcinomas. *Nat Med* 1997; 3: 231-4.
109. Dowdy SF et al. Physical interaction of the retinoblastoma protein with human D cyclins. *Cell* 1993; 73: 499-511.
110. Kato J, Matsushime H, Hiebert SW, Ewen ME, Sherr CJ. Direct binding of cyclin D to the retinoblastoma gene product (pRb) and pRb phosphorylation by the cyclin D-dependent kinase CDK4. *Genes Dev* 1993; 7: 331-42.
111. Matsushime H et al. Identification and properties of an atypical catalytic subunit (p34PSK-J3/cdk4) for mammalian D type G1 cyclins. *Cell* 1992; 71: 323-34.
112. Jiang W et al. Amplification and expression of the human cyclin D gene in esophageal cancer. *Cancer Res* 1992; 52: 2980-3.
113. Arber N et al. Increased expression of the cyclin D1 gene in Barrett's esophagus. *Cancer Epidemiol Biomarkers Prev* 1996; 5: 457-9.
114. Bani-Hani K et al. Prospective study of cyclin D1 overexpression in Barrett's esophagus: association with increased risk of adenocarcinoma. *J Natl Cancer Inst* 2000; 92: 1316-21.
115. Horowitz JM et al. Frequent inactivation of the retinoblastoma anti-oncogene is restricted to a subset of human tumor cells. *Proc Natl Acad Sci U S A* 1990; 87: 2775-9.
116. Jiang W et al. Altered expression of the cyclin D1 and retinoblastoma genes in human esophageal cancer. *Proc Natl Acad Sci U S A* 1993; 90: 9026-30.
117. Alao JP. The regulation of cyclin D1 degradation: roles in cancer development and the potential for therapeutic invention. *Mol Cancer* 2007; 6: 24.

118. Boynton RF et al. Frequent loss of heterozygosity at the retinoblastoma locus in human esophageal cancers. *Cancer Res* 1991; 51: 5766-9.
119. Huang Y et al. Altered messenger RNA and unique mutational profiles of p53 and Rb in human esophageal carcinomas. *Cancer Res* 1993; 53: 1889-94.
120. Reid BJ et al. Barrett's esophagus: ordering the events that lead to cancer. *Eur J Cancer Prev* 1996; 5 Suppl 2: 57-65.
121. Barrett MT et al. Evolution of neoplastic cell lineages in Barrett oesophagus. *Nat Genet* 1999; 22: 106-9.
122. Mu DQ, Peng YS, Xu QJ. Values of mutations of K-ras oncogene at codon 12 in detection of pancreatic cancer: 15-year experience. *World J Gastroenterol* 2004; 10: 471-5.
123. Lord RV, O'Grady R, Sheehan C, Field AF, Ward RL. K-ras codon 12 mutations in Barrett's oesophagus and adenocarcinomas of the oesophagus and oesophagogastric junction. *J Gastroenterol Hepatol* 2000; 15: 730-6.
124. Bos JL et al. Prevalence of ras gene mutations in human colorectal cancers. *Nature* 1987; 327: 293-7.
125. Oltvai ZN, Milliman CL, Korsmeyer SJ. Bcl-2 heterodimerizes in vivo with a conserved homolog, Bax, that accelerates programmed cell death. *Cell* 1993; 74: 609-19.
126. Adams JM, Cory S. The Bcl-2 protein family: arbiters of cell survival. *Science* 1998; 281: 1322-6.
127. Katada N et al. Apoptosis is inhibited early in the dysplasia-carcinoma sequence of Barrett esophagus. *Arch Surg* 1997; 132: 728-33.
128. Bailey T et al. Altered cadherin and catenin complexes in the Barrett's esophagus-dysplasia-adenocarcinoma sequence: correlation with disease progression and dedifferentiation. *Am J Pathol* 1998; 152: 135-44.
129. Tsukita S, Itoh M, Nagafuchi A, Yonemura S, Tsukita S. Submembranous junctional plaque proteins include potential tumor suppressor molecules. *J Cell Biol* 1993; 123: 1049-53.
130. McNeill H, Ozawa M, Kemler R, Nelson WJ. Novel function of the cell adhesion molecule uvomorulin as an inducer of cell surface polarity. *Cell* 1990; 62: 309-16.
131. Behrens J, Mareel MM, Van Roy FM, Birchmeier W. Dissecting tumor cell invasion: epithelial cells acquire invasive properties after the loss of uvomorulin-mediated cell-cell adhesion. *J Cell Biol* 1989; 108: 2435-47.

132. Dorudi S, Sheffield JP, Poulsom R, Northover JM, Hart IR. E-cadherin expression in colorectal cancer. An immunocytochemical and in situ hybridization study. *Am J Pathol* 1993; 142: 981-6.
133. Kadowaki T et al. E-cadherin and alpha-catenin expression in human esophageal cancer. *Cancer Res* 1994; 54: 291-6.
134. Tselepis C, Perry I, Jankowski J. Barrett's esophagus: dysregulation of cell cycling and intercellular adhesion in the metaplasia-dysplasia-carcinoma sequence. *Digestion* 2000; 61: 1-5.
135. Langer R et al. Prognostic significance of expression patterns of c-erbB-2, p53, p16INK4A, p27KIP1, cyclin D1 and epidermal growth factor receptor in oesophageal adenocarcinoma: a tissue microarray study. *J Clin Pathol* 2006; 59: 631-4.
136. Akiyama T, Sudo C, Ogawara H, Toyoshima K, Yamamoto T. The product of the human c-erbB-2 gene: a 185-kilodalton glycoprotein with tyrosine kinase activity. *Science* 1986; 232: 1644-6.
137. Holmes WE et al. Identification of heregulin, a specific activator of p185erbB2. *Science* 1992; 256: 1205-10.
138. Wen D et al. Neu differentiation factor: a transmembrane glycoprotein containing an EGF domain and an immunoglobulin homology unit. *Cell* 1992; 69: 559-72.
139. Yokota J et al. Amplification of c-erbB-2 oncogene in human adenocarcinomas in vivo. *Lancet* 1986; 1: 765-7.
140. Ross JS, McKenna BJ. The HER-2/neu oncogene in tumors of the gastrointestinal tract. *Cancer Invest* 2001; 19: 554-68.
141. Hardwick RH, Shepherd NA, Moorghen M, Newcomb PV, Alderson D. c-erbB-2 overexpression in the dysplasia/carcinoma sequence of Barrett's oesophagus. *J Clin Pathol* 1995; 48: 129-32.
142. Harley CB, Futcher AB, Greider CW. Telomeres shorten during ageing of human fibroblasts. *Nature* 1990; 345: 458-60.
143. Counter CM et al. Telomere shortening associated with chromosome instability is arrested in immortal cells which express telomerase activity. *EMBO J* 1992; 11: 1921-9.
144. Morales CP, Lee EL, Shay JW. In situ hybridization for the detection of telomerase RNA in the progression from Barrett's esophagus to esophageal adenocarcinoma. *Cancer* 1998; 83: 652-9.

145. Wilson KT, Fu S, Ramanujam KS, Meltzer SJ. Increased expression of inducible nitric oxide synthase and cyclooxygenase-2 in Barrett's esophagus and associated adenocarcinomas. *Cancer Res* 1998; 58: 2929-34.
146. Ambs S et al. Relationship between p53 mutations and inducible nitric oxide synthase expression in human colorectal cancer. *J Natl Cancer Inst* 1999; 91: 86-8.
147. Zhang F et al. Duodenal reflux induces cyclooxygenase-2 in the esophageal mucosa of rats: evidence for involvement of bile acids. *Gastroenterology* 2001; 121: 1391-9.
148. Cross AJ et al. A prospective study of red and processed meat intake in relation to cancer risk. *PLoS Med* 2007; 4: e325.
149. Cross AJ et al. Meat consumption and risk of esophageal and gastric cancer in a large prospective study. *Am J Gastroenterol* 2011; 106: 432-42.
150. Goldstein SR et al. Development of esophageal metaplasia and adenocarcinoma in a rat surgical model without the use of a carcinogen. *Carcinogenesis* 1997; 18: 2265-70.
151. Herrinton LJ, Friedman GD, Baer D, Selby JV. Transferrin saturation and risk of cancer. *Am J Epidemiol* 1995; 142: 692-8.
152. Hsing AW et al. Cancer risk following primary hemochromatosis: a population-based cohort study in Denmark. *Int J Cancer* 1995; 60: 160-2.
153. Knekt P, Jarvinen R, Dich J, Hakulinen T. Risk of colorectal and other gastrointestinal cancers after exposure to nitrate, nitrite and N-nitroso compounds: a follow-up study. *Int J Cancer* 1999; 80: 852-6.
154. Stevens RG, Graubard BI, Micozzi MS, Neriishi K, Blumberg BS. Moderate elevation of body iron level and increased risk of cancer occurrence and death. *Int J Cancer* 1994; 56: 364-9.
155. Tiniakos G, Williams R. Cirrhotic process, liver cell carcinoma and extrahepatic malignant tumors in idiopathic haemochromatosis. Study of 71 patients treated with venesection therapy. *Appl Pathol* 1988; 6: 128-38.
156. Larsson SC, Rafter J, Holmberg L, Bergkvist L, Wolk A. Red meat consumption and risk of cancers of the proximal colon, distal colon and rectum: the Swedish Mammography Cohort. *Int J Cancer* 2005; 113: 829-34.
157. Larsson SC, Wolk A. Meat consumption and risk of colorectal cancer: a meta-analysis of prospective studies. *Int J Cancer* 2006; 119: 2657-64.
158. Larsson SC, Orsini N, Wolk A. Processed meat consumption and stomach cancer risk: a meta-analysis. *J Natl Cancer Inst* 2006; 98: 1078-87.

159. Larsson SC, Bergkvist L, Wolk A. Processed meat consumption, dietary nitrosamines and stomach cancer risk in a cohort of Swedish women. *Int J Cancer* 2006; 119: 915-9.
160. Larsson SC, Johansson JE, Andersson SO, Wolk A. Meat intake and bladder cancer risk in a Swedish prospective cohort. *Cancer Causes Control* 2009; 20: 35-40.
161. Larsson SC, Wolk A. Red and processed meat consumption and risk of pancreatic cancer: meta-analysis of prospective studies. *Br J Cancer* 2012; 106: 603-7.
162. Chao A et al. Meat consumption and risk of colorectal cancer. *JAMA* 2005; 293: 172-82.
163. Ward MH et al. Risk of adenocarcinoma of the stomach and esophagus with meat cooking method and doneness preference. *Int J Cancer* 1997; 71: 14-9.
164. Ward MH et al. Heme iron from meat and risk of adenocarcinoma of the esophagus and stomach. *Eur J Cancer Prev* 2012; 21: 134-8.
165. Zacharski LR, Ornstein DL, Woloshin S, Schwartz LM. Association of age, sex, and race with body iron stores in adults: analysis of NHANES III data. *Am Heart J* 2000; 140: 98-104.
166. Knekt P et al. Body iron stores and risk of cancer. *Int J Cancer* 1994; 56: 379-82.
167. Zacharski LR et al. Decreased cancer risk after iron reduction in patients with peripheral arterial disease: results from a randomized trial. *J Natl Cancer Inst* 2008; 100: 996-1002.
168. Edgren G et al. Donation frequency, iron loss, and risk of cancer among blood donors. *J Natl Cancer Inst* 2008; 100: 572-9.
169. Chen X et al. An esophagogastrroduodenal anastomosis model for esophageal adenocarcinogenesis in rats and enhancement by iron overload. *Carcinogenesis* 1999; 20: 1801-8.
170. Goldstein SR, Yang GY, Chen X, Curtis SK, Yang CS. Studies of iron deposits, inducible nitric oxide synthase and nitrotyrosine in a rat model for esophageal adenocarcinoma. *Carcinogenesis* 1998; 19: 1445-9.
171. Boulton J et al. Overexpression of cellular iron import proteins is associated with malignant progression of esophageal adenocarcinoma. *Clin Cancer Res* 2008; 14: 379-87.
172. O'Donnell KA et al. Activation of transferrin receptor 1 by c-Myc enhances cellular proliferation and tumorigenesis. *Mol Cell Biol* 2006; 26: 2373-86.
173. Wu KJ, Polack A, Dalla-Favera R. Coordinated regulation of iron-controlling genes, H-ferritin and IRP2, by c-MYC. *Science* 1999; 283: 676-9.

174. Tselepis C et al. Upregulation of the oncogene c-myc in Barrett's adenocarcinoma: induction of c-myc by acidified bile acid in vitro. *Gut* 2003; 52: 174-80.
175. Brookes MJ et al. Modulation of iron transport proteins in human colorectal carcinogenesis. *Gut* 2006; 55: 1449-60.
176. Brookes MJ et al. A role for iron in Wnt signalling. *Oncogene* 2008; 27: 966-75.
177. Fleming RE, Bacon BR. Orchestration of iron homeostasis. *N Engl J Med* 2005; 352: 1741-4.
178. Aisen P, Enns C, Wessling-Resnick M. Chemistry and biology of eukaryotic iron metabolism. *Int J Biochem Cell Biol* 2001; 33: 940-59.
179. Huang X. Iron overload and its association with cancer risk in humans: evidence for iron as a carcinogenic metal. *Mutat Res* 2003; 533: 153-71.
180. Andrews NC. Forging a field: the golden age of iron biology. *Blood* 2008; 112: 219-30.
181. Chen X et al. Oxidative damage in an esophageal adenocarcinoma model with rats. *Carcinogenesis* 2000; 21: 257-63.
182. Chen X, Yang CS. Esophageal adenocarcinoma: a review and perspectives on the mechanism of carcinogenesis and chemoprevention. *Carcinogenesis* 2001; 22: 1119-29.
183. Tavani A, Negri E, Franceschi S, La Vecchia C. Risk factors for esophageal cancer in lifelong nonsmokers. *Cancer Epidemiol Biomarkers Prev* 1994; 3: 387-92.
184. Wetscher GJ et al. Reflux esophagitis in humans is a free radical event. *Dis Esophagus* 1997; 10: 29-32.
185. Birgegard G, Caro J. Increased ferritin synthesis and iron uptake in inflammatory mouse macrophages. *Scand J Haematol* 1984; 33: 43-8.
186. Yu Y, Kovacevic Z, Richardson DR. Tuning cell cycle regulation with an iron key. *Cell Cycle* 2007; 6: 1982-94.
187. Thelander L, Reichard P. Reduction of ribonucleotides. *Annu Rev Biochem* 1979; 48: 133-58.
188. Thelander L, Graslund A, Thelander M. Continual presence of oxygen and iron required for mammalian ribonucleotide reduction: possible regulation mechanism. *Biochem Biophys Res Commun* 1983; 110: 859-65.
189. Gao J, Richardson DR. The potential of iron chelators of the pyridoxal isonicotinoyl hydrazone class as effective antiproliferative agents, IV: The mechanisms involved in inhibiting cell-cycle progression. *Blood* 2001; 98: 842-50.

190. Kulp KS, Green SL, Vulliet PR. Iron deprivation inhibits cyclin-dependent kinase activity and decreases cyclin D/CDK4 protein levels in asynchronous MDA-MB-453 human breast cancer cells. *Exp Cell Res* 1996; 229: 60-8.
191. Darnell G, Richardson DR. The potential of iron chelators of the pyridoxal isonicotinoyl hydrazone class as effective antiproliferative agents III: the effect of the ligands on molecular targets involved in proliferation. *Blood* 1999; 94: 781-92.
192. Le NT, Richardson DR. Potent iron chelators increase the mRNA levels of the universal cyclin-dependent kinase inhibitor p21(CIP1/WAF1), but paradoxically inhibit its translation: a potential mechanism of cell cycle dysregulation. *Carcinogenesis* 2003; 24: 1045-58.
193. Lucas JJ et al. Effects of iron-depletion on cell cycle progression in normal human T lymphocytes: selective inhibition of the appearance of the cyclin A-associated component of the p33cdk2 kinase. *Blood* 1995; 86: 2268-80.
194. Brodie C et al. Neuroblastoma sensitivity to growth inhibition by deferrioxamine: evidence for a block in G1 phase of the cell cycle. *Cancer Res* 1993; 53: 3968-75.
195. Larrick JW, Cresswell P. Modulation of cell surface iron transferrin receptors by cellular density and state of activation. *J Supramol Struct* 1979; 11: 579-86.
196. Richardson DR, Baker E. The uptake of iron and transferrin by the human malignant melanoma cell. *Biochim Biophys Acta* 1990; 1053: 1-12.
197. Elford HL, Freese M, Passamani E, Morris HP. Ribonucleotide reductase and cell proliferation. I. Variations of ribonucleotide reductase activity with tumor growth rate in a series of rat hepatomas. *J Biol Chem* 1970; 245: 5228-33.
198. Clevers H. Wnt/beta-catenin signaling in development and disease. *Cell* 2006; 127: 469-80.
199. Munro SB, Turner IM, Farookhi R, Blaschuk OW, Jothy S. E-cadherin and OB-cadherin mRNA levels in normal human colon and colon carcinoma. *Exp Mol Pathol* 1995; 62: 118-22.
200. Orsulic S, Huber O, Aberle H, Arnold S, Kemler R. E-cadherin binding prevents beta-catenin nuclear localization and beta-catenin/LEF-1-mediated transactivation. *J Cell Sci* 1999; 112 ( Pt 8): 1237-45.
201. Hallberg L, Hulthen L. Prediction of dietary iron absorption: an algorithm for calculating absorption and bioavailability of dietary iron. *Am J Clin Nutr* 2000; 71: 1147-60.
202. McKie AT et al. An iron-regulated ferric reductase associated with the absorption of dietary iron. *Science* 2001; 291: 1755-9.

203. Gunshin H et al. Cloning and characterization of a mammalian proton-coupled metal-ion transporter. *Nature* 1997; 388: 482-8.
204. McKie AT et al. A novel duodenal iron-regulated transporter, IREG1, implicated in the basolateral transfer of iron to the circulation. *Mol Cell* 2000; 5: 299-309.
205. Kuo YM et al. Mislocalisation of hephaestin, a multicopper ferroxidase involved in basolateral intestinal iron transport, in the sex linked anaemia mouse. *Gut* 2004; 53: 201-6.
206. Chen H et al. Systemic regulation of Hephaestin and Ireg1 revealed in studies of genetic and nutritional iron deficiency. *Blood* 2003; 102: 1893-9.
207. Syed BA et al. Analysis of the human hephaestin gene and protein: comparative modelling of the N-terminus ecto-domain based upon ceruloplasmin. *Protein Eng* 2002; 15: 205-14.
208. Daniels TR, Delgado T, Helguera G, Penichet ML. The transferrin receptor part II: targeted delivery of therapeutic agents into cancer cells. *Clin Immunol* 2006; 121: 159-76.
209. Daniels TR, Delgado T, Rodriguez JA, Helguera G, Penichet ML. The transferrin receptor part I: Biology and targeting with cytotoxic antibodies for the treatment of cancer. *Clin Immunol* 2006; 121: 144-58.
210. Fleming MD et al. Nramp2 is mutated in the anemic Belgrade (b) rat: evidence of a role for Nramp2 in endosomal iron transport. *Proc Natl Acad Sci U S A* 1998; 95: 1148-53.
211. Ohgami RS, Campagna DR, McDonald A, Fleming MD. The Steap proteins are metalloreductases. *Blood* 2006; 108: 1388-94.
212. Collins JF, Franck CA, Kowdley KV, Ghishan FK. Identification of differentially expressed genes in response to dietary iron deprivation in rat duodenum. *Am J Physiol Gastrointest Liver Physiol* 2005; 288: G964-G971.
213. Gunshin H et al. Cybrd1 (duodenal cytochrome b) is not necessary for dietary iron absorption in mice. *Blood* 2005; 106: 2879-83.
214. Andrews NC. The iron transporter DMT1. *Int J Biochem Cell Biol* 1999; 31: 991-4.
215. Fleming MD et al. Microcytic anaemia mice have a mutation in Nramp2, a candidate iron transporter gene. *Nat Genet* 1997; 16: 383-6.
216. Hubert N, Hentze MW. Previously uncharacterized isoforms of divalent metal transporter (DMT)-1: implications for regulation and cellular function. *Proc Natl Acad Sci U S A* 2002; 99: 12345-50.

217. Mackenzie B, Takanaga H, Hubert N, Rolfs A, Hediger MA. Functional properties of multiple isoforms of human divalent metal-ion transporter 1 (DMT1). *Biochem J* 2007; 403: 59-69.
218. Garrick MD et al. Comparison of mammalian cell lines expressing distinct isoforms of divalent metal transporter 1 in a tetracycline-regulated fashion. *Biochem J* 2006; 398: 539-46.
219. Lee PL, Gelbart T, West C, Halloran C, Beutler E. The human Nramp2 gene: characterization of the gene structure, alternative splicing, promoter region and polymorphisms. *Blood Cells Mol Dis* 1998; 24: 199-215.
220. Ferreira C et al. Early embryonic lethality of H ferritin gene deletion in mice. *J Biol Chem* 2000; 275: 3021-4.
221. Torti FM, Torti SV. Regulation of ferritin genes and protein. *Blood* 2002; 99: 3505-16.
222. Bauminger ER et al. Iron (II) oxidation and early intermediates of iron-core formation in recombinant human H-chain ferritin. *Biochem J* 1993; 296 ( Pt 3): 709-19.
223. Towe KM. Structural distinction between ferritin and iron-dextran (imferon). An electron diffraction comparison. *J Biol Chem* 1981; 256: 9377-8.
224. Rudeck M, Volk T, Sitte N, Grune T. Ferritin oxidation in vitro: implication of iron release and degradation by the 20S proteasome. *IUBMB Life* 2000; 49: 451-6.
225. Address KJ, Basilion JP, Klausner RD, Rouault TA, Pardi A. Structure and dynamics of the iron responsive element RNA: implications for binding of the RNA by iron regulatory binding proteins. *J Mol Biol* 1997; 274: 72-83.
226. Sierzputowska-Gracz H, Theil EC. 15N NMR and CD studies of the IRE (iron regulatory element in ferritin mRNA with single base substitution in the hairpin loop. *Nucleic Acids Symp Ser* 1995; 203-6.
227. Hintze KJ, Theil EC. Cellular regulation and molecular interactions of the ferritins. *Cell Mol Life Sci* 2006; 63: 591-600.
228. Wessling-Resnick M. Iron imports. III. Transfer of iron from the mucosa into circulation. *Am J Physiol Gastrointest Liver Physiol* 2006; 290: G1-G6.
229. Donovan A et al. The iron exporter ferroportin/Slc40a1 is essential for iron homeostasis. *Cell Metab* 2005; 1: 191-200.
230. Ganz T. Hepcidin in iron metabolism. *Curr Opin Hematol* 2004; 11: 251-4.
231. Ganz T. Hepcidin--a peptide hormone at the interface of innate immunity and iron metabolism. *Curr Top Microbiol Immunol* 2006; 306: 183-98.

232. Lymboussaki A et al. The role of the iron responsive element in the control of ferroportin1/IREG1/MTP1 gene expression. *J Hepatol* 2003; 39: 710-5.
233. Ganz T. Cellular iron: ferroportin is the only way out. *Cell Metab* 2005; 1: 155-7.
234. Gordeuk VR et al. Iron overload in Africans and African-Americans and a common mutation in the SCL40A1 (ferroportin 1) gene. *Blood Cells Mol Dis* 2003; 31: 299-304.
235. Ganz T, Nemeth E. Iron sequestration and anemia of inflammation. *Semin Hematol* 2009; 46: 387-93.
236. Han O, Kim EY. Colocalization of ferroportin-1 with hephaestin on the basolateral membrane of human intestinal absorptive cells. *J Cell Biochem* 2007; 101: 1000-10.
237. Vulpe CD et al. Hephaestin, a ceruloplasmin homologue implicated in intestinal iron transport, is defective in the sla mouse. *Nat Genet* 1999; 21: 195-9.
238. Hinoi T et al. CDX2-regulated expression of iron transport protein hephaestin in intestinal and colonic epithelium. *Gastroenterology* 2005; 128: 946-61.
239. Neckers LM, Trepel JB. Transferrin receptor expression and the control of cell growth. *Cancer Invest* 1986; 4: 461-70.
240. Jing SQ, Trowbridge IS. Identification of the intermolecular disulfide bonds of the human transferrin receptor and its lipid-attachment site. *EMBO J* 1987; 6: 327-31.
241. MacGillivray RT et al. Two high-resolution crystal structures of the recombinant N-lobe of human transferrin reveal a structural change implicated in iron release. *Biochemistry* 1998; 37: 7919-28.
242. Pantopoulos K. Iron metabolism and the IRE/IRP regulatory system: an update. *Ann N Y Acad Sci* 2004; 1012: 1-13.
243. Omary MB, Trowbridge IS, Minowada J. Human cell-surface glycoprotein with unusual properties. *Nature* 1980; 286: 888-91.
244. Trinder D, Baker E. Transferrin receptor 2: a new molecule in iron metabolism. *Int J Biochem Cell Biol* 2003; 35: 292-6.
245. Kawabata H et al. Expression of transferrin receptor 2 in normal and neoplastic hematopoietic cells. *Blood* 2001; 98: 2714-9.
246. Johnson MB, Chen J, Murchison N, Green FA, Enns CA. Transferrin receptor 2: evidence for ligand-induced stabilization and redirection to a recycling pathway. *Mol Biol Cell* 2007; 18: 743-54.
247. Sharp P, Srai SK. Molecular mechanisms involved in intestinal iron absorption. *World J Gastroenterol* 2007; 13: 4716-24.

248. Rouault TA. The role of iron regulatory proteins in mammalian iron homeostasis and disease. *Nat Chem Biol* 2006; 2: 406-14.
249. Rouault T, Klausner R. Regulation of iron metabolism in eukaryotes. *Curr Top Cell Regul* 1997; 35: 1-19.
250. Klausner RD, Rouault TA, Harford JB. Regulating the fate of mRNA: the control of cellular iron metabolism. *Cell* 1993; 72: 19-28.
251. Guo B, Phillips JD, Yu Y, Leibold EA. Iron regulates the intracellular degradation of iron regulatory protein 2 by the proteasome. *J Biol Chem* 1995; 270: 21645-51.
252. Wallander ML, Leibold EA, Eisenstein RS. Molecular control of vertebrate iron homeostasis by iron regulatory proteins. *Biochim Biophys Acta* 2006; 1763: 668-89.
253. Hentze MW, Muckenthaler MU, Andrews NC. Balancing acts: molecular control of mammalian iron metabolism. *Cell* 2004; 117: 285-97.
254. De D, I, Ward DM, Kaplan J. Heparin regulation: ironing out the details. *J Clin Invest* 2007; 117: 1755-8.
255. Krause A et al. LEAP-1, a novel highly disulfide-bonded human peptide, exhibits antimicrobial activity. *FEBS Lett* 2000; 480: 147-50.
256. Nicolas G et al. Lack of hepcidin gene expression and severe tissue iron overload in upstream stimulatory factor 2 (USF2) knockout mice. *Proc Natl Acad Sci U S A* 2001; 98: 8780-5.
257. Park CH, Valore EV, Waring AJ, Ganz T. Heparin, a urinary antimicrobial peptide synthesized in the liver. *J Biol Chem* 2001; 276: 7806-10.
258. Nemeth E, Ganz T. Regulation of iron metabolism by hepcidin. *Annu Rev Nutr* 2006; 26: 323-42.
259. De D, I et al. The molecular mechanism of hepcidin-mediated ferroportin down-regulation. *Mol Biol Cell* 2007; 18: 2569-78.
260. Nemeth E et al. The N-terminus of hepcidin is essential for its interaction with ferroportin: structure-function study. *Blood* 2006; 107: 328-33.
261. Nemeth E, Ganz T. The role of hepcidin in iron metabolism. *Acta Haematol* 2009; 122: 78-86.
262. Babitt JL et al. Modulation of bone morphogenetic protein signaling in vivo regulates systemic iron balance. *J Clin Invest* 2007; 117: 1933-9.
263. Niederkofler V, Salie R, Arber S. Hemojuvelin is essential for dietary iron sensing, and its mutation leads to severe iron overload. *J Clin Invest* 2005; 115: 2180-6.

264. Gao J et al. Interaction of the hereditary hemochromatosis protein HFE with transferrin receptor 2 is required for transferrin-induced hepcidin expression. *Cell Metab* 2009; 9: 217-27.
265. Tanno T et al. High levels of GDF15 in thalassemia suppress expression of the iron regulatory protein hepcidin. *Nat Med* 2007; 13: 1096-101.
266. Peyssonnaud C et al. Regulation of iron homeostasis by the hypoxia-inducible transcription factors (HIFs). *J Clin Invest* 2007; 117: 1926-32.
267. Nemeth E et al. IL-6 mediates hypoferremia of inflammation by inducing the synthesis of the iron regulatory hormone hepcidin. *J Clin Invest* 2004; 113: 1271-6.
268. Shike H et al. Bass hepcidin is a novel antimicrobial peptide induced by bacterial challenge. *Eur J Biochem* 2002; 269: 2232-7.
269. Ponka P. Cell biology of heme. *Am J Med Sci* 1999; 318: 241-56.
270. Krishnamurthy P, Xie T, Schuetz JD. The role of transporters in cellular heme and porphyrin homeostasis. *Pharmacol Ther* 2007; 114: 345-58.
271. Zimmermann MB, Hurrell RF. Nutritional iron deficiency. *Lancet* 2007; 370: 511-20.
272. Hurrell RF. Fortification: overcoming technical and practical barriers. *J Nutr* 2002; 132: 806S-12S.
273. Quigley JG et al. Identification of a human heme exporter that is essential for erythropoiesis. *Cell* 2004; 118: 757-66.
274. Shayeghi M et al. Identification of an intestinal heme transporter. *Cell* 2005; 122: 789-801.
275. Gburek J et al. Megalin and cubilin are endocytic receptors involved in renal clearance of hemoglobin. *J Am Soc Nephrol* 2002; 13: 423-30.
276. Raffin SB, Woo CH, Roost KT, Price DC, Schmid R. Intestinal absorption of hemoglobin iron-heme cleavage by mucosal heme oxygenase. *J Clin Invest* 1974; 54: 1344-52.
277. Keel SB et al. A heme export protein is required for red blood cell differentiation and iron homeostasis. *Science* 2008; 319: 825-8.
278. Maliepaard M et al. Subcellular localization and distribution of the breast cancer resistance protein transporter in normal human tissues. *Cancer Res* 2001; 61: 3458-64.
279. Pavek P et al. Human breast cancer resistance protein: interactions with steroid drugs, hormones, the dietary carcinogen 2-amino-1-methyl-6-phenylimidazo(4,5-b)pyridine, and transport of cimetidine. *J Pharmacol Exp Ther* 2005; 312: 144-52.

280. Shaw GC et al. Mitoferrin is essential for erythroid iron assimilation. *Nature* 2006; 440: 96-100.
281. Dunn LL, Suryo RY, Richardson DR. Iron uptake and metabolism in the new millennium. *Trends Cell Biol* 2007; 17: 93-100.
282. Jonker JW et al. The breast cancer resistance protein protects against a major chlorophyll-derived dietary phototoxin and protoporphyria. *Proc Natl Acad Sci U S A* 2002; 99: 15649-54.
283. Shirihai OS, Gregory T, Yu C, Orkin SH, Weiss MJ. ABC-me: a novel mitochondrial transporter induced by GATA-1 during erythroid differentiation. *EMBO J* 2000; 19: 2492-502.
284. Kino K, Tsunoo H, Higa Y, Takami M, Nakajima H. Kinetic aspects of hemoglobin-haptoglobin-receptor interaction in rat liver plasma membranes, isolated liver cells, and liver cells in primary culture. *J Biol Chem* 1982; 257: 4828-33.
285. Latunde-Dada GO, Simpson RJ, McKie AT. Recent advances in mammalian haem transport. *Trends Biochem Sci* 2006; 31: 182-8.
286. Ascenzi P et al. Hemoglobin and heme scavenging. *IUBMB Life* 2005; 57: 749-59.
287. Higa Y, Oshiro S, Kino K, Tsunoo H, Nakajima H. Catabolism of globin-haptoglobin in liver cells after intravenous administration of hemoglobin-haptoglobin to rats. *J Biol Chem* 1981; 256: 12322-8.
288. Maniecki MB, Moller HJ, Moestrup SK, Moller BK. CD163 positive subsets of blood dendritic cells: the scavenging macrophage receptors CD163 and CD91 are coexpressed on human dendritic cells and monocytes. *Immunobiology* 2006; 211: 407-17.
289. Moestrup SK, Moller HJ. CD163: a regulated hemoglobin scavenger receptor with a role in the anti-inflammatory response. *Ann Med* 2004; 36: 347-54.
290. Hrkal Z, Vodrazka Z. [The molecular structure of serum hemopexin and its role in the metabolism of hemoglobins]. *Cas Lek Cesk* 1989; 128: 198-200.
291. Smith A, Morgan WT. Hemopexin-mediated transport of heme into isolated rat hepatocytes. *J Biol Chem* 1981; 256: 10902-9.
292. Hvidberg V et al. Identification of the receptor scavenging hemopexin-heme complexes. *Blood* 2005; 106: 2572-9.
293. Tolosano E et al. Enhanced splenomegaly and severe liver inflammation in haptoglobin/hemopexin double-null mice after acute hemolysis. *Blood* 2002; 100: 4201-8.

294. Wheby MS, Suttle GE, Ford KT, III. Intestinal absorption of hemoglobin iron. *Gastroenterology* 1970; 58: 647-54.
295. Latunde-Dada GO, Takeuchi K, Simpson RJ, McKie AT. Haem carrier protein 1 (HCP1): Expression and functional studies in cultured cells. *FEBS Lett* 2006; 580: 6865-70.
296. Qiu A et al. Identification of an intestinal folate transporter and the molecular basis for hereditary folate malabsorption. *Cell* 2006; 127: 917-28.
297. Yasuda S et al. Placental folate transport during pregnancy. *Biosci Biotechnol Biochem* 2008; 72: 2277-84.
298. Herz J, Strickland DK. LRP: a multifunctional scavenger and signaling receptor. *J Clin Invest* 2001; 108: 779-84.
299. Chen WJ, Goldstein JL, Brown MS. NPXY, a sequence often found in cytoplasmic tails, is required for coated pit-mediated internalization of the low density lipoprotein receptor. *J Biol Chem* 1990; 265: 3116-23.
300. Beisiegel U, Weber W, Bengtsson-Olivecrona G. Lipoprotein lipase enhances the binding of chylomicrons to low density lipoprotein receptor-related protein. *Proc Natl Acad Sci U S A* 1991; 88: 8342-6.
301. Ulery PG et al. Modulation of beta-amyloid precursor protein processing by the low density lipoprotein receptor-related protein (LRP). Evidence that LRP contributes to the pathogenesis of Alzheimer's disease. *J Biol Chem* 2000; 275: 7410-5.
302. Smith A, Ledford BE. Expression of the haemopexin-transport system in cultured mouse hepatoma cells. Links between haemopexin and iron metabolism. *Biochem J* 1988; 256: 941-50.
303. Johnsen M, Lund LR, Romer J, Almholt K, Dano K. Cancer invasion and tissue remodeling: common themes in proteolytic matrix degradation. *Curr Opin Cell Biol* 1998; 10: 667-71.
304. Barmina OY et al. Collagenase-3 binds to a specific receptor and requires the low density lipoprotein receptor-related protein for internalization. *J Biol Chem* 1999; 274: 30087-93.
305. Quigley JG et al. Cloning of the cellular receptor for feline leukemia virus subgroup C (FeLV-C), a retrovirus that induces red cell aplasia. *Blood* 2000; 95: 1093-9.
306. Worthington MT, Cohn SM, Miller SK, Luo RQ, Berg CL. Characterization of a human plasma membrane heme transporter in intestinal and hepatocyte cell lines. *Am J Physiol Gastrointest Liver Physiol* 2001; 280: G1172-G1177.

307. Lipovich L, Hughes AL, King MC, Abkowitz JL, Quigley JG. Genomic structure and evolutionary context of the human feline leukemia virus subgroup C receptor (hFLVCR) gene: evidence for block duplications and de novo gene formation within duplicons of the hFLVCR locus. *Gene* 2002; 286: 203-13.
308. Taylor CS, Willett BJ, Kabat D. A putative cell surface receptor for anemia-inducing feline leukemia virus subgroup C is a member of a transporter superfamily. *J Virol* 1999; 73: 6500-5.
309. Duffy SP et al. The Fowler syndrome-associated protein FLVCR2 is an importer of heme. *Mol Cell Biol* 2010; 30: 5318-24.
310. Doyle LA et al. A multidrug resistance transporter from human MCF-7 breast cancer cells. *Proc Natl Acad Sci U S A* 1998; 95: 15665-70.
311. Allikmets R, Schriml LM, Hutchinson A, Romano-Spica V, Dean M. A human placenta-specific ATP-binding cassette gene (ABCP) on chromosome 4q22 that is involved in multidrug resistance. *Cancer Res* 1998; 58: 5337-9.
312. Gupta N et al. Down-regulation of BCRP/ABCG2 in colorectal and cervical cancer. *Biochem Biophys Res Commun* 2006; 343: 571-7.
313. Bailey-Dell KJ, Hassel B, Doyle LA, Ross DD. Promoter characterization and genomic organization of the human breast cancer resistance protein (ATP-binding cassette transporter G2) gene. *Biochim Biophys Acta* 2001; 1520: 234-41.
314. Staud F, Pavek P. Breast cancer resistance protein (BCRP/ABCG2). *Int J Biochem Cell Biol* 2005; 37: 720-5.
315. Kage K et al. Dominant-negative inhibition of breast cancer resistance protein as drug efflux pump through the inhibition of S-S dependent homodimerization. *Int J Cancer* 2002; 97: 626-30.
316. Mogi M et al. Akt signaling regulates side population cell phenotype via Bcrp1 translocation. *J Biol Chem* 2003; 278: 39068-75.
317. Krishnamurthy P et al. The stem cell marker Bcrp/ABCG2 enhances hypoxic cell survival through interactions with heme. *J Biol Chem* 2004; 279: 24218-25.
318. Antolin I et al. Porphyrin accumulation in the Harderian glands of female Syrian hamster results in mitochondrial damage and cell death. *Anat Rec* 1994; 239: 349-59.
319. Gao J, Lovejoy D, Richardson DR. Effect of iron chelators with potent anti-proliferative activity on the expression of molecules involved in cell cycle progression and growth. *Redox Rep* 1999; 4: 311-2.
320. Kwok JC, Richardson DR. The iron metabolism of neoplastic cells: alterations that facilitate proliferation? *Crit Rev Oncol Hematol* 2002; 42: 65-78.

321. Steegmann-Olmedillas JL. The role of iron in tumour cell proliferation. *Clin Transl Oncol* 2011; 13: 71-6.
322. Sun D, Melman G, Letourneau NJ, Hays AM, Melman A. Synthesis and antiproliferating activity of iron chelators of hydroxyamino-1,3,5-triazine family. *Bioorg Med Chem Lett* 2010; 20: 458-60.
323. Whitnall M, Howard J, Ponka P, Richardson DR. A class of iron chelators with a wide spectrum of potent antitumor activity that overcomes resistance to chemotherapeutics. *Proc Natl Acad Sci U S A* 2006; 103: 14901-6.
324. Richardson DR, Baker E. Two saturable mechanisms of iron uptake from transferrin in human melanoma cells: the effect of transferrin concentration, chelators, and metabolic probes on transferrin and iron uptake. *J Cell Physiol* 1994; 161: 160-8.
325. Richardson DR. Iron chelators as therapeutic agents for the treatment of cancer. *Crit Rev Oncol Hematol* 2002; 42: 267-81.
326. Beckloff GL, Lerner HJ, Frost D, Russo-Alesi FM, Gitomer S. Hydroxyurea (NSC-32065) in biologic fluids: dose-concentration relationship. *Cancer Chemother Rep* 1965; 48: 57-8.
327. Gwilt PR, Tracewell WG. Pharmacokinetics and pharmacodynamics of hydroxyurea. *Clin Pharmacokinet* 1998; 34: 347-58.
328. Richardson DR. The therapeutic potential of iron chelators. *Expert Opin Investig Drugs* 1999; 8: 2141-58.
329. Witt L, Yap T, Blakley RL. Regulation of ribonucleotide reductase activity and its possible exploitation in chemotherapy. *Adv Enzyme Regul* 1978; 17: 157-71.
330. Takeda E, Weber G. Role of ribonucleotide reductase in expression in the neoplastic program. *Life Sci* 1981; 28: 1007-14.
331. Song S et al. Wnt inhibitor screen reveals iron dependence of beta-catenin signaling in cancers. *Cancer Res* 2011; 71: 7628-39.
332. Kemp JD et al. Inhibition of lymphoma growth in vivo by combined treatment with hydroxyethyl starch deferoxamine conjugate and IgG monoclonal antibodies against the transferrin receptor. *Cancer Res* 1995; 55: 3817-24.
333. Buss JL, Torti FM, Torti SV. The role of iron chelation in cancer therapy. *Curr Med Chem* 2003; 10: 1021-34.
334. Burkitt DP. Related disease--related cause? *Lancet* 1969; 2: 1229-31.
335. Fuchs CS et al. Dietary fiber and the risk of colorectal cancer and adenoma in women. *N Engl J Med* 1999; 340: 169-76.

336. Howe GR et al. Dietary intake of fiber and decreased risk of cancers of the colon and rectum: evidence from the combined analysis of 13 case-control studies. *J Natl Cancer Inst* 1992; 84: 1887-96.
337. Chen H et al. Dietary patterns and adenocarcinoma of the esophagus and distal stomach. *Am J Clin Nutr* 2002; 75: 137-44.
338. Lewis SJ, Heaton KW. Roughage revisited: the effect on intestinal function of inert plastic particles of different sizes and shape. *Dig Dis Sci* 1999; 44: 744-8.
339. Aozasa O, Ohta S, Nakao T, Miyata H, Nomura T. Enhancement in fecal excretion of dioxin isomer in mice by several dietary fibers. *Chemosphere* 2001; 45: 195-200.
340. Ikegami S, Umegaki K, Kawashima Y, Ichikawa T. Viscous indigestible polysaccharides reduce accumulation of pentachlorobenzene in rats. *J Nutr* 1994; 124: 754-60.
341. Davis TA, Volesky B, Mucci A. A review of the biochemistry of heavy metal biosorption by brown algae. *Water Res* 2003; 37: 4311-30.
342. Haug A, Larsen B. Biosynthesis of alginate. Epimerisation of D-mannuronic to L-guluronic acid residues in the polymer chain. *Biochim Biophys Acta* 1969; 192: 557-9.
343. Figueira MM, Volesky B, Ciminelli VS. Assessment of interference in biosorption of a heavy metal. *Biotechnol Bioeng* 1997; 54: 344-50.
344. Sreeram KJ, Yamini SH, Nair BU. Studies on the nature of interaction of iron(III) with alginates. *Biochim Biophys Acta* 2004; 1670: 121-5.
345. Sandberg AS et al. Alginate, small bowel sterol excretion, and absorption of nutrients in ileostomy subjects. *Am J Clin Nutr* 1994; 60: 751-6.
346. Hoshiyama Y, Sekine T, Sasaba T. A case-control study of colorectal cancer and its relation to diet, cigarettes, and alcohol consumption in Saitama Prefecture, Japan. *Tohoku J Exp Med* 1993; 171: 153-65.
347. Nakachi K, Imai K, Hoshiyama Y, Sasaba T. The joint effects of two factors in the aetiology of oesophageal cancer in Japan. *J Epidemiol Community Health* 1988; 42: 355-64.
348. Funahashi H et al. Seaweed prevents breast cancer? *Jpn J Cancer Res* 2001; 92: 483-7.
349. Kwon MJ, Nam TJ. A polysaccharide of the marine alga *Capsosiphon fulvescens* induces apoptosis in AGS gastric cancer cells via an IGF-IR-mediated PI3K/Akt pathway. *Cell Biol Int* 2007; 31: 768-75.

350. Philchenkov A, Zavelevich M, Imbs T, Zvyagintseva T, Zaporozhets T. Sensitization of human malignant lymphoid cells to etoposide by fucoidan, a brown seaweed polysaccharide. *Exp Oncol* 2007; 29: 181-5.
351. Reddy NR, Sathe SK, Salunkhe DK. Phytates in legumes and cereals. *Adv Food Res* 1982; 28: 1-92.
352. Graf E, Empson KL, Eaton JW. Phytic acid. A natural antioxidant. *J Biol Chem* 1987; 262: 11647-50.
353. Nielsen BK, Thompson LU, Bird RP. Effect of phytic acid on colonic epithelial cell proliferation. *Cancer Lett* 1987; 37: 317-25.
354. Shamsuddin AM, Ullah A. Inositol hexaphosphate inhibits large intestinal cancer in F344 rats 5 months after induction by azoxymethane. *Carcinogenesis* 1989; 10: 625-6.
355. Nelson RL, Yoo SJ, Tanure JC, Andrianopoulos G, Misumi A. The effect of iron on experimental colorectal carcinogenesis. *Anticancer Res* 1989; 9: 1477-82.
356. Keberle H. The biochemistry of Desferrioxamine and its relation to iron metabolism. *Ann N Y Acad Sci* 1964; 119: 758-68.
357. Giardina PJ, Grady RW. Chelation therapy in beta-thalassemia: the benefits and limitations of desferrioxamine. *Semin Hematol* 1995; 32: 304-12.
358. Richardson D, Ponka P, Baker E. The effect of the iron(III) chelator, desferrioxamine, on iron and transferrin uptake by the human malignant melanoma cell. *Cancer Res* 1994; 54: 685-9.
359. Richardson DR. Potential of iron chelators as effective antiproliferative agents. *Can J Physiol Pharmacol* 1997; 75: 1164-80.
360. Becton DL, Bryles P. Deferoxamine inhibition of human neuroblastoma viability and proliferation. *Cancer Res* 1988; 48: 7189-92.
361. Blatt J, Stitely S. Antineuroblastoma activity of desferoxamine in human cell lines. *Cancer Res* 1987; 47: 1749-50.
362. Thompson HJ, Kennedy K, Witt M, Juzefyk J. Effect of dietary iron deficiency or excess on the induction of mammary carcinogenesis by 1-methyl-1-nitrosourea. *Carcinogenesis* 1991; 12: 111-4.
363. Wang F, Elliott RL, Head JF. Inhibitory effect of deferoxamine mesylate and low iron diet on the 13762NF rat mammary adenocarcinoma. *Anticancer Res* 1999; 19: 445-50.
364. Hann HW, Stahlhut MW, Rubin R, Maddrey WC. Antitumor effect of deferoxamine on human hepatocellular carcinoma growing in athymic nude mice. *Cancer* 1992; 70: 2051-6.

365. Donfrancesco A et al. Effects of a single course of deferoxamine in neuroblastoma patients. *Cancer Res* 1990; 50: 4929-30.
366. Donfrancesco A et al. Deferoxamine, cyclophosphamide, etoposide, carboplatin, and thiotepa (D-CECaT): a new cytoreductive chelation-chemotherapy regimen in patients with advanced neuroblastoma. *Am J Clin Oncol* 1992; 15: 319-22.
367. Donfrancesco A et al. Deferoxamine followed by cyclophosphamide, etoposide, carboplatin, thiotepa, induction regimen in advanced neuroblastoma: preliminary results. Italian Neuroblastoma Cooperative Group. *Eur J Cancer* 1995; 31A: 612-5.
368. Blatt J, Huntley D. Enhancement of in vitro activity against neuroblastoma by doxorubicin and deferoxamine. *J Natl Cancer Inst* 1989; 81: 866-70.
369. Estrov Z et al. In vitro and in vivo effects of deferoxamine in neonatal acute leukemia. *Blood* 1987; 69: 757-61.
370. Dezza L et al. Effects of desferrioxamine on normal and leukemic human hematopoietic cell growth: in vitro and in vivo studies. *Leukemia* 1989; 3: 104-7.
371. Gao J, Richardson DR. Multiple effects of iron chelators on molecules controlling cell cycle progression. *Transfus Sci* 2000; 23: 247-8.
372. Cappellini MD. Exjade(R) (deferasirox, ICL670) in the treatment of chronic iron overload associated with blood transfusion. *Ther Clin Risk Manag* 2007; 3: 291-9.
373. Galanello R et al. Effect of food, type of food, and time of food intake on deferasirox bioavailability: recommendations for an optimal deferasirox administration regimen. *J Clin Pharmacol* 2008; 48: 428-35.
374. Nick H et al. Development of tridentate iron chelators: from desferrithiocin to ICL670. *Curr Med Chem* 2003; 10: 1065-76.
375. Nick H et al. ICL670A: preclinical profile. *Adv Exp Med Biol* 2002; 509: 185-203.
376. Galanello R et al. Safety, tolerability, and pharmacokinetics of ICL670, a new orally active iron-chelating agent in patients with transfusion-dependent iron overload due to beta-thalassemia. *J Clin Pharmacol* 2003; 43: 565-72.
377. Nisbet-Brown E et al. Effectiveness and safety of ICL670 in iron-loaded patients with thalassaemia: a randomised, double-blind, placebo-controlled, dose-escalation trial. *Lancet* 2003; 361: 1597-602.
378. Piga A et al. Randomized phase II trial of deferasirox (Exjade, ICL670), a once-daily, orally-administered iron chelator, in comparison to deferoxamine in thalassemia patients with transfusional iron overload. *Haematologica* 2006; 91: 873-80.
379. Cappellini MD et al. A phase 3 study of deferasirox (ICL670), a once-daily oral iron chelator, in patients with beta-thalassemia. *Blood* 2006; 107: 3455-62.

380. Galanello R et al. Phase II clinical evaluation of deferasirox, a once-daily oral chelating agent, in pediatric patients with beta-thalassemia major. *Haematologica* 2006; 91: 1343-51.
381. Gattermann N et al. Deferasirox in iron-overloaded patients with transfusion-dependent myelodysplastic syndromes: Results from the large 1-year EPIC study. *Leuk Res* 2010; 34: 1143-50.
382. Aggarwal BB. Nuclear factor-kappaB: the enemy within. *Cancer Cell* 2004; 6: 203-8.
383. Di Tucci AA et al. Correction of anemia in a transfusion-dependent patient with primary myelofibrosis receiving iron chelation therapy with deferasirox (Exjade, ICL670). *Eur J Haematol* 2007; 78: 540-2.
384. Kicic A, Chua AC, Baker E. Effect of iron chelators on proliferation and iron uptake in hepatoma cells. *Cancer* 2001; 92: 3093-110.
385. Leitch HA. Improving clinical outcome in patients with myelodysplastic syndrome and iron overload using iron chelation therapy. *Leuk Res* 2007; 31 Suppl 3: S7-S9.
386. Messa E et al. Deferasirox is a powerful NF-kappaB inhibitor in myelodysplastic cells and in leukemia cell lines acting independently from cell iron deprivation by chelation and reactive oxygen species scavenging. *Haematologica* 2010; 95: 1308-16.
387. Chantrel-Groussard K et al. The new orally active iron chelator ICL670A exhibits a higher antiproliferative effect in human hepatocyte cultures than O-trensox. *Eur J Pharmacol* 2006; 541: 129-37.
388. Gun J, Ekeltchik I, Lev O, Shelkov R, Melman A. Bis-(hydroxyamino)triazines: highly stable hydroxylamine-based ligands for iron(III) cations. *Chem Commun (Camb)* 2005; 5319-21.
389. Ekeltchik I, Gun J, Lev O, Shelkov R, Melman A. Bis(hydroxyamino)triazines: versatile and high-affinity tridentate hydroxylamine ligands for selective iron(III) chelation. *Dalton Trans* 2006; 1285-93.
390. Bernhardt PV et al. Iron chelators of the dipyriddyketone thiosemicarbazone class: precomplexation and transmetalation effects on anticancer activity. *J Med Chem* 2009; 52: 407-15.
391. Kalinowski DS et al. Design, synthesis, and characterization of novel iron chelators: structure-activity relationships of the 2-benzoylpyridine thiosemicarbazone series and their 3-nitrobenzoyl analogues as potent antitumor agents. *J Med Chem* 2007; 50: 3716-29.
392. Kalinowski DS, Sharpe PC, Bernhardt PV, Richardson DR. Structure-activity relationships of novel iron chelators for the treatment of iron overload disease:

- the methyl pyrazinylketone isonicotinoyl hydrazone series. *J Med Chem* 2008; 51: 331-44.
393. Buss JL, Greene BT, Turner J, Torti FM, Torti SV. Iron chelators in cancer chemotherapy. *Curr Top Med Chem* 2004; 4: 1623-35.
394. Messa E et al. Deferasirox treatment improved the hemoglobin level and decreased transfusion requirements in four patients with the myelodysplastic syndrome and primary myelofibrosis. *Acta Haematol* 2008; 120: 70-4.
395. Lescoat G et al. Antiproliferative and apoptotic effects in rat and human hepatoma cell cultures of the orally active iron chelator ICL670 compared to CP20: a possible relationship with polyamine metabolism. *Cell Prolif* 2007; 40: 755-67.
396. Ohyashiki JH et al. The oral iron chelator deferasirox represses signaling through the mTOR in myeloid leukemia cells by enhancing expression of REDD1. *Cancer Sci* 2009; 100: 970-7.
397. Easton JB, Houghton PJ. mTOR and cancer therapy. *Oncogene* 2006; 25: 6436-46.
398. Jansson PJ, Sharpe PC, Bernhardt PV, Richardson DR. Novel thiosemicarbazones of the ApT and DpT series and their copper complexes: identification of pronounced redox activity and characterization of their antitumor activity. *J Med Chem* 2010; 53: 5759-69.
399. Yuan J, Lovejoy DB, Richardson DR. Novel di-2-pyridyl-derived iron chelators with marked and selective antitumor activity: in vitro and in vivo assessment. *Blood* 2004; 104: 1450-8.
400. Jansson PJ, Hawkins CL, Lovejoy DB, Richardson DR. The iron complex of Dp44mT is redox-active and induces hydroxyl radical formation: an EPR study. *J Inorg Biochem* 2010; 104: 1224-8.
401. Richardson DR et al. Dipyriddy thiosemicarbazone chelators with potent and selective antitumor activity form iron complexes with redox activity. *J Med Chem* 2006; 49: 6510-21.
402. Liu ZD, Liu DY, Hider RC. Iron chelator chemistry. *Adv Exp Med Biol* 2002; 509: 141-66.
403. Barnham KJ, Masters CL, Bush AI. Neurodegenerative diseases and oxidative stress. *Nat Rev Drug Discov* 2004; 3: 205-14.
404. Richardson DR, Tran EH, Ponka P. The potential of iron chelators of the pyridoxal isonicotinoyl hydrazone class as effective antiproliferative agents. *Blood* 1995; 86: 4295-306.
405. Bandyopadhyay S et al. The Drg-1 gene suppresses tumor metastasis in prostate cancer. *Cancer Res* 2003; 63: 1731-6.

406. Kovacevic Z, Chikhani S, Lovejoy DB, Richardson DR. Novel thiosemicarbazone iron chelators induce up-regulation and phosphorylation of the metastasis suppressor, NdrG1: A new strategy for the treatment of pancreatic cancer. *Mol Pharmacol* 2011.
407. Kurdistani SK et al. Inhibition of tumor cell growth by RTP/rit42 and its responsiveness to p53 and DNA damage. *Cancer Res* 1998; 58: 4439-44.
408. Kovacevic Z et al. The metastasis suppressor, N-myc downstream regulated gene 1 (NdrG1), upregulates p21 via p53-independent mechanisms. *Carcinogenesis* 2011; 32: 732-40.
409. Marzano C, Pellei M, Tisato F, Santini C. Copper complexes as anticancer agents. *Anticancer Agents Med Chem* 2009; 9: 185-211.
410. Yu Y, Wong J, Lovejoy DB, Kalinowski DS, Richardson DR. Chelators at the cancer coalface: desferrioxamine to Triapine and beyond. *Clin Cancer Res* 2006; 12: 6876-83.
411. Daniel KG, Gupta P, Harbach RH, Guida WC, Dou QP. Organic copper complexes as a new class of proteasome inhibitors and apoptosis inducers in human cancer cells. *Biochem Pharmacol* 2004; 67: 1139-51.
412. Gupte A, Mumper RJ. Elevated copper and oxidative stress in cancer cells as a target for cancer treatment. *Cancer Treat Rev* 2009; 35: 32-46.
413. Myhre O, Andersen JM, Aarnes H, Fonnum F. Evaluation of the probes 2',7'-dichlorofluorescein diacetate, luminol, and lucigenin as indicators of reactive species formation. *Biochem Pharmacol* 2003; 65: 1575-82.
414. Noursri E et al. Antitumor activity and mechanism of action of the iron chelator, Dp44mT, against leukemic cells. *Am J Hematol* 2009; 84: 170-6.
415. Lovejoy DB et al. Antitumor Activity of Metal-Chelating Compound Dp44mT Is Mediated by Formation of a Redox-Active Copper Complex That Accumulates in Lysosomes. *Cancer Res* 2011; 71: 5871-80.
416. Rockett JC, Larkin K, Darnton SJ, Morris AG, Matthews HR. Five newly established oesophageal carcinoma cell lines: phenotypic and immunological characterization. *Br J Cancer* 1997; 75: 258-63.
417. Harrison T, Graham F, Williams J. Host-range mutants of adenovirus type 5 defective for growth in HeLa cells. *Virology* 1977; 77: 319-29.
418. Naldini L, Blomer U, Gage FH, Trono D, Verma IM. Efficient transfer, integration, and sustained long-term expression of the transgene in adult rat brains injected with a lentiviral vector. *Proc Natl Acad Sci U S A* 1996; 93: 11382-8.

419. Southern PJ, Berg P. Transformation of mammalian cells to antibiotic resistance with a bacterial gene under control of the SV40 early region promoter. *J Mol Appl Genet* 1982; 1: 327-41.
420. Di Martino E et al. IGFBP-3 and IGFBP-10 (CYR61) up-regulation during the development of Barrett's oesophagus and associated oesophageal adenocarcinoma: potential biomarkers of disease risk. *Biomarkers* 2006; 11: 547-61.
421. Mosmann T. Rapid colorimetric assay for cellular growth and survival: application to proliferation and cytotoxicity assays. *J Immunol Methods* 1983; 65: 55-63.
422. Ahmed SA, Gogal RM, Jr., Walsh JE. A new rapid and simple non-radioactive assay to monitor and determine the proliferation of lymphocytes: an alternative to [3H]thymidine incorporation assay. *J Immunol Methods* 1994; 170: 211-24.
423. Riemer J, Hoepken HH, Czerwinska H, Robinson SR, Dringen R. Colorimetric ferrozine-based assay for the quantitation of iron in cultured cells. *Anal Biochem* 2004; 331: 370-5.
424. Shoemaker RH et al. Application of a human tumor colony-forming assay to new drug screening. *Cancer Res* 1985; 45: 2145-53.
425. Rodriguez LG, Wu X, Guan JL. Wound-healing assay. *Methods Mol Biol* 2005; 294: 23-9.
426. Paddison PJ, Caudy AA, Bernstein E, Hannon GJ, Conklin DS. Short hairpin RNAs (shRNAs) induce sequence-specific silencing in mammalian cells. *Genes Dev* 2002; 16: 948-58.
427. Paddison PJ, Caudy AA, Hannon GJ. Stable suppression of gene expression by RNAi in mammalian cells. *Proc Natl Acad Sci U S A* 2002; 99: 1443-8.
428. McIntyre GJ, Fanning GC. Design and cloning strategies for constructing shRNA expression vectors. *BMC Biotechnol* 2006; 6: 1.
429. Vermeulen A et al. The contributions of dsRNA structure to Dicer specificity and efficiency. *RNA* 2005; 11: 674-82.
430. Gregory RI, Chendrimada TP, Cooch N, Shiekhattar R. Human RISC couples microRNA biogenesis and posttranscriptional gene silencing. *Cell* 2005; 123: 631-40.
431. Hughes CS, Postovit LM, Lajoie GA. Matrigel: a complex protein mixture required for optimal growth of cell culture. *Proteomics* 2010; 10: 1886-90.
432. Johnsen M, Lund LR, Romer J, Almholt K, Dano K. Cancer invasion and tissue remodeling: common themes in proteolytic matrix degradation. *Curr Opin Cell Biol* 1998; 10: 667-71.

433. Steegmann-Olmedillas JL. The role of iron in tumour cell proliferation. *Clin Transl Oncol* 2011; 13: 71-6.
434. Broderick R, Nasheuer HP. Regulation of Cdc45 in the cell cycle and after DNA damage. *Biochem Soc Trans* 2009; 37: 926-30.
435. Broderick R et al. Cell cycle-dependent mobility of Cdc45 determined in vivo by fluorescence correlation spectroscopy. *PLoS One* 2012; 7: e35537.
436. Morton DB, Griffiths PH. Guidelines on the recognition of pain, distress and discomfort in experimental animals and an hypothesis for assessment. *Vet Rec* 1985; 116: 431-6.
437. Melcher AA, Mort D, Maughan TS. Epirubicin, cisplatin and continuous infusion 5-fluorouracil (ECF) as neoadjuvant chemotherapy in gastro-oesophageal cancer. *Br J Cancer* 1996; 74: 1651-4.
438. Takashima N et al. Gene expression profiling of the response of esophageal carcinoma cells to cisplatin. *Dis Esophagus* 2008; 21: 230-5.
439. Richardson DR, Kalinowski DS, Lau S, Jansson PJ, Lovejoy DB. Cancer cell iron metabolism and the development of potent iron chelators as anti-tumour agents. *Biochim Biophys Acta* 2009; 1790: 702-17.
440. Kovacevic Z et al. The medicinal chemistry of novel iron chelators for the treatment of cancer. *Curr Top Med Chem* 2011; 11: 483-99.
441. Kalinowski DS, Richardson DR. The evolution of iron chelators for the treatment of iron overload disease and cancer. *Pharmacol Rev* 2005; 57: 547-83.
442. Hormi-Carver K et al. Unlike esophageal squamous cells, Barrett's epithelial cells resist apoptosis by activating the nuclear factor-kappaB pathway. *Cancer Res* 2009; 69: 672-7.
443. Yen CJ et al. Bile acid exposure up-regulates tuberous sclerosis complex 1/mammalian target of rapamycin pathway in Barrett's-associated esophageal adenocarcinoma. *Cancer Res* 2008; 68: 2632-40.
444. Enzinger PC, Ilson DH, Kelsen DP. Chemotherapy in esophageal cancer. *Semin Oncol* 1999; 26: 12-20.
445. Harpole DH, Jr. et al. The prognostic value of molecular marker analysis in patients treated with trimodality therapy for esophageal cancer. *Clin Cancer Res* 2001; 7: 562-9.
446. Urschel JD, Vasan H. A meta-analysis of randomized controlled trials that compared neoadjuvant chemoradiation and surgery to surgery alone for resectable esophageal cancer. *Am J Surg* 2003; 185: 538-43.

